University of Bath

PHD

Design and synthesis of selective inhibitors of poly(ADP-ribose)polymerase-2

Sunderland, Peter

Award date:
2010

Awarding institution:
University of Bath

Link to publication

Alternative formats
If you require this document in an alternative format, please contact:
openaccess@bath.ac.uk

Copyright of this thesis rests with the author. Access is subject to the above licence, if given. If no licence is specified above, original content in this thesis is licensed under the terms of the Creative Commons Attribution-NonCommercial 4.0 International (CC BY-NC-ND 4.0) Licence (https://creativecommons.org/licenses/by-nc-nd/4.0/). Any third-party copyright material present remains the property of its respective owner(s) and is licensed under its existing terms.

Take down policy
If you consider content within Bath's Research Portal to be in breach of UK law, please contact: openaccess@bath.ac.uk with the details. Your claim will be investigated and, where appropriate, the item will be removed from public view as soon as possible.

Download date: 05. May. 2023

Design and synthesis of selective inhibitors of poly(ADP-ribose)polymerase-2

submitted by

Peter Thomas Sunderland

for the degree of PhD

of the University of Bath

2010

The research work in this thesis has been carried out in the Department of Pharmacy and Pharmacology, under the supervision of Dr Michael D. Threadgill and Dr Andrew Thompson.

COPYRIGHT

Attention is drawn to the fact that copyright of this thesis rests with its author. This copy of the thesis has been supplied on condition that anyone who consults it is understood to recognise that its copyright rests with its author and that no quotation from the thesis and no information derived from it may be published without the prior written consent of the author.

This thesis may not be consulted, photocopied or lent to other libraries without the permission of the author for three years from the date of acceptance of the thesis.

……

……

Abstract

The poly(ADP-ribose) polymerases (PARPs) are a family of enzymes that catalyse the transfer of ADP-ribose polymers onto acceptor proteins. The biology and biochemistry of PARP-1 has been extensively studied and, for many years, this was thought to be the sole protein responsible for poly(ADP-ribosyl)ation reactions. However, the functions of the remaining members of the PARP family remain unclear. PARP-2 is responsible for 10-15% of the poly(ADP-ribosyl)ation reactions in the cell and, like PARP-1, is activated by damage to DNA. Recently, the biological importance of PARP-2 has been illustrated by studies using knockout mice and antisense RNA. The protein has been shown to have an important role in DNA repair, telomeric integrity, inflammation and cellular differentiation; but the picture is cloudy. There is currently a major requirement for isoform-selective inhibitors of PARP-2 to use as tools to study the functions of the enzyme. This work focuses upon the design and synthesis of these molecules and their biological evaluation.

Three sets of target compounds were proposed, based on the structure of the murine PARP-2 active site with our lead compound 5-AIQ docked. An initial series of 5-substituted 5-AIQs with carboxylic acids tethered were prepared by alkylation of 5-AIQ or Heck reaction with 5-iodoisoquinolin-1-one but these molecules did not show selectivity for PARP-2 over PARP-1. A further set of 5-acylaminoisoquinolin-1-ones were prepared by treating 5-AIQ with the appropriate acid chloride and were more promising. 5-benzamidoisoquinolinone displayed a 9-fold selectivity for PARP-2 over PARP-1 in our assays. This was in contrast to the best literature compound which had a *ca*. 3-fold selectivity for PARP-2 in our system (reported 60-fold selectivity).

3-substituted compounds were initially prepared using the established chemistry of the Hurtley reaction but two new routes were developed. The first of these involved an initial Friedel-Crafts reaction of 5-nitroisocoumarin and rearrangement followed by decarbonylation / decarboxylation. The second is likely to become the most efficient way to synthesise 3-aryl-5-nitroisoquinolin-1-ones and involves Suzuki reaction with 3-

chloro-1-methoxyisoquinoline as the key step. The 3-substituted compounds were generally highly potent against PARP-1/2 in comparison with 5-AIQ but were not selective.

Several approaches were explored in the synthesis of 4-substituted isoquinolin-1-ones but by far the most successful were palladium-catalysed couplings with protected 4-bromo-5-nitroisoquinolin-1-ones. The most promising 4-substituted compound was 5-amino-4-(4-trifluromethyl)isoquinolin-1-one which was *ca.* 8-fold selective for PARP-2.

A series of 3,5- and 4,5-disubstituted 5-AIQs was generated using previously developed chemistry. Biological evaluation showed these compounds were not significantly active against either PARP isoform.

A new synthesis of our lead compound 5-AIQ was developed in which the only purification steps were filtration and recrystallisation. This has become by far the most efficient way to synthesise this important molecule.

Acknowledgements

I would like to firstly thank my lead supervisor Prof. Mike Threadgill for patience, enthusiasm and guidance throughout this work. I would also like to thank Dr. Andy Thompson for help with molecular modelling and Dr. Niall Martin for support and encouragement throughout my studies.

Much gratitude also goes to colleagues and friends in the lab who have helped and taught me in the 3.5/3.7 lab. Dan, Lisa, Archana, Anna, Victoria, Rich and Emilie, thanks to you all.

A big thank-you to Dr. Tim Woodman for NMR support during this work and for proof-reading the thesis.

Much appreciation goes to the Dept. of Pharmacy & Pharmacology University of Bath and KuDOS Ltd. for sponsorship.

Finally, thanks to all my friends and family for their help during this degree, especially Dad for proof-reading.

We are all in the gutter, but some of us are looking at the stars. Oscar Wilde

Contents

Abbreviations

List of Figures, Schemes and Tables

Figures

Schemes

Scheme 5. Synthesis of 5-nitroisocoumarin *via* enamine formation. (i) DMFDMA, DMF, reflux; (ii) SiO_2.

Scheme 6. Preferred route to 5-AIQ. (i) MeOH, H^+, reflux, 84%; (ii) DMFDMA, DMF, reflux, SiO_2, 42%; (iii) NH_3, 2-methoxyethanol, reflux, 71%; (iv) H_2, 10% Pd/C, EtOH, H^+, 66%.

Scheme 7. Synthesis of **59** *via* an alkylation of 5-AIQ. (i) diisopropylethylamine, ethyl bromoacetate, 19%; (ii) aq. HCl, 87%.

Scheme 8. Attempted synthesis of **60** which gave **61**, hydrolysis yielded **62**. (i) NaH, methyl propenoate 67%; (ii) aq. HCl, 85%.

Scheme 9. Attempted synthesis of 5-iodoisoquinolin-1-one *via* Curtius rearrangement of 72. (i) EtCN, $Pd(OAc)_2$, propenoic acid, Et_3N; (ii) $SOCl_2$; (iii) NaN_3, H_2O; (iv) Heat, $(MeOCH_2CH_2OCH_2CH_2)_2O$.

Scheme 10. Synthesis of the targets **27** and **26** *via* Heck reaction of 5-iodoisoquinolin-1-one. (i) Pd/C, H_2, 89%; (ii) $NaNO_2$, HCl, KI, 58%; (iii) NH_3, 2-methoxyethanol, 62%; (iv) Propenoic acid, Et_3N, Pd(II) acetate, 97%; (v) Pd/C, H_2, 66%.

Scheme 11. Synthesis of 1-oxoisoquinoline-5-carboxylic acid **28**. (i) $KOBu^t$, ethyl formate, **76** 14%, **77** 13%; (ii) KOH, EtOH, 83%.

Scheme 12. Synthesis of 5-cyanoisoquinolin-1-one **76** *via* Pinner-type reaction of **41**. (i) DMFDMA, 3 d, 71%; (ii) MeOH, HCl, 55%.

Scheme 13. General outcomes of the Pinner reation .

Scheme 14. Expected pathways when **78** is subjected to Pinner conditions.

Scheme 15. Proposed mechanism for the formation of **76** from **78**.

Scheme 16. New, higher-yielding synthesis of 5-bromoisoquinolin-1-one **64**. (i) Br_2, 65%; (ii) $AcOH/H_2O$, 70%.

Scheme 17. Attempted synthesis of the ester **93** *via* palladium-catalysed coupling of **64** and ethyl acetoacetate. (i) $Pd(OAc)_2$, P^tBu_3, K_3PO_4, toluene.

Scheme 18. Attempted synthesis of **93** *via* palladium-catalysed couplings with diethyl malonate.

Scheme 19. Proposed synthesis of **98** *via* Stille reaction to form **96**. (i) $Pd_2(dba)_3$, SPhos, trimethylallyl tin, toluene; (ii) O_3; (iii) PCC.

Scheme 20. Acylation of 5-AIQ with various acid chlorides. (i) Pyridine, 90°C, 16 h, 55-86%.

Scheme 21. Hg^{2+}-catalysed cyclisation of methyl 3-nitro-2-phenylethynylbenzoate **30** to give 5-nitro-3-phenylisocoumarin **31** which can be converted into the corresponding isoquinolin-1-one **32** by reaction with ammonia. (i) $(Ph_3P)PdCl_2$, CuI, ethynylbenzene; (ii) $HgSO_4$, H_2SO_4, acetone; (ii) 2-methozyethanol, NH_3; (iv) Pd/C, H_2.

Scheme 22. Hurtley reation of 2-bromo-3-nitrobenzoic acid with **β**-diketones (left to right) and reaction of methyl 2-iodo-3-nitrobenzoate with arylethynes under Castro-Stevens conditions (right to left), to give 3-aryl-5-nitroisocoumarins, precursors to isoquinolin-1-ones. (i) NaOEt, Cu; (ii) Pyridine, heat; (iii) 2-methoxyethanol, NH_3; (iv) Pd/C, H_2.

Scheme 23. Formation of 3-arylisocoumarins by Hurtley reaction of **34** or **122**, followed by deacylation. (i) Cu, $KOBu^t$, 2-methylpropan-2-ol; (ii) NaCl, 170°C.

Scheme 24. Synthesis of **34** by mercuration followed by bromination. (i) NaOH, $Hg(OAc)_2$, AcOH, (ii) AcOH, Br_2, NaBr, 74% (overall).

Scheme 25. Synthesis of β-diketones *via* Claisen-condensation-type reactions. (i) $BF_3.(AcOH)_2$, 68-84%

Scheme 26. The different tautomers of **128** evidenced by ^1H NMR. The intramolecular hydrogen bonds offer increased stability.

Scheme 27. Two possible products are possible depending upon whether the Hurtley intermediate **136** undergoes debenzoylation or deacylation.

Scheme 28. Synthesis of 3-substituted isoquinolin-1-ones *via* Hurtley reaction. (i) Cu, $KOBu^t$, 2-methylpropan-2-ol, 12-33%; (ii) NH_3, 2-methoxyethanol, 24-80%; (iii) Pd/H_2, HCl, 42-79%.

Scheme 29. Resonance forms of the lactams **142** and **143**.

Scheme 30. Probable products formed if Friedel-Crafts alkylations or acylations were attempted directly on 5-AIQ

Scheme 31. Friedel-Crafts acylations of **38**. (i) Ac_2O, H^+, 36%; (ii) PhCOCl, $AlCl_3$, 26%.

Scheme 32. ^{13}C-Labelling study.

Scheme 33. Proposed mechanism for the formation of **31** following Friedel-Crafts reaction of 5-nitroisocoumarin **56**.

Scheme 32. Retrosynthetic analysis for **167**.

Scheme 35. Synthesis of **158** *via* Suzuki coupling with **171**. (i) HNO_3/H_2SO_4, 91%; (ii) MeOH, Na, 92%; (iii) $Pd_2(dba)_3$, SPhos, K_3PO_4, 3-MePhB$(OH)_2$, toluene, 67%; (iv) HBr, 85%; (v) Pd/C, H_2, 69%; overall yield 33%.

Scheme 36. Synthesis of 5-cyano-4-methylisocoumarin **177**, 5-cyanoisoquinolin-1-one **178** and 5-cyanoisocoumarin **177** from 2,6-dicyanotoluene **41**. (i) $KOBu^t$, ethyl formate, 76 14%, 77 13%; (ii) DMFDMA, 71%; (iii) MeOH, HCl, 55%; (iv) $KOBu^t$, ethyl formate, 0%; (v) DMFDMA, 0%; (vi) DMFDMA, TsOH, 12%; (vii) diisopropylamine, 13%.

Scheme 37. Proposed mechanism for the formation of the aldehyde **176**.

Scheme 38. Bromination of 2-methyl-5-nitroisoquinolin-1-one **180**, as reported by Horning.[171]

Scheme 39. Bromination of **38** to form **49** and reduction of the nitro function. (i) Br_2, AcOH; (ii) Sn(II)Cl_2, EtOH; (iii) Heat.

Scheme 40. Attempted Suzuki cross-couplings of **49** (R = NO_2) and **184** (R = NH_2).

Scheme 41. Synthesis of 4-bromo-1-methoxy-5-nitroisoquinoline **46**. (i) DMF, oxalyl chloride, 89%; (ii) MeOH, Na, 82%.

Scheme 42. Synthesis of **190** *via* lithiation of **46**. (i) *n*-BuLi , THF; (ii) MeI, 9%.

Scheme 43. Reported synthesis of the hindered biaryl **193** *via* Suzuki cross-coupling.[172] (i) $Pd_2(dba)_3$, SPhos, K_3PO_4, toluene, 93%

Scheme 44. Synthesis of **195** and **197**. (i) $Pd_2(dba)_3$, SPhos, K_3PO_4, ArB$(OH)_2$, toluene, **194** 86% and **198** 81%; (ii) HBr, **196** 65% and **199** 65%; (v) Pd/C, H_2, **195** 51% and **197** 53%.

Scheme 45. Synthesis of **200.** (i) BnOH, NaH, DMF, 201 71% and 202 12%; (ii) $Pd_2(dba)_3$, SPhos, K_3PO_4, 4-MeOPhB$(OH)_2$, toluene, 61%; (iii) Pd/C, H_2, 47%.

Scheme 46. Synthesis of the hindered **205**. (i) $Pd_2(dba)_3$, SPhos, K_3PO_4 ,phenanthren-9-ylboronic acid, toluene, 42%; (iii) Pd/C, H_2.

Scheme 47. Synthesis of **207** *via* Stille cross-coupling. (i) Me_4Sn, $Pd_2(dba)_3$, SPhos, toluene, 72%; (ii) HBr, 70%; (iii) Pd/C, H_2, HCl, 65%.

Scheme 48. Attempted Buchwald-Hartwig couplings with **46**. (i) $Pd_2(dba)_3$, SPhos, K_3PO_4, PhXH, toluene. **208** 34%, **209** 0%, **210** 0%.
Scheme 49. Synthesis of disubstituted isoquinolin-1-ones. (i) ArCOCl, pyridine.
Scheme 50. A novel synthesis of 5-AIQ. (i) HNO_2/H_2SO_4, 92%; (ii) $AcOH/H_2O$, 82%; (iii) Pd/C, H_2, 70%.

Tables

Table 11. Cytotoxicity of selected isoquinolin-1-ones against HT29 human colon carcinoma cells.

Abbreviations

3-AB	3-aminobenzamide
Ac	acetyl
AIF	apoptosis-mediating factor
5-AIQ	5-aminoisoquinolin-1-one
ANK	ankyrin
AP-2	activator protein-2
ARC	ANK repeat cluster
BER	base excision repair
BRCA1	breast cancer susceptibility protein
BRCT	breast cancer susceptibility protein, C-terminus
Bu	butyl
CHO	Chinese hamster ovary
CBP	CREB-binding protein
CPC	chromosomal passenger complex
CREB	camp response element binding protein
Da	Dalton
DBD	DNA binding domain
DNBS	dinitrobenzene sulfonic acid
DSB	double strand breaks
Et	ethyl
Et_3N	triethylamine
EtOAc	ethyl acetate
EtOH	ethanol
HMBC	heteronuclear multiple bond connectivity
HMQC	heteronuclear multiple quantum correlation
HR	homologous recombination
hTERC	human telomerase RNA component
hTERT	human telomerase reverse transcriptase
ICAM-1	intercelluar adhesion molecule-1

iNOS	inducible nitric oxide
Me	methyl
MMS	methyl methanesulfonate
MNU	*N*-methyl-*N*-nitrosourea
MVP	major vault protein
NAD^+	nicotinamide adenine dinucleotide
NBS	*N*-bromosuccinimide
NIS	*N*-iodosuccinimide
NHEJ	non-homologous end joining
PAR	poly(ADP-ribose)
NLS	nuclear localisation signal
PARG	poly(ADP-ribose) glycohydrolase
PARP	poly(ADP-ribose) polymerase
PMN	polymorphonuclear leukocyte
PPARγ	peroxisome proliferator activated receptor-γ
RNS	reactive nitrogen species
ROS	reactive oxygen species
SSB	single strand breaks
SSBR	single strand break repair
SPhos	2-(2',6'-dimethoxybiphenyl)-dicyclohexylphosphine
TCDD	2,3,7,8-tetrachlorodibenzo-*p*-dioxin
TCR	T-cell receptor
TEF-1	transcription enhancer factor-1
TEP-1	telomerase associated protein
TNBS	trinitrobenzenesulfonic acid
TRF-1	telomeric repeat binding factor-1
TRF-2	telomeric repeat binding factor-2
Tankyrase-1	TRF1-interacting, ankyrin-related ADP-ribose
VRNA	vault RNA
WAT	white adipose tissue
XRCC1	X-ray repair cross complementing I

1. Introduction

1.1 The PARP superfamily

The poly(ADP-ribosyl)ation of proteins involves the transfer of multiple ADP-ribose units onto glutamic acid residues of the targets, resulting in the formation of polymers. The formation of poly(ADP-ribose) (PAR) was first reported in 1963[1] and, since then, there has been an intense research focus into both the functions of the polymer and of the family of enzymes behind its synthesis, the poly(ADP-ribose) polymerases (PARPs).

1.2 PARP-1

1.2.1 Molecular Structure

The PARPs are found in most eukaryotes, with the notable exception of yeasts.[2] The first isoform to be discovered and characterised was poly(ADP-ribose)polymerase-1 (PARP-1). The human gene for PARP-1 comprises 23 exons and is located on chromosome 1 at position q41-q42, contained within 43 Kb of DNA.[3] Initial proteolytic studies of the enzyme revealed three main functional domains,[4] which have been further subdivided into the six domains as shown in Figure 1.

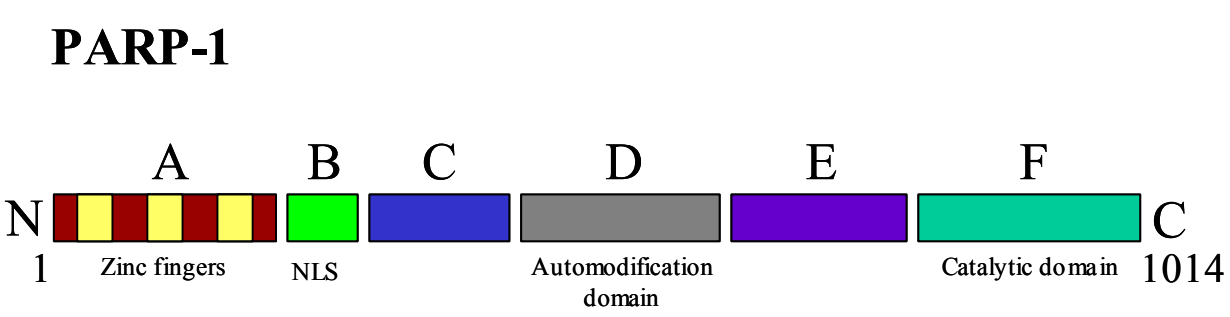

Figure 1. The domain structures of PARP-1

Four domains from the six depicted have now been designated with a function. The DNA-binding domain (DBD) is found close to the N terminus and was originally thought to contain just two zinc-binding sites[5] but a third zinc finger structure was reported in 2008.[6] The initially discovered zinc-binding domains are essential for DNA binding, unlike their newly discovered counterpart, which appears to have a role in protein-protein interactions and the DNA-dependant activation of PARP-1, although the role of this third zinc finger is still controversial.

Domain B, the nuclear localisation signal (NLS), contains the PARP nuclear-homing sequence which is essential for nuclear translocation.[7] Also present in the domain is a cleavage site for a number of apoptotic proteases.[8] Amongst these, caspase-3 has been identified as being primarily responsible for the breakdown of PARP-1 during programmed cell death.[9]

The Automodification domain, or domain D, contains a breast-cancer susceptibility sequence (BRCA1), C-terminus (BRCT) motif which is found in numerous proteins involved in cell-cycle control and DNA repair and recombination.[10] It is known that proteins possessing the *ca.* 100-amino-acid motif can form heterodimers[11] and, therefore, its presence in PARP-1 provides a platform for protein-protein interactions and for dimerisation. In lower organisms, such as *Drosophila*, a leucine zipper has been found in domain D[12] and it has been postulated that this motif is responsible for protein-protein interactions in such species. Interestingly the leucine zipper is poorly conserved in vertebrates, suggesting that the presence of the BRCT domain has rendered it redundant.

Close to the carboxy terminus lies domain F, the catalytic domain. Alignment and comparison of the amino-acid sequences of PARP-1 from multiple species shows that domain F has been highly conserved throughout evolution. Analysis of the crystal structure of the chicken PARP-1 catalytic fragment revealed common features with the active sites of some bacterial toxins, which are mono-ADP-ribosyl transferases,[13] and random mutagenesis of residues in the active site has demonstrated that the conserved

E988 is essential for elongation of the PAR chain.[14] Scheme 1 shows the reactions catalysed by PARPs containing the catalytic fragment.

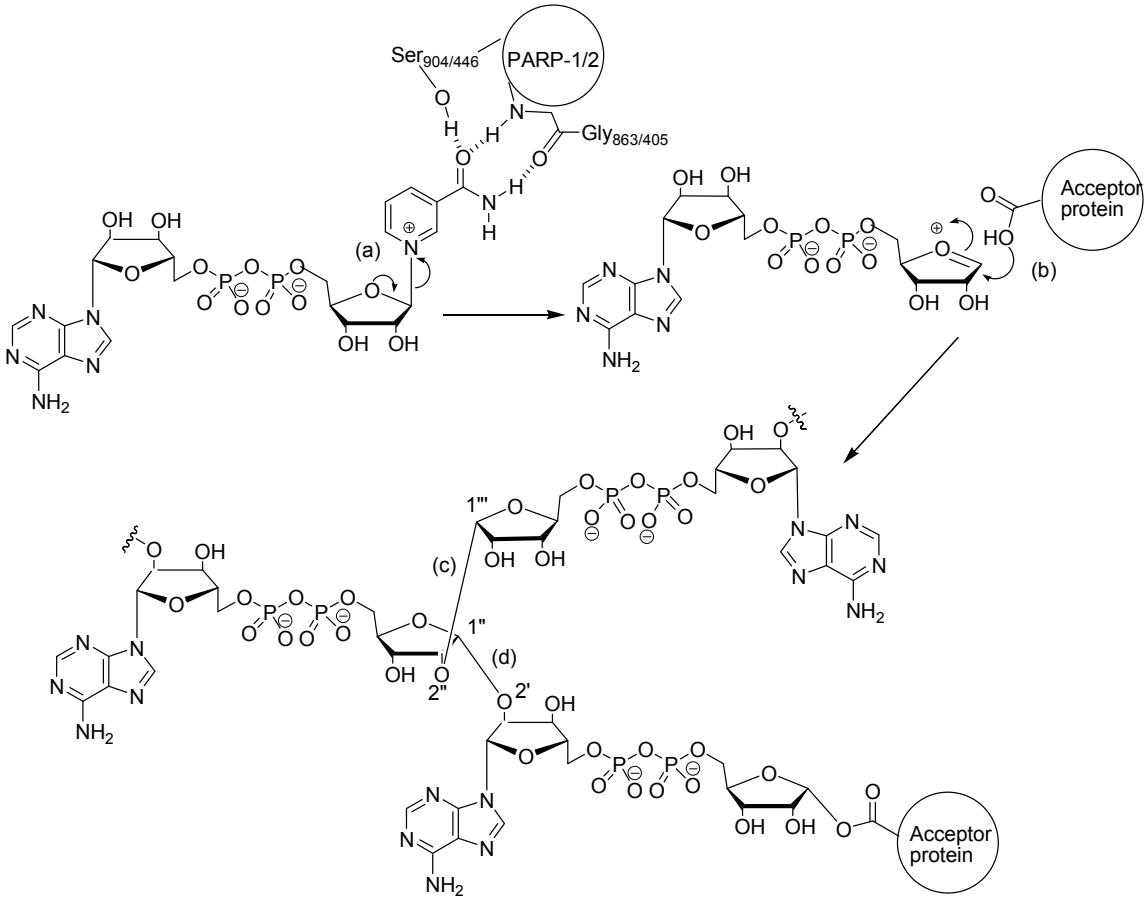

Scheme 1. PAR-generating reactions catalysed by PARPs. a) Generation of cyclic oxonium ion following weakening of the C–N bond. b) Initiation, the cation is quenched by a nucleophilic glutamate residue from an acceptor protein. c) Branching, *via* the 2′′-OH of the nicotinamide-ribose. d) Elongation, *via* the 2′′-OH of the adenine-ribose.

The first step of the PARP-catalysed reaction is removal of the nicotinamide as a leaving group. This is facilitated by a trio of strong hydrogen bonds to the primary amide, which stretches and weakens the glycosidic C–N bond. This process generates the intermediate highly electrophilic oxonium ion (Scheme 1). The "Initiation" then involves the

nucleophilic attack of the anionic γ-carboxylate of a glutamate residue from an acceptor protein at the α-face of the anomeric carbon of the cyclic oxonium ion. Elongation and branching rely on the same chemistry, quenching of the oxonium ion *via* an oxygen nucleophile but supplied by a 2'-hydroxy group of a ribose of the growing polymer. Each molecule of NAD^+ contains two ribose units and these are identified as either the adenine-ribose or the nicotinamide-ribose, depending on their relative positions. If the adenine-ribose 2'-OH is utilised to quench the cyclic oxonium ion, elongation of the PAR chain occurs. Quenching by the nicotinamide-ribose 2'-hydroxy creates a branch-point in the chain, which occurs approximately once in every thirty-to-fifty ADP-ribose units polymerised.[15]

Automodification of the enzymes themselves is the principal regulator of PARP activity, as the process ultimately leads to termination of catalytic activity due to electrostatic repulsion between the poly(ADP)ribosylated enzyme and DNA.

The PAR polymer has a short biological half-life of less than one minute *in vivo*, owing to degradation by the enzyme poly(ADP-ribose) glycohydrolase (PARG). PARG hydrolyses the glycosidic (1" → 2') linkages in linear and the (1" → 2") linkages in branched PAR to produce ADP-ribose.[16] Following the actions of PARG, one ADP-ribose unit is left, linked through a carboxylate group on a glutamate residue to the acceptor protein. ADP-ribose protein lyase is the enzyme responsible for the removal of this last residue *via* hydrolysis of the ester bond between the protein and the ADP-ribose monomer.[17]

1.2.2 DNA Repair

The major heterologous acceptors of PAR generated by PARP-1 are proteins involved in nuclear functions, including DNA repair and replication, transcription and chromatin-structure modulation, suggesting that PARP-1 is involved in the regulation of these processes. The poly(ADP-ribosyl)ation of histones is thought to be particularly important as the build up of anionic charge leads to a relaxation of chromatin structure, allowing components of the DNA-repair pathway access to the DNA.[18] PARP-1 interacts directly

(through the BRCT motif) with multiple components of the base excision repair (BER) and single-strand-break repair (SSBR) pathways.

The crucial role of PARP-1 in DNA repair is also evidenced by the hypersensitivity of cells to DNA-damaging agents which have been treated with PARP-1 inhibitors[19]. For example, Huet and Laval[20] showed Chinese Hamster Ovary (CHO) cells had decreased DNA repair and decreased survival when treated with bleomycin in combination with 3-aminobenzamide **1a**, rather than with bleomycin alone. Another group[21] used X-rays as the DNA-damaging agent and showed that co-treatment with **1a** resulted in diminished survival in V79-B310H cells.

Until highly PARP-1-selective inhibitors are available, perhaps a better strategy to investigate the importance of PARP-1 alone in DNA repair is to use PARP-1 antisense mRNA.[22] Stevnsner and co-workers[23] used nitrogen mustard **2** (HN2) to damage DNA in HeLa S3 cells expressing PARP-1 antisense mRNA and showed that these cells displayed decreased gene specific repair and survival. Similar observations were made by Ding *et al.*[24, 25]who used methyl methanesulfonate **3** (MMS) as an alternative DNA damaging agent.

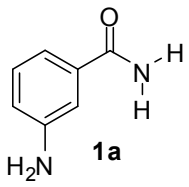

1a

Figure 2. The structure of the PARP inhibitor 3AB **1a**.

In addition, studies on PARP-1-knockout mice (which develop normally and are fertile) have shown markedly increased sensitivity to ionising radiation and alkylating agents.[22] When PARP-$1^{-/-}$ mice were exposed to γ-rays (8 Gy), the majority died within 4-6 days, whereas approximately 50% of the wild-type mice survived an identical exposure for three weeks.[26] In a different experiment, using the alkylating agent N-methyl-N-

nitrosourea **4** (MNU), the authors reported that all PARP-1 deficient mice had died four weeks after intraperitoneal injection. In contrast, 60% of the control mice survived and lived for over eight weeks post-injection. Interestingly, it has been shown that PARP-1 knockouts do not recruit the scaffold protein X-ray repair cross complementing I (XRCC1) to single strand breaks (SSB) and have delayed SSBR,[15] suggesting a possible mechanism for their hypersensitivity to DNA-damaging agents.

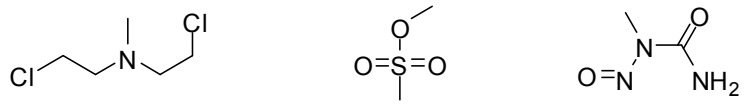

2 **3** **4**

Figure 3. The structures of the alkylating agents HN2 **2**, MMS **3** and MNU **4**.

PARP-1 plays a major role in the initial stages of SSBR, which are outlined below.

1) The SSBR pathway begins with the detection of SSBs and this is achieved by PARP-1 (and possibly other PARP isoforms[19, 27]) binding to the damaged site through its zinc fingers.
2) The DNA-bound PARP-1 is activated resulting in PAR production and chromatin relaxation following histone poly(ADP-ribosyl)ation (note that this process is transient as the PAR polymers are rapidly degraded by PARG).
3) With the chromatin in a relaxed state, PARP-1 interacts with and recruits XRCC1 to the site of damage. This protein acts as a molecular scaffold[28] and allows the assembly of the SSBR complex through interaction with the multiple components involved (most importantly DNA polymerase and DNA ligase).
4) In order that the final two stages of SSBR can take place, the damaged 3' and 5' 'ends' of DNA must be restored to their original undamaged state. Multiple enzymes are involved in this process including XRCC1, PNKP and APTX.
5) Gap filling is the penultimate stage of SSBR and involves the replacement of a single lost nucleotide (short-patch repair) or two or more nucleotides

(long-patch repair). DNA polymerases perform this insertion and Pol β has been shown to be of particular importance.[29]

6) The final stage of SSBR is ligation of the inserted nucleotide(s). Short-patch repair sites are generally ligated by DNA ligase 3 whereas DNA ligase 1 is important in the ligation step of long-patch repair.

PARP-2 is also implicated in these processes and this will be discussed in a later section. The role of PARP-1 in the repair of double-strand breaks (DSBs) is unclear. The two major mechanisms for the repair of DSBs are homologous recombination (HR) and non-homologous end joining (NHEJ) and there is evidence to suggest that PARP-1 is not required for the efficient running of these processes.[30] However, Audebert *et al*.[31] showed that DSB repair was slowed in PARP-1 deficient cells and in cells pre-treated with a PARP-1 inhibitor; suggesting that there may be a PARP-1 dependant DSB pathway.

Ataxia telangiectasia mutated (ATM) is a protein kinase that is crucial in DSB repair, phosphorylating several key proteins in the pathway. Ku86 is part of the Ku hetero-dimer[32] which is thought to bind to damaged DNA ends and recruit essential factors in the DSB repair pathway.[33] The fact that PARP-1/ATM and PARP-1/Ku86 double knockouts are not viable has been attributed to the loss of SSBR through loss of PARP-1 activity and DSB repair through the loss of ATM or Ku86. The above evidence points to a minor role for PARP-1 in DSB repair but a crucial role in SSBR.

1.2.3 Mitosis

The initial stages of mitosis involve chromosomal segregation and this occurs at a structure known as the spindle, which is based on microtubules. Several PARPs localise to the spindle. The work of Chang *et al.*[34] showed that PAR is enriched in the spindle and also required for its assembly and structure, as hydrolysis of PAR led to inhibition of the formation and maintenance of the spindles.

The Aurora kinases were discovered in 1995[35] and are involved in the regulation of many processes involved in mitosis. Aurora-B is part of the chromosomal passenger complex (CPC) that plays an essential role in guiding the stage-to-stage progress through and completion of mitosis. In order that duplicated DNA can be segregated in mitosis, the chromosomes must first be condensed. The key mediator in this process is histone 3. Aurora-B regulates the activity of histone 3 *via* phosphorylation at serines 10 and 28[36] and PARP-1 has been shown to interact specifically with Aurora-B through the BRCT domain.[37] Damage to DNA during mitosis would result in poly(ADP-ribosylation) of the kinase, subsequent deactivation and a reduction in phosphorylation at serines 10 and 28 on histone 3. This is significant as the likely result is prevention of chromosomal condensation and a subsequent halting of progression of metaphase. This suggests a regulatory role of PARP-1 in mitosis. Additionally, PARP-1 has been found localised both to the centrosomes (the major microtubule organising centres) and the chromosomes in the interphase and cytokinesis (cell division) phases of mitosis.[38]

1.2.4 Transcriptional regulation and *NF-κB*

PARP-1 is involved in transcriptional regulation and acts either through direct interactions with transcription factors or by modifications of chromatin structure. Numerous transcription factors and co-factors are stimulated by PARP-1 including b-Myb, transcription enhancer factor-1 (TEF-1), nuclear factor (NF)-κB,[39] activator protein-2 (AP-2) and PAX6.[40]

NF-κB

The term NF-κB covers a family of inducible transcription factors that are important in the regulation of various genes involved in inflammation and the immune response, the most studied form of NF-κB is a heterodimer consisting of two subunits, p50 and p65. In order for NF-κB to promote the expression of genes, several co-factors are required and the two most important of these are the histone acetyltransferases p300 and cAMP response element-binding protein (CREB)-binding protein (CBP). PARP-1 has also been

shown to act as a co-factor for NF-κB,[41] interacting with both subunits. Hassa *et al.*[39] obtained some clues to the possible molecular mechanisms at work when they showed PARP-1 is acetylated by p300/CBP and that this was required for the association of PARP-1 with p50 and subsequent activation of NF-κB. The potential importance of the PARP-1/p50 interaction was demonstrated by Tulin and Spradling[42] who showed that *Drosophila* mutants with diminished levels of the protein displayed a similar phenotype, consisting of immune-system defects, as mice lacking the p50 gene. This research also shows that the PARP-1 mediated regulation of NF-κB has been conserved throughout evolution.

In DNA repair, the poly(ADP-ribosyl)ation of histones by PARP-1 results in a relaxation of chromatin structure and this may also occur in transcription. Chromatin exists in a number of different structural states that have differing levels of transcriptional activity; for example, metaphase chromosomes are highly condensed whereas interphase chromosomes are much more disperse. Kim *et al.*[43] showed that PARP-1 binds to the functional unit of chromatin, the nucleosome, and that activation of the enzyme, followed by removal, was required for transcription to occur. The group also showed that PARP-1 was activated in the absence of DNA damage (by using nick-free, circular DNA templates) but the mechanism of this activation remains an open question. Another group showed that poly(ADP-ribosyl)ation was required[44] for the formation of long-term memory in *Aplysia* and postulated that a PARP-1-mediated decondensation of chromatin structure allowed the high level of transcription required (for the formation of long term memory), to take place.

1.2.5 Inflammation and inflammatory diseases

As mentioned above, PARP-1 is involved in the regulation of NF-κB[45] and AP-1,[46] which are important transcription factors involved in controlling the expression of pro-inflammatory mediators; therefore, the protein has a role in inflammation. In addition, a key feature of inflammatory disease is oxidative stress. This is an imbalance of the antioxidant / pro-oxidant species in the cell, favouring oxidation. Once the normal

cellular protective systems are exhausted (e.g. glutathione redox cycle) there is a build up of reactive oxygen and nitrogen species. These species damage DNA and therefore cause activation of PARP-1 and, when in excess, overactivation. This overactivation can lead to cell death and this has been shown to be important in many disease states, which involve inflammation. The role of PARP-1 in cell death can be explained by two mechanisms. Firstly, depletion of cellular NAD^+ causes a depletion of ATP as the cell attempts to resynthesise and replenish stores of the lost NAD^+. The loss of ATP will lead to cellular death by necrosis. The second pathway is mediated through apoptosis-mediating factor (AIF). Persistent poly-ADP-ribosylation reactions have been shown to cause the relocation of AIF from the mitochondria to the nucleus, where subsequent DNA fragmentation occurs; this leads to cell death by apoptosis.[47] PARP-1 is a target of caspases 3 and 7 during apoptosis and these proteases break down PARP-1 into two fragments: p24 and p89. This fragmentation inactivates PARP-1 and can be seen as a marker for the occurrence of apoptosis.

1.2.6 Asthma

Activation of PARP-1 was directly linked to asthma by Boulares *et al.* in 2003.[48] The group used a mouse model of asthma, which was induced by ovalbumin. The detection of PAR was used as evidence of PARP-1 activation and 3-aminobenzamide **1a** (3-AB) was used to inhibit PARP-1. Administration of 3-AB diminished PAR to undetectable levels, reduced the expression of inducible nitric oxide (iNOS) and reduced cell migration. In order to validate the results (3-AB is a weak and non-selective PARP inhibitor), PARP-$1^{-/-}$ mice were also investigated and the phenotype provided protection from the disease in the model. A similar model (but in guinea pigs) was used by Suzuki *et al.*,[49] who showed that administration of 3-AB or 5-aminoisoquinolin-1-one **5** (5-AIQ) reduced the severity of cough and occurrence of dyspnoea in the animals.

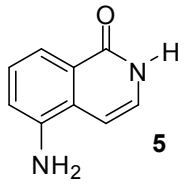

5

Figure 4. The structure of 5-AIQ **5**.

These studies suggest that PARP-1 plays a crucial role in asthma but the results of experiments using knockout mice in asthma must be viewed with caution. There are two stages to creating an animal model of asthma: sensitisation, which involves priming the animal with the antigen, and elicitation, where the inflammatory response is triggered in the presensitised animal. As knockout mice will never possess a particular gene, both stages of the model will be influenced. Therefore further studies are required using selective inhibitors of PARP-1 and, indeed, other PARP isoform-selective inhibitors to determine the role of PARP-1 and of the other PARP isoforms in asthma.

1.2.7 Ischaemia-reperfusion injury

Occlusion of blood vessels supplying oxygenated blood to tissues will result in those tissues becoming ischaemic. Rapid reperfusion of these tissues with oxygenated blood results in the generation of free radicals (oxygen is an oxidising diradical ·O-O·) and other oxidants. The generated species then cause SSBs in DNA and other cellular damage (such as modifications of lipids and proteins), resulting in activation of PARP-1. If the level of PARP-1 activation is great, then its substrate, NAD^+, is consumed. The cell will then attempt to resynthesise NAD^+ from nicotinamide, utilising ATP. The resultant cellular deficiency in NAD^+ and ATP negatively impacts processes such as glycolysis, which ultimately leads to cell death by necrosis, unless the balance is redressed. The rationale for the use of PARP-1 inhibitors in ischaemia-reperfusion injury is to prevent depletion of cellular NAD^+ and, therefore, cell death, which ultimately results in protection of the organ concerned.

Inhibitors of PARP-1 have been shown to be of excellent therapeutic benefit when administered in animal models of ischaemia-reperfusion injury of various organs including the kidney, liver and heart (*i.e.* myocardial infarction). In a rat model of

myocardial infarction which involved coronary artery occlusion followed by reperfusion, 5-AIQ was shown to cause a significant, dose-related reduction in infarct size.[50] The doses of 5-AIQ required in this study were low, ranging from 0.03-0.3 mg kg^{-1}, this is in constrast to similar studies with the lipophilic PARP inhibitor 3-AB **1a** which required a significantly higher dose (> 10 mg kg^{-1}) to produce similar effects.[51, 52]

Another study[53] used a separate rat model of shock / resuscitation and assessed liver microcirculation and function both with and without pre-treatment with 5-AIQ. The group found that the controls suffered from compromised liver function and that 5-AIQ ameliorated this effect. The dose of 5-AIQ used in this study was 3 mg kg^{-1} and lower dosing schedules were not attempted in this work. In order to assess the protective effects of 5-AIQ on renal injury caused by ischaemia-reperfusion, Chatterjee *et al.*[54] used hydrogen peroxide to induce oxidative stress in rat renal proximal tubular cells and incubated the cells with varying concentrations of the PARP inhibitor. In addition, the researchers tested the efficacy of 5-AIQ *in vivo* by subjecting rats to renal bilateral ischaemia-reperfusion both with and without treatment with 5-AIQ. 5-AIQ was found to significantly reduce cell injury and death caused by oxidative stress in the isolated tissue and also in the *in vivo* models. In the rat model 5-AIQ also showed extreme promise in protecting rats from multiple organ injury and dysfunction caused by haemorrhage and resuscitation.[55] In this study, the *i.v.* dose of 5-AIQ required was 30 μg kg^{-1}, some 330-fold lower than that of the benchmark inhibitor at the time 3-AB **1a** (10 mg kg^{-1}).

1.2.8 Inflammatory bowel diseases

Although the precise aetiology of inflammatory bowel diseases is currently unknown, numerous animal and clinical studies have demonstrated the importance of the formation of reactive nitrogen species (RNS) and reactive oxygen species (ROS) in the development of the disorders. For example, polymorphonuclear leukocytes (PMNs) derived from patients with ulcerative colitis have increased levels of oxygen free radicals, in comparison with those derived from healthy patients.[56] As the generation of free

radicals is linked to activation of PARP-1, the role of this enzyme has been examined in such disorders.

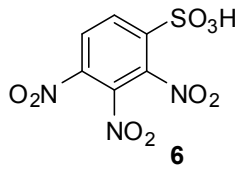

6

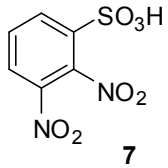

7

Figure 5. Structure of TNBS **6** and DNBS **7**.

Zingarelli *et al.*[57] induced colitis in PARP-1$^{-/-}$ and wild-type mice using trinitrobenzenesulfonic acid **6** (TNBS). The group observed that whilst the wild-type mice displayed symptoms of ulceration and chronic erosion for up to seven days, the PARP-1 knockout mice were completely recovered within six days. Symptoms of colitis were associated with an increase in intercellular adhesion molecule-1 (ICAM-1), infiltration by neutrophils, peroxidation of lipids and nitrosative damage, which were diminished in the mutant mice, indicating a role for PARP-1 in the activation of these processes. Similar results were obtained in the work of Cuzzocrea *et al.*[58] who examined the value of the PARP inhibitors 5-AIQ and 3-AB in a dinitrobenzene sulfonic acid **8** (DNBS)-induced model of colitis. Here, PARP-1 inhibition (evidenced by a reduction in PAR staining) caused a diminution in myeloperoxidase activity, ICAM-1 up-regulation and colon injury.

It is, therefore, unsurprising that researchers have examined the role of PARP-1 and other isoforms in such disorders and several groups have established a link between increased PARP activity and colitis in rodent models.[59-61]

1.2.9 Arthritis

The chronic inflammation in rheumatoid arthritis has been linked to superoxide anions which would suggest a potential role for PARP-1 in the disease. Additionally, autoantibodies against PARP-1 have been found to be present in patients with rheumatoid arthritis and other autoimmune diseases.[62, 63] Peroxynitrite ($ONOO^-$) is the cytotoxic product formed when superoxide reacts with nitric oxide and (mainly due to its capability to cross cell membranes and long half-life) is thought to be the primary mediator of DNA damage in inflammatory diseases, *in vivo*.[64] The work of Pacher *et al.*[65] demonstrated that a reduction in PARP activity by pre-treatment with an inhibitor or by introducing the PARP-$1^{-/-}$ phenotype, protected fibroblasts from peroxynitrite-induced injury. The authors also found that oral treatment with a PARP inhibitor resulted in delayed clinical signs of arthritis and improved histological status (a sign of reduced tyrosine nitration) in a collagen-induced model of arthritis in mice. These data point to a possible clinical application of PARP-1/2 inhibitors in the treatment of arthritis but further studies are required.

1.3 PARP-2

1.3.1 Molecular Structure

The PARP-2 gene encodes for a 62 kDa protein and is localised at chromosome 14 at position q11.2 in humans and C1 in mouse.[66] The mouse protein consists of three functional domains (Figure 6).

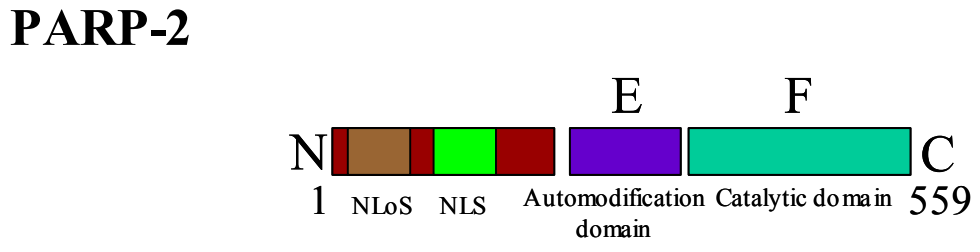

Figure 6. The domain structure of PARP-2.

Figure 7. Domain structure of PARP-2

The DNA-binding domain (Figure 6, residues 1-64) of PARP-2 is distinct from the corresponding PARP-1 domain and, interestingly, lacks the zinc fingers that are essential for binding to DNA by this latter isoform of the enzyme. This domain is, however, rich in basic amino-acids (*ca*. 25% Lys or Arg)[66] and these residues probably play a major role in binding to DNA. The differences in structure of the DNA domains of PARPs 1 and 2 may also reflect the differences in the DNA structures which the two enzymes recognize and the fact that PARP-2 binds to SSBs less efficiently than does PARP-1. The PARP-2 DBD contains both a NLS and a nucleolar localisation Signal (NoLS). Lying between the DBD and domain E, there is a DNRD (AspAsnArgAsp) caspase-3/7 cleavage site.[67] Domain E is the site responsible for the protein-protein interactions that PARP-2 shares with various partners which include PARP-1, XRCC1 and DNA ligase 3.[15] In addition, this domain acts as the automodification domain in PARP-2. Domain F, or the catalytic domain, of mouse and human PARP-2 are highly conserved and both show high homology with the human PARP-1 catalytic domain domain (69% in the case of human PARP-2[66]).

1.3.2 PARP-2 targets, partners and functions

PARP-2 is significantly less active in terms of catalytic activity, compared with PARP-1, and accounts for approximately 5-10% of the total cellular PARP activity.[15] The enzyme has been shown to heterodimerise with PARP-1 and shares many of its functions and targets; however, it has emerged that PARP-2 has some different protein targets and potential functions to PARP-1.

1.3.3 DNA Repair

PARP-2, like PARP-1, is activated by DNA damage and is considered to be a sensor of DNA strand breaks. The two proteins heterodimerise and homodimerise *in vivo* in addition to poly(ADP-ribosyl)ating each other. However, the major heterologous target of PAR synthesised by PARP-2 is the core histone, H2B, rather than H1, but the significance of this difference has not yet been elucidated. The precise role of PARP-2 in

SSBR and BER is not yet clear. The protein interacts through its E domain with several key players in BER, including XRCC1, DNA pol B and DNA ligase III, which would suggest that it is somehow involved in the process of BER. In addition to accepting PAR synthesised by PARP-2, XRCC1 is also a negative regulator of the activity of the enzyme (as it is with PARP-1[68]). The mechanism of this negative regulation is to reduce the rate of automodificaiton of the enzymes by binding to the automodification domain. This results in the PARP isoforms remaining at the DNA lesion rather than becoming detached and available for further rounds of DNA repair. It is likely that this negative feedback loop is in place to prevent excessive XRCC1 recruitment by PARPs 1 and 2.

Schreiber *et al.*[15] showed that PARP-2$^{-/-}$ mouse embryonic fibroblasts (MEFs) display a delay in the repair of alkylated bases following treatment with *N*-methyl-*N*-nitrosourea (MNU) and the importance of PARP-1 in BER has been outlined above. Interestingly, the authors noted that the loss of PARP-2 had a similar impact to the loss of PARP-1, even though PARP-1 is expressed in increased levels, suggesting that perhaps it is the PARP-1/2 heterodimer that is important for efficient BER.

Somewhat contradictory results were obtained by Fisher *et al.*[69] who used hydrogen peroxide to induce SSBRs in human A549 cells and depleted PARP-1 and PARP-2 using siRNA. Although the authors found that a reduction in PARP-1 significantly reduced the rate of SSBR, a reduction in PARP-2 had only a minor effect, even when PARP-1 was also knocked down. A possible explanation for this unexpected result is an incomplete knock down of the proteins but further studies are required to clarify the role of PARP-2 in SSBR and selective inhibitors of PARP-2 would be valuable tools for this purpose.

1.3.4 Telomeric integrity

Telomeres are the complexes of protein and DNA found at the ends of the chromosomes, which contain multiple duplex T_2AG_3 repeats. Telomeres have a protective role, preventing the progressive loss of the chromosome ends with each round of replication and also preventing the ends from being processed as DSBs, which would lead to non-

homologous end-joining or homologous recombination. The classical view of telomeres was that they were arranged as linear double-stranded repeats but Griffith *et al*.[70] showed that the telomeric DNA loops back on itself, forming a lasso structure termed a t-loop (telomere-loop). This process requires a single-strand 3' overhang and is mediated by telomeric repeat binding factor-2 (TRF2) which also has a role in telomere protection through association with various DNA-repair and damage signalling factors.[71, 72] PARP-2 has been shown to interact with TRF2[73] and affects its ability to bind DNA through both a non-covalent interaction of PAR with the DNA binding domain of TRF2 and a covalent modification at the dimerisation domain. These interactions and modifications would open up the t-loop structure and, much in the same way PARP-1 facilitates the repair of DNA, allow access of the DNA-repair enzymes to the site of damage. An alternative telomeric structure was proposed by de Lange,[74] in which the DNA forms dimers and tetramers involving G-quadruplexes; it is possible that both structures co-exist.

Dantzer *et al*.[73] showed that PARP-$2^{-/-}$ mouse embryonic fibroblasts (MEFs) displayed normal telomere length and telomerase activity when compared to wild-type cells. However, these cells showed increased numbers of chromatid and chromosome breaks and of chromosome ends that lacked detectable T_2AG_3 repeats. These results from knockout mice suggest that PARP-2 has a functional role in the maintenance of telomeres but further work using selelective inhibitors of this isoform are required to gain insights into the precise molecular mechanisms at work.

1.3.5 Inflammation

As mentioned above, PARP-1 is implicated in inflammation due to its regulation of NF-κB and the fact that its over-activation by pro-inflammatory mediators leads to cell death by necrosis. It is unlikely that the over-activation of PARP-2 alone will deplete cellular NAD^+ levels, as it accounts for only *ca*. 10% of the total PARP activity in the cell. At present, little is known about the role of PARP-2 in the regulation of genes involved in inflammation but some lines of evidence suggest a possible role. Firstly, administration of the PARP-2 antisense oligonucleotide (ISIS 110251) in the interleukin-

10-deficient mouse (an animal model of colitis) resulted in a marked improvement in colonic inflammatory disease in this model and, in addition, a subsequent normalisation of colonic function was observed.[75]

Secondly, PARP-2-knockout mice were also protected from focal cerebral ischaemia relative to wild-type controls. In global ischaemic insult, the mutants had worse outcomes than PARP-$1^{-/-}$ mice (which showed neuroprotection) in the hippocampus but with no effect in the cortex.[76] Further studies are required to deduce the molecular mechanisms involved in these responses and the precise role that PARP-2 plays in inflammation, highlighting the immediate requirement for isoform-selective inhibitors of PARP-2.

1.3.6 Cellular differentiation

The study of PARP-2 knockout mice has provided evidence for specific roles of the isoform (*i.e.* PARP-1 independent) in cellular differentiation, which include the development of T lymphocytes,[77] germ cells[15] (specifically spermatogenesis) and adipocytes (adipogenesis).[78]

1.3.7 T Lymphocytes

Yelamos *et al.*[77] reported that the deletion of PARP-2 but not of PARP-1 led to a significant diminution in $CD4^{+}CD8^{+}$ double-positive (DP) thymocytes, which was associated with a decrease in DP cell survival. The authors also noted an increased expression of the pro-apoptotic protein, Noxa, in the PARP-$2^{-/-}$ thymocytes, which also showed a reduced expression of T-cell receptor (TCR). These results suggest that PARP-2 has a role in survival of T-cells during the process of thymopoiesis and may regulate the programmed cell death (apoptosis) of thymocytes. Elucidation of the precise molecular mechanisms at work will require more studies and the use of PARP-2-selective inhibitors.

1.3.8 Germ Cells

PARP-2 is widely expressed in the seminiferous epithelium and is evenly distributed across the seminiferous tubules, this is in contrast to PARP-1 where expression is limited to the peripheral cell layer which contains rapidly deviding spermatogonia.[15] This differening expression pattern for the two isoforms suggests distinct roles in spermatogenesis and perhaps a more prominent role for PARP-2.

The multistage process of spermatogenesis involves one round of mitosis and two rounds of meiosis and results in the formation of haploid gametes from diploid spermatogonium. PARP-2-knockout mice display a phenotype which suggests an important role of the protein in the development of sperm cells. The mice display hypofertility and irregularities at numerous stages in the progression of spermatogenesis.[79] Firstly, X- and Y- linked genes are upregulated, as meiotic chromosome deactivation is not fully effective. Secondly, nuclear elongation is delayed, which adversely affects spermatogenesis. Finally, chromosome mis-segregation at metaphase 1 is observed, associated with a loss of centromeric heterochromatin integrity. Interestingly, PARP-1-knockout mice do not display hypofertility. These data would suggest a crucial role for PARP-2 but not PARP-1, in the development of sperm cells and it is possible that defects in the normal functioning of the enzyme are a cause of hypo-fertility in humans.

1.3.9 Adipocytes

PARP-2 knockout mice display lipodystrophy, with decreased weight of white adipose tissue (WAT) and disorders in the differentiation of preadipocytes to adipocytes, when compared with wild-type mice.[78] A proposed mechanism for this phenotype is that PARP-2 regulates the expression of peroxisome proliferator activated receptor-γ (PPARγ) as part of the RXR-PPARγ transcription complex. Evidence for this theory was provided by Bai *et al.*[78] who showed that PARP-2 siRNA diminished ligand-dependant activation and the basal activity of PPARγ. The group also showed, by chromatin immunoprecipitation, that PARP-2 interacted with the PPARγ/RXR complex, forming a

heterodimer. PPARγ plays a vital part in the function of WAT by controlling the expression of several WAT proteins. These interesting results require further investigation, pointing to a role of PARP-2 in obesity and a potential role for PARP-2 inhibitors as novel treatments for this increasingly important condition.

1.4 PARP-3

The gene for human PARP-3 is located on chromosome 3 at position p21.1-p22.2[80]. The protein contains 540 amino acids and consists of three domains. The N-terminal domain is unique to PARP-3 and contains a concise targeting motif in exon 1, responsible for its function of localising the enzyme to the centrioles. The centrioles reside within the centrosome, a structure that forms near the nucleus during interphase and is important in the processing of microtubules. PARP-3 preferentially locates to the daughter centriole[81] and a splicing variant lacking the targetting motif leads to accumulation in the nucleus. An E domain is present in PARP-3, the function of which has not been elucidated. The 489-amino-acid catalytic domain shares *ca*. 35% sequence similarity with the other PARP catalytic domains and has 61% similarity with the human PARP-1 domain.

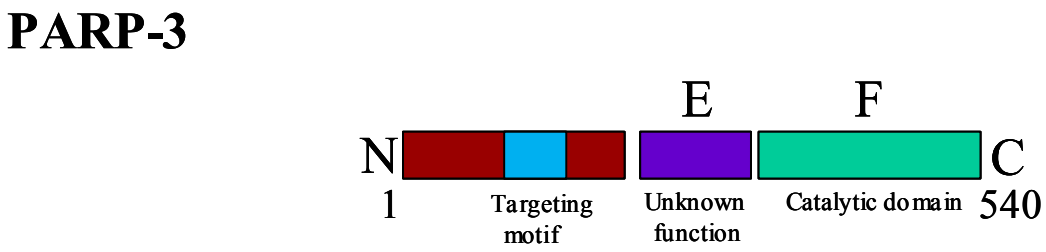

Figure 7. The molecular structure of PARP-3.

Although no automodification domain is present, the protein is capable of automodification in the presence of biotinylated NAD^+, as illustrated by Western blot analysis.[82] Currently, the functions of PARP-3 are unclear but it has been reported that over-expression of the protein interferes with the G1/S cell cycle progression but not with centrosomal duplication or amplification[81]. PARP-3 may, therefore, function in the maturation of the preferred daughter centriole until the G1-S restriction point (the cell-

cycle checkpoint between G1 and S phase). The crystal structure of the human PARP-3 catalytic domain has recently become available,[82] allowing the rational design of selective PARP-3 inhibitors. This will aid in the elucidation of any specific functions. The catalytic domains of PARPs 1 and 3 contain some key differences, which could potentially be exploited in the quest for selective inhibitors. In PARP-3, the pocket between the donor site and the N-terminal α-helix bundle is slightly opened in comparison to PARP-1 as the D-loop is four amino acids shorter. Additional differences also exist in a loop near the PARP signature motif and in a loop near the active site.

1.5 PARP-4

PARP-4 or vault PARP (V-PARP) is the largest member of the PARP family with a molecular weight of 192.6 kDa. It is found located in the vault complex in the cytoplasm and also in the nucleus and at the mitotic spindle (not associated with the vault complex).[83] The gene for PARP-4 is located on chromosome 13q11, with 34 exons coding for its 1724 amino acids. In mammals, vault particles are barrel-shaped ribonucleoprotein complexes found in the cytoplasm, consisting of PARP-4, major vault protein (MVP), telomerase associated protein (TEP-1) and an untranslated vault RNA (VRNA).

The functions of the vault particles are currently unknown but they are highly conserved throughout evolution, suggesting a fundamental role in cellular survival. A role in cellular transport was proposed by Kickhoefer *et al.*[84] in 1996. MVP is over-expressed in numerous non-P-glycoprotein-expressing tumour cell lines and it has been linked to multidrug resistance.[85]

Unusually, the catalytic domain of PARP-4 is found at the N-terminus rather than at the C-terminus as with the other PARPs discovered so far. The presence of a BRCT domain points to a possible role of the protein in DNA repair and, supporting this theory, PARP-

4-knockout mice show an increased susceptibility to both N,N-dimethylhydrazine-induced colon tumourigenesis and urethane-induced lung tumourigenesis (although to a lesser extent).[86]

1.6 PARP-5 and 6, the tankyrases

PARP-5 or TRF1-interacting, ankyrin-related ADP-ribose (tankyrase-1) was discovered as a partner of the human telomeric repeat binding factor 1 (TRF-1) in a two-hybrid screen carried out by Smith *et al*.[87] in 1998. The 142 kDa protein consists of four domains. At the N-terminus lies the HPS domain, named after the continuous repeats of histidine, proline and serine; the function of this domain is currently unknown. The ankyrin (ANK) domain spans 842 amino-acids and contains 24 repeats of the ANK motif, important in protein-protein interactions and placing PARP-5 into the ANK family. The ANK family of proteins have a structural role and link membrane based proteins to those found in the cytoplasm.[88] Uniquely to PARP-5 the ANK domain is further divided into five ARC (ANK repeat cluster) subunits, stevewhich each act as a TRF-1 binding site. A sterile alpha module (SAM) is responsible for the reversible polymerisation of PARP-5 (i.e. to form a polyprotein)[89] and is found adjacent to the catalytic domain.

PARP-6 or tankyrase-2 is closely related to PARP-5. The 127 kDa protein lacks the HPS domain but the other three domains are present and show high homology with PARP-5. It is of interest to note that PARP-5 or PARP-6a single-knockouts are viable but the double knockout is embryonic lethal.[90] This indicates, similarly to PARPs -1 and –2, that the enzymes share redundant functions but that tankyrase activity is absolutely required for normal development.

The telomeres were introduced above, in relation to PARP-2. Telomeres are not completely replicated and gradually shorten over time, however, they are resynthesised by the enzyme telomerase. This is a ribonucleoprotein reverse transcriptase consisting of two subunits, the human telomerase RNA component (hTERC) and the human telomerase reverse transcriptase (hTERT) catalytic portion. TRF-1 acts as a negative

regulator of telomerase activity through the recognition of specific DNA sequences in telomeres. The tankyrases poly(ADP-ribosyl)ate TRF-1 and the build up of negative charge is likely to block the binding of TRF-1 to telomeric DNA (as has been shown *in vitro*[91]). Therefore activation of the tankyrases will lead to elongation of telomeres; the mechanism of activation is currently unknown but Cook *et al.* showed that tankyrase-1 is not activated by DNA damage.[92]

In normal cells, the level of telomerase activity is low but most cancer cells have high levels,[92] which probably contributes to their immortality. It is possible to indirectly inhibit telomerase by stabilising the telomeric DNA in a G-quadruplex structure thus preventing the initial elongation step by the enzyme.[93] Alternatively, the hTERT[94] or hTERC[95] subunits can be directly inhibited. Regardless of the mechanism, inhibition of telomerase leads to the shortening of telomeres and cellular senescence or apoptosis, which suggests that specific inhibitors may be of value in cancer therapy.

One problem associated with the direct inhibition of telomerase is that shorter telomeres have fewer TRF-1-binding sites and, therefore, fewer molecules of TRF-1, enhancing the apparent activity of any non-inhibited telomerase. Alternative approaches would be the direct inhibition of TRF-1 or the use of selective inhibitors of the tankyrases, which would decrease the access of telomerase to its substrate by blocking the poly(ADP-ribosyl)ation of TRF-1. TRF-2, another telomeric binding protein involved in telomere protection, was introduced in relation to PARP-2. Currently, it is not known if there is any interaction between the tankyrases and TRF-2 but it would seem that PARP-2 has a more prominent role in its regulation. Again, selective inhibition of the relevant PARP isoform is required to help to answer the many open questions in this area. Until these tools are available, the generation of PARP-2/PARP-5 and PARP-2/PARP-6 double knockouts would, if viable, give further insights into the biological roles of these isoforms.

1.7 PARP-7, PARP-12 and PARP-13

PARP-12, PARP-13 and PARP-7 (ti-PARP) all have a similar domain structures containing CCCH (CysCysCysHis) zinc fingers close to the N-terminus, a central WWE (TrpTrpGlu) domain and a catalytic F domain.[96] The WWE domain is probably a site for protein-protein interactions, whilst the zinc fingers differ in structure to those found in PARPs 1 and 2 and may bind to RNA rather than DNA. The transcription of PARP-12 is induced by 2,3,7,8-tetrachlorodibenzo-*p*-dioxin (TCDD) and this is controlled by the dioxin-bound aryl hydrocarbon receptor (AHR).[97]

Interestingly one isoform of PARP-13 was initially identified as ZAP,[98] a protein found in rats associated with resistance to retroviral infection, which binds to viral RNA. It is not currently known if the PARP-13 isoform containing the F domain also has a role in viral immunity.

1.8 PARP-9, PARP-14 and PARP-15

PARPs 9, 14 and 15 all share common structural features with one to three macro domains being linked to a catalytic PARP domain.[96] The macro domain was first discovered in macroH2A (a histone variant) and is important in chromosomal inactivation and transcriptional repression.[99] The macro domain of PARP-9 can bind to PAR[100] and may have phosphoesterase activity, which suggests the protein may function as a regulator of the size of the polymer.

1.9 PARP-10

PARP-10 contains an RNA-recognition motif (RRM) near to the N-terminus, then a glycine-rich domain before the catalytic domain.[101] The isoform is known to interact with c-Myc, an important regulator of transcription, controlling cell proliferation. Both the RRM and the glycine-rich domain present in PARP-10 have been found to be of importance in RNA-binding nucleolin, a partner of c-Myc. PARP-10 has been shown to inhibit the cellular transformation caused by c-Myc and Ha-Ras. The protein also

poly(ADP-ribosyl)ates histone H2A, suggesting a role in the regulation of chromatin structure.

1.10 Other PARPs

Very little is currently known about the remaining PARPs - PARP-6, 8, 11 and 16. Other than a WWE sequence in PARP-11,[96] no domains of note have been discovered in these PARPs, so their possible functions are also unknown.

1.11 PARGs

The PARGs are responsible for breaking down PAR into free ADP-ribose molecules and possess both endo- and exoglycosidase activity. Mammalian PARG genes encode a minimum of four isoforms. PARGs-102, 99 and 59/60 are found in high abundance in the cytoplasm, whilst PARG-110/111 is found in low abundance in the nucleus. Unsurprisingly, PARG-110/111 contains two nuclear localisation signals in exon 1, the other PARG isoforms lack exon 1 and this probably explains their differing primary locations. Mice with deletions of exons 2 and 3, resulting in a loss of PARG-110, 102 and 99, have normal phenotypes but have an increased susceptibility to streptozotocin-induced diabetes.[102] The mice are also more susceptible to alkylating agents and ionising radiation than are wild type mice. The deletion of all four PARG isoforms is embryonic-lethal and fibroblast cells lacking PARG activity are also hypersensitive to cytotoxic DNA-damaging agents.

1.12 Inhibitors of PARPs

In the early years of research into inhibitors of the PARPs, it was assumed there was only a single isoform of the enzyme which is now known as PARP-1.

1.12.1 Early PARP inhibitors

It was rationalised that the nicotinamide portion of NAD^+ was required for 'PARP' inhibition and the first competitive inhibitors were 5-methylnicotinamide **8a** and nicotinamide[103] **8b**. However, it was soon shown that these molecules were not specific (for example, nicotinamide is also an inhibitor of adenosine 3',5'-cyclic monophosphate phosphodiesterase, mono(ADP-ribosyl)transferases[104] and SIRT-1). Additionally, the presence of the ring nitrogen meant that these compounds were substrates for NAD-metabolising enzymes. This problem was circumvented in 1975 when Shall first reported benzamide **1b** as an inhibitor of PARP[105] but the hydrophobic nature and low solubility of this compound meant that it was not suitable for *in vivo* testing.

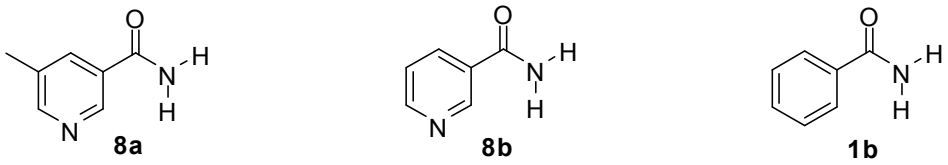

Figure 8. The structures of 5-methylnicotinamide **8a**, nicotinamide **8b** and benzamide **1b**.

1.12.2 Benzamides

Purnell and Whish[106] examined a series of 3-substituted benzamides, amongst other compounds, in 1980. It was rationalised that the introduction of polar substituents would improve water-solubility compared with the parent compound. The compounds were assessed for activity against PARP by measuring percentage inhibition at a concentration of 50 μM and also by measuring the amount of NAD^+ incorporated into an acid insoluble fraction. The authors found that all the benzamides were more potent than nicotinamide in their system and that the most potent benzamides were the unsubstituted compound **1b** and 3-methoxybenzamide **1c**. Percentage inhibition (at 50 μM) was above 90%, except in the case of 3-nitrobenzamide **1d**.

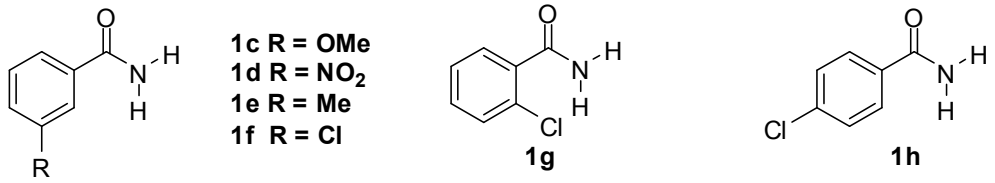

Figure 9. A selection of the benzamides reported by Purnell and Whish[106] and Banasik.[107]

In a comprehensive study of over one hundred and thirty compounds, Banasik reported the IC_{50} values of a series of substituted benzamides.[107] From the values reported, it was clear that 3-substitution was well tolerated; 3-aminobenzamide **1a** (IC_{50} = 33 μM), 3-methylbenzamide **1e** ((IC_{50} = 19 μM) and 3-chlorobenzamide **1f** (IC_{50} = 22 μM) were examples of potent 3-substituted benzamide inhibitors. Substitution in the 2- or 4-positions caused a drop in potency; the 2-Cl **1g** (IC_{50} = 1000 μM) and 4-Cl **1h** (IC_{50} = 300 μM) analogues were relatively weak inhibitors. Disubstitution was not favoured; the difluoro- **1i** (IC_{50} = 180 μM) was moderate but disubstitution with larger groups in **1j** (IC_{50} = 1200 μM) and **1k** (IC_{50} = 2500 μM) led to a dramatic drop in potency.

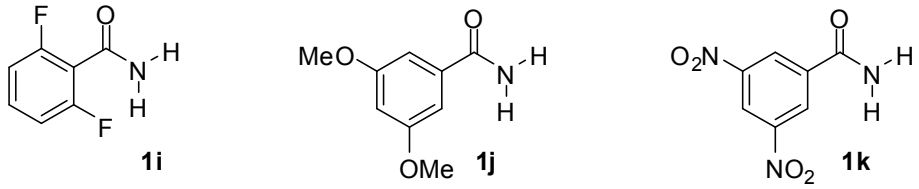

Figure 10. The disubstituted benzamides **1i**, **1j**, and **1k.**

The importance of the carboxamide with at least one amide proton for PARP inhibitory activity was demonstrated early on as thioamides[108] and N-alkylated[109] derivatives suffered from a dramatic loss of activity.

More potent inhibitors were discovered by Suto[110] and by Banasik[104] who reported the 3,4-dihydroisoquinolinones in which the carboxamide is fixed in conformation by the ethano bridge.

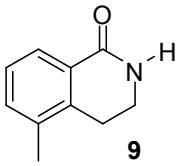

9

Figure 11. The structure of the 3,4-dihydroisoquinolin-1-one **9**.

These compounds were found to be several times more potent than conformationally free PARP inhibitors, with the 3,4-dihydroisoquinolin-1-one **9** proving to be over 50-fold more potent than 3-AB **1a**. The authors concluded that maintenance of the carboxamide in the *anti* conformation was crucial for potent activity.

Many different classes of PARP inhibitors have since been synthesised in which the carboxamide function is held in the required conformation as part of a heterocyclic ring, *e.g.* isoquinolin-1-ones, tricyclic benzimidazoles, quinazolin-4-ones.

1.12.3 Benzimidazole-4-carboxamides and benzoxazole-4-carboxamides

An interesting approach was developed by a group at the University of Newcastle who used an intramolecular hydrogen bond to hold the carboxamide in the active conformation in their series of benzimidazole-4-carboxamides[111] and benzoxazole-4-carboxamides.[109]

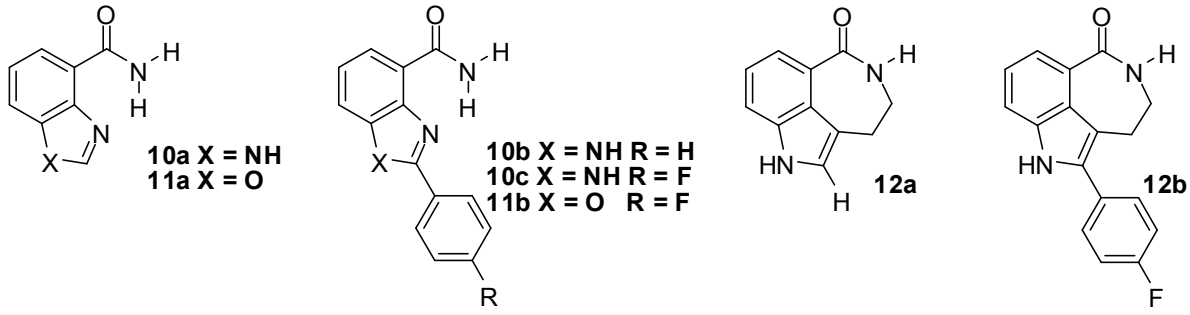

Figure 12. Structures of some benzimidazole-4-carboxamides, benzoxazole-4-carboxamides and tricyclic PARP inhibitors.

This strategy proved successful and the compounds generally had potencies far superior to similar molecules lacking the hydrogen bond. The compounds were tested in a cell-based assay and the most potent examples were found to be the 2-phenyl compounds. In general the benzimidazoles e.g. **10b** (EC_{50} = 990 nM) performed better than the corresponding benzoxazoles e.g. **11b** (EC_{50} = 2100 nM). Particulary potent in their assay system was the 4-fluorophenyl derivative **10c** (EC_{50} = 60 nM). Several groups have trapped the amide bond in the required confirmation by means of a covalent bond, in a tricyclic system.[112, 113] Again, in general, the 2-phenyl-substituted compounds showed increased potency; for example, Agouron found that whilst the parent compound **12a** had a K_i of 38 nM, the 4-fluorophenyl derivative **12b** was several times more potent with a k_i of 4 nM. Substitution at other positions of the molecule such as the lactam ring in general did not lead to increased potency in this series.

1.12.4 Quinazolinones and phthalazin-1-ones

Banasik[104] reported that quinazolin-4-one **13a** had IC_{50} = 9.5 μM but sustitution at the 2-position increased potency, for example **13b** and **13c** have IC_{50} values of *ca.* 200 nM.[113] 8-substituted analogues have also been investigated and hydroxy or methyl groups are better than a methoxy group at this position.

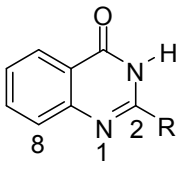

13a R = H
13b R = Me
13c R = Ph

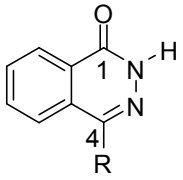

14a R = H
14b R = Bn

Figure 13. Some simple quinazolin-1-ones and phthalazin-1-ones.

Phthalazin-1-one **14a** was also reported as an inhibitor by Banasik.[104] Its IC_{50} was moderate and it was not until Kudos Pharmaceuticals began substituting in the 4-position of this heterocycle that potency began to improve significantly. The simple 4-benzylphthalazin-1-one **14b** had IC_{50} = 770 nM in their assay but, when the benzene ring was *meta*-substituted, potency increased and the N-phenylpropionamide **14c** was particularly potent (IC_{50} = 20 nM) but was not a suitable drug candidate, owing to concerns over pharmacokinetics.[114] PF_{50} was used as a measure of cellular potency and this potentiation factor was calculated as the ratio of the IC_{50} growth curve of HeLa B cells treated with MMS divided by the IC_{50} of the growth curve of cells treated with both MMS and PARP inhibitor. In the cell based assays, test compounds were used at a fixed concentration of 200 nM. In order to increase metabolic stability, the group modified the anilide group to a lactam ring in **14d** (IC_{50} = 120 nM) but this also resulted in a drop in potency. This drop was reversed by the introduction of a second carbonyl group to the lactam in **14e** (IC_{50} = 13 nM) but cellular potency was poor (PF_{50} = 1.94). Both PARP-1 inhibitory potency and cellular potency were increased by the introduction of a fluorine atom in the para position of the benzyl moiety in **14f** (IC_{50} = 5 nM, PF_{50} = 5.62). Interestingly, **14f** was also tested against other PARP isoforms and showed a similar level of activity against PARP-1 but was *ca.* 100-fold less potent against PARPs -4 and -5.

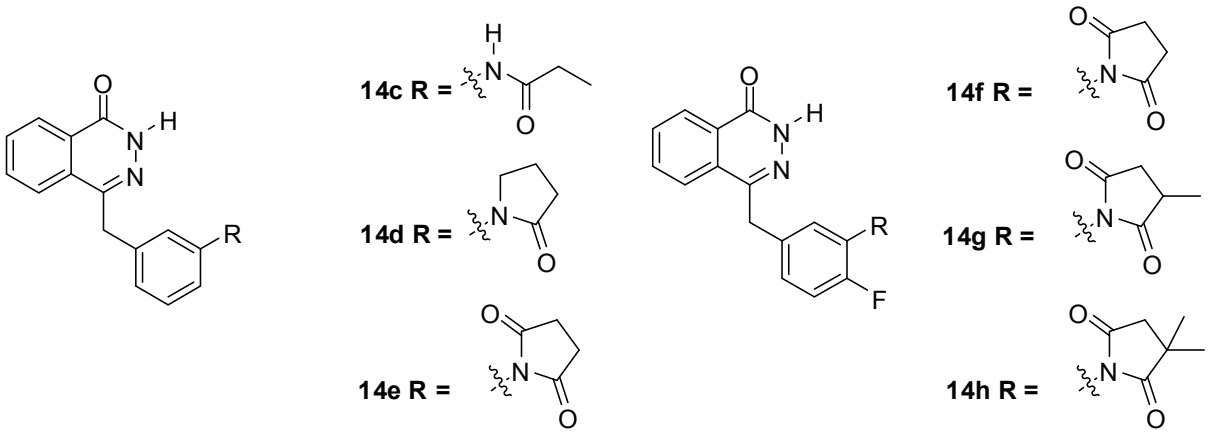

Figure 14. A selection of phthalazin-1-ones developed by Kudos Pharmaceuticals.

Indeed the introduction of a *p*-fluoro substituent seemed to generally increase general potency in the 4-benzyl series. A further increase in cellular activity was noted with **14g** (IC_{50} = 3.8 nM, PF_{50} = 18.2) in which a methyl group was introduced α to the imide carbonyl. It was proposed that this increase was possibly due to enhanced cellular penetration due to increasing lipophilicity but when a geminal dimethyl functionality was introduced in **14h** (IC_{50} = 9.8, PF_{50} = 2.9) a drop in cellular potency was noted.

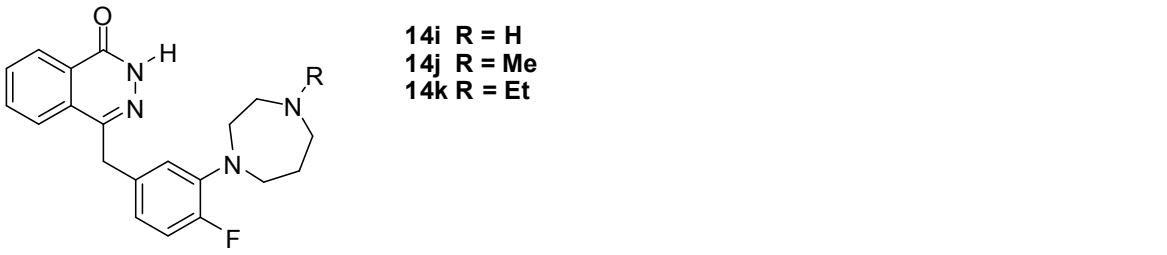

Figure 15. The homopiperazine derivatives **14i**, **14j** and **14k**

Other structural modifications at the *m*-position of the benzyl moiety, such as introducing a homopiperazine ring, also gave rise to highly potent PARP-1 inhibitors. For example, the homopiperazines **14i, 14j** and **14k** are single-digit nanomolar inhibitors of the enzyme.[115]

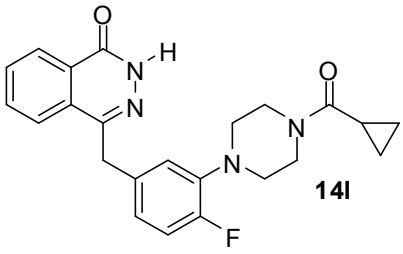

Figure 16. The structure of the clinical candidate **14l** developed by Kudos Pharmaceuticals

However, it was found that the acylpiperazine **14l** was not only a highly potent inhibitor (IC_{50} = 5 nM) but also possessed the best pharmacokinetic profile, was orally active and active *in vivo* in an SW620 colorectal cancer xenograft model. Due to these factors **14l** was selected for clinical development for the treatment of BRCA1- and BRCA2-deficient cancers.[116]

1.12.5 Isoindolines

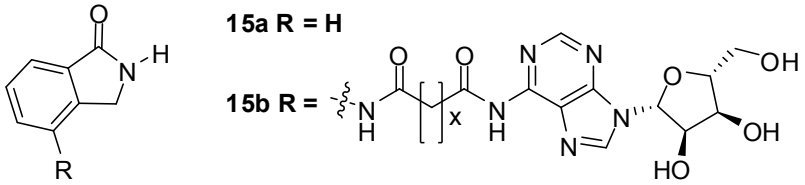

Figure 17. Isoindoline PARP inhibitors.

The unsubstituted isoindoline **15a** is a relatively poor inhibitor of PARP-1, as are the simple 5-substituted analogues (EC_{50} > 10 μM) in a cell-protection assay. However, more complex substitution at the 5-position, for example an adenosine group attached *via* an alkyl chain **15b**, significantly improves potency. It should be noted that many classes of inhibitor are not potent in this type of assay, due to poor uptake across the cell membrane and not necessarily poor inibition of PARP.

1.12.6 Dihydroisoquinolinones and Isoquinolinones

This research centres on the isoquinolinones and structure-activity relationships (SAR) will be discussed in more detail below but a brief introduction is given here. Following the initial report of isoquinolin-1-one as an inhibitor of PARP (IC_{50} = 6.2 μM) by Banasik,[104] Suto[110] investigated the SAR of various 5-substituted analogues. Elaboration at this position proved successful, with the 5-hydroxy analogues proving to be most potent with IC_{50}s of 140 nM and 100 nM for the 3,4-unsaturated **17** and 3,4-saturated **18** compounds, respectively.

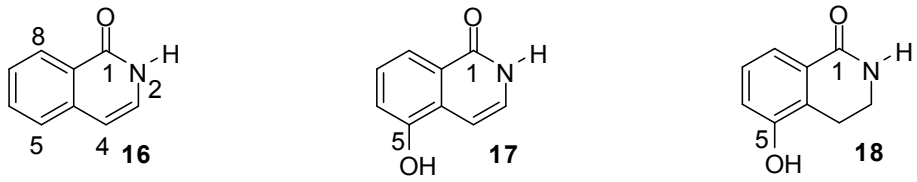

Figure 18. Structures of the isoquinolin-1-one PARP inhibitors **16**, **17** and **18.**

Suto[110] also reported 5-AIQ **5** as a PARP inhibitor for the first time with an IC_{50} of 260 nM. This was notable as, upon conversion to its HCl salt, the compound became highly water-soluble. Although Suto did not investigate the compound further, the fact that he had synthesised a water-soluble PARP inhibitor was highly significant as the *in vivo* potency of the compound would be greatly increased by this modification (see above for comparisons with lipophillic PARP inhibitors in *in vivo* models of disease). It us unsurprising that the vast majority of inhibitors up to this point were not water-soluble as the required planar benzamide pharmacophore is also a molecular signature for lipophilicity. The huge promise shown by 5-AIQ and the lack of 3- and 4-substituted analogues in the literature led us to select it as our lead compound for this research (see below).

A summary of the structure-activity relationships deduced thus far is presented in Figure 19.

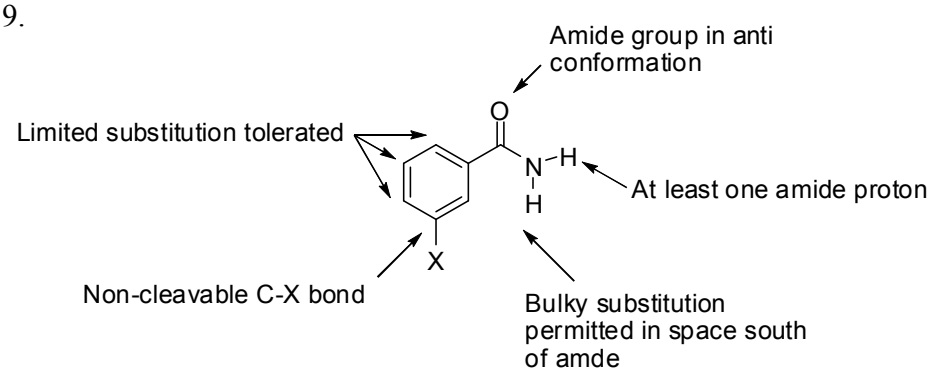

Figure 19. PARP inhibitor SAR to date.

1.12.7 Clinical trial development of PARP inhibitors

Recently, a group at Abbott Laboratories[117] have has identified a series of substituted pyrazolo[1,5-*a*]quinazolin-5(4H)-ones as potent inhibitors of PARP-1, with their lead pre-clinical candidate **19** showing excellent enzymatic and cellular potency and cross-species oral bioavailability. The PARP inhibitor AG-014699[118] **12c** has recently completed a Phase 2 clinical trial in combination with temozolomide in patients with metastatic malignant melanoma; of the 40 evaluable patients, seven partial responses were seen. The compound developed by Kudos Pharmaceuticals **14l** KU-0059436/AZD2281 was shown to selectively inhibit BRCA1-[119] and BRCA2-deficient[120] mammary cell growth, in combination with platinum drugs and as stand alone therapy.[116] The compound has entered Phase 2 clinical trials as monotherapy in BRCA-deficient ovarian or breast cancer patients and in combination with a variety of cytotoxic drugs for a range of tumours.

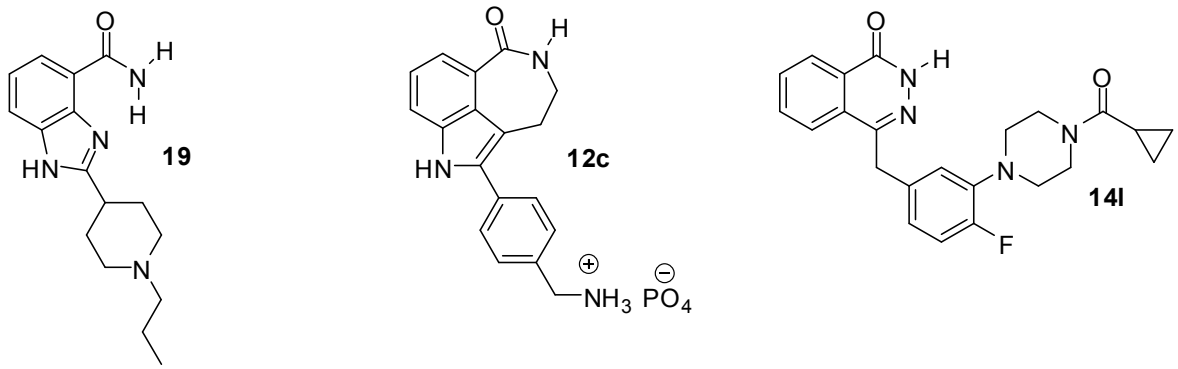

Figure 20. Structures of the PARP inhibitors **19** and **12c** and **14l**.

1.12.8 PARP-2 inhibitors reported in the literature

There are very few selective PARP-1 or PARP-2 inhibitors reported in the literature at present. Perkins *et al.*[121] developed an assay for PARPs 1 and 2, based on the observation that heterologous expression of either isoform in cells of the yeast *Saccharomyces cerevisiae* resulted in growth inhibition; therefore, the endpoint of the assay was reversal of this inhibition. The authors used this assay to identify the compounds ICX56290675 **20** and ICX56258231 **21** with eight-fold selectivity for PARP-1 and three-fold selectivity for PARP-2 respectively (note that **21** is possibly a hydrolytically activated prodrug for the corresponding phthalazinone **14b**). Iwashita *et al.*[122] discovered an inhibitor FR261529 **22** with five-fold selectivity for PARP-2 over PARP-1; these discoveries were made through random screening of compound libraries or by chance in the search for PARP-1 inhibitors rather than by rational drug design.

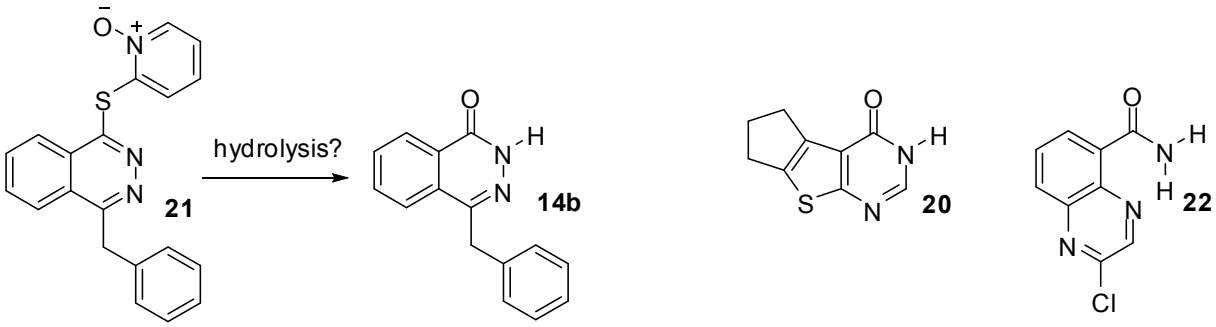

Scheme 2. Structures of selective PARP-1 and PARP-2 inhibitors discovered by random screening.

In 2004, the crystal structure of the catalytic fragment of murine PARP-2 was solved[123] at 2.8 Å resolution, seven years after the data for the chicken PARP-1 catalytic fragment were made available.[13] The high degree of homology of the PARP catalytic domain between different species means PARP inhibitors are unlikely to show a wide species-difference in their inhibitory activity between chicken, mouse and human PARPs, although any differences in important residues must be noted.

The key residues involved in PARP-1 inhibitor binding were deduced by Ruf *et al.*[124] who studied the co-crystals of PARP-1 chicken catalytic fragment with the inhibitors **20**, 4ANI **23**, 3MBA **1c** and NU1025 **13d** bound. The authors identified hydrogen bonding between Gly863-NH, Gly863-O, and Ser904-OH and the lactam or amide group of the bound inhibitors; additionally, hydrophobic interactions were identified between PD128763 and Tyr907. The two key hydrogen-bonding residues in chicken PARP-1 are conserved in both human and mouse PARP-2 (Gly405 and Ser446) as is the tyrosine residue (Tyr449).

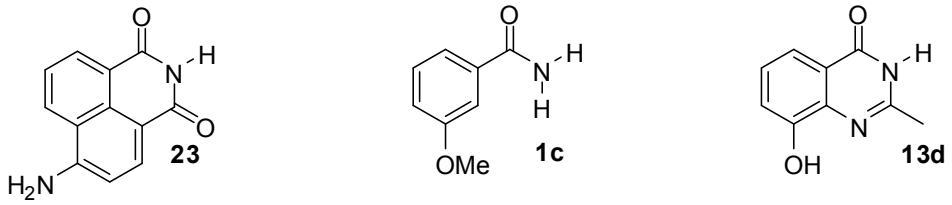

Figure 21. Structures of the PARP inhibitors **23**, **1c** and **13d**.

Ishida *et al.*[125] attempted to rationalise the selectivity of the quinazolinone **13e** for PARP-1 (10-fold over PARP-2) and **22** for PARP-2 (5-fold over PARP-1 see above) by a combination of X-ray structural study *via* PARP-1 co-crystals and homology modelling using murine PARP-2 as a template.

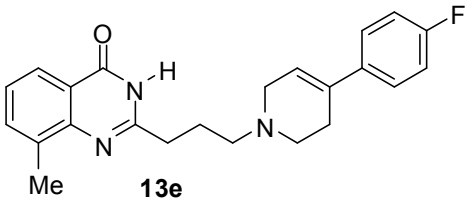

13e

Figure 22. The PARP-1 selective quinazolinone **13e**

The expected three hydrogen bonds between the lactam/carboxamide function of the inhibitors and Gly863/Ser904 in PARP-1 and Gly405/Ser446 in PARP-2 were seen. Additionally, a π-π interaction between the heterocyclic aromatic core of **13e** and Tyr907/Tyr869 in PARP-1 and Tyr449/438 in PARP-2 was observed. The 4-phenyltetra-hydropyridine moiety of **13e** lay in a hydrophobic pocket lined by the residues Leu769, Ile879 and Pro881 in PARP-1. In PARP-2, Leu769 is replaced by Gly314 and this single amino-acid difference resulted in a loss of hydrophobicity in the pocket and, hence, a loss of potency of **13e** against PARP-2.

The non-hydrogen-bonded nitrogen of the quinoxaline ring in **22** formed favourable contacts with the carboxylate of Glu988 in PARP-1; this residue is conserved in PARP-2 (Glu534), suggesting that the binding mode was also conserved. The authors speculated that the replacement of Asp766 and Glu763 in human PARP-1 with Glu311 and Gln308 in human PARP-2 resulted in more favourable interactions with the chlorophenyl moiety of **22** and therefore the observed increase in potency.

The small changes in the amino-acid sequence between the murine PARP-2 catalytic fragment and the chicken PARP-1 active site make the design of selective inhibitors feasible as the above authors have suggested. On initial inspection of the two structures

two key differences can be noted, firstly the hydrophobic binding pocket is larger in PARP-2 (and maybe lacking hydrophobicity around Gly314 – see above) suggesting that more three dimensional bulk will be tolerated in this area. The second key difference is the replacement of the neutral polar Gln308 in chicken PARP-1 with the basic Lys308 in murine PARP-2, which could be exploited by building an acidic function to an inhibitor which would sit close in space to the residue in the PARP-2 active site.

2. Research aims and objectives

The functions of PARP-2 remain unclear, although tools such as knockout mice and antisense RNA offer some clues. Additionally, the effects of PARP-2 (and PARP-1) are mediated *via* two mechanisms, the catalytic activity of the enzyme and also through protein-protein interactions. As PARP-2-knockout mice would never express the protein, both mechanisms are knocked out, whereas, with a pharmacological inhibitor, only the enzymatic activity would be lost.

There is currently a major need for potent and selective inhibitors of PARP-2 to study the function of the enzyme and the effect of inhibiting catalytic activity alone. The inhibitors discovered thus far have been found by random screening of PARP-1 inhibitor libraries and the current selectivity is modest; by using rational drug design significant improvements should be possible in terms of potency and selectivity.

5-AIQ is a potent inhibitor of PARP-1 with excellent *in vivo* activity in animal models of disease and will serve as a template for our designed inhibitors.

The major aim of this research is to develop isoform-selective inhibitors of PARP-2. In order to exploit the differences between the catalytic sites of PARP-1 and PARP-2, a bulky aromatic substituent will be introduced at the 3- or 4-position of the 5-AIQ to fit into the larger hydrophobic pocket in PARP-2. Therefore sets of 3- and 4-substituted 5-AIQs will be prepared.

An acidic function will be introduced at the 5-position of the molecule; this will be either tethered to the exocyclic 5-amine of 5-AIQ through CH_2 units or directly attached at the 5-position of isoquinolin-1-one. Other synthetic modifications at the 5-position will be considered, if appropriate.

All synthesised inhibitors will be evaluated for PARP-1 and PARP-2 inhibitory activity by KuDOS Pharmaceuticals and IC_{50} values will be generated where possible.

The key objective of the work is to design and synthesise inihibitors of PARP-2 with a higher degree of isoform-selectivity than any published compound. Obtaining samples of literature compounds and assessing them in our assays will measure this.

3. Results and Discussion

3.1 Molecular modelling

Using the crystal structures of PARP-1 (PDB code 4PAX, chicken PARP I with NU1025 **13d** (inhibitor, Ruf *et al.*[124]) and PARP-2 (PDB code 1GSO, murine PARP-2, Oliver *et al.*[123]) as starting structures, the binding pocket was established (by eye) and compared. This was achieved by uploading the relevant PDB files in UCSF Chimera (Version 1) and locating the known key substrate-binding residues in the active sites of the two isoforms.

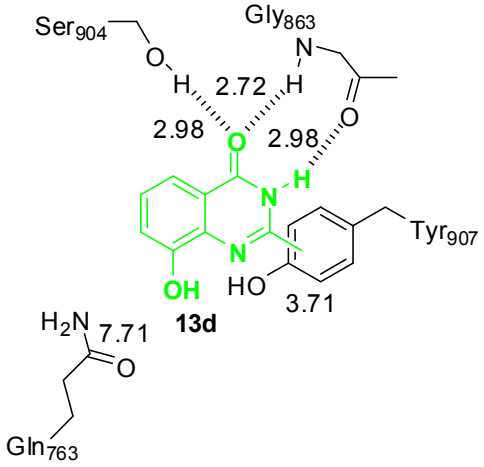

Figure 23. Observed interactions and distances between **13d** and the PARP-1 active site; all distances are in Ångstroms.

Initial studies with PARP-1 involved measuring and mapping the binding pocket, together with key interactions between the bound NU1025 **13d** inhibitor and the pocket. Comparisons were also made to PARP-1 without an inhibitor present by uploading the PDB file 2PAW (corresponding to the catalytic fragment of chicken PARP-1 with no inhibitor bound) into UCSF Chimera. This was to establish and confirm previous observations that the receptor binding pocket is relatively rigid and does not change conformation upon binding the substrate or an inhibitor ligand. The observed significant

interactions and distances in the PARP-1 model are shown in Figure 23, these distances would be used when docking 5-AIQ into PARP-2. Comparison of the binding pocket with and without a bound inhibitor showed little significant difference.

The distances observed in the PARP-1 study (Figure 23) were then used to dock a minimised and charged (Gastieger + Hückel) 5-AIQ into the binding pocket of PARP-2. This was achieved by transferring the protein structures from UCSF Chimera into Hyperchem (Version 7.5). Once docked (by eye), the structure was transferred back into UCSF Chimera and restraints were added (as observed in the PARP-1 model) and the ligand was subjected to molecular dynamics (300 K for 5 ps, the last 1 ps was then averaged) and then re-minimised. The binding pocket and ligand (5.0 Å from ligand) were then subjected to molecular dynamics (300 K for 5 ps, the last 1 ps was then averaged) and the complete complex (enzyme and 5-AIQ) was minimised to give the final model.

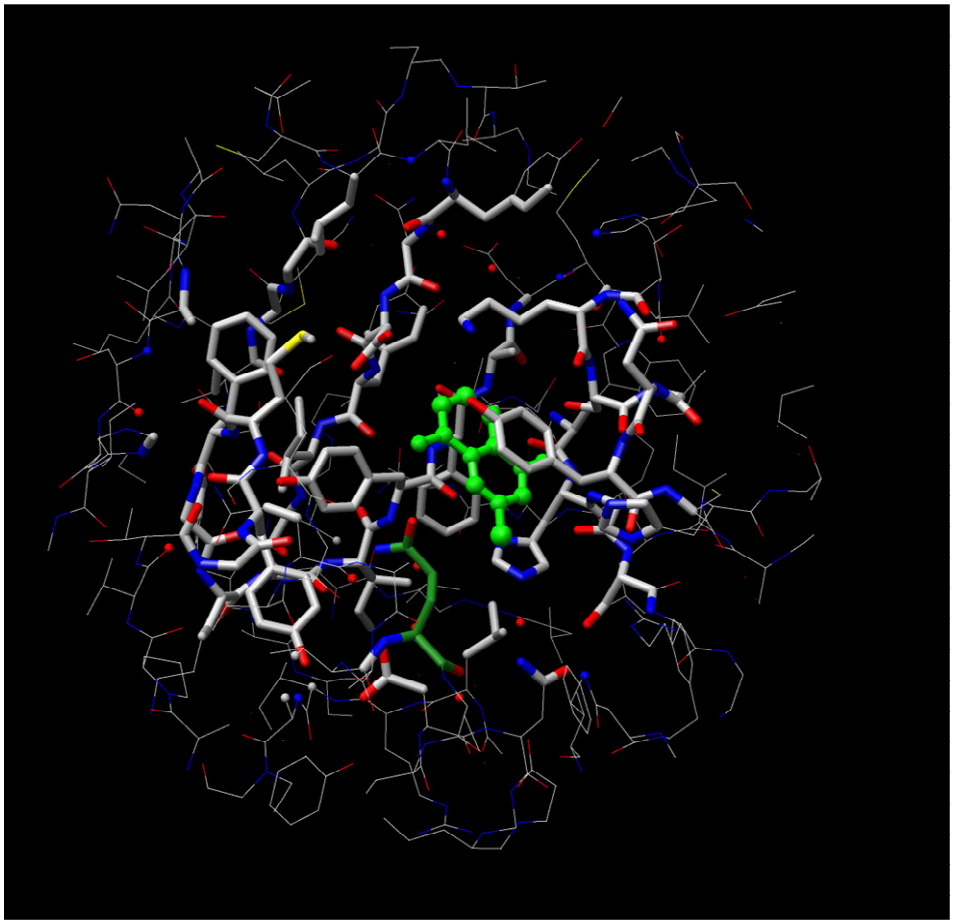

Figure 24. Model of the catalytic fragment of PARP-2 with **13d** docked and Lys308 shown in green.

In this model, Lys308 sat relatively close in space (3.08 Å) to the 5-amino function in 5-AIQ. The side chain of this residue was mobile but a stronger interaction between the acidic function and the lysine occurs when the two groups are close in space. Therefore, our CH_2 tether was short (1-2 units from the amine or 1-3 units if attached directly to the carbocyclic ring).

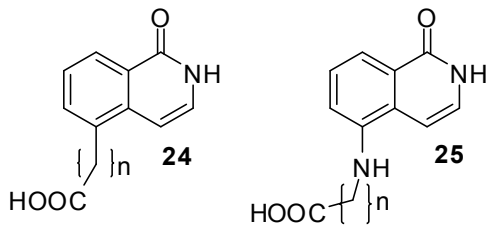

Figure 25. Structures of isoquinolin-1-ones with carboxylic acids tethered to the 5-position. a) n = 1-2; b) n = 1-3.

It was observed that the hydrophobic pocket in PARP-2 had a larger volume than the corresponding space in PARP-1, in our model. The pocket lies south of the 3- and 4-positions in the docked 5-AIQ core and this difference will be exploited by functionalising these positions with bulky substituents.

3.2 PARP-1 Assay

There are numerous PARP-1 assays reported in the literature and many of them rely on the use of radiolabelled substrate, either ^{3}H- or ^{32}P-labelled NAD^{+}.[126] The assay developed by Purnell and Whish[106] used nuclei isolated from the thymus of a freshly slaughtered pig, rather than pure enzyme. The authors calculated percentage inhibition of PARP activity by measuring the amount of [^{3}H]adenosine-NAD^{+} incorporated into an acid-insoluble fraction, following initiation of the PARP reaction, when no inhibitor was present. This was then compared with the value when an inhibitor was present.

The assay reported by Cheung and Zhang[127] involves the use of biotinylated NAD^{+} in addition to ^{3}H-NAD^{+}. The PAR polymers produced bind to avidin-SPA beads also present in the reaction mixture, resulting in excitation of the scintillant and amplification of the signal. The signal produced from the free [^{3}H]adenosine-NAD^{+} dissipates in aqueous solution, therefore the free ligands and complexes do not need to be separated, which greatly increases throughput.

An alternative ELISA-based assay was developed by Decker *et al.*[127] PARP activity is measured using UV absorption and no radioisotopes are required. The assay is highly sensitive but the frequent washing steps required in ELISA assays decreases throughput and renders them prone to operator error.

Another assay bypassing the use of radioisotopes has been reported by Trevigen Inc. and is commercially available. The assay uses biotinylated NAD^+ in wells coated with histone acceptor proteins. The extent of incorporation of biotin into the PAR polymers and, therefore, activity of the enzyme is measured using a conjugated streptavidin detection system which gives a colorimetric readout. A similar minaturised assay, based on the same principles, has been developed by Lee *et al*.[128]

KuDOS Pharmaceuticals Ltd. kindly agreed to screen the compounds for PARP-1 activity though an established collaboration. This company has developed a FlashPlate scintillation proximity assay[129] for the high-throughput screening of compound libraries. The principles of the assay briefly follow. PARP-1 is purified from HeLa nuclear extracts in-house and 96-well FlashPlates (NEN) are coated with scintillant. After the incubation of the inhibitor with PARP-1, the reagents (NAD^+, ^3H-NAD^+ and DNA) are added to the wells to initiate the PARP-catalysed reaction. Column 11 is a positive control which does not contain test compound and column 12 is a negative control lacking DNA. As a result of the PARP reaction, PARP-1 will automodify itself and the resulting structures will contain ^3H-labelled adenine. Following termination of the reaction (cold AcOH), the PARP-1-^3H-ADP-ribose complexes will come into close proximity with the FlashPlate walls which leads to signal amplification. Unreacted ^3H-NAD^+ will remain free in solution and therefore less likely to come close enough to the well walls to be amplified. The assay plates are read on a TopCount scintillation counter.

In order to obtain IC_{50} values, eight different concentrations of inhibitor were used in a range surrounding the expected value. The recorded counts for TopCount are then transferred to the program ActivityBase which calculates the mean positive and negative

counts per minute (cpm) from columns 11 and 12. The percentage inhibition is calculated using the following equation:

$$\% \text{ Inhibition} = 100 - [(\text{cpm of well} - \text{mean -ve cpm}) / (\text{mean +ve cpm} - \text{mean –ve cpm}) \times 100]$$

Percentage inhibition can then be plotted against enzyme concentration and the IC_{50} of the inhibitor can be calculated.

3.3 PARP-2 Assay

To date, there are very few assays of PARP-2 activity reported in the literature. Perkins *et al.*[121] developed a novel cell based screen in yeast. The assay relies on the fact that PARP-2 enzymatic activity causes growth inhibition in the organism; therefore reversal of this effect is a measure of PARP-2 inhibitory activity.

KuDOS Pharmaceuticals Ltd. evaluated the compounds for inhibition of PARP-2 catalytic using their ELISA based assay, developed in-house. The principles of the assay are as follows. 96-Well plates (Fisher Scientific) are coated with rabbit anti-PARP-2 polyclonal antibody (Abcam Nunc-Immuno MaxiSorp) to which murine PARP-2 (Alexis Biochemicals) is bound. Column 11 of the plates is a positive control containing no test inhibitor and column 12 is a negative control containing no PARP-2 protein. Following incubation with test inhibitors, the plates are washed and scintillation fluid is added; they can then be read on a TopCount scintillation counter.

The mean counts per minute (cpm) for all wells can then be obtained using the program ActivityBase. From these values, percentage inhibition can be calculated using the following equation:

$$\% \text{ Inhibition} = 100 - [(\text{cpm of well} - \text{mean -ve cpm}) / (\text{mean +ve cpm} - \text{mean –ve cpm}) \times 100]$$

Percentage inhibition can then be plotted against enzyme concentration and the IC_{50} of the inhibitor can be calculated.

3.4 5-Substituted Isoquinolinones

The initial synthetic targets were the secondary amines with the general structure **25** which could be feasibly synthesised from 5-AIQ and suitable two- or three-carbon electrophiles carrying a (masked) ω-carboxylic acid. It was envisaged that alkylations at the nucleophilic amino group would proceed smoothly and this was the case when a weak base was used in combination with ethylbromoacetate.

3.4.1 Synthesis of 5-AIQ

Three different routes to 5-AIQ have been reported in the literature. Wenkert *at al.*[130] first reported the synthesis of 5-AIQ in 1964. This route starts from the complete isoquinoline core already carrying a nitrogen substituent at the 5- position and is simply a series of adjustments of the oxidation levels. Commercially available **50** was N-oxidised to **51** in good yield. Polonowski rearrangement of this N-oxide with acetic anhydride generated **38** which was subsequently reduced to the target 5-AIQ **5**.

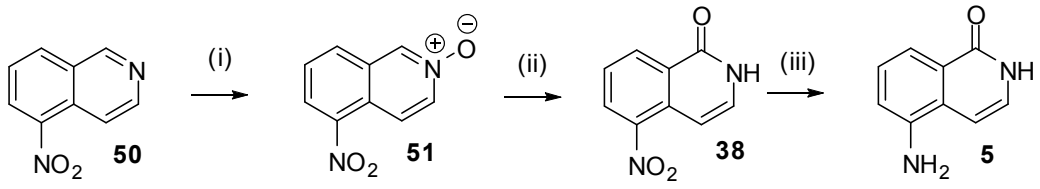

Scheme 3. Reported synthesis of 5-AIQ *via* Polonowski rearrangement of **51**. (i) AcOH, H_2O_2; (ii) Ac_2O, heat; (iii) Pd/C, H_2.

In our laboratory, the rearrangement step has been found to be low yielding and unreliable[131] and this led us to examine other routes.

An alternative novel synthesis was recently developed by Woon *et al.*[132] In this route, the 3-carbon and the ring-nitrogen are introduced as nucleophilic cyanide. Radical bromination of the Ar-Me group of the ester **52** led to the mono-brominated product **53**. Nucleophilic displacement of bromide with cyanide gave the nitrile **54**. Interestingly, this step could only be achieved with the expensive tetraethylammonium cyanide but not with simple alkali metal cyanides, even in the presence of phase-transfer catalysts. Selective reduction of **54** with DIBAL-H at -78°C furnished the imine, which cyclised *in situ* to the key intermediate **38**. This was again converted to 5-AIQ by reduction of the nitro group. Unfortunately the yields of the displacement and reductive cyclisation steps were low, resulting in a poor overall yield of only 8%.

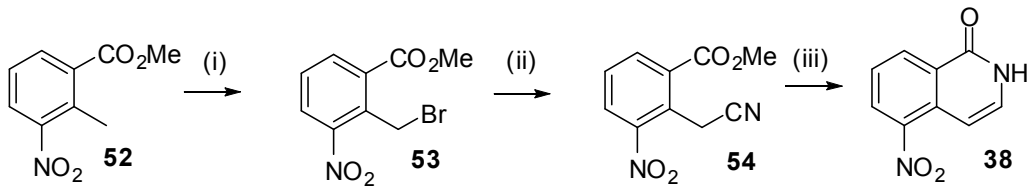

Scheme 4. Synthesis of 5-nitroisoquinolin-1-one *via* radical bromination of **52**. (i) Br_2, $(PhCO_2)_2$, CCl_4, hv, reflux; (ii) Et_4NCN, MeCN; (iii) DIBAL-H.

The final route reported[55] also involved introduction of the 3-carbon. This was achieved through formation of the enamine **55** *via* condensation of **52** with dimethylformamide dimethyl acetal (DMFDMA). Immediate passage of the crude reaction mixture of **55** down a silica gel chromatography column provided enough acidity to protonate the basic enamine nitrogen, catalysing the hydrolysis of **55** to an intermediate aldehyde. The enol form of this aldehyde cyclised *in situ*. This cyclisation meant that 5-nitroisocoumarin **56** was both formed and purified in one step.

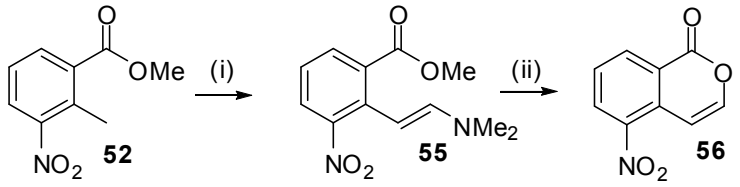

Scheme 5. Synthesis of 5-nitroisocoumarin *via* enamine formation. (i) DMFDMA, DMF, reflux; (ii) SiO_2.

Saturation of a solution of **56** in 2-methoxyethanol with ammonia and boiling under reflux, followed by palladium-catalysed hydrogenation of the nitro group yielded **5** in an overall yield of 17%. Although this yield was not ideal, it was nearly double that of the only other reliable published synthesis (*via* radical bromination of **52**) and could be performed on scales of up to 8 g. This method was therefore chosen to obtain starting material for the synthesis of the initial 5-substituted targets.

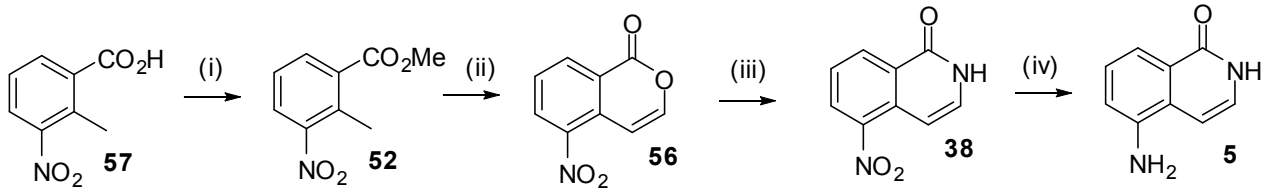

Scheme 6. Preferred route to 5-AIQ. (i) MeOH, H^+, reflux, 84%; (ii) DMFDMA, DMF, reflux, SiO_2, 42%; (iii) NH_3, 2-methoxyethanol, reflux, 71%; (iv) H_2, 10% Pd/C, EtOH, H^+, 66%.

3.4.2 Alkylations of 5-AIQ

The one-carbon CH_2 tether was introduced by alkylating the exocyclic amino-nitrogen of 5-AIQ with ethyl bromoacetate, using N,N-diisopropylethylamine as base. The function of the base was to free the amine from its salt; as a weak base was chosen, lactam proton abstraction would not occur. The yield obtained for this step to form **58** was somewhat disappointing (19%) but, as only a small amount of compound was required for

biological testing, the reaction conditions were not optimised. Hydrolysis with aqueous hydrochloric acid gave the first target **59** as the hydrochloride salt in good yield in a final convenient step. An attempt to grow crystals of **59**, in order to confirm its structure by X-ray crystallography, resulted in formation of the methyl ester due to the use of methanol as the recrystallisation solvent (discussed in a later section).

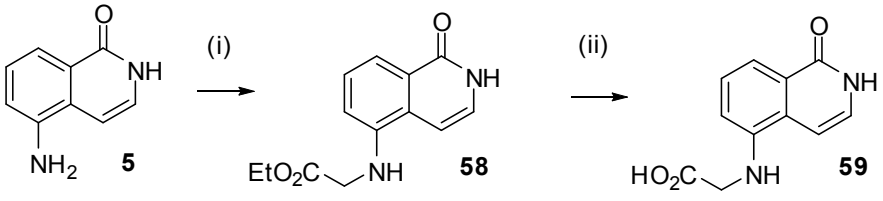

Scheme 7. Synthesis of **59** *via* an alkylation of 5-AIQ. (i) diisopropylethylamine, ethyl bromoacetate, 19%; (ii) aq. HCl, 87%.

In order to attach a two-carbon tether, it was assumed the amino group of 5-AIQ would act as a Michael donor when reacted with the Michael acceptor, methyl propenoate. Sodium hydride was used to catalyse the reaction and, upon initial inspection of the NMR spectrum of **60**, it was assumed the desired ester **61** had been formed in 67% yield. Some doubt was cast upon this assumption by the chemical shift of the protons adjacent to the amine nitrogen, at 4.09ppm. This value appears somewhat downfield for -CH_2NAr protons and would be more appropriate for protons adjacent to a lactam. It was feasible that the strong base, sodium hydride had removed the lactam proton in addition to forming the free amine at the 5-position. The resultant anion would be more nucleophilic than the aromatic amino group and, therefore, more likely to react with methyl propenoate forming methyl 3-(5-amino-1-oxoisoquinolin-2(1H)-yl)propanoate **60** rather than the expected ester **61**. Upon acid-hydrolysis, the resultant carboxylic acid **62** was subject to analysis using Heteronuclear Multiple Quantum Correlation (HMQC) and Heteronuclear Multiple Bond Connectivity (HMBC) NMR experiments. HMQC experiments show strong proton-carbon couplings and therefore which protons are directly connected to particular carbons. HMBC experiments inform about weaker proton-carbon couplings and therefore which protons are separated from the carbons in

question by two to three bonds. The partial HMBC spectrum of **62** is shown below, along with assignments (full assignment of **62** can be found in the experimental section). Two key lines of evidence for the proposed structure are strong three-bond HMBC couplings between the 1-C and the $NC\underline{H_2}$ alkyl protons and also between the 3-C and the same protons. If the alkylation had taken place at the 5-amino position, these protons would be five bonds away and highly unlikely to couple strongly to the 1- and 3- carbons.

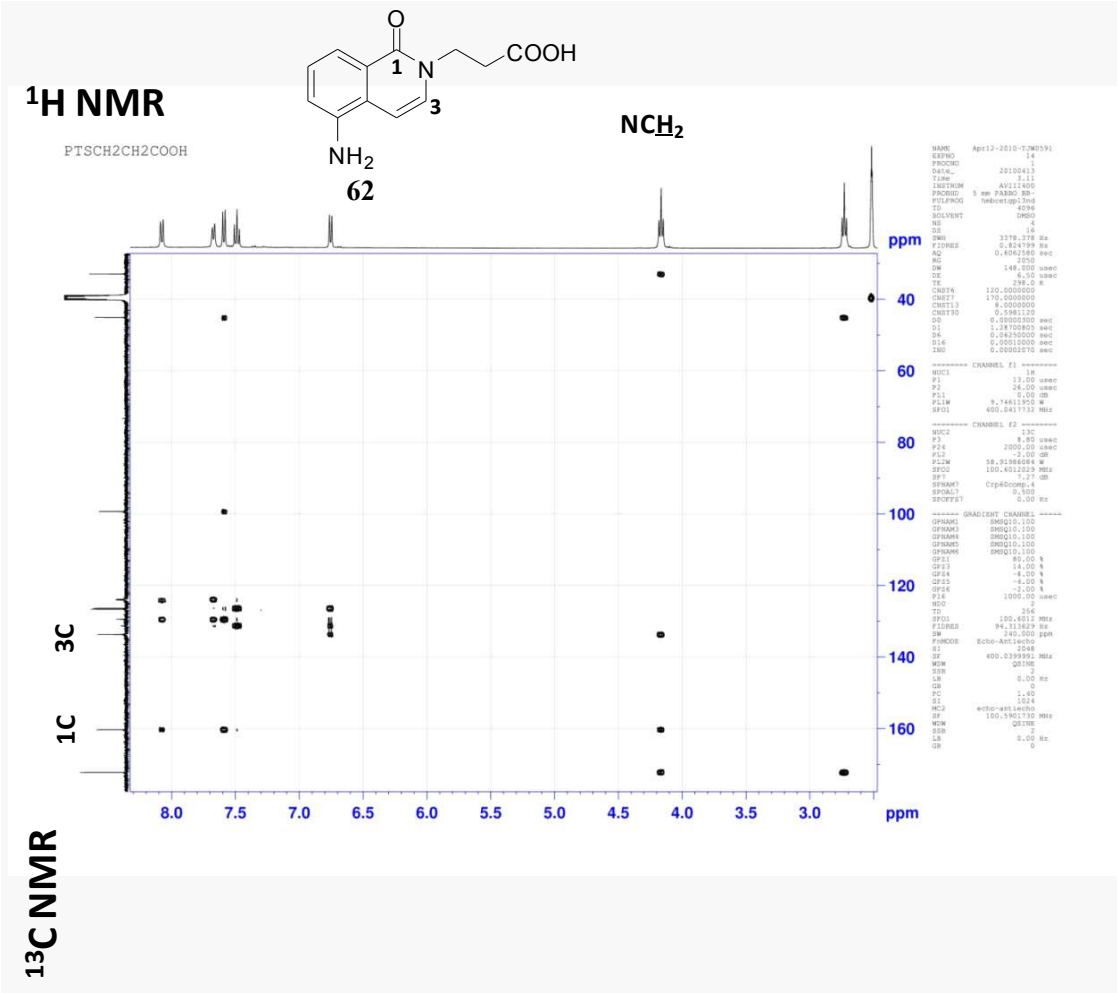

Figure 26. Partial HMBC spectrum of **62**.

Therefore, treatment of 5-AIQ with sodium hydride and methyl propenoate did not give the expected **61**. Instead, the lactam proton was removed and alkylation took place at 2-N yielding **60**.

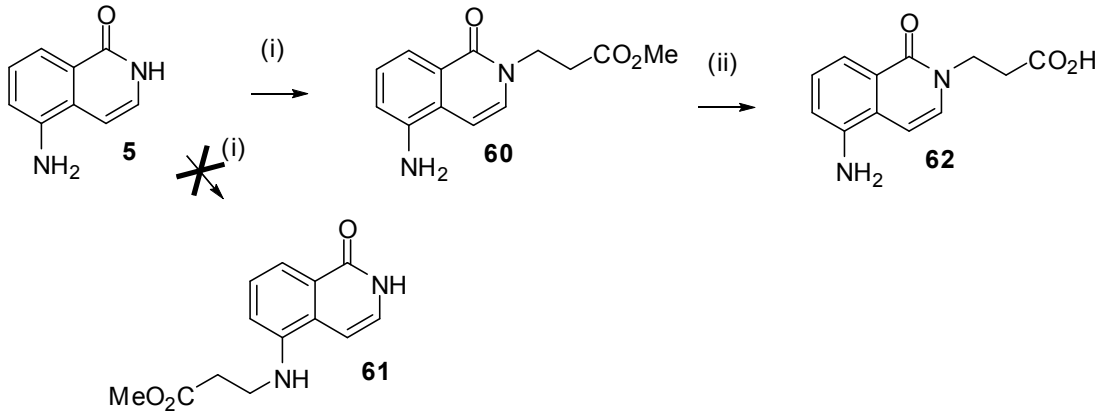

Scheme 8. Attempted synthesis of **60** which gave **61**, hydrolysis yielded **62**. (i) NaH, methyl propenoate 67%; (ii) aq. HCl, 85%.

3.4.3 Synthesis and Heck reaction of 5-iodoisoquinolin-1-one

The next targets were the acids **28**, **63** and **27**, with the carboxylic acid or carbon tether attached directly to the ring.

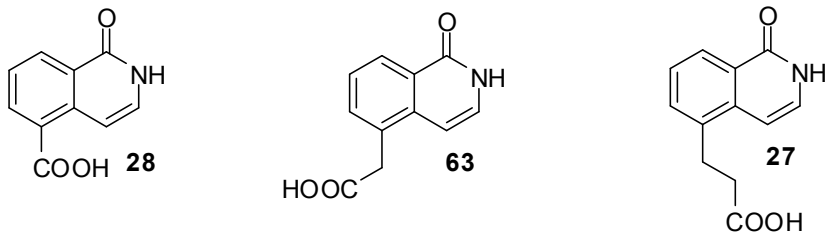

Figure 27. The carboxylic acid targets **28**, **63** and **27**.

To attach a two-carbon tether directly to the aromatic ring, it was planned to use palladium-catalysed chemistry and the Heck reaction of either 5-bromoisoquinolin-1-one **64** or 5-iodoisoquinolin-1-one **65**. Initially discovered in the 1970s, the Heck reaction was independently reported by both Heck[133]and Mizoroki[134] and involves the

palladium(0)-catalysed arylation or alkenylation of alkenes by aryl or alkenyl halides (or *pseudo*-halides) in the presence of base. The mechanism of the Heck reaction is not fully understood but is best represented by a catalytic cycle; the reaction involves four key steps.

- Oxidative addition
- Migratory insertion (carbopalladation)
- β–hydride elimination
- Reductive elimination

Before the Heck reaction could be attempted, the starting aryl halide was required and this was either 5-bromoisoquinolin-1-one **64** or 5-iodoisoquinolin-1-one **65**. Berry *et al.*[135] reported the synthesis of 5-bromoisoquinoline *via* a one-pot Curtius rearrangement of 3-(2-bromophenyl)propenoyl azide and *trans→cis* isomerism and cyclisation of the intermediate isocyanate at high temperature. The starting acyl azide was prepared in two steps from 2-bromoiodobenzene **69**, using an iodine-selective Heck coupling reaction described by Plevyak *et al.*[136] but using propanenitrile rather than acetonitrile as solvent; the higher boiling solvent allowed the avoidance of the use of a sealed tube to perform the reaction at 100°C to form *E*-2'-bromocinnamic acid **70**. This was readily converted to the acyl chloride **71** by reaction with thionyl chloride. The acyl azide **72** was formed by reaction with sodium azide in water. However, the thermal Curtius rearrangement / isomerisation / cyclisation in tetraglyme proved troublesome, with little or none of the desired isoquinolin-1-one **64** formed (by TLC and/or MS analysis). In contrast to Curtius reactions which usually occur at <120°C,[137, 138] *trans→cis* isomerisms require much higher temperatures to take place. The difficulties encountered in this synthesis of **64** were therefore probably due to problems maintaining the very high temperature (260°C) required for the isomerisation / cyclisation step to occur. Similar attempts to cyclise 3-(2-iodoophenyl)propenoyl azide to form 5-iodoisoquinolin-1-one also failed.

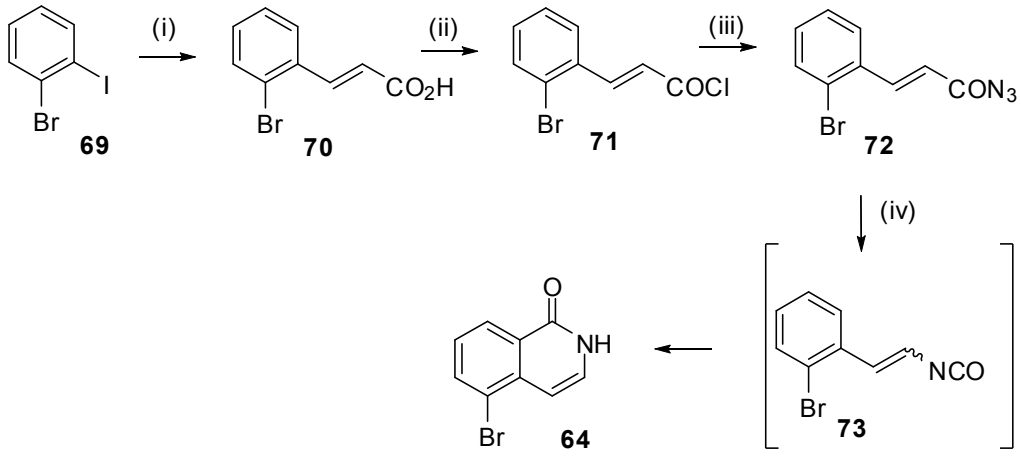

Scheme 9. Attempted synthesis of 5-iodoisoquinolin-1-one *via* Curtius rearrangement of **72**. (i) EtCN, $Pd(OAc)_2$, propenoic acid, Et_3N; (ii) $SOCl_2$; (iii) NaN_3, H_2O; (iv) Heat, $(MeOCH_2CH_2OCH_2CH_2)_2O$.

An alternative approach was therefore investigated. The preferred starting material was the 5-iodo compound **65** as iodine is a better leaving group than bromine therefore aryl iodides tend to perform better in palladium-catalysed couplings. It was envisaged that the 5-iodo function could be introduced *via* diazotisation of the amino group in 5-aminoisocoumarin **74** or 5-aminoisoquinolin-1-one **5**, followed by displacement with iodide ion. The isocoumarin **56** was made as usual and palladium-catalysed reduction of the nitro group furnished the corresponding amine. Close monitoring of this reaction by TLC was essential, as a slower reduction of the 3,4-double bond was also possible under the conditions. The diazotisation step was achieved with sodium nitrite and hydrochloric acid in water and subsequent nucleophilic displacement with potassium iodide (KI) gave 5-iodoisocoumarin **75** in moderate yield. The established procedure (a number of alternatives are reported in the literature but this is by far the most straightforward and efficient) of saturation with ammonia and reflux in 2-methoxyethanol was used to convert **75** to the isoquinolin-1-one **65**.

The method of Watson *et al.*[131] was then employed for the Heck reaction, using propanenitrile as solvent, triethylamine as base and palladium(II) acetate as catalyst or, more accurately, precatalyst. This gave **26** in excellent yield and palladium-catalysed

hydrogenation of the alkene, in methanol, also went smoothly to form the target intermediate 5-iodoisoquinolinone **27**.

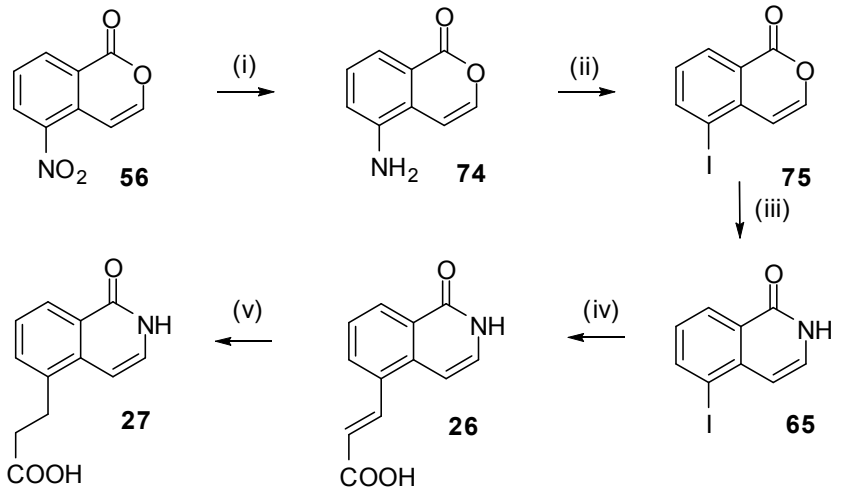

Scheme 10. Synthesis of the targets **27** and **26** *via* Heck reaction of 5-iodoisoquinolin-1-one. (i) Pd/C, H_2, 89%; (ii) $NaNO_2$, HCl, KI, 58%; (iii) NH_3, 2-methoxyethanol, 62%; (iv) Propenoic acid, Et_3N, Pd(II) acetate, 97%; (v) Pd/C, H_2, 66%.

3.4.4 Synthesis of 1-Oxo-1,2-dihydroisoquinoline-5-carboxylic acid

1-Oxo-1,2-dihydroisoquinoline-5-carboxylic acid **28** is a known compound and is accessible by hydrolysis of 5-cyanoisoquinolin-1-one **76**.[131] Compound **76** was originally synthesised in low yield by Wenkert *et al.*[130] by condensation of 2,6-dicyanotoluene **41** with ethyl formate under basic conditions, then acidic workup. When this procedure was followed, a small amount of the isocoumarin **77** was also recovered in low yield.

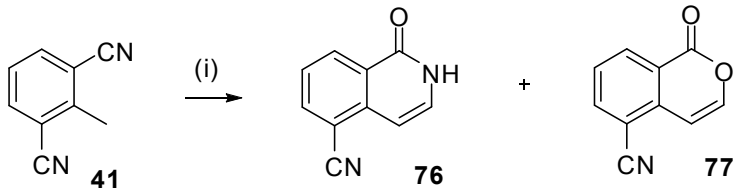

Scheme 11. Synthesis of 1-oxoisoquinoline-5-carboxylic acid **28**. (i) KOBu^t, ethyl formate, **76** 14%, **77** 13%; (ii) KOH, EtOH, 83%.

An alternative synthetic method was developed by Watson *et al.*[131] and this method was also followed. Thus, the enamine **78** was formed, following condensation of 2,6-dicyanotoluene **41** with DMFDMA, as originally reported by Ponticello and Baldwin.[139] Then Pinner-type reaction gave **76** in moderate yield.

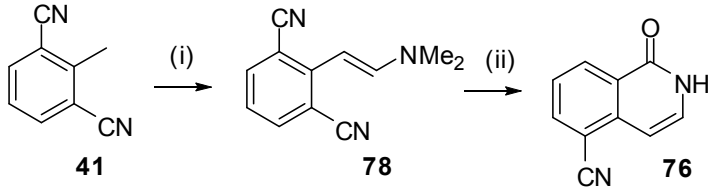

Scheme 12. Synthesis of 5-cyanoisoquinolin-1-one **76** *via* Pinner-type reaction of **41**. (i) DMFDMA, 3 d, 71%; (ii) MeOH, HCl, 55%.

The Pinner reaction[140] involves the treatment of nitriles e.g. **79** with anhydrous hydrochloric acid in the presence of alcohols resulting in a condensation to form imino ether hydrochloride salts **80**. These salts are unstable and there are a number of possible products depending upon the workup conditions, for example treatment with weak base would result in the formation of the imino ether **81** whereas using aqueous acid would furnish the ester **82**.

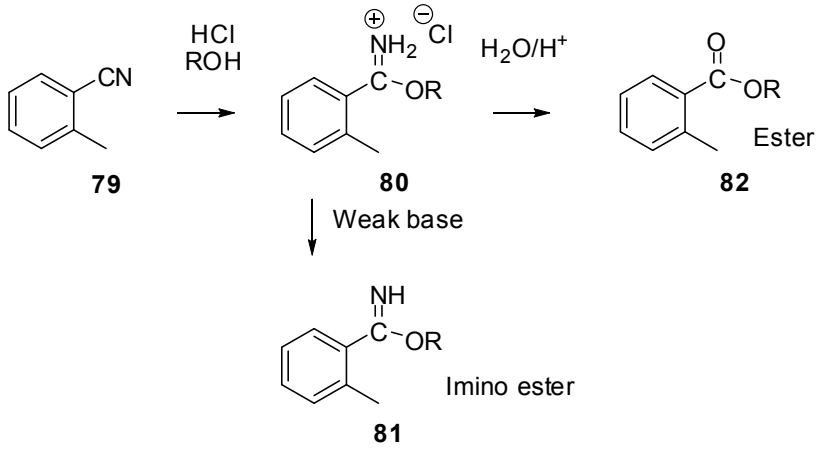

Scheme 13. General outcomes of the Pinner reation .

The planned Pinner-type reaction of the enamine **78** involved treatment of the starting material, in an excess of anhydrous methanol, with dry hydrogen chloride gas followed by aqueous workup. If the reaction was to follow a typical Pinner pathway, the formation of one or two products could be expected, depending on whether one or two of the cyano groups was converted to the methyl ester. If a single cyano group reacted, one would expect the intermediate ester **84** to cyclise to form 5-cyanoisocoumarin **77**. Therfore, conversion of both cyano groups would give the intermediate ester **85** which would lead to the isocoumarin **86**.

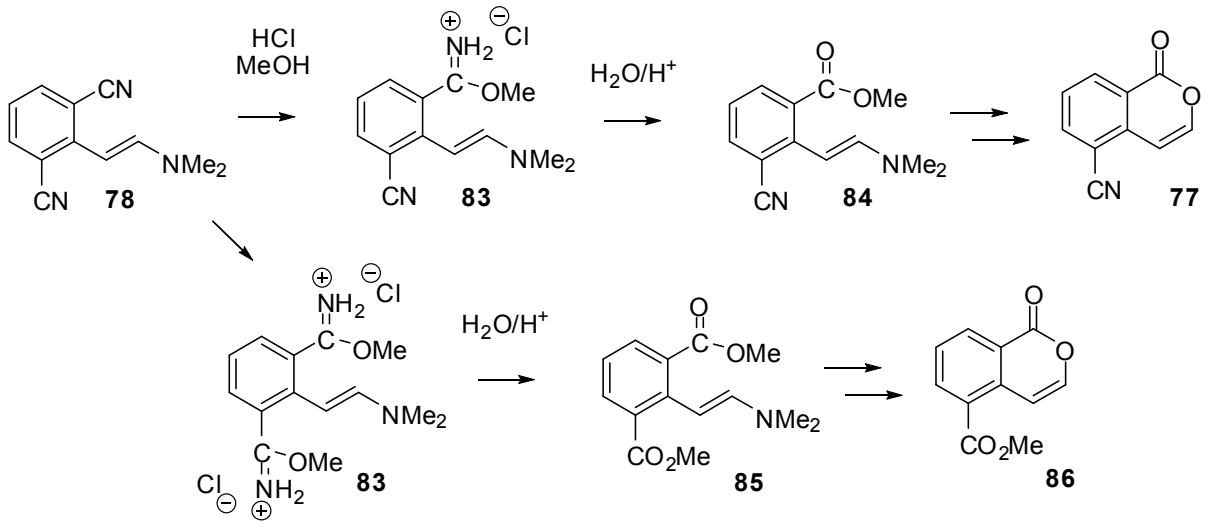

Scheme 14. Expected pathways when **78** is subjected to Pinner conditions.

However, Watson *et al.*[131] reported that the only isolable product from Pinner reaction of **78** was 5-cyanoisoquinolin-1-one **76**. The formation of this product could be rationalised by an intramolecular attack of the nitrogen lone pair of the imino ether on to the dimethyl iminium ion in **87**, which could be formed by protonation and rearrangement of **88.** The loss of dimethylamine from **89** would give **76**. This would take place in anhydrous conditions and therefore before any of the expected methyl esters could form.

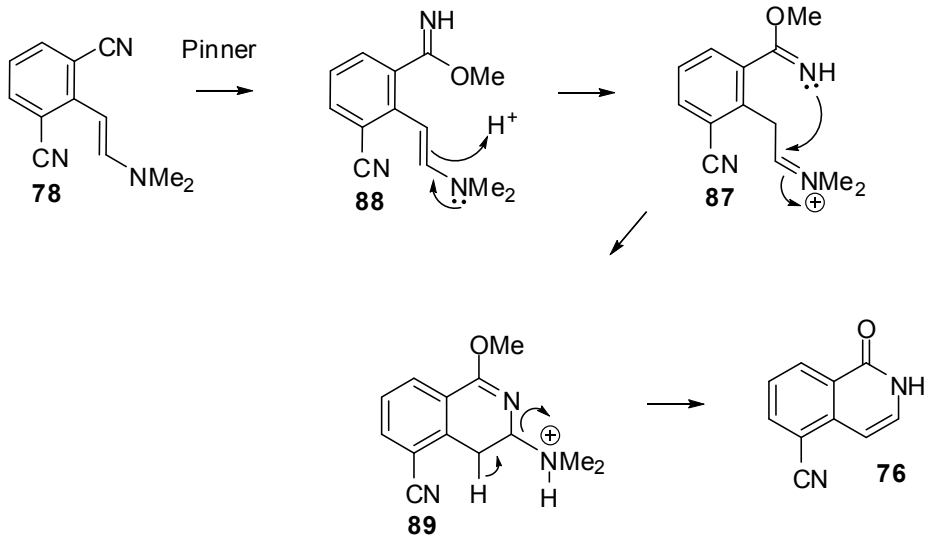

Scheme 15. Proposed mechanism for the formation of **76** from **78**.

The overall yield of this second route was much better than the previous synthesis but a major disadvantage was the prolonged reaction times (>3 d) required to form the enamine. As only a small amount of **28** was needed for biological evaluation, the prolonged reaction times required to form the enamine in the second route were avoided and Wenkert's more expedient but less efficient synthesis was chosen. With **76** in hand, the last remaining step was hydrolysis of the cyano group. The published vigorous base-catalysed hydrolysis gave the target compound **28** in good yield.

3.4.5 Novel synthesis of 5-bromoisoquinolin-1-one 64

Several methods were considered in order to introduce a single CH_2 unit, followed by a carboxylic acid, to the isoquinolin-1-one core. All the approaches relied upon the use of a 5-haloisocoumarin or 5-haloisoquinolin-1-one as starting material. A more efficient route to these compounds was required, as the current multistep approach was low yielding (16% overall yield from the starting 2-methyl-3-nitrobenzioc acid) and time consuming.

Isoquinolin-1-ones could be accessed by hydrolysis of 1-chloroisoquinolines; there are examples of such conversions (or similar) in the literature.[141-143] Therefore, 5-bromo-1-chloroisoquinoline is a simple functional group interconversion (FGI) away from the required 5-bromoisoquinolin-1-one **64** and the aim was to synthesise this precursor. The key step in a short synthesis would be the installation of bromine in the 5-position of the isoquinoline core. Gordon and Pearson[144] reported that isoquinoline could be brominated selectively in the 5-position using a technique they termed the "swamping catalyst method" in which gaseous bromine was added to a mixture of molten aluminium chloride and isoquinoline over a sintered condenser. Some years later, Braye *et al.*[145] used the same technique to brominate the commercially available 1-chloroisoquinoline **90** selectively in the 5-position to give **91** which was exactly the conversion required in the present work. This chemistry was found to be both high yielding (*ca*. 65%) and reproducible, with the added bonus of avoiding column chromatography. As predicted, conversion to 5-bromoisoquinolin-1-one was straightforward and was achieved in a mixture of acetic acid and water at 100°C. This new route to **64** required fewer steps and had a far greater overall yield (46%) than all other previous published syntheses.

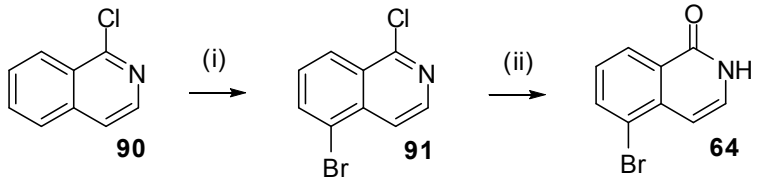

90 **91** **64**

Scheme 16. New, higher-yielding synthesis of 5-bromoisoquinolin-1-one **64**. (i) Br_2, 65%; (ii) $AcOH/H_2O$, 70%.

3.4.6 Attempted synthesis of 2-(1-oxo-1,2-dihydroisoquinolin-5-yl)acetic acid 63

The next step was to attempt direct attachment of a CH_2CO_2Et unit at the 5-position of the isoquinolin-1-one and the first approach was a palladium-catalysed coupling reaction of 5-bromoisoquinolin-1-one **64** and the enolate of ethyl acetoacetate **92** in the presence of base, followed by *in situ* deacetylation.

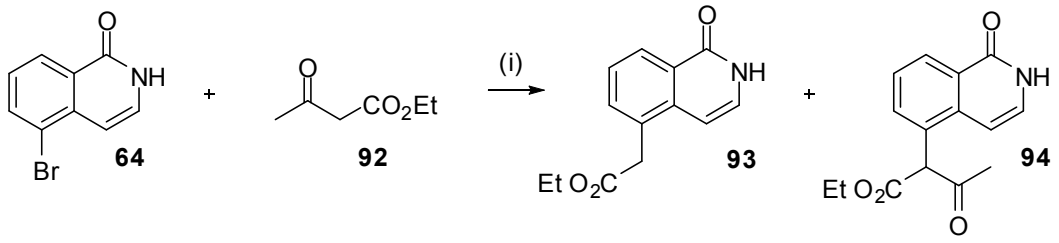

Scheme 17. Attempted synthesis of the ester **93** *via* palladium-catalysed coupling of **64** and ethyl acetoacetate. (i) $Pd(OAc)_2$, P^tBu_3, K_3PO_4, toluene.

Paluki and Buchwald developed this type of chemistry and originally reported the palladium(II) catalysed α-arylation of ketones in 1997[146] using aryl halides and ketones in the presence of base, catalyst and ligand. The authors suggested that the reaction proceeded by the *in situ* generation of palladium as the coordinatively unsaturated and reactive 14 electron oxidation state (usually coordinated to two ligands but represented as Pd(0)Ln) and oxidative addition with the aryl halide. Substitution of the halide with the enolate of the ketone and reductive elimination would furnish the α-aryl ketone and regenerate the catalyst. The authors were keen to extend this protocol to esters, as many important drug molecules (e.g. Non-Steroidal Anti-Inflammatory drugs (NSAIDs)) are derivatives of α-aryl esters. The same group reported the successful palladium-catalysed α-arylation of esters in 2001,[147] which, in the case of the more readily enolised β-keto esters, were deacylated under the reaction conditions. Unfortunately, the protocol could not be extended to 5-haloisoquinolin-1-ones and, despite prolonged efforts with a range of reaction conditions including variation of solvent, catalyst, ligand and base,[148] only starting material was recovered from the reaction mixture. Seeking an explanation for this unexpected lack of reactivity, it was speculated that the use of 5-haloisoquinolin-1-ones was perhaps an issue, as these compounds have limited solubility in many organic solvents and can also co-ordinate to palladium, possibly diminishing the catalytic activity of the metal. The reaction was therefore repeated using the isocoumarin **75** but again only starting material was recovered. Finally, the catalyst was varied, switching to a copper(I) iodide-catalysed reaction[149] but no improvement in reactivity was achieved.

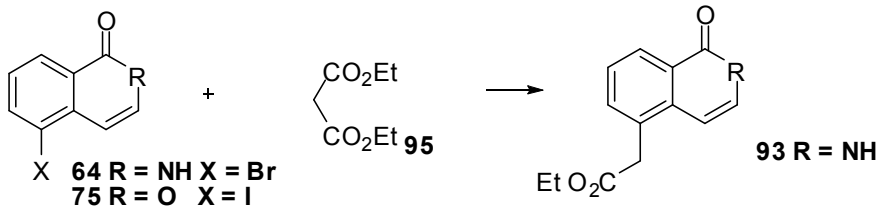

Scheme 18. Attempted synthesis of **93** *via* palladium-catalysed couplings with diethyl malonate.

Özdemir *et al.*[150] have reported the successful synthesis of arylacetic acid derivatives from diethyl malonate **95** and various aryl halides catalysed by a palladium(1,3-dialkylimidazolidin-2-ylidene) species formed *in situ*. The group noted that the arylations in their study generally required milder reaction conditions than had previously been reported.[151] In the present work, this reaction was investigated using the starting 5-bromoisoquinolin-1-one **64** or 5-iodoisocoumarin **75** under a variety of conditions but the only isolable products were the starting aryl halide with traces of dehalogenated starting materials. The formation of the latter indicates that there is some formation of the aryl-Pd species but that this fails to react with the enolate.

The earlier success of the Heck reaction led us back to more conventional palladium-catalysed chemistry and the Stille reaction. In 1978, Kerdesky and Stille[152] first used palladium-catalysed reactions of organotin compounds and acid chlorides to synthesise ketones. Stille developed this chemistry[153, 154] and the Pd(0)-catalysed coupling of an alkyl, aryl or alkenyl halide and an organostannane is now known as the Stille cross-coupling. It was planned to couple allyltributylstannane with **75**, anticipating the formation of **96**, as allyl groups are known to be transmetallated selectively from allyltrialkylstannanes in preference to the alkyl groups. This approach introduces a three-carbon unit but the terminal carbon could be cleaved oxidatively by ozonolysis (or osmium tetroxide / sodium periodate), followed by oxidation of the intermediate aldehyde **97** to give **98**. The Stille reaction gave a complex mixture of products and mass

spectrometric analysis showed that none of the desired 5-allylisocoumarin had been formed.

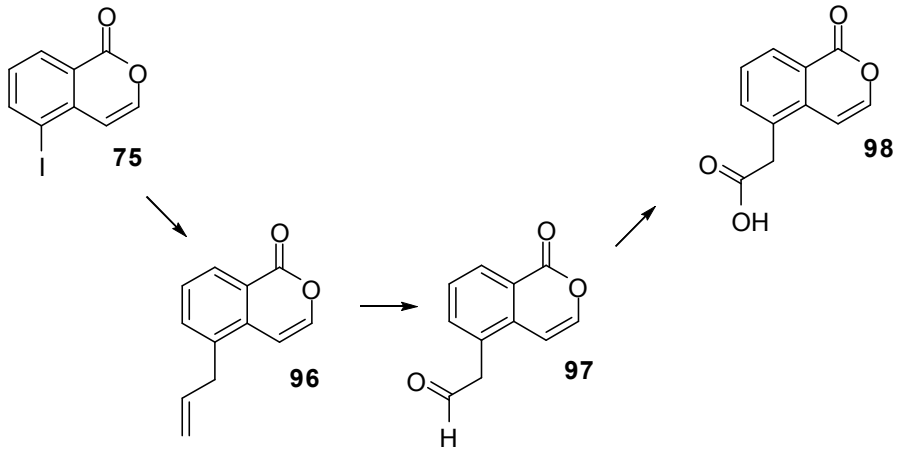

Scheme 19. Proposed synthesis of **98** *via* Stille reaction to form **96**. (i) $Pd_2(dba)_3$, SPhos, trimethylallyl tin, toluene; (ii) O_3; (iii) PCC.

As none of these approaches were successful, the synthetic efforts were paused in favour of obtaining biological data to guide future synthesis. The benchmark inhibitor 5-AIQ was tested to serve as a reference point for potency and selectivity.

3.4.8 Initial SAR of 5-substituted isoquinolin-1-ones

Ideally, compounds would be tested using the same assay for each PARP isoform but Kudos were unable to extend the protocol used in their Flashplate PARP-1 assay to PARP-2. The initial IC_{50} values of the early targets, obtained using the assays developed by Kudos Pharmaceuticals, are presented in Table 1.

Table 1. Inhibition of the activities of PARP-1 and PARP-2 by 5- and 2-(ω-carboxyalkyl)isoquinolin-1-ones; data for 5-AIQ **5** are shown for comparison.

Cpd. No.	Structure	PARP-1 IC_{50} (μM)	PARP-2 IC_{50} (μM)	Selectivity ($IC_{50\ (PARP-1)}$ / ($IC_{50\ (PARP-2)}$)
5	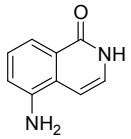	0.94	1.05	0.89
59	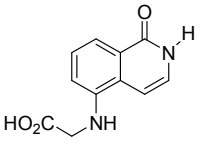	1.56	0.55	2.85
62	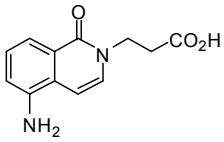	0.55	1.59	0.35
28	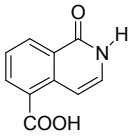	>25	>25	-
26	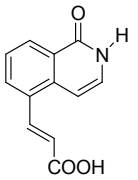	6.58	4.67	1.41
27	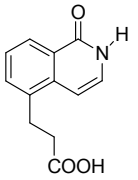	8.45	2.96	2.85

As expected, 5-AIQ did not discriminate between the two PARP isoforms to a significant extent and had an IC_{50} of *ca.* 1 μM for each. The secondary amine **59** was slightly PARP-2 selective (2.85 fold) whilst remaining moderately potent for each isoform. When the amine function is replaced with a CH_2 in **27**, activity against both isoforms is reduced by approximately 6-fold. A possible explanation for this reduction in potency is that the amine NH in **59** forms favourable contacts with residues in the active sites of both isoforms and these are lost in **27**. Interestingly, it has been proposed that a water-

mediated hydrogen bond between the amino group of 5-AIQ and the Glu988 carboxylate contributes to the increased potency of the inhibitor.[155] The more rigid alkene **26** showed a minor increase in potency for PARP-1 and was slightly less potent towards PARP-2 than its saturated counterpart. However the differences observed are too small to suggest that free rotation about the alkane plays a significant role in activity against either isoform.

The propanioc acid **62** retained activity for both isoforms and was slightly PARP-1 selective. In fact, **62** was the most potent PARP-1 inhibitor of the series evaluated. This result was somewhat unexpected given that the vast majority of SAR studies with PARP-1 inhibitors show that one amide proton is absolutely required, in order that the three key hydrogen bonds with Gly863 and Ser904 in the PARP-1 catalytic site are formed. It is feasible that **62** could bind to the active sites of PARP-1 (and -2) in two different ways. /Firstly, the amide carbonyl could form two hydrogen bonds, one with the Gly863 NH and a second with the Ser904, in the traditional way. The third contact could be achieved thanks to the flexibility of the propanoic acid side chain, with the carboxylic acid hydroxy replacing the amide hydrogen. However it is likely that the acid would be deprotonated at physiological pH, therefore this binding mode is not probable.

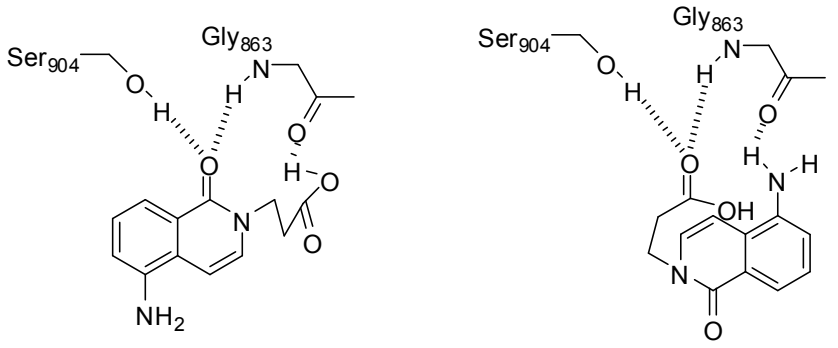

Figure 28. Possible binding modes of **62** in the PARP-1 active site.

Alternatively, the compound could fit into the PARP-1 active site in a different manner. The carboxylate carbonyl could form two hydrogen bonds with Gly863 and Ser904 and an amine proton could participate in the final bond. These two possible binding modes are shown in Figure 28.

Interestingly, Eltze *et. al.*[156] have recently reported a selection of imidazoquinolinone, imidazopyridine and isoquinolindione compounds which lack an amide NH but possess other binding motifs. Many of these were potent PARP-1/2 inhibitors.

It was surprising that the carboxylic acid **28** showed an apparent lack of activity as Watson *et al.*[131] had shown this compound was a moderately potent PARP inhibitor, inhibiting PARP activity by 79% at a concentration of 13.2 μM, in comparison with a control. This result illustrates that caution must be exercised when comparing compounds tested in different assays as very different results can be obtained.

3.4.9 Further modifications at the 5-position of 5-AIQ

The modest selectivity and potency of the initial targets led us to consider other modifications at the 5-position of 5-AIQ. Interestingly, while these modifications were being considered, Pellicciari *et al.*[157] published a paper reporting the synthesis and biological evaluation of a series of 5-benzoyloxyisoquinolin-1-ones and also some saturated (*i.e.* 3,4-dihydro) analogues. Initially, the group screened the compounds at a concentration of 10 μM against bovine PARP-1 and murine PARP-2 and calculated percentage activity, compared to control. The more promising compounds (in terms of apparent selectivity) were taken forward for further biological characterisation. The methods developed by Banasik *et al.*[107] were then used to assay the compounds, again using bovine PARP-1 and murine PARP-2. Thus PARP activity was assessed by measuring the radioactivity of [^{3}H]adenosine-NAD$^+$ incorporated into acid insoluble material, following the PARP reaction. The group reported that 5-benzoyloxyisoquinolin-1-one **99** showed a 60-fold selectivity for PARP-2 over PARP-1 using this assay. In addition, **99** and the potent PARP-1 (and 2) inhibitor PJ34 **100** were tested in whole cells using fibroblasts derived from PARP-1 knockout mice or wild-type controls. The vast majority of the PARP-catalytic activity in the PARP-1$^{-/-}$ cells would be due to PARP-2, whereas, in the wild-type cells, PARP-1 would account for 85-90% and PARP-2 10-15%. It was shown that PJ34 caused a 76% drop in PARP(1 + 2) activity (when compared with

control) in the wild-type cells whereas **99** only caused a 9% drop. In the PARP-$1^{-/-}$ cells, PJ34 **100** caused a 76% reduction in PARP(-2) activity whilst treatment with **99** resulted in a 90% drop. The authors claim that these data show PJ34 inhibits PARPs 1 and 2 but **99** only inhibits PARP-2.

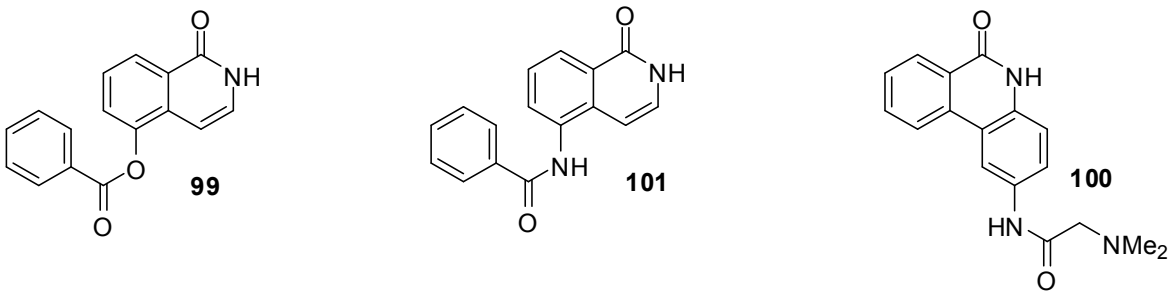

Figure 29. The PARP-2 selective ester **99** and proposed amide **101**, and the unselective PJ34 **100**

A potential problem with use of the the Pellicciari compound **99** is the presence of a phenyl ester group, which one would expect to be easily hydrolysed under physiological conditions, therefore limiting its usefulness in *in vivo* experiments. With this in mind, it was planned to synthesise a series of benzamides, with the general structure shown in Scheme 20, in which the tethering amide bond would be much more stable *in vivo* than the isosteric ester in Pellicciari's series.

In order to generate the series, 5-AIQ was treated with various commercially available acid chlorides using pyridine as solvent. The functions of the pyridine were twofold, firstly to act as a base to quench the HCl formed in the reaction and secondly to act a nucleophilic catalyst, activating the acid chloride. In general, the acylations worked well and the isolation of products was achieved by evaporation of solvent and recrystallisation.

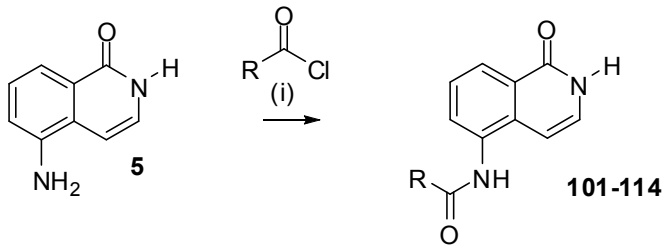

Scheme 20. Acylation of 5-AIQ with various acid chlorides. (i) Pyridine, 90°C, 16 h, 55-86%.

3.4.10 Further SAR of 5-substituted isoquinolin-1-ones

Table 2 shows the relevant yields and IC_{50} values of the compounds in this series. Additionally, the IC_{50} values of Pellicciari's[157] compound **99** and the quinoxaline **22** (claimed by Iwashita *et al*[122] to be 5-fold selective for PARP-2) obtained in the assays are shown as small amounts were available to us for testing. Before comparing the results obtained in this study with other studies, it should be noted that the species from which the enzymes are isolated from or accessed by recombinant DNA technology, may vary. Pellicciari compared bovine PARP-1 with murine PARP-2, Iwashita did not disclose the assay conditions and Kudos Pharmaceuticals compare human PARP-1 with murine PARP-2.

Table 2. Inhibition of the activities of PARP-1 and PARP-2 by 5-amidoisoquinolin-1-ones; data for 5-AIQ **5**, 5-benzoyloxyisoquinolin-1-one **99** and 2-(4-chlorophenyl)quinoxaline-5-carboxamide **22** are shown for comparison

Cpd No.	5-substituent	Yield	PARP-1 IC_{50} (μM)	PARP-2 IC_{50} (μM)	Selectivity ($IC_{50\ (PARP-1)}$ / ($IC_{50\ (PARP-2)}$)	Reported selectivity ($IC_{50\ (PARP-1)}$ / ($IC_{50\ (PARP-2)}$)
5	H_2N- (5-AIQ)	-	0.94	1.05	0.89	-
101	PhCONH-	86%	13.9	1.5	9.3	-
102	4-BrPhCONH	81%	33.2	25	1.3	
103	4-Me-PhCONH-	82%	13.4	6.5	2.1	-

104	4-I-PhCONH-	76%	7.6	1.3	5.8	-
105	4-O_2N-PhCONH-	71%	3.0	1.6	1.9	-
106	4-F_3C-PhCONH-	72%	10.7	3.3	3.2	-
107	4-F-PhCONH-	68%	18.0	3.6	5.0	-
108	4-Cl-PhCONH-	77%	11.2	3.9	2.9	-
109	2-I-PhCONH-	61%	4.5	3.2	1.4	-
110	2-Me-PhCONH-	63%	31.6	5.6	5.6	-
111	(thiophen-3-yl)CONH-	61%	22.4	7.0	3.2	-
112	cHex-CONH-	68%	>80	27.9	>2.9	-
113	Bu^{t}CONH-	55%	>100	29	3.4	-
114	(adamantan-1-yl)-CONH-	59%	>50	19.9	>2.5	-
99	$PhCO_2$-		4.10	1.49	2.75	60[157]
22	[2-(4-ClPh)-quinoxaline-5-$CONH_2$]		0.03	0.09	0.33	4.71[122]

In general, better yields were achieved with aromatic (61-86%) over aliphatic acid chlorides (59-69%). Substitution of the aromatic ring led to lower yields. Electron-neutral substituents in the *para*-position were better tolerated than electron-withdrawing groups and, as expected, *ortho*-substitution caused a significant reduction in yield.

In terms of selectivity, the most promising compound was N-(1-oxo-1,2-dihydro-isoquinolin-5-yl)benzamide **101**, which was 9.3-fold selective for PARP-2 over PARP-1. Substitution of the benzene ring in the acyl group generally reduced potency towards both isoforms but the effect on PARP-2 activity was generally more pronounced, so the

compounds became less selective. However, the most potent inhibitor of PARP-2 was 4-iodo-N-(1-oxo-1,2-dihydroisoquinolin-5-yl)benzamide **104** with an IC_{50} value of 1.3 μM; unfortunately, this compound also showed an increased potency towards PARP-1 and as a consequence, was only 5.8-fold selective. A bulkier electron-withdrawing group increased potency towards PARP-1, as illustrated by **106** (IC_{50} = 10.7 μM) and the most potent PARP-1 inhibitor **105** (IC_{50} = 3.0 μM); PARP-2 activity was only moderately affected. A smaller electron-withdrawing group decreased PARP-1 activity and 4-fluoro-N-(1-oxo-1,2-dihydroisoquinolin-5-yl)benzamide **107** had an IC_{50} value of 18.0 μM. Switching to the corresponding thiophene-2-carboxamide **111** led to a *ca.* 2-fold drop in PARP-1 activity but a *ca.* 5-fold drop in PARP-2 activity and therefore a drop in selectivity. The alkyl carboxamides **112** and **113** suffered from a dramatic loss in PARP-1/2 activity but again the effect was more pronounced for PARP-2 so the compounds became less selective for this isoform. The same was true for **114** which was synthesised to test the effect of steric bulk with aromaticity.

With these promising data in hand, the next stage in the research would be the synthesis of a series of 3- and 4-subsituted isoquinolin-1-ones and evaluation of these molecules as inhibitors of PARP-1/2. The purpose of the preparation of these compound sets would be to test if structural modifications in the 3- and 4- positions had a similar impact on PARP-1/2 inhibitory activity, as modifications in the 5-position. It was hoped that a bulky subsitituent in one of these positions would lead to an increased inhibitory potency against PARP-2 over PARP-1, owing to the larger hydrophobic-binding pocket (in conparrison with PARP-1) in this isoform.

3.5 3-Substituted isoquinolin-1-ones

The strategy to synthesise the series of 3-substituted isoquinolin-1-ones was to follow literature precedent but novel routes would also be investigated as required.

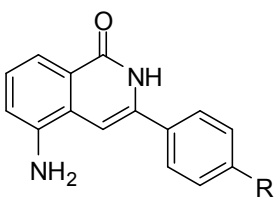

33 R = H
115 R = Cl
116 R = CF_3
117 R = OMe
118 R = Me

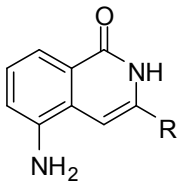

119 R = Me
120 R = Et
121 R = Pentyl

Figure 30. Target 3-aryl and 3-alkylisoquinolin-1-ones.

The first eight compounds required were the 3-arylisoquinolin-1-ones **33** and **115-118** and the 3-alkylisoquinolin-1-ones **119**, **120** and **121**. Three of these examples were chosen to test the effect of varying alkyl chain length (**119-121**) on PARP inhibitory activity. The other five molecules were designed to test the effect of varying the electronics of the 3-phenyl ring: **117** is highly electron-rich, **118** is electron-rich to a lesser extent, **116** is electron-deficient and **33** and **115** are electron neutral.

There are currently a number of routes to 3-arylisoquinolin-1-ones in the literature including Hg^{2+}-catalysed cyclisation of methyl 3-nitro-2-phenylethynylbenzoate **30**.[158]

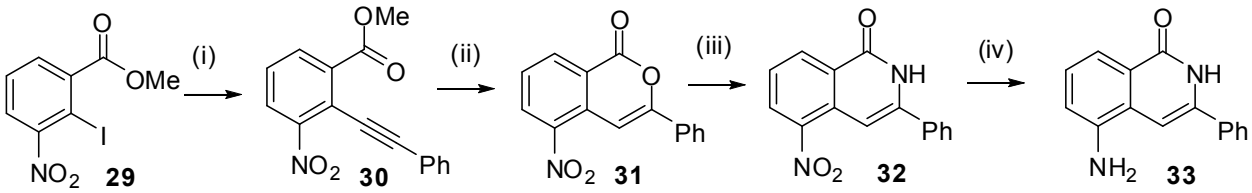

Scheme 21. Hg^{2+}-catalysed cyclisation of methyl 3-nitro-2-phenylethynylbenzoate **30** to give 5-nitro-3-phenylisocoumarin **31** which can be converted into the corresponding isoquinolin-1-one **32** by reaction with ammonia. (i) $(Ph_3P)PdCl_2$, CuI, ethynylbenzene; (ii) $HgSO_4$, H_2SO_4, acetone; (ii) 2-methozyethanol, NH_3; (iv) Pd/C, H_2.

Other routes include Hurtley reaction of 2-bromo-3-nitrobenzoic acid **34** with β-diketones[158] and reaction of methyl 2-iodo-3-nitrobenzoate **36** with arylethynes under

Castro-Stevens conditions.[158]

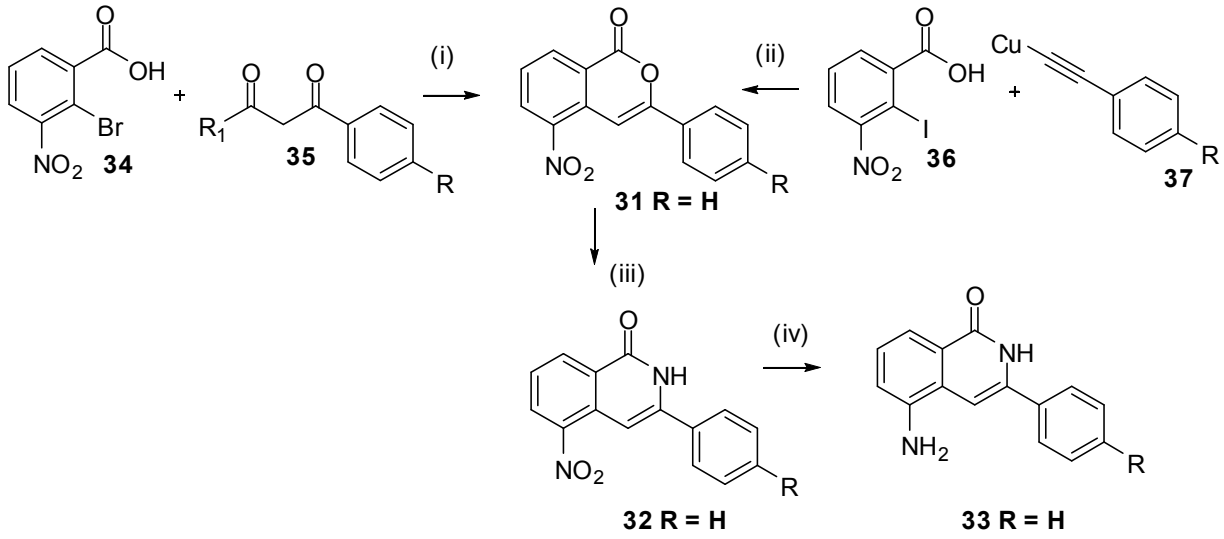

Scheme 22. Hurtley reation of 2-bromo-3-nitrobenzoic acid with β-diketones (left to right) and reaction of methyl 2-iodo-3-nitrobenzoate with arylethynes under Castro-Stevens conditions (right to left), to give 3-aryl-5-nitroisocoumarins, precursors to isoquinolin-1-ones. (i) NaOEt, Cu; (ii) Pyridine, heat; (iii) 2-methoxyethanol, NH_3; (iv) Pd/C, H_2.

The mercury catalysed cyclisation could only be applied to methyl 3-nitro-2-phenylethynylbenzoate and not other arylethynes; this meant it was only useful for the synthesis of 5-nitro-3-phenylisocoumarin **31**. The second literature route was limited to phenyl, 4-methylphenyl and 4-methoxyphenyl arylethynes and therefore the corresponding 3-arylisocoumarins. Far more versatile was the final route utilising the Hurtley reaction, as a range of 3-aryl and 3-alkylisocoumarins could be accessed and this pathway was chosen.

3.5.1 Hurtley reaction

Hurtley[159] first reported the condensation of 2-bromobenzoic acid **122** with a range of β-diketones with either copper (II) acetate or copper powder as catalyst and in the presence of ethanolic sodium ethoxide. Further investigations by Cirrigotis *et al.*[160] showed that the carboxylic acid was essential and switching to analogues such as esters caused the reaction to fail. The group also showed that the reaction proceeded with 2-iodobenzoic-acid, albeit in much lower yield and that a source of copper was essential. Two years later, Ames *et al.*[161] reported the formation of the isocoumarin **123** by Hurtley coupling of 2-bromo-3-nitrobenzoic acid **34** with pentane-2,4-dione **124**, followed by deacylation of the intermediate **125** and ring-closure with sodium chloride at 170°C.

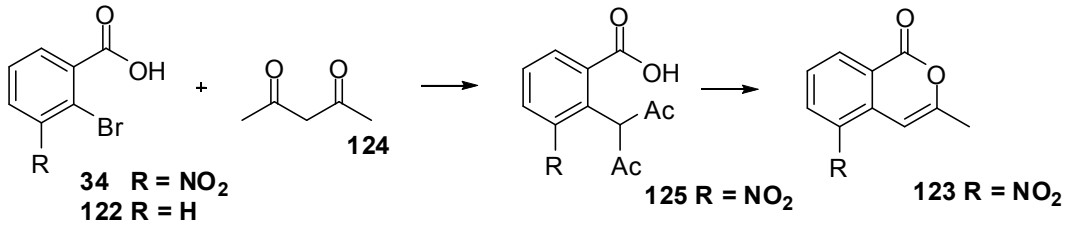

Scheme 23. Formation of 3-arylisocoumarins by Hurtley reaction of **34** or **122**, followed by deacylation. (i) Cu, KOBu^t, 2-methylpropan-2-ol; (ii) NaCl, 170°C.

The work of Woon[162] significantly extended the scope of the use of the Hurtley reaction to form 5-nitro-3-substituted isocoumarins from 2-bromo-3-nitrobenzioic acid and β-diketones. The main findings of the research are summarised below.

- It was possible to form 5-nitro-3-substituted isocoumarins in a single step using Hurtley's original conditions but β-diketone cleavage side products were also formed.
- The use of a potassium *t*-butoxide/*t*-butanol system abolished the formation of β-diketone cleavage side products.
- Copper powder was an effective catalyst.
- The use of unsymmetrical β-diketones lead to the formation of two products.

As quantities of **33**, **117**, **120** and **121** were available from a previous project, these compounds were evaluated directly. In the meantime, the method of Woon[162] was followed in synthesising 2-bromo-3-nitrobenzoic acid and the β-diketones required as starting materials for the Hurtley reaction. The *ortho*-bromo acid **34** was prepared from 3-nitrophthalic acid **126** in good yield (74%) by regioselective mercuration / decarboxylation and electrophilic bromination of **127**.

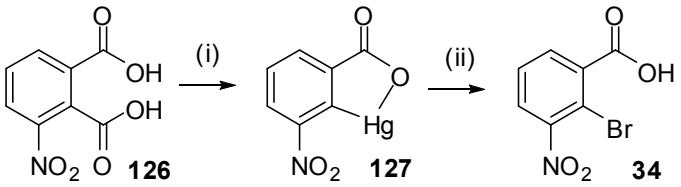

Scheme 24. Synthesis of **34** by mercuration followed by bromination. (i) NaOH, $Hg(OAc)_2$, AcOH, (ii) AcOH, Br_2, NaBr, 74% (overall).

Heptane-2,4-dione **124** was commercially available and the remaining β-diketones **128-130** were synthesised by acylating the corresponding acetophenones **131-133** with acetic anhydride **134** using a boron trifluoride-acetic acid complex.

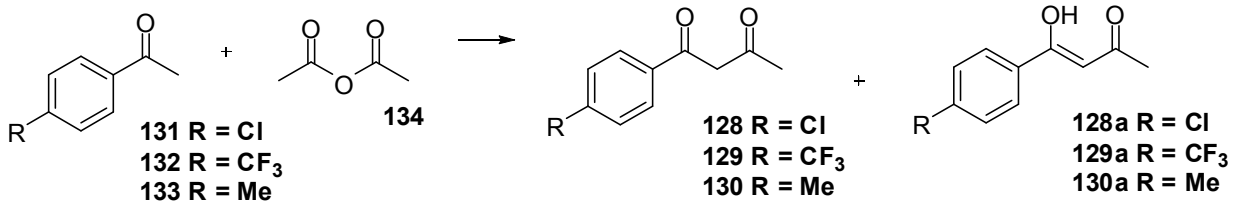

Scheme 25. Synthesis of β-diketones *via* Claisen-condensation-type reactions. (i) $BF_3.(AcOH)_2$, 68-84%

The desired products were obtained in moderate to good yields (68-84%) and in each case there was evidence of the presence of both the keto and enol form in the ^1H NMR spectrum. For example, the signals at δ 6.13 and 16.09 in the ^1H NMR spectrum of 1-(4-chlorophenyl)butane-1,3-dione **128** are characteristic of enol alkene and hydroxy protons respectively, whereas the signal at δ 4.07 is due to the keto CH_2 protons.

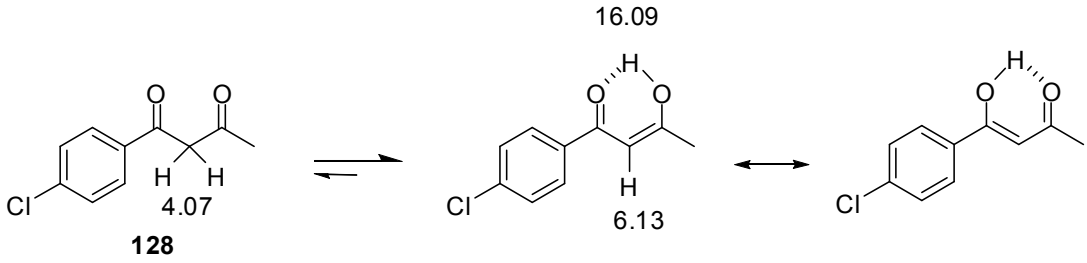

Scheme 26. The different tautomers of **128** evidenced by ^{1}H NMR. The intramolecular hydrogen bonds offer increased stability.

The most prevalent tautomer was the enol form (generally >90%); this is unsurprising as intramolecular hydrogen bonding leads to the formation of a stable six membered ring in this form.

With the starting materials in hand, the Hurtley reactions could be attempted. As expected, Hurtley reaction of the unsymmetrical β-diketones led to two products. The major product was the required 3-arylisocoumarin (e.g. **135**) and was probably formed by deacetylation of the Hurtley intermediate (e.g. **136**), whilst the minor product 3-methyl-5-nitroisocoumarin **123** was most likely formed by debenzoylation of the same intermediate.

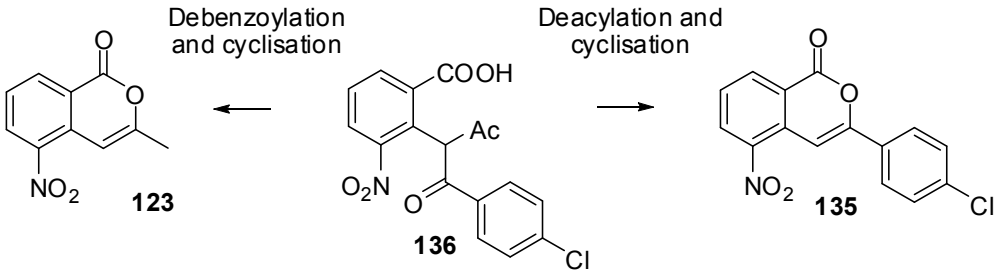

Scheme 27. Two possible products are possible depending upon whether the Hurtley intermediate **136** undergoes debenzoylation or decaylation.

It is interesting that the 3-arylisocoumarin is the major product as electronically debenzoylation is favoured over deacylation due to the fact that benzoyl carbonyl carbons are less electrophillic than their acetyl counterparts. This suggests that steric effects dominate and the smaller acetyl group is preferentially lost. In line with the reported

synthesis, the yields were low, ranging from 12% to 33%, but optimisation was not important at this stage.

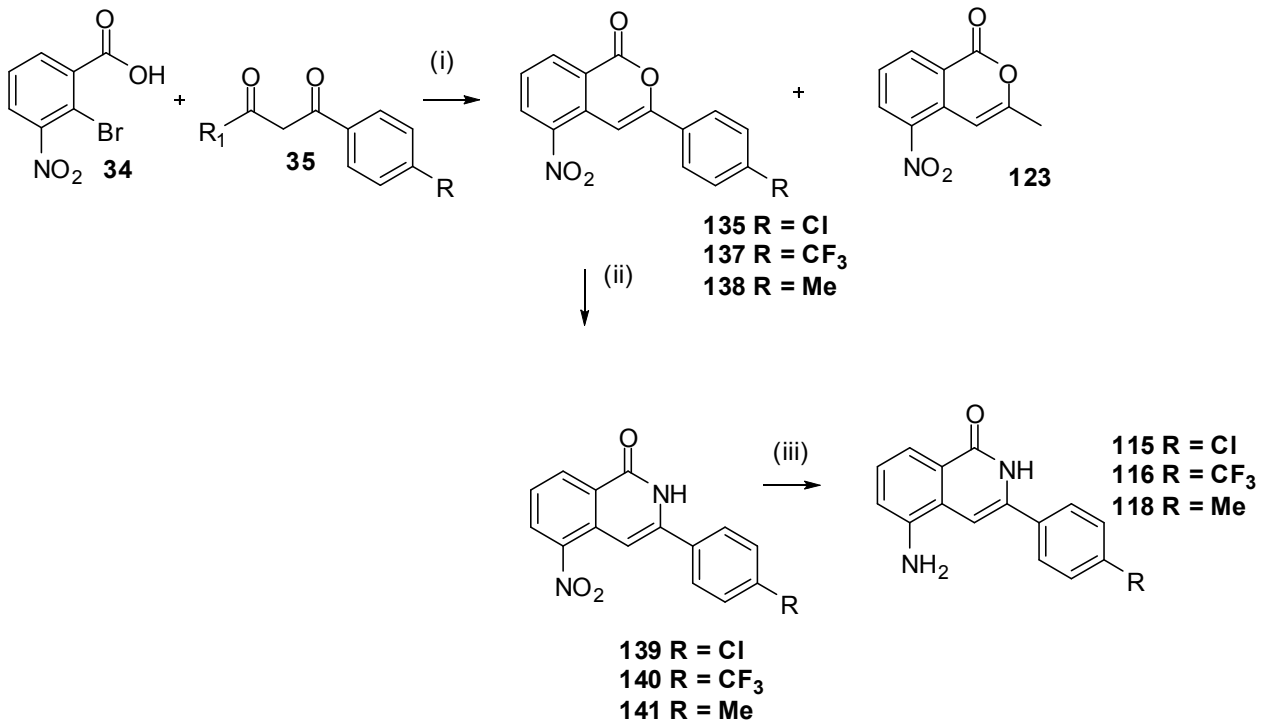

Scheme 28. Synthesis of 3-substituted isoquinolin-1-ones *via* Hurtley reaction. (i) Cu, $KOBu^t$, 2-methylpropan-2-ol, 12-33%; (ii) NH_3, 2-methoxyethanol, 24-80%; (iii) Pd/H_2, HCl, 42-79%.

With the synthesis of the 5-nitro-3-arylisocoumarins achieved, all that remained was to convert these to the corresponding isoquinoline-1-ones and then reduce the nitro function. These steps were achieved in good yields using the established procedures of saturation with ammonia and reflux in 2-methoxyethanol followed by palladium-catalysed hydrogenation of the nitro function.

3.5.2 Friedel-Crafts reaction

Attention was then turned to the synthesis of 4-substituted isoquinolin-1-ones. It was rationalised that the most nucleophilic carbon of isoquinolin-1-ones is at the 4-position due to mesomeric donation of the lone pair of the nitrogen in the amide.

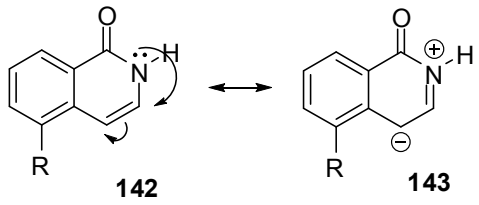

Scheme 29. Resonance forms of the lactams **142** and **143**.

The first strategy to exploit this electronic difference was electrophilic substitution *via* Friedel-Crafts alkylation or acylation. These reactions involve the Lewis-acid catalysed introduction of a keto or alkyl group on to an aromatic by reaction with an alkyl halide (or alkene) or acyl halide (or anhydride), respectively. The presence of the nucleophilic amino group on 5-AIQ meant it was not feasible to attempt Friedel-Crafts acylation reactions directly on this molecule as this would result in acylation of the amine. In addition the amine would act as an *o*-/*p*-directing group in the Friedel-Crafts alkylation, activating the carbocyclic ring and causing substitution in the 6- and 8-positions. In order avoid this issue, 5-nitroisoquinolin-1-one **38** was chosen as the starting material; although the nitro group in this molecule is sterically larger than the amino function in 5-AIQ, possibly hindering substitution in the neighbouring 4-position, it deactivates the carbocyclic ring and is not itself nucleophilic.

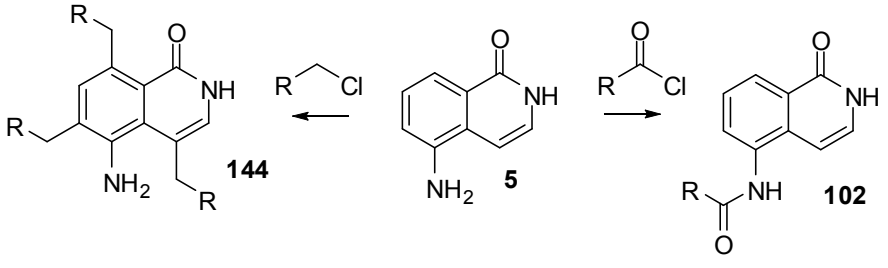

Scheme 30. Probable products formed if Friedel-Crafts alkylations or acylations were attempted directly on 5-AIQ

Benzoyl chloride was chosen as both reactant and solvent; its high boiling point allowed that a range of temperatures could be studied and an excess of electrophile was unlikely to affect the path of the reaction. The strong Lewis acid, aluminium chloride ($AlCl_3$) was used as a catalyst for the first series of experiments, which involved gradually increasing the temperature from room temperature until product was formed (as shown by TLC analysis). No reaction occurred until the temperature reached 150°C and a product significantly less polar than the starting material was formed in low yield after 3 days. Unfortunately, upon analysis by ^{1}H and ^{13}C NMR, this molecule was not the desired 4-benzoyl-5-nitroisoquinolin-1-one but the N-substituted 2-benzoyl-5-nitroisoquinolin-1-one **145,** in low yield (26%). It is likely that steric crowding at the 4-position led to the formation of this product.

A Friedel-Crafts alkylation was attempted with benzyl chloride in nitrobenzene, again using $AlCl_3$ as catalyst, but no reaction occurred even at temperatures up to 180°C. Efforts were therefore focused on acylation reactions from this point.

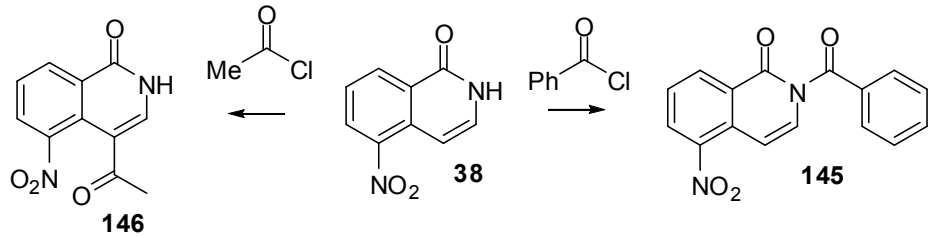

Scheme 31. Friedel-Crafts acylations of **38**. (i) Ac_2O, H^+, 36%; (ii) PhCOCl, $AlCl_3$, 26%.

For the next experiments, a less sterically demanding electrophile was chosen, formed from acetic anhydride under Brønsted acid-catalysis. A range of temperatures was again investigated. The desired product, 4-acetyl-5-nitroisoquinolin-1(*2H*)-one **146** formed at 100°C and the reaction went to completion after 22 h. Interestingly, none of the N-substituted product was formed under these conditions, probably due to the change in catalyst from a Lewis to a Brønsted acid affecting the nucleophilicity at this position. A Lewis acid is likely to form a complex here whereas a Brønsted acid would simply protonate the attacking electrophile rendering it more reactive. The IR spectrum of **146** was interesting in that the ketone carbonyl absorption 1761 cm^{-1} is unusually high for an

aryl ketone. The probable cause of this is that the ketone is forced out of plane and orthogonal to the isoquinolin-1-one by the *peri* nitro group. The resultant loss of conjugation would cause the change in IR absorption. Initial attempts to reduce the ketone with sodium borohydride resulted in a complex mixture. In a further attempt to introduce a benzoyl group to the 4-position, benzoic anhydride was used as the electrophile under Brønsted acid catalysis but no reaction occurred, even under forcing conditions.

Following the failure of the attempts to benzoylate the 4-position of **38**, focus was turned to the more reactive 5-nitroisocoumarin **56**, as the switch to the lactone would prevent substitution occurring at the 2-position. Initially, **56** was treated with benzoyl chloride in a range of solvents, gradually increasing the temperature and using $AlCl_3$ as catalyst. The reaction proceeded slowly (Table 3 entry **B**) at 100°C with nitromethane as solvent; a single product was formed in poor yield, as shown by TLC. Preliminary analysis of this product by ^{1}H NMR showed the characteristic doublet, triplet, doublet coupling pattern of the 6-H, 7-H and 8-H of the isocoumarin and also the presence of a phenyl group, pointing to formation of the expected 4-benzoyl-5-nitroisocoumarin. However, further analysis by ^{13}C NMR revealed that only one carbonyl group was present with a signal at δ 160.3, corresponding to the lactone carbonyl in isocoumarins. This observation was confirmed by IR, as only one carbonyl absorption at 1739 cm^{-1} was present in the IR spectrum of the product. The MS also showed the MW to be 28 Da lower than that of the intended product. Further characterisation of the product by HMBC and HMQC NMR experiments revealed the product to be 5-nitro-3-phenylisocoumarin **31** and this was confirmed by comparison of the NMR spectrum and melting point with an authentic sample and by co-elution by TLC.

The chemistry of this new reaction was interesting and a series of experiments was designed to test the effects of solvent, Lewis acid and temperature on it. A strong Lewis acid such as $AlCl_3$ or $SnCl_4$ (entries **C** and **F**) was essential and no reaction occurred with the weaker Lewis acids $ZnCl_2$ and $Zn(OTf)_2$ (entries **H** and **I**), even under forcing conditions for extended reaction times. The effect of temperature is compared in Entries **C**, **D** and **E** (100°C, 150°C and 180°C). The reaction rate was increased at 150°C; this

temperature also gave the greatest yield (42%); increasing the temperature to 180°C led to a lower yield, probably owing to degradation of reactants or intermediates.

The greatest yields and shortest reaction time were achieved with nitrobenzene as solvent. Comparison with use of nitromethane (Entries **C** and **J**) at 100°C suggested that the nature of the solvent had only a minor effect and the reaction temperature was paramount. However nitromethane and nitrobenzene are oxidising agents, so an experiment was conducted in the non-oxidising, high-boiling solvent pentachloroethane (Entry **K**); some product **31** was formed but in poor yield. Having optimised the conditions (Entry **D**), the generality of this new reaction was tested by using a range of acid chlorides. The presence of an electron-donating group in the aromatic acid chloride

Table 3. Outcomes of reactions of acyl chlorides with 5-nitroisocoumarin **56** under various Friedel-Crafts conditions.

Entry	Acyl chloride	Lewis acid	Solvent	Reaction temp. (°C)	Reaction time (d)	Product	Yield (%)
A	PhCOCl	$AlCl_3$	DCM	40	7	**SM**[a]	0
B	PhCOCl	$AlCl_3$	$MeNO_2$	80	7	**SM**[a]	0
C	PhCOCl	$SnCl_4$	$PhNO_2$	100	7	**31**	21
D	PhCOCl	$SnCl_4$	$PhNO_2$	150	3	**31**	42
E	PhCOCl	$SnCl_4$	$PhNO_2$	180	3	**31**	27
F	PhCOCl	$AlCl_3$	$PhNO_2$	150	3	**31**	38
G	PhCOCl	$Sn(OTf)_2$	$PhNO_2$	150	3	**31**	19
H	PhCOCl	$ZnCl_2$	$PhNO_2$	150	3	**SM**[a]	0
I	PhCOCl	$Zn(OTf)_2$	$PhNO_2$	150	3	**SM**[a]	0
J	PhCOCl	$SnCl_4$	$MeNO_2$	100	5	**31**	17
K	PhCOCl	$SnCl_4$	C_2HCl_5	150	3	**31**	13
L	$Ph^{13}COCl$	$SnCl_4$	$PhNO_2$	150	3	**27**	39
M	4-$O_2NC_6H_4COCl$	$SnCl_4$	$PhNO_2$	150	3	**34**	10
N	4-$F_3CC_6H_4COCl$	$SnCl_4$	$PhNO_2$	150	3	**35**	11
O	4-$EtOC_6H_4COCl$	$SnCl_4$	$PhNO_2$	150	3	**SM**[a]	0
P	4-ClC_6H_4COCl	$SnCl_4$	$PhNO_2$	150	3	**36**	29
Q	4-MeC_6H_4COCl	$SnCl_4$	$PhNO_2$	150	3	**37**	23
R	3-MeC_6H_4COCl	$SnCl_4$	$PhNO_2$	150	3	**38**	21
S	4-$FC_6H_4CH_2COCl$	$SnCl_4$	$PhNO_2$	150	3	[b]	0
T	$Me(CH_2)_4COCl$	$SnCl_4$	$PhNO_2$	150	3	[b]	0

[a] Only **56** recovered. [b] Mixture of decomposition products

(Entry **O**) prevented any reaction but the 3-arylisocoumarin products were formed when electron-withdrawing groups were present (Entries **M** and **N**), although the yield was adversely affected. Groups with little electronic effect gave the expected products in satisfactory yields (Entries **P**, **Q** and **R**). The reaction did not proceed with aliphatic acid chlorides and only mixtures of decomposition products were obtained.

Our initial investigations into this reaction gave some clues as to the possible mechanism by which the 3-aryl products were formed. The strong Lewis acidity and forcing conditions required suggested that the primary step might be the formation of the Friedel-Crafts 4-acylated product and the poor yield with the non-oxidising pentachloroethane indicated that an oxidation step was possibly involved. In order to gain further insights into the mechanism, a ^{13}C labelling study using ^{13}C-carbonyl-labelled benzoyl chloride was conducted under the optimum conditions, which yielded **148**.

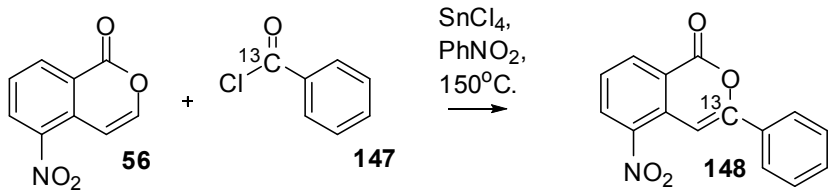

Scheme 32. ^{13}C-Labelling study.

The ^{1}H NMR spectrum of **148** contained a broad doublet at δ 7.87 ppm with a coupling constant of 5.5 Hz, corresponding to 4-H. In the unlabelled product **31**, the corresponding signal is a broad singlet. These data confirm that the ^{13}C from the labelled acid chloride has been incorporated into the product at position 8a, 5, 4a or 3, as the coupling constant is only consistent with $^{2}J_{C\text{-}H}$ or $^{3}J_{C\text{-}H}$ but not $^{1}J_{C\text{-}H}$ which would be much greater (>100 Hz). The exact location of the ^{13}C was proved by ^{13}C NMR spectrum, primarily by the greatly enhanced peak at δ 156.8 which had previously been assigned as corresponding to 3-C following HMBC and HMQC experiments. This was supported by the observation of one-bond carbon-carbon couplings between the 3-C and adjacent carbons with $^{1}J_{C\text{-}C} = 68$

Hz between 3-C and 1'-C and $^{1}J_{C\text{-}C}$ = 75 Hz between 3-C and 4-C. Additionally, longer range two- and three-bond couplings were observed with *J* values between 0 and 5 Hz and, as anticipated, the ^{3}J values were larger.

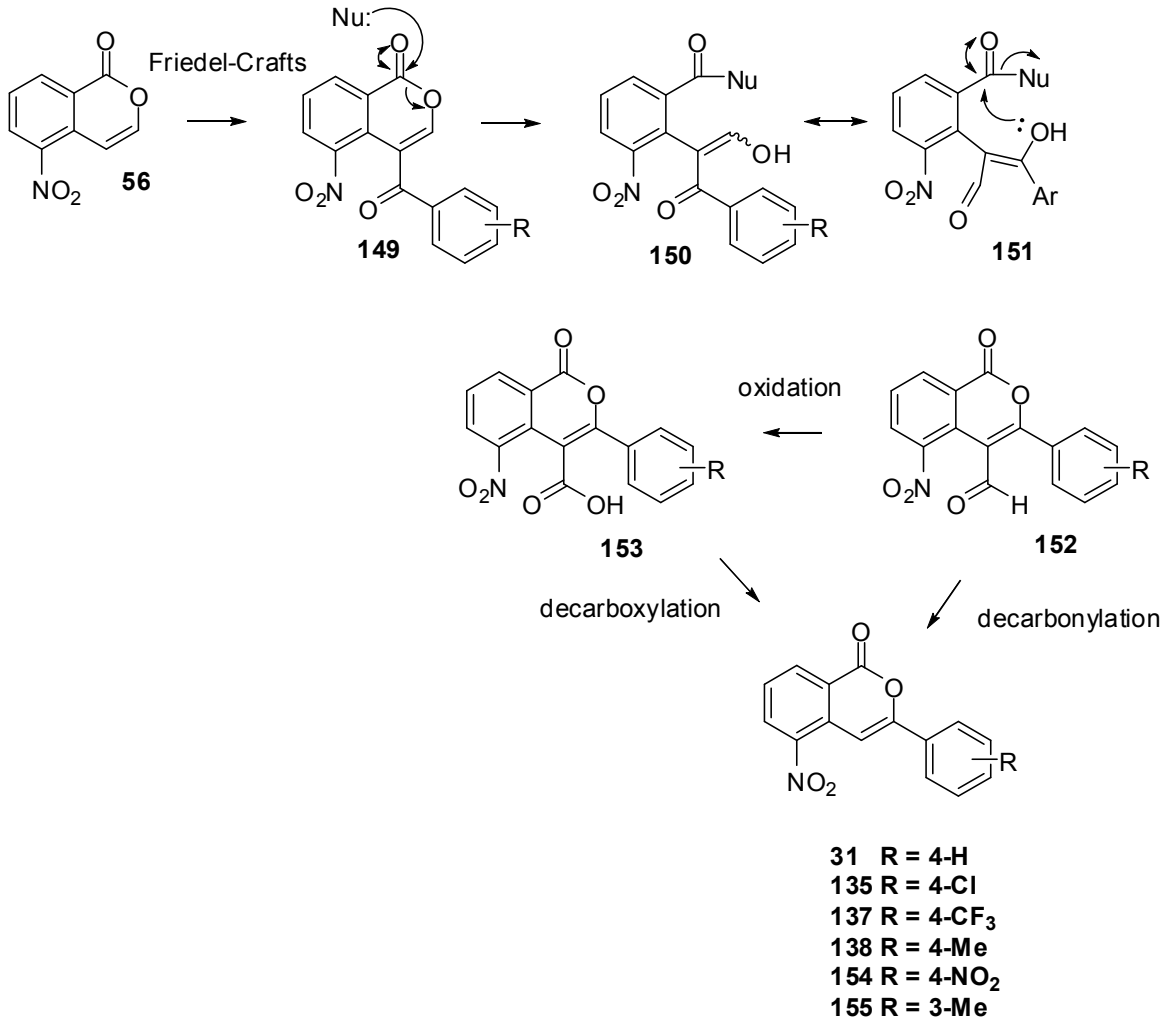

Scheme 33. Proposed mechanism for the formation of **31** following Friedel-Crafts reaction of 5-nitroisocoumarin **56**.

Having proved that the carbon framework of the benzoyl group was incorporated intact rather than the carbonyl detaching from the phenyl group, it was possible to propose a

mechanism for the reaction path, following our previous observations. The initial Friedel-Crafts product **149** is formed as shown by the requirement for forcing conditions and strong Lewis acidity. Next, a nucleophile in the reaction mixture, which could be a triflate or a chloride ion, attacks the ester carbonyl of the isocoumarin giving rise to the enol **150** which can tautomerise to the enol **151**. After cyclisation, the product **31** could be formed either by direct decarbonylation of **152** or by oxidation to the corresponding carboxylic acid **153** and decarboxylation. In view of the literature reports that 6,8-dihydroxy-4-formyl-3-methylisocoumarin is stable in hot aqueous formic acid[163] and that decarboxylations of isocoumarin-4-carboxylic acids have been used synthetically to obtain isocoumarins,[164, 165] a direct decarbonylation is unlikely and initial oxidation then loss of the carboxylic acid unit is more likely. This view is supported by the low yield obtained with the non-oxidising solvent, pentachloroethane (Entry **K**).

Although serendipity had played a part in the discovery of this novel route to 5-nitro-3-arylisocoumarins it was, nevertheless, synthetically useful despite moderate yields. The table below compares the yields obtained with this new reaction with those obtained using the Hurtley route.

Table 4. Comparrison of the chemical yields obtained when various isocoumarins are synthesised by either the Hurtley route or the Friedel-Crafts route.

3-Substiuent and compound number	Yield (% Hurtley from **34**)	Yield (% Friedel-Crafts from **56**)
Ph **31**	78	42
4-MePh **138**	20	37
4-F_3CPh **137**	12	11
4-ClPh **135**	33	29
4-NO_2Ph **154**	0	10
4-MeOPh **156**	60	0
3-Me **123**	23	0

In general, the two routes have similar yields from the starting bromobenzoic acid or isocoumarin but differences exist in the substituents which are tolerated; for example it is

not possible to synthesise 5-nitro-3-(4-nitrophenyl)isocoumarin **154** using the Hurtley route but the Friedel-Crafts route allows this. Conversely, the Hurtley route tolerates alkyl substituents and electron-rich aromatics whereas the new route does not.

3.5.3 Initial SAR with 3-substituted isoquinolin-1-ones

The IC_{50} values of the first series of 3-substituted isoquinolin-1-ones tested are shown in the table below along with the values obtained for 5-AIQ for comparison.

Table 5. Inhibition of the activities of PARP-1 and PARP-2 by 3,5-disubstituted isoquinolin-1-ones and isocoumarins; data for 5-AIQ **5** are shown for comparison

Cpd. No.	Structure	PARP-1 IC_{50} (μM)	PARP-2 IC_{50} (μM)	Selectivity ($IC_{50\ (PARP-1)}$ / ($IC_{50\ (PARP-2)}$)
5	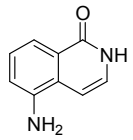	0.94	1.05	0.89
33	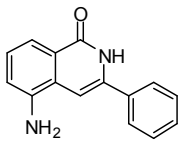	0.72	0.48	1.5
115	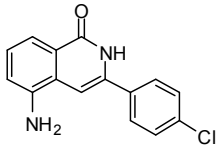	0.19	0.16	1.2
116	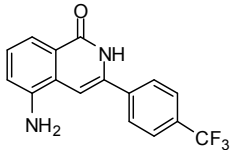	0.27	0.17	1.6
117	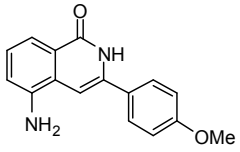	0.50	0.73	0.7
118	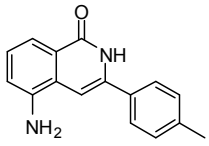	0.06	0.12	0.5

120	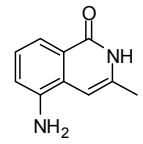	0.19	0.26	0.73
121	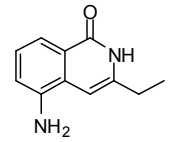	0.45	0.83	0.54
122	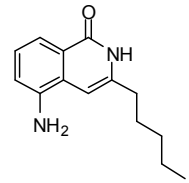	>25000	>25000	-

The first point to note is that the 3-substituted compounds were generally some 10-fold more potent against both PARPs -1 and -2 than the 5-substituted series and also 2-10-fold more potent than 5-AIQ, except in the case of 5-amino-3-pentylisoquinolin-1-one **122**, where all activity was lost. The most potent compound was the 3-(4-methylphenyl)-substituted **118** which was slightly PARP-1 selective and *ca.* 10-fold more potent than the 3-phenyl **33**. Adjusting the electronic configuration of the phenyl ring did not have a significant impact on potency and electron-neutral substituents were preferred. The electron-deficient **116** was slightly more potent than the electron-rich **117** but the 3-(4-chlorophenyl)-substituted **115** showed the greatest potency of the three. It is tempting to speculate that the 3-arylisoquinolin-1-ones show increased potency over 5-AIQ thanks to the bulky aryl substituent occupying a lipophilic-binding pocket in the PARP1/2 active sites. However, the smaller 3-alkyl substituted compounds (3-Me and 3-Et) show a similar level of activity and this casts doubt on the requirement for a sterically large hydrophobic group in this position.

Unfortunately, the series showed very little selectivity for either isoform; however, the significant increase in potency was promising. It was decided that some further examples would be examined; as potent non-isoform-selective PARP inhibitors are useful molecules in their own right and it was plausible that selectivity could be gained by subsequent modifications in other positions.

The most potent PARP-1/2 inhibitor synthesised thus far was 5-amino-3-(4-methylphenyl)isoquinolin-1-one **118**. In order to ascertain if the position of the methyl group on the aromatic ring had any effect on potency or selectivity, the *o*- **157** and *m*- **158** analogues were prepared. In addition, 5-nitro-3-(4-iodophenyl)isocoumarin **159** and the corresponding isoquinolin-1-ones **160** and **161** would be synthesised; the iodo-phenyl function would serve as a starting point for further modifications, if required, through palladium-catalysed chemistry.

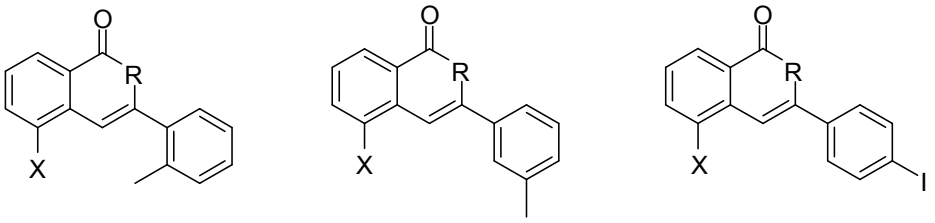

157 X = NH_2 R = NH
162 X = NO_2 R = NH
163 X = NO_2 R = O

158 X = NH_2 R = NH
164 X = NO_2 R = NH
155 X = NO_2 R = O

159 X = NO_2 R = O
160 X = NO_2 R = NH
161 X = NH_2 R = NH

Figure 31. The secondary 3-substituted targets.

The now established Friedel-Crafts-like procedure was used to prepare the next set of isocoumarins. Reaction with ammonia in the usual way gave the isoquinolin-1-ones. Pd/C mediated hydrogenation was used to reduce the nitro group in **162** and **164**. In order to prevent any reductive de-iodination of **160**, tin (II) chloride in EtOH was used as the reducing system, rather than H_2Pd/C. The yields for the three steps are shown in Table 6.

Table 6. Chemical yields obtained when **157**, **158** and **161** were synthesised *via* Friedel-Crafts reaction of **56**.

3-substituent and compound number	% Yield (Friedel-Crafts reaction)	% Yield (Reaction with ammonia)	% Yield (Reduction of Nitro group)	% Overall yield (from **56**)
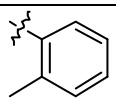 **157**	25	46	56	3
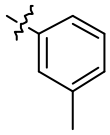 **158**	21	59	62	4
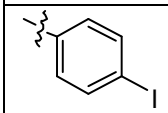 **161**	34	55	51	5

The new compounds were sent for biological evaluation and attention was turned to developing a more efficient route to 3-arylisoquinolin-1-ones as the overall yields for the current routes were poor.

3.5.4 A novel route to 5-amino-3-arylisoquinolin-1-ones

From earlier work, it was known that 1-chloroisoquinolines were precursors to isoquinolin-1-ones. Therefore, compounds with the general structure of **166** would be only two (functional group interconvcersions) FGIs away from the target 3-aryl 5-AIQs **167**. These compounds would be accessible by palladium-catalysed couplings and disconnection of the aryl group would give the dihalide **168**. However, this could present a problem; palladium-catalysed coupling onto this compound may give the disubstituted product **169**, as both halogens are activated by being adjacent to the ring nitrogen. In fact, the two chlorines in 1,3-dichloroisoquinolines show an inherent difference in reactivity and it is reported to be possible to perform selective Suzuki couplings on such molecules[166] to give 1-aryl-3-chloroisoquinolines **170**. Of course, this is opposite to the required regioselectivity of coupling.

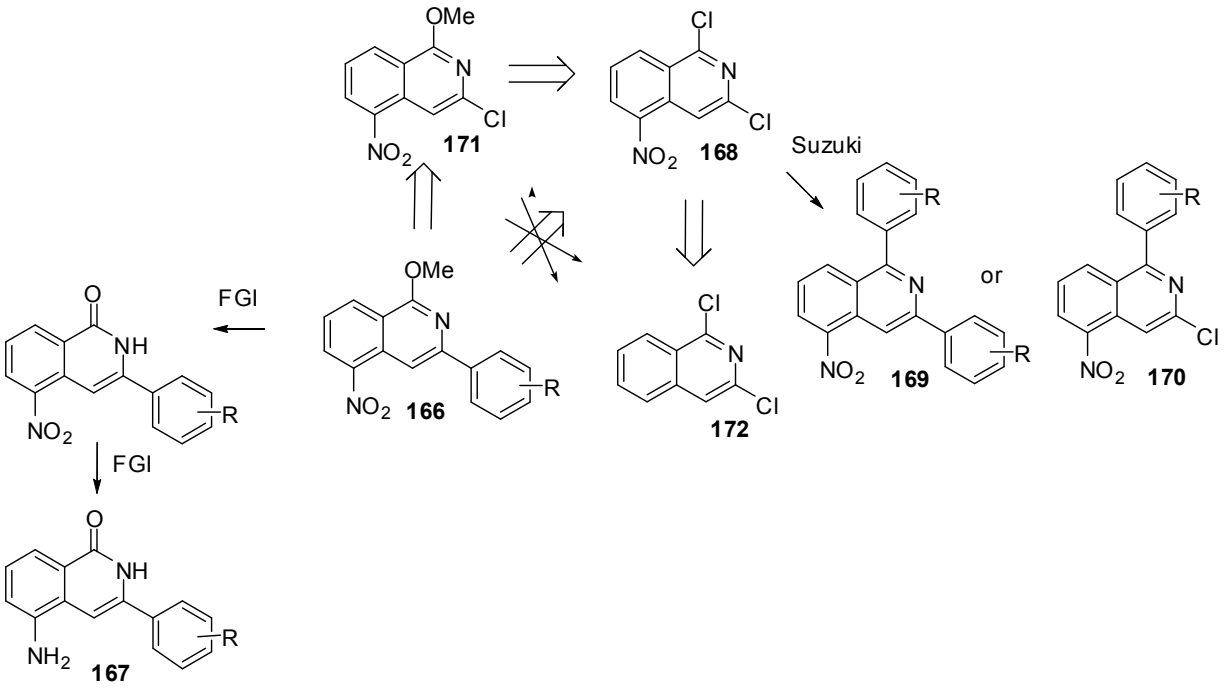

Scheme 34. Retrosynthetic analysis for **167**.

This difference in coupling reactivity was highly likely to remain in 5-nitro-1,3-dichloroisoquinolines however; it may be expected to translate into differences in electrophilic reactivity and thus could be exploited to protect selectively the 1-chloro position as the methoxy lactim **171**. The final disconnection would be the 5-nitro group and we were encouraged by reports that nitration of 1-chloroisoquinoline gave 1-chloro-5-nitroisoquinoline as the sole product in very good yield that selective nitration in the 5-position would be possible.[167, 168] Therefore, the forward synthesis was attempted. Classical nitration of **172** with concentrated nitric and sulfuric acids, ensuring that the isoquinoline was fully protonated in the reaction mixture to deactivate the heterocyclic ring, gave a single product **168**, in excellent yield. The double-doublet, triplet, double-doublet coupling pattern in the ^{1}H NMR spectrum of the product provided evidence that nitration had occurred in either the 8- or 5-positions. The absence of a Nuclear Overhauser Enhancement Spectroscopy (NOESY) interaction between the 4-H and any other protons pointed to the absence of a proton in the 5-position and that electrophilic substitution had occurred here.

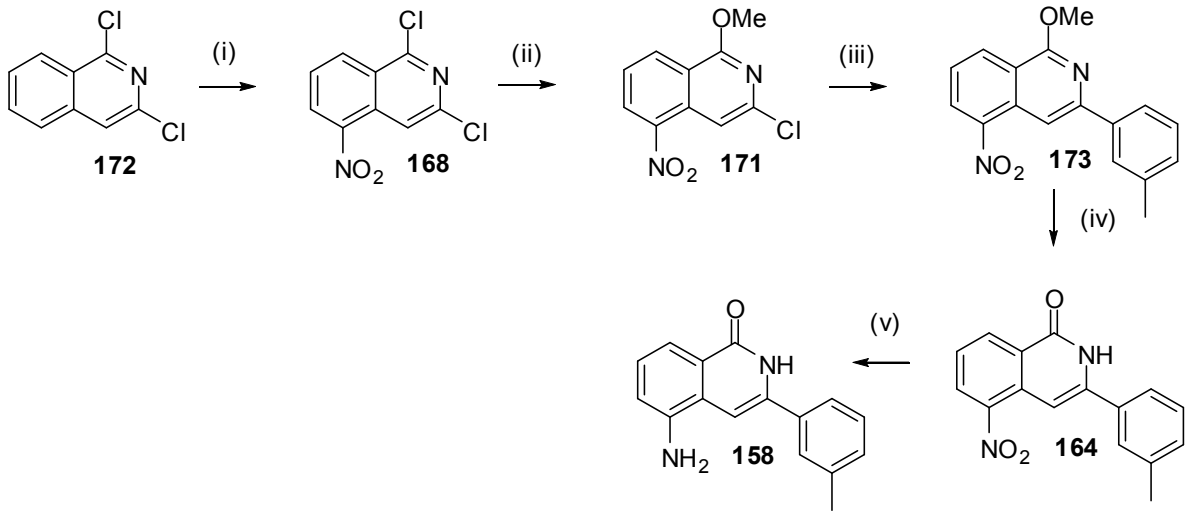

Scheme 35. Synthesis of **158** *via* Suzuki coupling with **171**. (i) HNO_3/H_2SO_4, 91%; (ii) MeOH, Na, 92%; (iii) $Pd_2(dba)_3$, SPhos, K_3PO_4, 3-MePhB$(OH)_2$, toluene, 67%; (iv) HBr, 85%; (v) Pd/C, H_2, 69%; overall yield 33%.

Pleasingly, reaction with sodium methoxide, formed *in situ* in methanol, displaced only the 1-Cl and gave 3-chloro-1-methoxy-5-nitroisoquinoline **171** as the sole product in good yield; none of the unwanted 1,3-dimethoxy-5-nitroisoquinoline or 1-chloro-3-methoxy-5-nitroisoquinoline were formed. This protected 3-chloro-5-nitroisoquinolin-1-one was a suitable substrate upon which to perform palladium-catalysed couplings. An initial Stille coupling with tetramethyltin and tetrakis(triphenylphosphine) palladium in DMF failed and attentions were turned to the Suzuki-coupling.

In order to evaluate this new route in comparison with the previously developed Friedel-Crafts-type synthesis, it was decided that **158** would be synthesised and the overall yields would be compared. Compound **171** was treated with 3-methylphenylboronic acid in refluxing toluene using a $Pd_2(dba)_3$/SPhos catalyst system with K_3PO_4 as base. The sole product was **173**, which was obtained in 67% yield. Aqueous hydrobromic acid was chosen to deprotect the lactim to furnish the isoquinolin-1-one, as a literature report had outlined a similar demethylation using this reagent.[169] The deprotection was achieved in excellent yield and the remaining nitro-reduction had been performed previously. The overall yield for the synthesis of **158** from commercially available starting material was 33%, an eight-fold improvement on the Friedel-Crafts-type route. Therefore, a second novel and efficient route has been developed for the synthesis of 3-arylisoquinolin-1-ones in this work. Both routes introduce diversity at a relatively late stage in the synthesis, which is important as the number of repetitive steps is reduced when producing libraries of compounds. It is likely that the route based on the Suzuki coupling will tolerate a wider range of functionality than all other routes (for example, electron-rich, electron-deficient and sterically hindered boronic acids), such is the versatility of this reaction.

3.4.10 Further SAR with 3-arylisoquinolin-1-ones

The biological data for the 3-arylisoquinolin-1-ones **157**, **158** and **161** are shown in Table 7, along with **118** and 5-AIQ for comparison.

Table 7. Inhibition of the activities of PARP-1 and PARP-2 by isomeric 3-(methylphenyl)-5-AIQs and by 3-(4-iodophenyl)-5-AIQ; data for 5-AIQ **5** are shown for comparison

Cpd. No.	Structure	PARP-1 IC_{50} (μM)	PARP-2 IC_{50} (μM)	Selectivity ($IC_{50\ (PARP-1)}$ / ($IC_{50\ (PARP-2)}$)
5	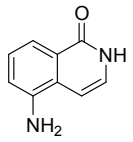	0.94	1.05	0.89
118	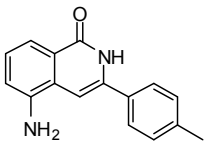	0.06	0.12	0.5
157	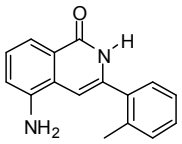	5.68	10.78	0.53
158	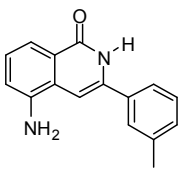	6.15	2.93	2.10

161	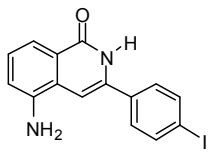	1.14	0.37	3.09

Somewhat unexpectedly, the position of the methyl group on the 3-phenyl ring had a dramatic effect on potency and the *o*- and *m*- derivatives **157** and **158** were some 100-fold less potent against PARP-1 than was **118**. The *p*-iodophenyl **161** showed a similar level of activity against PARP-1 as 5-AIQ but increased potency against PARP-2 rendering it *ca*. 3-fold selective. When compared to the *p*-chlorophenyl derivative **115**, the larger halogen causes a near 6-fold drop in PARP-1 activity and only a 2-fold drop in PARP-2 activity. This suggests that increase bulk in the *p*-phenyl group in the 3-position may be better tolerated in PARP-2. However the 3-*p*-methoxyphenyl **117** and 3-*p*-methylphenyl **118** analogues are slightly PARP-1 selective which contradicts this proposal. A possible explanation for the drop in activity in **157** and **158** is that the lipophilic binding pocket in PARP-1/2 is long and narrow and will therefore tolerate *p*-phenyl-substituents but not *o*- or *m*-.

Due to the lack of selectivity of the 3-substituted isoquinolin-1-ones it was decided that no further examples would be prepared and focus was turned back to the 4-substituted targets.

3.6 4-Substituted isoquinolin-1-ones

Various strategies were employed to attempt to introduce bulky lipophilic substituents to the 4-position of 5-AIQ. The first of these, electrophilic substitution *via* the Friedel-Crafts reaction, was unsuccessful and has been discussed above.

3.6.1 Alkylations and condensations of 2,6-dicyanotoluene

The two literature routes to 5-cyanoisoquinolin-1-one **76** have been discussed above; both of these involve condensations of 2,6-dicyanotoluene **41** and could feasibly be modified, by extension of the methyl group of the substrate, to give 4-alkyl-5-cyano-isoquinolin-1-ones. The first route to be examined was condensation of **41** with ethyl formate and it was postulated that substitution at the benzylic position of the starting dicyano compound, and subsequent reaction under the same conditions, would give the desired products. The methyl group of **41**, which is activated by the flanking nitriles, was deprotonated with lithium bis(trimethylsilyl)amide; this anion was methylated with iodomethane, based on a procedure by Mao and Boekelheide.[170] This process proceeded smoothly in excellent yield; however, the resulting 2,6-dicyanoethylbenzene **174** failed to condense with ethyl formate, even under more forcing conditions.

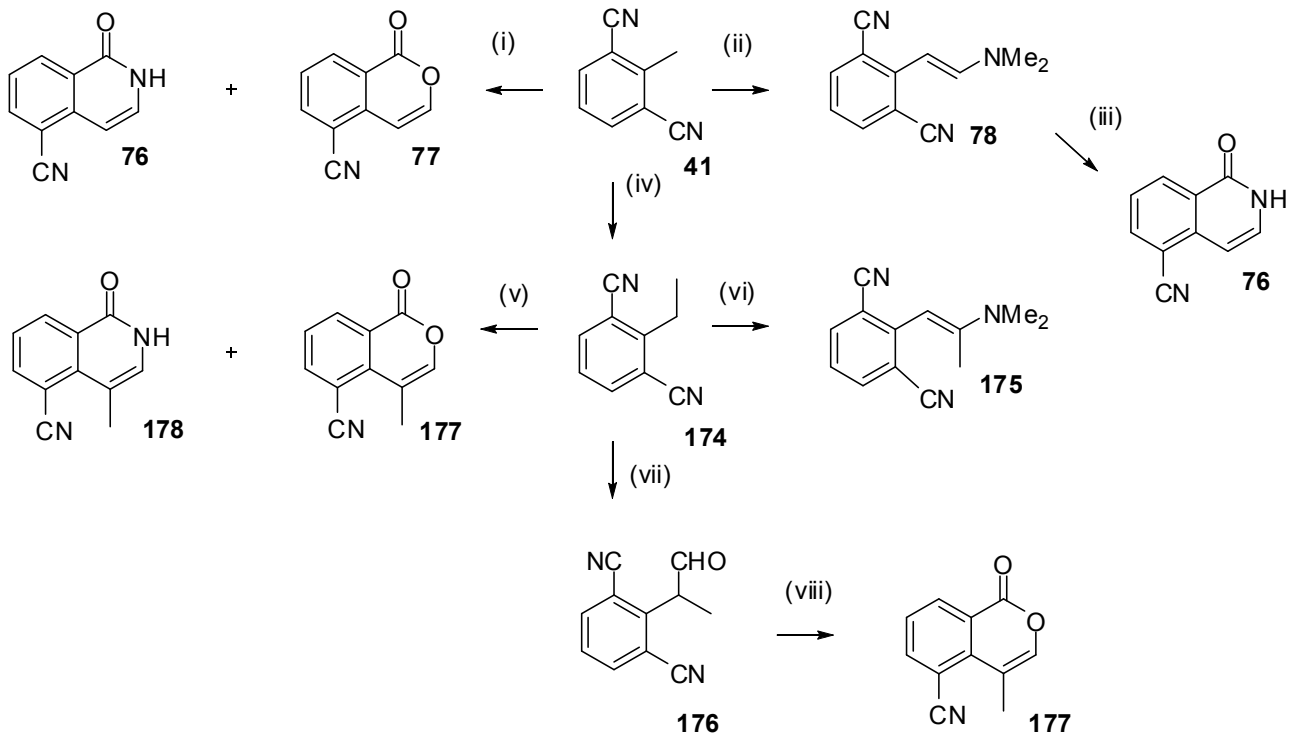

Scheme 36. Synthesis of 5-cyano-4-methylisocoumarin **177**, 5-cyanoisoquinolin-1-one **178** and 5-cyano-isocoumarin **177** from 2,6-dicyanotoluene **41**. (i) KOBu^t, ethyl formate, **76** 14%, **77** 13%; (ii) DMFDMA, 71%; (iii) MeOH, HCl, 55%; (iv) LHMDS, MeI, 94%; (v) KOBu^t, ethyl formate, 0%; (vi) DMFDMA, 0%; (vii) DMFDMA, TsOH, 12%; (viii) diisopropylamine, 13%.

The second synthesis of **76** involved condensation of **41** with DMFDMA to form an intermediate enamine **78**. It was attempted to cause the ethyl analogue **174** to react with DMF/DMA under the same conditions, anticipating the formation of enamine **175**; however, NMR and TLC analysis showed that, despite prolonged reaction times, the starting material remained unchanged. In order to increase the electrophilicity of the "carbonyl" carbon in DMFDMA, a catalytic amount of acid was added to the reaction and the mixture was stirred for a further two days. Separation and analysis of the resulting complex mixture of products by chromatography revealed that, although none of the expected enamine **175** was formed, the corresponding aldehyde **176** was obtained, but in very low yield (12%).

It is likely that the aldehyde is formed from the intermediate enamine by hydrolysis on the slightly acidic silica. This process is analogous to the formation of 5-nitroisocoumarin **56** from methyl 2-(2-dimethylaminoethenyl)-3-nitrobenzoate **55** by passage through a silica column. However, the enol of the aldehyde **176** does not cyclise by nucleophilic attack on the adjacent nitrile carbon, in contrast to the cyclisation of the enol methyl 2-(2-hydroxyethenyl)-3-nitrobenzoate into the adjacent ester carbonyl.

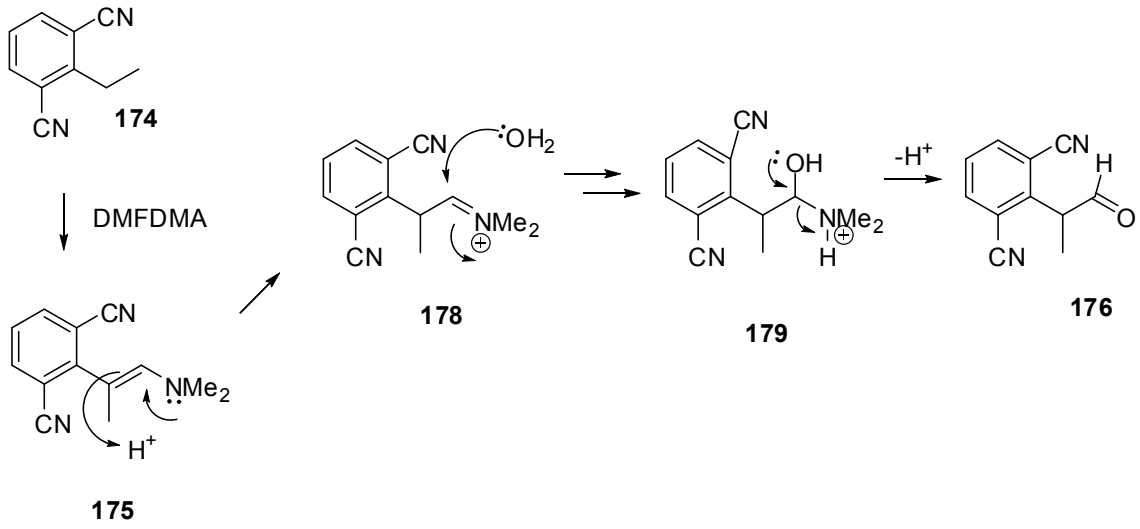

Scheme 37. Proposed mechanism for the formation of the aldehyde **176**.

It was anticipated that formation of the enolate of **176** would result in cyclisation to the isocoumarin **177** upon aqueous workup. This was the case, treatment of **176** with diisopropylamine gave **177** but, again, the yield was disappointing (13%). The ^{1}H NMR spectrum of **177** was interesting, as an allylic coupling was observed between 3-H and the methyl group, with a ^{4}J value of 1.2 Hz. Attempts to convert **177** to the isoquinolin-1-one using the standard protocol failed and alternative routes to the 4-substituted targets were investigated.

3.6.2 Attempted iodination and successful bromination of 5-nitroisoquinolin-1-one

The 4-position of 5-nitroisoquinolin-1-one is the most nucleophilic (see above). This electronic difference had already bee n exploited in forming 4-acyl-5-nitroisoquinolin-1-one and it was feasible that other electrophilic substitution reactions, such as acid-catalysed bromination or iodination, would be possible. As the ultimate aim was to perform palladium-catalysed couplings upon the 4-halo-isoquinolinone, the preferred 4-substituent was iodine as this is a potentially better leaving group than is bromine. Unfortunately, treatment of **56** with iodine in acetic acid gave only starting material, even after heating at 100°C for 24 h, and the same was true when the more electrophilic N-iodosuccinimide was employed as the iodinating agent. At this point, a switch to bromine was considered; bromine is more electrophilically reactive than is iodine and Horning *et al.*[171] had reported that treatment of 2-methyl-5-nitroisoquinolin-1-one **180** with one molar equivalent of bromine at room temperature gave a 1:1 mixture of 4-bromo-2-methyl-5-nitroisoquinolin-1-one **181** and the bromohydrin 4-bromo-3-hydroxy-5-nitroisoquinolin-1-one **182**, upon aqueous workup.

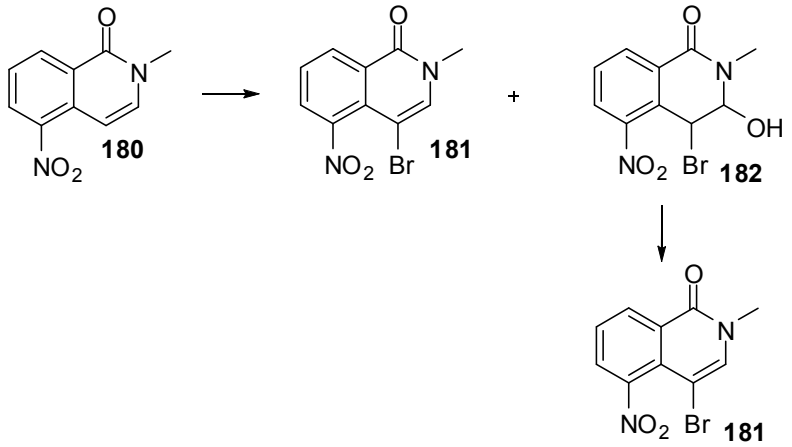

Scheme 38. Bromination of 2-methyl-5-nitroisoquinolin-1-one **180**, as reported by Horning.[171]

The group noted that **182** could be dehydrated to **181** when heated to its melting point. As it was unlikely that substitution at the 1-position would affect the reaction pathway (all Horning's reactions were conducted using N-alkylated isoquinolin-1-ones), the reaction of 5-nitroisoquinolin-1-one **38** with bromine under the same conditions was attempted.

This gave the anticipated mixture of 4-bromo-5-nitroisoquinolin-1-one **49** and 4-bromo-3-hydroxy-5-nitroisoquinolin-1-one **183**, upon aqueous workup. Upon heating the bromohydrin **183** to its melting point, **49** was obtained and the overall yield was a satisfactory 53%.

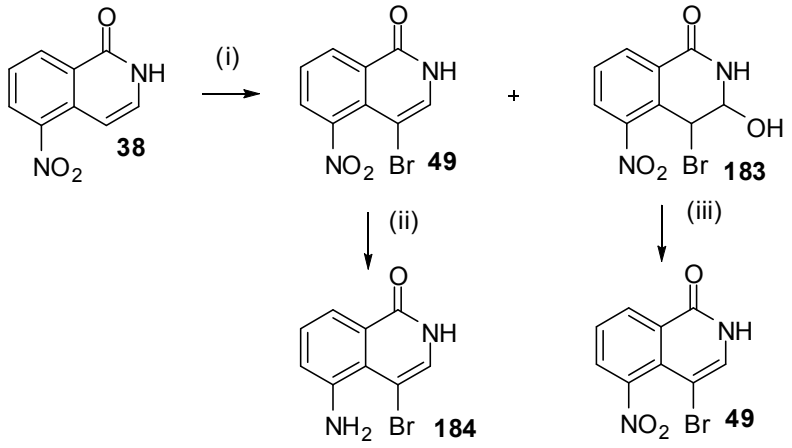

Scheme 39. Bromination of **38** to form **49** and reduction of the nitro function. (i) Br_2, AcOH; (ii) $Sn(II)Cl_2$, EtOH; (iii) Heat.

A slight variation in reaction conditions (heating a concentrated solution at 60°C for 16 h) resulted in precipitation of the desired product **49** upon cooling, whilst the bromohydrin remained in solution. This variation caused the overall yield to increase to 66% and the vast majority of **49** was isolated without the need for column chromatography.

3.6.3 Attempted palladium and copper-catalysed cross-couplings with 4-bromo-5-nitroisoquinolin-1-one

The following cross-couplings were now attempted:

- Suzuki
- Stille
- Ullman

The first of these was the Suzuki coupling; compound **49** was treated with with phenylboronic acid in DMF, with sodium carbonate as base and tetrakis(triphenyl-phosphine)palladium ($Pd(Ph_3P)_4$) as catalyst, over a range of temperatures (80-150°C). Only starting material was recovered and it was reasoned that the bulky nitro group, adjacent to the bromine, was causing sufficient steric hindrance to prevent the coupling from taking place. Therefore, the nitro function was reduced to the leaner amino group using tin(II) chloride, prior to performing the coupling reactions. The use of hydrogen in the presence of palladium metal was avoided in order to avoid any reductive debromination of **49**. The Suzuki reaction was then repeated with **184** as starting material but this compound also failed to react

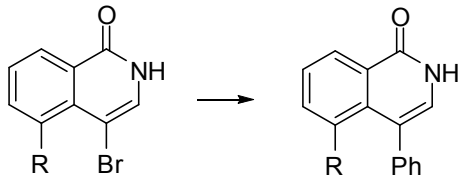

Scheme 40. Attempted Suzuki cross-couplings of **49** (R = NO_2) and **184** (R = NH_2).

A change in conditions was required and Barder et al.[172] had reported a series of Suzuki couplings using extremely hindered aryl halides and phenyl boronic acids, in high yields. The group attributed the success of these transformations to the use of the novel ligand, 2-(2',6'-dimethoxybiphenyl)-dicyclohexylphosphine (SPhos) **185**. Encouraged by these reports, the Suzuki reaction was repeated using Barder's conditions. **49** or **184** were stirred with tris(dibenzylideneacetone)dipalladium (Pd_2dba_3)/SPhos, potassium phosphate (K_3PO_4) and two equivalents of phenyl boronic acid, in DMF or toluene. No reaction took place and, as a result, our attentions turned to the Stille cross-coupling. **49** and **184** were both treated with tetraphenyltin and catalytic $Pd[Ph_3P]_4$ in DMF but the only products isolated were the starting aryl halides or small quantities of debrominated material.

The Ullmann reaction involves the condensation of two aryl halides in the presence of an excess of copper powder or copper (II) salts at high temperature. The exact mechanism for the reaction is unknown but it is likely the process involves the formation of a Ar-

Cu(I) species which undergoes oxidative addition with one equivalent of aryl halide and then reductive elimination to give the biaryl. It was hoped that the high temperature required for the Ullmann coupling would render the 4-bromoisoquinolin-1-ones **49** and **184** reactive. However, no coupling took place and only a mixture of debrominated and starting material was recovered even after heating to 180°C for 3 d.

The failure of **49** or **184** to undergo organometalic cross-couplings meant that an alternative approach must be sought and the first of these was *via* lithiation of a protected derivative of **49**.

3.6.4 Synthesis of 4-bromo-1-methoxy-5-nitroisoquinoline

It was rationalised that **49** could undergo lithium-for-bromine exchange, allowing the formation of 4-substituted compounds by treatment with appropriate electrophiles. However, the presence of an exchangeable lactam proton was a concern, as it was conceivable that self-quenching could occur, depending on the relative rates of lithium-bromine exchange *versus* proton abstraction. In order to circumvent this problem, the protection of the lactam as a methoxy-lactim was proposed. A report in the literature[169] outlined the conversion of 4-bromoisoquinolin-1-one **186** to 4-bromo-1-methoxy-isoquinoline **187** by treatment of **186** with Vilsmeier's reagent to form the 1-chloro derivative **188**, followed by treatment with sodium methoxide (the final conversion was also very similar to the conversion of 1,3-dichloro-5-nitroisoquinoline to 3-chloro-1-methoxy-5-nitroisoquinoline which had earlier been achieved in high yield).

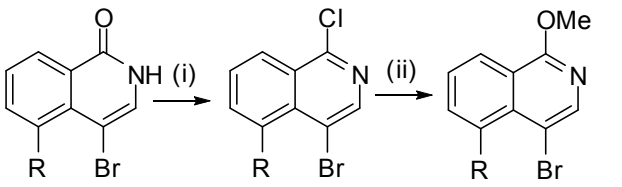

49 R = NO_2
186 R = H

188 R = H
189 R = NO_2

46 R = NO_2
187 R = H

Scheme 41. Synthesis of 4-bromo-1-methoxy-5-nitroisoquinoline **46**. (i) DMF, oxalyl chloride, 89%; (ii) MeOH, Na, 82%.

Pleasingly, it was found that this protocol could be extended to the 5-nitro analogues and 4-bromo-1-chloro-5-nitroisoquinoline **189** was formed in very good yield (89%) following the reported procedure. Displacement of the chlorine with methoxide to **46** was unexpectedly slow (3 d) and low yielding (56%) when sodium methoxide was added as a solid to the reaction mixture. A significant reduction in reaction time (16 h) and yield (82%) was achieved when sodium methoxide was formed *in situ*, as per the earlier synthesis of 3-chloro-1-methoxy-5-nitroisoquinoline **171**.

3.6.5 Lithiations of 4-bromo-1-methoxy-5-nitroisoquinoline

The protected lactam **46** was treated with butyllithium (BuLi) at -78°C in order to form the anion at the 4-position; this carbanion was quenched with iodomethane. ^{1}H NMR and TLC analysis of the crude material showed a complex mixture of products which were purified by column chromatography. It was possible to isolate the desired 1-methoxy-4-methyl-5-nitroisoquinoline **190** in very low yield (9%).

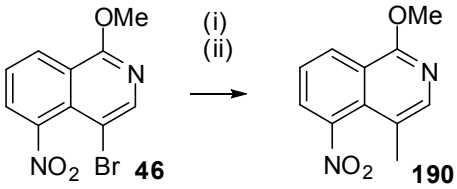

Scheme 42. Synthesis of **190** *via* lithiation of **46**. (i) *n*-BuLi , THF; (ii) MeI, 9%.

Unfortunately, the protocol could not be extended to the use of other electrophiles and this, along with the poor yield of the first reaction, led us to examine other routes.

3.6.6 Palladium-catalysed cross-couplings with 4-bromo-1-methoxy-5-nitroisoquinoline

It had initially been proposed that steric hindrance had prevented any palladium-catalysed cross-coupling involving **49** from taking place. However, there are numerous examples in the literature of high-yielding Suzuki cross-coupling reactions between extremely hindered substrates. One example is the reaction of the boronic acid **191** with the aryl halide **192** to form **193**, which was achieved in 93% yield.[172]

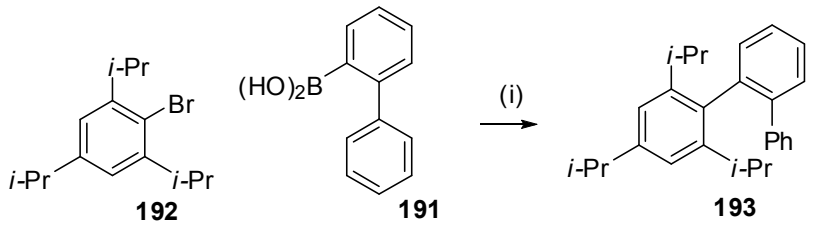

Scheme 43. Reported synthesis of the hindered biaryl **193** *via* Suzuki cross-coupling.[172] (i) $Pd_2(dba)_3$, SPhos, K_3PO_4, toluene, 93%

Therefore, it was thought that the protected lactam **46** may be a suitable candidate for Suzuki coupling and that the change in electronic distribution and solubility compared to **49** may bring a change in reactivity.

This was the case, as **49** was caused to react with phenylboronic acid under the now standard Suzuki reaction conditions ($Pd_2(dba)_3$, SPhos, K_3PO_4, toluene, 100°C) and gave **194** as the sole product in very good 86% yield. Conversion to the 5-aminoisoquinolin-1-one **195** was straightforward in two steps using the established procedures of

demethylation with hydrobromic acid to give **196** then palladium-catalysed reduction of the nitro function with hydrogen.

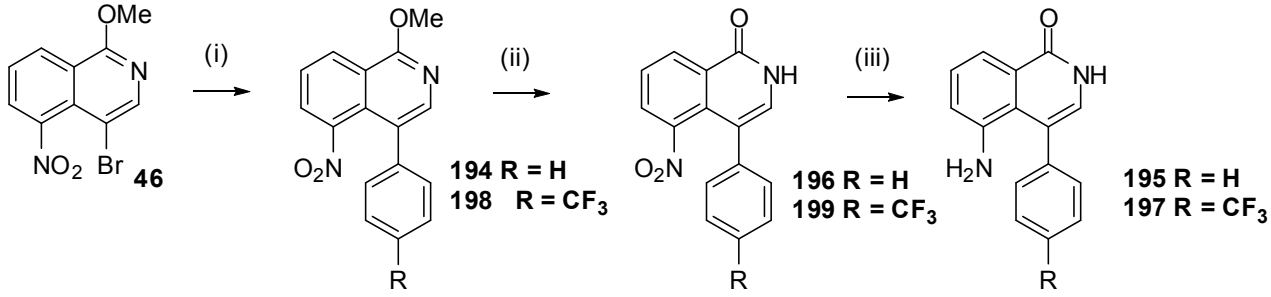

Scheme 44. Synthesis of **195** and **197**. (i) $Pd_2(dba)_3$, SPhos, K_3PO_4, $ArB(OH)_2$, toluene, **194** 86% and **198** 81%; (ii) HBr, **196** 65% and **199** 65%; (v) Pd/C, H_2, **195** 51% and **197** 53%.

Also required was the *p*-trifluoromethylphenyl derivative **197** and this was to be prepared using the same three-step synthesis. It was pleasing that the yield of the Suzuki reaction was only slightly affected (reduced by 5%) when the electron-deficient 4-trifluoromethylphenylboronic acid was employed as reactant. As electron-deficient boronic acids are less nucleophilic than their electron-rich counterparts, they undergo transmetallation more slowly. Additionally, they are more prone to homocoupling.[173]

The final 4-aryl compound to be synthesised in this series was the electron-rich *p*-methoxyphenyl analogue **200**. It would not be possible to prepare this by the route that had been developed, as the deprotection step would also result in the demethylation of the methoxy substituent. A different form of protection was required and the formation of the benzyloxylactim was preferred. This would allow deprotection of the lactam and reduction of the nitro group in one step *via* catalytic hydrogenation. The lactim was prepared by first forming the anion of benzyl alcohol with sodium hydride in DMF then adding **189** in solution in DMF and refluxing for 16 h.

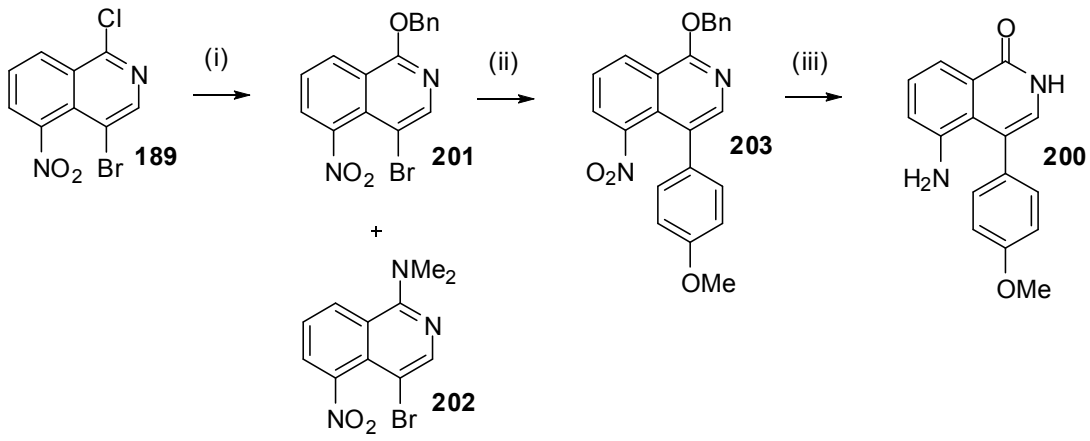

Scheme 45. Synthesis of **200**. (i) BnOH, NaH, DMF, **201** 71% and **202** 12%; (ii) $Pd_2(dba)_3$, SPhos, K_3PO_4, 4-MeOPhB$(OH)_2$, toluene, 61%; (iii) Pd/C, H_2, 47%.

The benzyl ether **201** was formed in good 71% yield and a small amount of the side product **202** was also isolated. It is likely that this was formed from dimethylamine, itself formed by decompositon of DMF, reacting at the electrophilic 1-C in **189**. The Suzuki coupling to **203** was effective and the deprotection / reduction proceeded in 47% yield, which was adequate especially as two transformations were achieved in a single step.

Following the success of the Suzuki couplings using the novel protected lactam substrates **46** and **201**, it was speculated as to why such difficulties had been encountered with the unprotected molecule **49**. One explanation is that the lactam carbonyl may coordinate to the palladium, rendering it catalytically inactive. Alternatively, the main factor determining reactivity may be solubility in organic solvents. The lactam function renders the molecule much more polar and intramolecular hydrogen bonding reduces solubility in the solvents used in cross-coupling reactions. When this is masked as a lactim, polarity is decreased and solubility in organic solvents is increased.

One factor that was initially considered to be of high importance in determining whether or not a cross-coupling reaction would occur was steric hindrance. It was proposed that

the highly hindered **204** would be synthesised to test the scope of the reaction in terms of larger substrates.

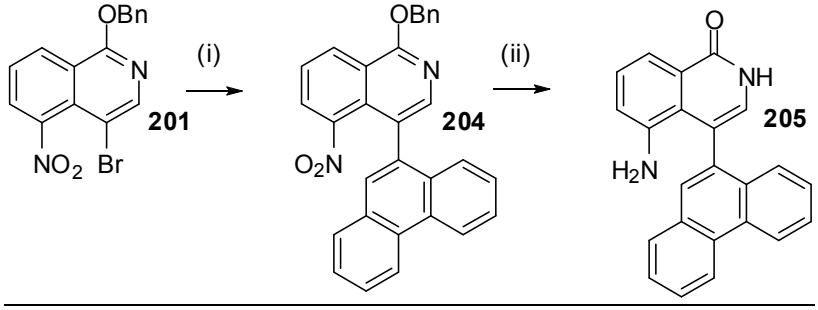

Scheme 46. Synthesis of the hindered **205**. (i) $Pd_2(dba)_3$, SPhos, K_3PO_4 ,phenanthren-9-ylboronic acid, toluene, 42%; (iii) Pd/C, H_2.

Although the yield was significantly lower than for the couplings of the less hindered phenylboronic acids, coupled product **204** was formed in acceptable yield. This was pleasing as the *peri* nitro group is likely to cause significant crowding at the 4-position of the product when adjacent to a group as bulky as a phenanthryl. The selection of couplings performed thus far illustrates the versatility of the Suzuki cross coupling with **46** in that electron-deficient, electron-rich, electron-neutral and now severly sterically hindered boronic acid substrates are tolerated. Crystals were grown in order to confirm the 3D structure of the molecule and this is discussed in a later section.

The deprotection / reduction step appeared to result in conversion to the amine **205**, as shown by mass spectrometry and tlc analysis. However, **205** was insoluble in all solvents suitable for NMR spectroscopic analysis, so full characterisation was not possible. This also meant that the molecule was not suitable for biological evaluation as the PARP-1/2 assays were performed in DMSO.

3.6.7 Stille cross-coupling with 4-bromo-1-methoxy-5-nitroisoquinoline

The low yields and unpredictability of the lithiation reactions of **46** meant that a more efficient route was required for the synthesis of 5-nitro-4-alkylisoquinolin-1-ones was required. Following the success of the Suzuki-coupling, the alkyl version of this reaction was considered but earlier attempts to introduce a benzyl substituent at the 4-position by this method had failed, therefore Stille coupling of **46** with tetramethyltin was attempted. The same tris(dibenzylideneacetone)dipalladium(0)/SPhos catalyst and toluene solvent system (the Stille coupling does not require a base) as the Suzuki reaction were employed. Due to the low boiling point of tetramethyltin (74-75°C), the reaction was conducted at 70°C.

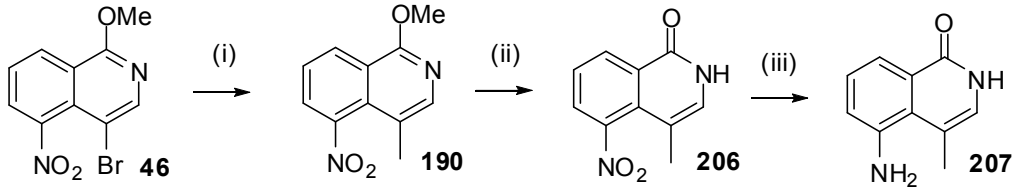

Scheme 47. Synthesis of **207** *via* Stille cross-coupling. (i) Me_4Sn, $Pd_2(dba)_3$, SPhos, toluene, 72%; (ii) HBr, 70%; (iii) Pd/C, H_2, HCl, 65%.

TLC analysis showed the reaction proceeded very slowly and there was incomplete conversion to product after 7 d. Upon workup, only a small amount of starting material was isolated and the yield of 72% was obtained. Conversion to **206** and then the final amino **207** compound was straightforward using the previously established methods.

Although time pressures prevented further investigation of this novel route to 4-substituted isoquinolin-1-ones, it is likely that numerous other aryl, alkenyl, alkyl and allyl substituents will be tolerated as couplings with tetramethyltin are generally more difficult to perform than with other organotin reagents.

3.6.8 SAR with 4-substituted isoquinolin-1-ones

Table 8 shows the biological data for the 4-substituted-5AIQs and 5-AIQ for comparison.

Table 8. Inhibition of the activities of PARP-1 and PARP-2 by 4-substituted isoquinolin-1-ones; data for 5-AIQ **5** are shown for comparison

Cpd. No.	Structure	PARP-1 IC_{50} (μM)	PARP-2 IC_{50} (μM)	Selectivity ($IC_{50\ (PARP-1)}$ / ($IC_{50\ (PARP-2)}$)
5	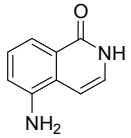	0.94	1.05	0.89
184		0.56	0.22	2.55
207	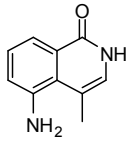	*Not evaluated owing to solubility problems*		-
196	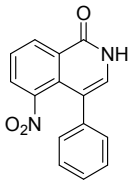	3.80	2.50	1.52
195	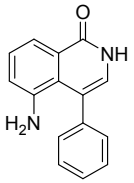	0.52	0.48	1.08
200	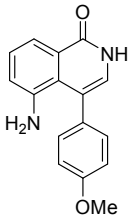	4.70	2.18	2.16

197	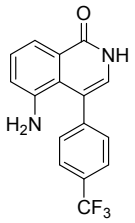	4.11	0.54	7.61
205	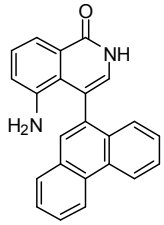	*Not evaluated owing to solubility problems*		-

205 and 207 were not evaluated due to solubility problems in the solvent (DMSO) the assays were performed in. The 4-bromo derivative 184 showed increased potency over both isoforms than 5-AIQ and was slightly (2.5 fold) selective for PARP-2. The 5-nitro-4-phenyl derivative 196 showed activity against both isoforms and was approximately 3-fold less potent than was 5-AIQ; this was expected, as electron withdrawing groups in the 5-position of isoquinolin-1-ones are known to reduce potency.[110] Conversely, 195 was 2-fold more potent than was 5-AIQ against both isoforms. An electron-donating substituent reduced potency against both isoforms but activity against PARP-1 was affected more therefore 200 was *ca.* 2-fold selective for PARP-2. An electron-withdrawing group only reduced activity against PARP-2 very slightly, whilst reducing activity against PARP-1 by a factor of eight, meaning that 197 was 7.6-fold selective for PARP-2.

3.6.9 Buchwald-Hartwig cross-coupling

To investigate further the scope of the cross-coupling reactions possible with **46**, a series of Buchwald-Hartwig reactions were attempted. Thus **46** was treated with a range of phenol derivatives under the standard conditions. The anticipated products would be precursors to compounds that were broadly isosteric to 4-benzylisoquinolin-1-ones which would be of interest as potentially selective PARP-2 inhibitors.

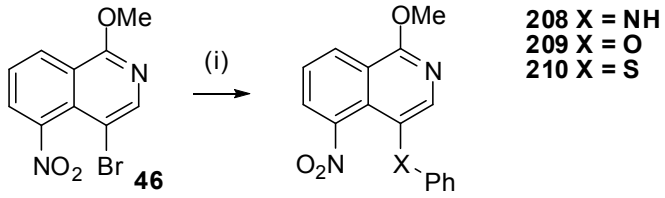

Scheme 48. Attempted Buchwald-Hartwig couplings with **46**. (i) $Pd_2(dba)_3$, SPhos, K_3PO_4, PhXH, toluene. **208** 34%, **209** 0%, **210** 0%.

The sole successful coupling was that between **46** and aniline in low yield. A report[174] that the Pd-ligand and the solvent could have a dramatic effect on the outcome of Buchwald-Hartwig reactions was encouraging and these adjustment of these variables was investigated. The structures of the various ligands that were studied are shown in Figure 32.

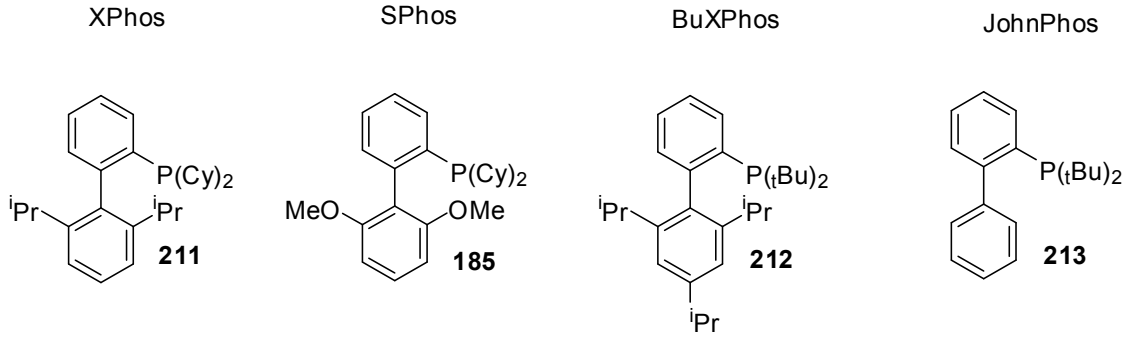

Figure 32. Ligands for the Buchwald-Hartwig reaction. **211** = XPhos, **185** = SPhos, **212** = BuXPhos, **213** = JohnPhos.

The nature of the base can also have a significant influence on outcome of the Buchwald-Hartwig reaction and the use of potassium *t*-butoxide ($KOBu^t$) was investigated. None of the variations allowed that **209** or **210** could be formed but it was possible to increase the yield of **208**.

Table 9 shows the yields obtained when Buchwald-Hartwig reaction conditions with **46** were varied.

Table 9. Chemical yields obtained when reactions conditions were varied in Buckwald-Hartwig couplings of **46** with aniline.

	Toluene / K_3PO_4	DMF / K_3PO_4	Dioxane / K_3PO_4	Toluene / $KOBu^t$	DMF / $KOBu^t$	Dioxane / $KOBu^t$
XPhos **211**	30	36	38	32	38	34
SPhos **185**	32	38	36	34	40	45
BuXPhos **212**	11	5	10	9	9	14
JohnPhos **213**	0	0	0	0	0	0

The ligand JohnPhos was ineffective and this was perhaps due to the fact that this compound is relatively electron-poor in comparison with the other ligands used in this synthesis. Electron-rich ligands tend to hasten the 'oxidative addition' step in palladium-catalysed coupling and tend to perform better in difficult syntheses. BuXPhos was not as effective as SPhos and XPhos and the strong base $KOBu^t$ performed better than K_3PO_4. The optimum conditions were an SPhos/$Pd_2(dba)_3$ catalyst system with $KOBu^t$ as base and dioxane as solvent; these conditions resulted in a 45% yield.

3.7 X-ray crystallography of 1-methoxy-5-nitro-4-phenylisoquinoline (194), 1-(benzyloxy)-4-bromo-5-nitroisoquinoline (201) and 1-(benzyloxy)-5-nitro-4-(phenanthren-9-yl)isoquinoline (204) and methyl 2-(1-oxo-1,2-dihydroisoquinolin-5-ylamino)acetate (214)

A hexane / EtOAc system was used to grow large crystals of **194,** shown in Figure 39.

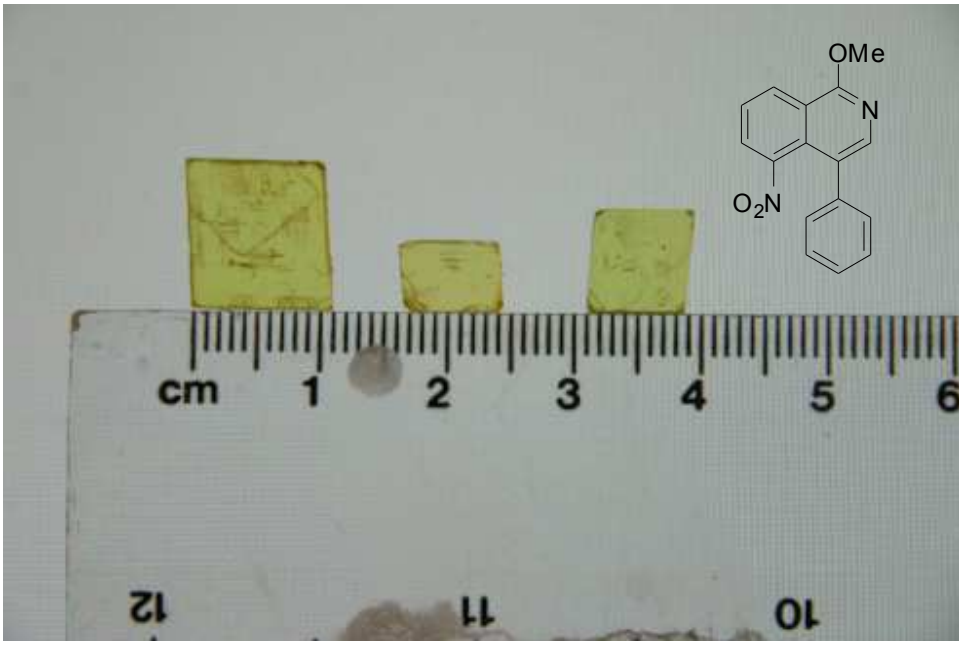

Figure 33. Large crystals of 1-methoxy-5-nitro-4-phenylisoquinoline **194** shown on a ruler.

The X-ray crystallographic structure of **194** is shown in Figure 38.

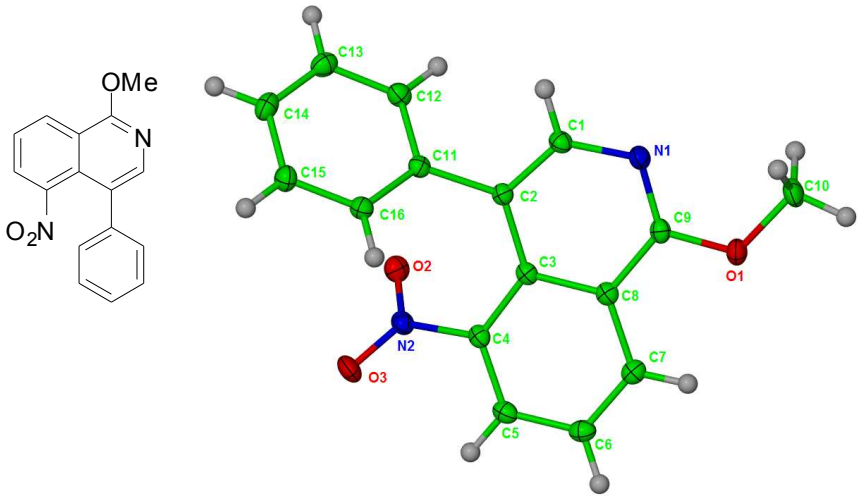

Figure 34. X-ray crystallographic structure of **194**.

The obtained structure confirms the successful Suzuki coupling of **46** with phenylboronic acid despite previous failures with the unprotected lactone **49.** The molecule exists as a monomer in this crystal structure due to the absence of sufficient H-bond donor/acceptor groups. It can be seen that the phenyl ring remains in plane with the isoquinoline core and this would be expected in order that conjugation could occur. The *peri* nitro group is, however, bent out of plane illustrating the steric crowding at the 4,5-positions. As one would expect, the methoxy group points away from the molecule.

The X-ray crystallographic structure of **201** is shown in Figure 35.

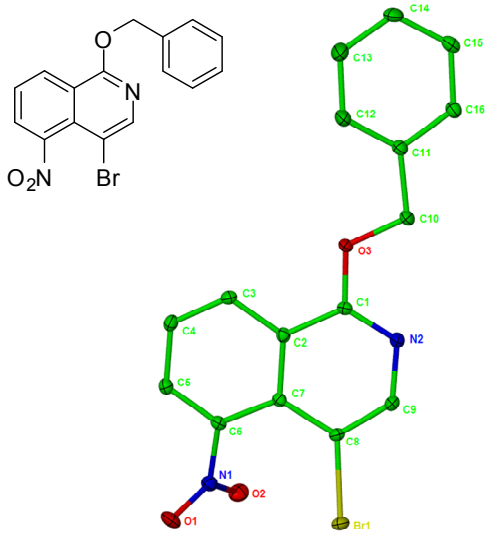

Figure 35. X-ray crystallographic structure of **201**.

The structure confirms the successful protection of **46** as the benzyloxylactim. The molecule is essentially planar with the benzyloxy function pointing away from the core. Again, the nitro group is *peri* to a large group in the 4-position (bromine). This results in the nitro funtion bending out of the plane of the isoquinoline core to a similar degree as observed in the crystal structure of **194** when the 4-substituent was a phenyl group. Akin to **194**, the molecule exists as a monomer in crystalline form.

The X-ray crystallographic structure of **204** is shown in Figure 36.

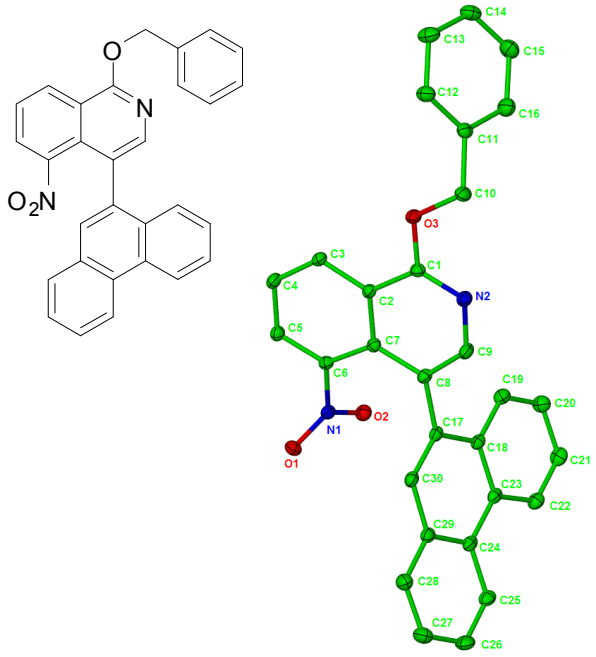

Figure 36. X-ray crystallographic structure of **204**.

This crystal proves the structure of **204** and confirms the successful Suzuki coupling of **201** with the bulky phenanthren-9-ylboronic acid. The severe steric crowding in **204** can be observed in the X-ray crystallographic structure. The presence of the extremely bulky 4-substituent has a profound effect. Both the phenanthrenyl group and the *peri* nitro group are twisted out of plane to the isoquinoline and are parallel to one another. This is in contrast to **194** where the smaller phenyl ring remains in plane and most probably conjugated with the isoquinolinone core but the nitro group is twisted out of plane. It can be observed from the crystal that free rotation of the phenanthrene group is highly unlikely and this would suggest that the molecule exists as a pair of atropisomers. The benzyloxy function points away from the isoquinoline and the molecule is monomeric in this crystalline form.

The X-ray crystallographic structure of **214** is shown in Figure 37.

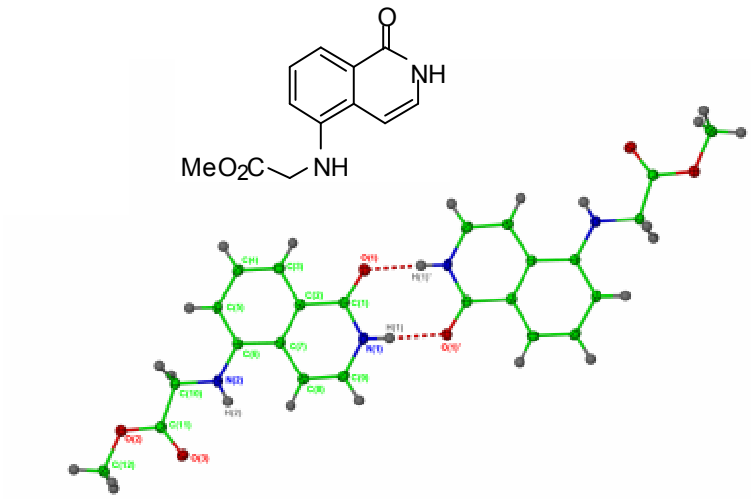

Figure 37. X-ray crystallographic structure of **214**.

Crystals of compound **59** were grown in methanol in order to confirm its structure. Unfortunately this resulted in esterification, probably catalysed by residual HCl in the sample, and formation of the methyl ester **214.** However, the two structures are very similar and it can be observed that in the X-ray crystallographic structure of **214** the compound is a dimer due to the presence of two intermolecular hydrogen bonds. The two lactam hydrogens act as hydrogen bond donors whilst the ring carbonyls act as acceptors. It is likely that these H-bonds are present in most isoquinolin-1-ones and contribute to the high melting points and crystalline structure of these molecules. No H-bonding is observed ester portion of the molecule. The ester groups point away from the isoquinolin-1-one core but remain broadly in plane.

3.8 Disubstituted isoquinolin-1-ones

In general, substituting at the 3- and 4-positions of 5-AIQ had caused an increase in potency against PARP-1/2 and benzoylation at the 5-position had caused an increase in selectivity for PARP-2 over PARP-1. It was hoped that a combination of these modifications in the same molecule would lead to a potent and selective inhibitor of PARP-2. Four compounds would be prepared the 3-methyl-5-benzoyl **215**, 3-phenyl-5-benzoyl **216**, 4-phenyl-5-benzoyl **217** and, to test if substitution in the *p*-position of the benzoyl phenyl ring had any biological effect, **218** would also be synthesised. This set would be screened for actrivity and further examples prepared, if required.

3.8.1 Synthesis of disubstituted isoquinolin-1-ones

The 3- or 4-substituted isoquinoline-1-one core of the molecule would be prepared using the methods established. Therefore 5-amino-3-methlyisoquinolin-1-one **119** was prepared by Hurtley reaction of pentane-1,4-dione with **34**, reaction with ammonia and reduction of the nitro group in the standard way (Pd/C and H_2). The 3-phenyl analogue **33** was prepared by Friedel-Crafts reaction of **56** with benzoyl chloride then conversion to the final amine in the usual way. Finally, the 5-amino-4-phenylisoquinolin-1-one **195** was prepared by Suzuki reaction of **46** with phenyl boronic acid followed by deprotection / reduction as discussed above.

The substituted 5-AIQs were then benzoylated in pyridine using the standard protocol except for **216** were column chromatography was required for purification.

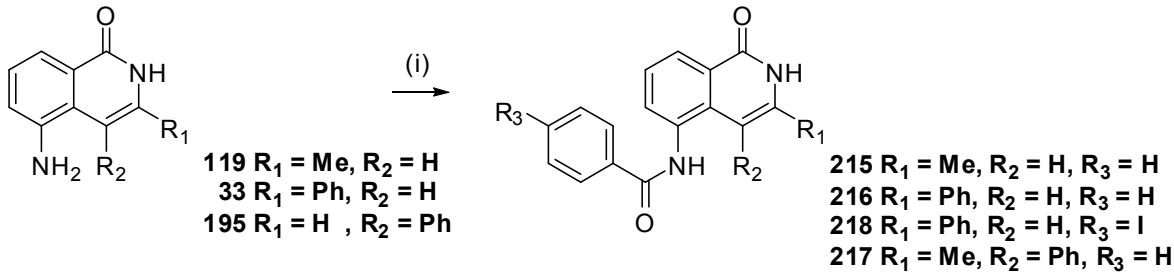

Scheme 49. Synthesis of disubstituted isoquinolin-1-ones. (i) ArCOCl, pyridine.

3.8.2 SAR of disubstituted isoquinolin-1-ones

The chemical yields and biological data for the disubstituted compounds are presented in Table 10.

Table 10. Acylation yields and inhibition of the activities of PARP-1 and PARP-2 by 5-benzamido-3-substituted and -4-substituted isoquinolin-1-ones; data for 5-AIQ **5** are shown for comparison.

Cpd. No.	Structure	Acylation yield	PARP-1 IC_{50} (μM)	PARP-2 IC_{50} (μM)	Selectivity ($IC_{50\ (PARP-1)}$ / ($IC_{50\ (PARP-2)}$)
5	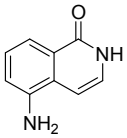	-	0.94	1.05	0.89
215	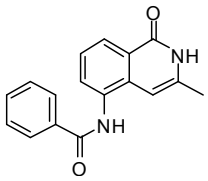	72%	16.6	6.3	2.6
216	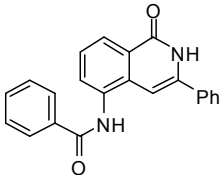	64%	>100	38.3	>2.6

218	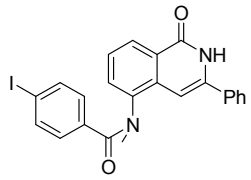	62%	>100	28.4	>3.5
217	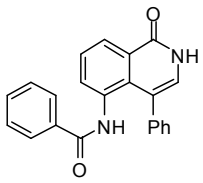	36%	>100	>100	-

The yields obtained following the synthesis of the disubstitued compounds were generally good when using the standard procedure (reaction of the 3- or 4-aryl 5-amino-isoquinoline-1-one with the relevant acid chloride in pyridine). Purification issues caused a drop in the yield of **217** as problems were encountered when attempting to recrystallise the compound and column chromatography was required.

A drastic drop in potency towards PARP-1 was observed with the disubstituted compounds. Unfortunately, this drop was mirrored with PARP-2, although to a lesser extent in **215**, **216** and **218**, which were approximately 3-fold selective for this isoform. The 4,5-disubstituted **217** was devoid of activity against either isoform.

The disappointing lack of potency or significant selectivity of this compound set meant that no further examples were prepared.

3.9 A novel and highly efficient synthesis of 5-AIQ

It has been detailed above that the current routes to 5-AIQ are unsatisfactory. The Polonovski rearrangement is unreliable and low yielding in our hands. The DMFDMA condensation is limited by the necessity for column chromatography, restricting the scale of the reaction and resulting in a low overall yield of 18%. The reductive cyclisation route is multistep; requiring column chromatography at many stages and has a poor overall yield of 9%.

Towards the end of this work, the synthetic route to 5-AIQ was modified, significantly increasing the overall yield and eliminating the need for chromatography. In designing a new and efficient synthesis for 5-AIQ from commercially available starting material, the order of events was important. 1-Chloroisoquinoline **90** can be converted to the corresponding isoquinolin-1-one *via* hydrolysis. The most nucleophilic carbon in isoquinolin-1-one is C4, therefore nitration at the lactam stage would give 4-nitroisoquinolin-1-one and with this in mind we chose to nitrate **90** in which the heterocylic ring is deactivated by the chloro-substituent and electrophilic attack is favoured at C5.

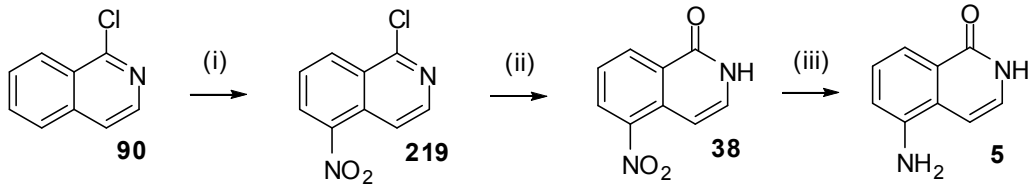

90 **219** **38** **5**

Scheme 50. A novel synthesis of 5-AIQ. (i) HNO_2/H_2SO_4, 92%; (ii) $AcOH/H_2O$, 82%; (iii) Pd/C, H_2, 70%.

This first step proceeded smoothly in the desired 5-position giving **219** in 92% yield. Conversion to the isoquinolin-1-one **38** was achieved by hydrolysis with acetic acid and water. Then catalytic hydrogenation with 10% Pd/C in EtOH and HCl gave 5AIQ:HCl in an overall yield of 53%. The only purification steps required in this synthesis are filtration and recrystallisation, allowing for large scale preparation of this important molecule.

4. MTS Cell proliferation assay

4.1 Background to MTS assay

The MTS cell proliferation assay is a colorimetric assay which is used as a rapid means of assessing the cytotoxicity of a particular compound. The brief principles of the assay are that (3-(4,5-dimethylthiazol-2-yl)-5-(3-carboxymethoxyphenyl)-2-(4-sulfophenyl)-2H-tetrazolium) (MTS), when incubated with phenozine metosulphate and living cells is reduced by mitochondrial reductases to formazan. Formazan is UV active and therefore its concentration can be measured. Cytotoxic compounds reduce the amount of formazan formed and IC_{50} values can be generated by screening a range of concentrations and plotting the data obtained.

4.2 Biological results

A selection of the PARP inhibitors synthesised were screened using the MTS assay and the results are presented in Table 10.

Table 10. Cytotoxicity of selected isoquinolin-1-ones against HT29 human colon carcinoma cells.

Compound No.	Structure	IC_{50} (μM)
5	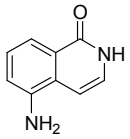	>500
120	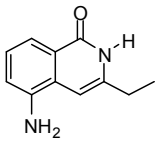	>500
116	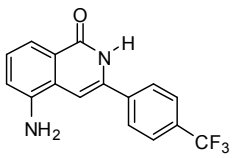	>500

33	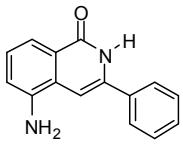	2.2
117	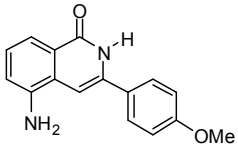	85.2
115	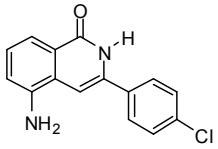	17.9
32	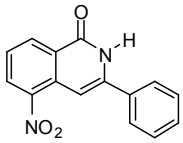	>500
121	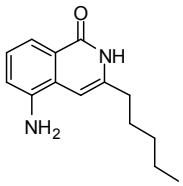	34.0
207	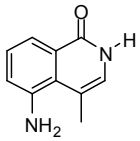	>500
195	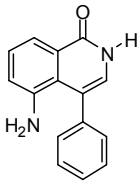	17.9
196	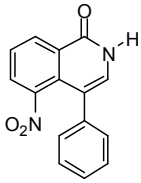	>500
101	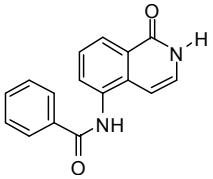	>500

None of the 5-substituted compounds tested were active in the assay. Of the 4-substituted compounds only **195** (IC_{50} = 17.9) was active. Over half of the 3-substituted compounds showed activity and the 3-phenyl **33** (IC_{50} = 2.2) was highly active. Substitution of the phenyl ring caused a reduction in activity and the *p*-trifluoromethylphenyl **117** was inactive. The 3-ethyl **120** was not active but extension of the alkyl chain to 3-pentyl **121** (IC_{50} = 34.0) rendered the molecule active. Activity in the MTS assay did not correspond with PARP-1 or PARP-2 activity which suggests an off-target effect.

5. Conclusions and future work

5.1 Conclusions

The inital aims and objectives of this project were to synthesise a series of 5-substituted isoquinolin-1-ones with carboxylic acids tethered to the 5-position and series of 3- and 4-substituted isoquinolin-1-ones with bulky lipophilic groups in the relevant positions. All synthesised inhibitors would be evaluated for PARP-1 and PARP-2-inhibitory activity. During the course of the work, a further set of 5-substituted compounds were required, based around a selective PARP-2 inhibitor reported in the literature. A final set of disubstituted targets were proposed in the hope that the combined functionalities would lead to potent and selective PARP-2 inhibitors.

The first 5-substituted target isoquinolinone-5-$NHCH_2CO_2H$ **59** was synthesised in acceptable yield by alkylation of 5-AIQ with ethyl bromoacetate, followed by hydrolysis. Problems were encountered in the synthesis of the homologue **61;** treatment of 5-AIQ with methyl propenoate in the presence of sodium hydride resulted in abstraction of the lactam proton and alkylation at the 2-position forming **60**. The isoquinolinone-5-propenoic acid **26** was prepared in in excellent yield using the Heck reaction of **65** with propenoic acid. Reduction to the alkane using Pd/C and H_2 provided another initial target **27**. The acid **28** was prepared following literature precedent by hydrolysis of **76**. Several methods were attempted to synthesise **63** including palladium-catalysed coupling of **75** with either diethyl malonate or ethylacetoacetate and Stille reaction **75** with trimethylallyltin. None of these were successful but the requirement for quantities of 5-bromoisoquinolin-1-one **64** meant that a new synthesis for this molecule was developed. The key step involved the selective installation of bromine in the 5-position of 1-chloroisoquinoline using the swamping catalyst method. This new synthesis was significantly more reliable and efficient than all other published syntheses of **64**.

The initial 5-substituted compounds were evaluated for activity against PARPs-1 and -2. Surprisingly, the most potent PARP-1 inhibitor was **60** which lacked an amide NH. In general, the inhibitors were not selective for either isoform, although **59** and **27** showed a *ca.* 3-fold selectivity for PARP-2 over PARP-1. A further series of 5-acylaminoisoquinolin-1-ones was generated in good yields by treating 5-AIQ with the appropriate acid chloride in pyridine. The biological results from this series were more promising and the inhibitor which showed the highest degree of selectivity (*ca.* 9-fold) for PARP-2 was the unsubstituted 5-benzamidoisoquinolinone **101**. The PARP-2 selective inhibitors **22** and **99** that have been reported in the literature were also evaluated. It was interesting that **22** was 3-fold PARP-1 selective (reported selectivity 4.71 for PARP-2) in our assays. **99** showed *ca*. 3-fold selectivity for PARP-2 in our system, in contrast to the reported 60-fold selectivity.

The initial 3-alkyl and 3-arylisoquinolin-1-ones were prepared using the established route of Hurtley reaction of **34** with the appropriate β-diketone to form the isocoumarin, followed by reaction with ammonia and then palladium-catalysed reduction to the amine. A novel route to 3-aryl-5-nitroisocoumarins by Friedel-Crafts reaction of **56** with various acid chlorides was developed. The reaction was optimised for Lewis acid ($SnCl_4$), reaction temperature (150^oC) and solvent ($PhNO_2$). The scope of the reaction was found to be limited to electron-deficient or electron-neutral acid chlorides. Reaction of **56** with [^{13}C]-carbonyl benzoyl chloride gave **148** in which the ^{13}C is located in the 3-position of the heterocycle, proving that the benzoyl carbon framework is incorporated intact. The yields of this new synthesis were comparable with the Hurtley route and therefore it is synthetically useful. In addition, the Friedel-Crafts route allows for the synthesis of 3-aryl-5-nitroisocoumarins with electron-withdrawing substituents on the phenyl ring (*e.g.* **154**), whereas the Hurtley route does not. However, the Hurtley route allows access to 3-alkyl-5-nitroisocoumarins and the Friedel-Crafts route does not. The Friedel-Crafts route was used to prepare the remaining 3-aryl compounds. A novel route to **158** was developed following the synthesis of 3-chloro-1-methoxy-5-nitroisoquinoline **171** which served as an ideal intermediate for Suzuki coupling with 3-methylphenylboronic acid. The overall yield of this synthesis was much greater than that of the Friedel-Crafts route.

It is likely that this route will allow for later synthesis of a diverse range of 5-amino-3-arylisoquinolin-1-ones due to the versatility of the Suzuki reaction. An attempt to introduce a 3-methyl substituent to **171** using the Stille reaction failed.

The synthesised 3-substituted compounds were assayed for activity against the two PARP isoforms studied. In general both the 3-alkyl and 3-aryl the compounds were between 2- and 10-fold more potent than 5-AIQ against both PARP isoforms but there were some exceptions. All activity was lost with **121** and the position of the methyl group on the 3-phenyl ring had a dramatic effect on potency; the *o*- and *m*- derivatives **157** and **158** were some 100-fold less potent against PARP-1 than **118**. The *p*-iodophenyl derivative **161** was 3-fold selective for PARP-2 but none of the compounds showed any major selectivity.

Several approaches were investigated for the synthesis of 4-substituted 5-aminoisoquinolin-1-ones. Friedel-Crafts reaction of **38** with benzoyl chloride and $AlCl_3$ gave the undesired 2-substituted **145**. A switch to a Brønsted acid catalyst and acetic anhydride gave the desired 4-substituted **146** but all attempts to reduce the ketone failed. Methylation of the carbanion derived from 2,6-dicyanotoluene **41**, followed by condensation with DMFDMA, gave the aldehyde **176** which cyclised to the isocoumarin **177** upon formation of the enolate with diisopropylamine. However, the yields were very low and conversion to the isoquinolin-1-one did not occur when standard protocol was followed. Following the improved synthesis of 4-bromo-5-nitroisoquinolin-1-one **49**, both palladium and copper-catalysed coupling reactions were attempted. These reactions failed, probably owing to poor solubility in the reaction medium, and the protected derivative **46** was prepared. It was possible to form the 4-methyl analogue **190** by lithiation of **46** and treatment with methyl iodide. This procedure did not extend to not extend to other electrophiles and the yield was poor. A much higher yield of **190** was obtained following Stille coupling of **46** with tetramethyltin and conversion to the target isoquinolin-1-one was straightforward. The Suzuki reaction of **46** was employed to synthesise the 4-substituted **195** and **197** in high yields and the structure of **195** was confirmed by X-ray crystallography. Standard Suzuki conditions of $Pd_2(dba)_3$, SPhos,

potassium phosphate and toluene were developed. For the synthesis of **200**, a different protected intermediate was required. This was prepared by reaction of **189** with sodium benzyloxide and the structure of the formed **201** was confirmed by X-ray crystallography. The coupling of **201** and 4-methoxyphenylboronic acid was successfully performed and deprotection and reduction of the nitro group were achieved in acceptable yield in a single step. The scope of the reaction for sterically hindered substrates was tested by the preparation of **204** which was formed in moderate yield. The X-ray crystallographic structure of **204** showed that the 4-substituent and the *peri* nitro group were twisted out of plane to the isoquinoline. A series of Buchwald-Hartwig reactions were attempted with **46** but the only success was with aniline, forming **208**. The reaction was optimised for ligand (SPhos), base ($KOBu^t$) and solvent (1,4-dioxane).

The 4-arylisoquinolin-1-ones were assessed for activity against PARP-1 and PARP-2. Compound **195** was 2-fold more potent than was 5-AIQ against both isoforms and was therefore not selective. A drop in potency against PARP-1 was observed with **200** and also **197** which was *ca.* 8-fold selective for PARP-2.

A short series of 3,5- and 4,5-disubstituted 5-AIQs was generated utilising the chemistry that had been developed throughout this work. Upon biological evaluation it was observed that these modifications caused a drastic drop in potency towards both PARP isoforms. The disappointing biological data meant that no further disubstituted compounds were prepared.

A selection of the synthesised compounds was tested in the MTS cell proliferation assay (HT29 human colon carcinoma cells). Some of the 3-substituted compounds showed low micromolar activity but the 4- and 5-substituted compounds were not active. Activity in this assay was not correlated with PARP-1 or PARP-2-activity, which suggests an off-target effect.

Finally, a new three-step synthesis of 5-AIQ was developed in which the only purification procedures required were filtration and recrystallisation. The overall yield of

this route was considerably higher than all other published routes. In addition, it was also reliable (unlike the Polonowski rearrangement of **51**) and could be performed on large scales (unlike the formation of **56** by reaction of **52** with DMFDMA).

In this work, the chemistry of isoquinolin-1-ones has been significantly advanced. Novel and synthetically useful routes to 3-, 4- and 5-substituted isoquinolin-1-ones have been developed. Biological evaluation of the compounds showed that five had a better selectivity profile for PARP-2 over PARP-1 than the best literature compound **99**, in our assays. It would appear that modifications at the 4- and 5-positions of 5-AIQ are of paramount importance for selectivity.

5.2 Future work

The promising biological activity of many of the compounds synthesised in this project warrants further investigation. Ideally, the compounds should be tested in the same assay systems when comparing inhibitory activity against different PARP isoforms. Therefore, future work could focus on the development of a Flash Plate assay for PARP-2 or, if this was not possible, an ELSIA based assay for PARP-1. It would also be of interest to test the most selective inhibitors of PARP-2 from this project *in vivo*, for example comparing the effect of the inhibitors on PARP activity in cells derived from PARP-1 and PARP-2 knockout mice and also from wild-type mice. These further biological tests would give insights into the true selectivity of the compounds.

It would appear that modifications at the 4- and 5-positions of 5-AIQ are of paramount importance for selectivity. 5-substituted 5-AIQs have been extensively studied and future work could focus on the synthesis of 5-amino-4-arylisoquinolin-1-ones in which the phenyl ring is decorated with electron-withdrawing substituents. Additionally, as only one example has been studied, a further selection of 4-alkyl 5-AIQs could be prepared by Stille reaction of **46** with suitable substrates followed by deprotection and reduction.

The palladium-catalysed chemistry to prepare 3-arylisoquinolin-1-ones from **171** also deserves further investigation as this is likely to be the most efficient and versatile route to these compounds. The activity of some of the 3-arylisoquinolin-1-ones in the MTS assay is interesting and this potential off-target effect could be investigated. It is possible that inhibition of a different PARP isoform causes the observed cytotoxicity, therefore testing this series and further examples in other isoform-specific assays would be of interest.

As the effect of 3,4-disubstitution in isoquinolin-1-ones on PARP inhibitory activity has not been investigated, these compounds could be prepared in future work. This could possibly be achieved by selective bromination of protected 3-alkyl or 3-arylisoquinolin-1-ones followed by palladium catalysed coupling chemistry.

Finally, although the 3,5-disubstituted compounds suffered from a dramatic drop in potency against both PARP isoforms, it was possible to retain some activity against PARP-2 whilst almost abolishing activity against PARP-1. For this reason, a small number of further examples could be prepared in an attempt to improve the potency and selectivity of this series.

6. Experimental

General Procedures

All melting points were determined using a Reichert-Jung Thermo Galen Kofler block and are uncorrected. IR spectra were recorded on a Perkin-Elmer RXI FT-IR spectrometer, either as a liquid (film) or as a KBr disc (KBr). υ_{max} values are given in cm^{-1}. NMR spectra were recorded on either JEOL-Varian GX 270 (270.05 MHz ^{1}H; 67.8 MHz ^{13}C) or Varian Mercury EX 400 (399.65 MHz ^{1}H; 100.4 MHz ^{13}C; 376.05 MHz ^{19}F) spectrometers. Tetramethylsilane was used as an internal standard for samples dissolved in $CDCl_3$ and $(CD_3)_2SO$. Multiplicities are indicated as follows; s (singlet), br (broad singlet), d (doublet), dd (doublet doublet), dt (doublet triplet), t (triplet), q (quartet) and m (multiplet). Coupling constants (*J*) are expressed in Hz. Where indicated, 2-D experiments were used to assign ^{1}H NMR and ^{13}C NMR signals. Mass spectra were Electrospray (ES) at the University of Bath Mass Spectrometry Service using a VG 7070 Mass Spectrometer, the University of Bath Department of Pharmacy and Pharmacology High Resolution Mass Spectrometry Service using a Bruker microOTOF™. Elemental analysis (CHN) was carried out at the School of Pharmacy, University of London, Microanalysis Service. Thin layer chromatography (TLC) was performed on silica gel 60 F_{254}-coated aluminium sheets (Merck) and visualisation was accomplished by UV light (254 nm). Flash column chromatography was performed using silica gel 60 (0.040-0.063 mm, Merck) as the stationary phase.

Reagents were purchased from Aldrich, Lancaster or Acros chemical companies and were used without further purification. Solutions in organic solvents were dried over magnesium sulfate and solvents were evaporated under reduced pressure. Experiments were conducted at ambient temperature, unless otherwise stated.

5-Aminoisoquinolin-1-one hydrochloride (5)

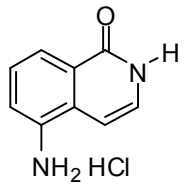

To 5-nitroisoquinolin-1-one **38** (1.6 g, 8.4 mmol) in EtOH (100 mL) and aq. HCl (34%, 4 mL), a slurry of 10% Pd on charcoal (1.0 g) in EtOH (20 mL) was added. The mixture was stirred under H_2 for 2 h. The suspension was then filtered through Celite®. The Celite® pad and residue were suspended in water (600 mL) and heated. The hot suspension was filtered through a second Celite® pad. Evaporation of the solvent and drying gave **5** (1.1 g, 66%) as white crystals: mp 248-252°C (decomp.) (lit.[130] 250-260°C (decomp.)); ^{1}H NMR (D_2O) δ 6.76 (1 H, d, *J* = 7.5 Hz, 4-H), 7.39 (1 H, d, *J* = 7.5 Hz, 3-H), 7.59 (1 H, t, *J* = 8.0 Hz, 7-H), 7.79 (1 H, d, *J* = 8.0 Hz, 6-H), 8.27 (1 H, d, *J* = 8.0 Hz, 8-H).

***E*-3-(1-Oxoisoquinolin-5-yl)propenoic acid (26)**

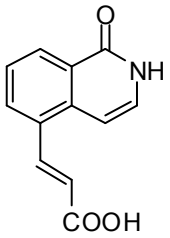

5-Iodoisoquinolin-1-one **65** (200 mg, 0.74 mmol), propenoic acid (0.06 mL, 70 mg, 0.49 mmol), palladium (II) acetate (16 mg, 74 μmol) and triethylamine (0.26 mL, 186 mg, 1.84 mmol) in propanenitrile (0.6 mL) were heated under reflux for 1 h. Hydrochloric acid (2 M, 20 mL) was added and the precipitate was collected and dried to give **26** (152 mg, 97%) as a pale green solid; R_f = 0.05 (hexane / ethyl acetate, 1:1); mp 314-318°C (lit.[131] 315-318°C); ^{1}H NMR ($(CD_3)_2SO$) δ 6.58 (1 H, d, *J* = 15.8 Hz, =$CHCO_2$), 6.74 (1 H, d, *J* = 7.3 Hz, 4-H), 7.30 (1 H, d, *J* = 7.3, Hz, 3-H), 7.52 (1 H, t, *J* = 7.7 Hz, 7-H), 8.10

(1 H, d, *J* = 15.8 Hz, ArCH=), 8.12 (1 H, d, *J* = 7.7 Hz, 8-H), 8.27 (2 H, d, *J* = 7.7 Hz, 6-H), 11.47 (1 H, br s, NH), 12.60 (1 H, br s, CO_2H).

3-(1-Oxoisoquinolin-5-yl)propanoic acid (27)

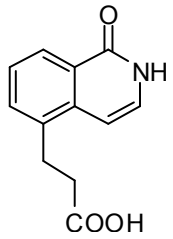

To the alkene **26** (160 mg, 8.4 mmol) in EtOH (20 mL) and aq. HCl (34%, 4 mL), a slurry of 10% Pd on charcoal (100 mg) in EtOH (5 mL) was added. The mixture was stirred under H_2 for 2 h and then filtered through Celite®. Evaporation of the solvent from the filtrate and drying gave **27** (105 mg, 66%) as white crystals: mp 260-263°C; ^{1}H NMR ($(CD_3)_2SO$) δ 2.54 (2 H, t, *J* = 7.8 Hz, ArCH_2), 3.09 (2 H, t, *J* = 7.8 Hz, CH_2COOH), 3.17-3.42 (1 H, br, CO_2H), 6.62 (1 H, d, *J* = 7.4 Hz, 4-H), 7.21 (1 H, br d, *J* = 7.8 Hz, 3-H), 7.38 (1 H, t, *J* = 7.4 Hz, 7-H), 7.55 (1 H, d, *J* = 7.4 Hz, 6-H), 8.07 (1 H, d, *J* = 7.4 Hz, 8-H), 11.29 (1 H, br s, NH); ^{13}C NMR δ 27.4, 34.8, 100.7, 125.1, 125.9, 126.5, 128.9, 132.2, 136.1, 136.3, 162.0, 173.7. MS (ESI +ve) *m/z* 240.0682 (M + Na) ($C_{12}H_{11}NaNO_3$ requires 240.0637); 218.0819 (M + H) ($C_{16}H_{15}N_2O$ requires 218.0817).

1-Oxoisoquinoline-5-carboxylic acid (28)

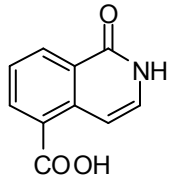

5-Cyanoisoquinolin1-one **76** (427 mg, 2.5 mmol) was heated under reflux with potassium hydroxide in ethanol (20% w/v, 12 mL), under nitrogen, until the production of ammonia ceased (3 d). The mixture was acidified with concentrated hydrochloric acid and the solvent was evaporated. The residue was taken up into methanol and filtered. Concentration of the filtrate gave **28** (0.394 g, 83%) as a white solid; R_f = 0.2

(chloroform / methanol / acetic acid, 100:10:1); mp >300°C (lit.[131] >300 °C); ^{1}H NMR (CD_3OD) δ 7.28 (1 H, d, *J* = 7.7 Hz, 4-H), 7.56 (1 H, t, *J* = 7.7 Hz, 7-H), 7.76 (1 H, d, *J* = 7.7 Hz, 3-H), 8.42 (1 H, d, *J* = 7.7 Hz, 8-H), 8.58 (1 H, d, *J* = 7.7 Hz, 6-H).

5-Nitro-3-phenylisocoumarin (31)

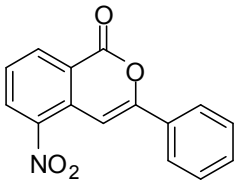

$SnCl_4$ (148.5 mg, 0.57 mmol) was added to **56** (100 mg, 0.52 mmol) in $PhNO_2$ (1.0 mL). After 30 min, benzoyl chloride (140.5 mg, 1.04 mmol) was added and the mixture was stirred at 150°C under Ar for 3 d. The cooled mixture was quenched with ice-water (2.0 mL) and extracted with EtOAc (2 × 20 mL). The combined extracts were washed (NaOH, brine) and dried ($MgSO_4$). Evaporation and chromatography (hexane / EtOAc 15:1) gave **31** (40 mg, 42%) as a pale yellow solid: R_f = 0.57 (hexane/EtOAc 4:1); mp 145-146°C (lit.[158] mp 142-143°C); IR ν_{max} 1739 (C=O), 1626 (C=C), 1525 & 1341 (NO_2) cm^{-1}; ^{1}H NMR δ 7.48-7.51 (3 H, m, Ph 3,4,5-H_3), 7.59 (1 H, t, *J* = 7.8 Hz, 7-H), 7.85 (1 H, brs, 4-H), 7.92 (2 H, m, Ph 2,6-H_2), 8.48 (1 H, dd, *J* = 8.2, 1.2 Hz, 6-H), 8.61 (1 H, ddd, *J* = 8.2, 1.2, 0.8 Hz, 8-H); ^{13}C NMR δ 96.3, 122.3, 125.9, 127.1, 129.0, 131.1, 131.2, 131.6, 131.9, 135.8, 144.2, 156.8, 160.3.

2-Hydroxymercuri-3-nitrobenzoic acid (127)

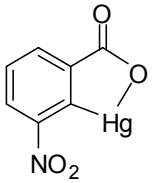

2-Bromo-3-nitrobenzoic acid (34)

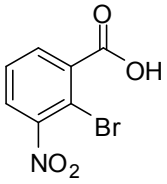

3-Nitrophthalic acid (10.5 g, 50 mmol) in hot aqueous NaOH (10%, 40 mL) was added to $Hg(OAc)_2$ (17.5 g, 55 mmol) in hot AcOH (2.5 mL) and H_2O (70 mL). The mixture was heated at 170°C for 70 h and was then filtered. The precipitate was washed (H_2O, then EtOH) and dried to give 2-hydroxymercuri-3-nitrobenzoic acid **127** as a cream solid. Compound **134** was then heated under reflux in aqueous NaOH (3.5%, 250 mL). Aqueous HCl (2 M, 6 mL) was then slowly added, with vigorous stirring, and the solution was allowed to cool to room temperature. AcOH (3 mL) was then added. The cream precipitate dissolved upon addition of a mixture of NaBr (6.0 g, 59 mmol) and Br_2 (9.5 g, 60 mmol) in H_2O (10 mL). The solution was heated under reflux for 24 h, cooled and neutralised with aqueous NaOH. It was then filtered and acidified (aq. HCl (9 M)). The precipitate formed was filtered, dried and recrystallised (EtOH) to give **34** (9.1 g, 74%) as a white solid: R_f = 0.24 (hexane / EtOAc 1:4); mp 183-185°C (lit.[162] mp 187-188°C); ^{1}H NMR ($(CD_3)_2SO$) δ 7.70 (1 H, t, *J* = 7.9 Hz, 5-H), 7.93 (1 H, dd, *J* = 7.9, 1.5 Hz, 4-H), 8.08 (1 H, dd, *J* = 7.9, 1.5 Hz, 6-H).

5-Nitroisoquinolin-1-one (38)

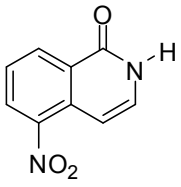

Method A:

Compound **56** (1.5 g, 7.9 mmol) in 2-methoxyethanol (45 mL) was saturated with NH_3 and boiled under reflux for 2 h. The solvent and excess reagent were evaporated until 10 mL remained. The concentrate was stored at 4°C for 16 h and the precipitated crystals

were filtered, washed (H_2O, then EtOH) and recrystallised (EtOH) to give **38** (1.1 g, 73%) as pale yellow crystals: R_f = 0.49 (hexane / EtOAc 2:3); mp 244–246°C (decomp.) (lit.[162] mp 247-249°C); ^{1}H NMR ($(CD_3)_2SO$) δ 6.97 (1 H, dd, *J* = 7.7, 0.7 Hz, 4-H), 7.45 (1 H, dd, *J* = 7.7, 1.8 Hz, 3-H), 7.66 (1 H, t, *J* = 7.7 Hz, 7-H), 8.46 (1 H, dd, *J* = 7.7, 1.5 Hz, 6-H), 8.58 (1 H, ddd, *J* = 7.7, 1.5, 0.7 Hz, 8-H), 11.80 (1 H, brs, NH).

Method B:

1-Chloro-5-nitroisoquinoline **212** (5.00g, 24 mmol) was added to aq AcOH (100 mL) and the mixture was stirred at 100°C for 40 h. The cooled suspension was then poured onto ice; the precipitated crystals were filtered, washed (H_2O) and recrystallised (EtOH) to give **38** (3.74 g, 82%) as pale yellow crystals; data as above.

4-Bromo-1-methoxy-5-nitro-isoquinoline (46)

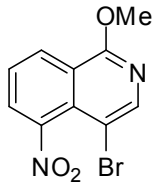

Method A:

Compound **189** (0.78 g, 2.70 mmol) and NaOMe (0.28 g, 4.9 mmol) were heated under reflux in dry MeOH (20 mL) for 3 d. The excess solvent was evaporated until 5 mL remained; the residue was diluted with H_2O and extracted ($CHCl_3$). Evaporation of the solvent and drying gave **46** (0.43 g, 56%) as a yellow solid: R_f = 0.68 (hexane / EtOAc 5:1); mp 154-157°C; ^{1}H NMR ($CDCl_3$) δ 4.18 (3 H, s, OMe), 7.63 (1 H, t, *J* = 7.8 Hz, 7-H), 7.88 (1 H, dd, *J* = 7.8, 1.1 Hz, 6-H), 8.29 (1 H, s, 3-H), 8.48 (1 H, dd, *J* = 7.8, 1.1 Hz, 8-H); ^{13}C NMR δ 54.6, 104.2, 110.0, 121.9, 126.3, 126.9, 128.5, 146.2, 147.0, 160.3; Anal. Found: C, 42.43; H, 2.63; N, 9.69. Calc. For for $C_{10}H_7BrN_2O_3$: C, 42.43; H, 2.49; N, 9.90%.

Method B:

To **189** (5.0 g, 17.4 mmol) in dry MeOH (90 mL) was added finely divided sodium (0.70 g, 31 mmol) and the mixture was heated under reflux for 16 h. The excess solvent was then evaporated until 20 mL remained and the residue was diluted with H_2O and extracted ($CHCl_3$). Evaporation of the solvent and drying gave **46** (4.0 g, 82%): data as above.

4-Bromo-5-nitroisoquinolin-1-one (49)

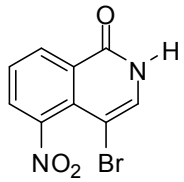

(±)-4-Bromo-3-hydroxy-5-nitro-3,4-dihydroisoquinolin-1-one (183)

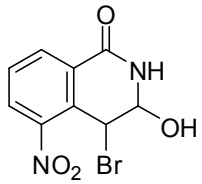

Method A:

Br_2 (0.84 g, 5.3 mmol) in AcOH (1 mL) was slowly added to a suspension of **38** (1.0 g, 5.3 mmol) in AcOH (30 mL). After 2 h, the cooled mixture was poured onto ice H_2O (60 mL) and stirred for 5 min. Extraction (CH_2Cl_2), drying, evaporation and chromatography (hexane/EtOAc 6:1) gave **49** (0.53 g, 37%) as a pale orange solid: R_f = 0.54 (hexane / EtOAc 1:1); mp 229-232°C (lit.[175] mp 233-235°C); ^{1}H NMR ($(CD_3)_2CO$) δ 7.73 (1 H, s, 3-H), 7.77 (1 H, t, *J* = 7.8 Hz, 7-H), 8.10 (1 H, dd, *J* = 7.8, 1.6 Hz, 6-H), 8.61 (1 H, dd, *J* = 8.6, 1.9 Hz, 8-H).

Further elution gave **183** (0.24 g, 30%) as a pale yellow solid: mp 170-172°C (lit.[175]mp 175-177°C); ^{1}H NMR ($(CD_3)_2CO$) δ 5.52 (1 H, dd, *J* = 5.7, 1.2 Hz, 3-H), 6.73 (1 H, d, *J* = 5.9 Hz, 4-H), 7.82 (1 H, t, *J* = 7.9 Hz, 7-H), 8.00 (1 H, dd, *J* = 7.9, 1.5 Hz, 6-H), 8.30 (1 H, dd, *J* = 7.7, 1.5 Hz, 8-H), 8.55 (1 H, br, NH).

Method B:

Br_2 (5.0 g, 31.8 mmol) in AcOH (5 mL) was slowly added to a suspension of **38** (6.0 g, 32 mmol) in AcOH (15 mL). The mixture was heated to 60°C and stirred for 16 h, then cooled and poured onto ice H_2O (60 mL). The precipitate was collected, washed (MeOH) and dried to give **49** (4.5 g, 52%). Also isolated was **183** (2.4 g, 26%) as a pale yellow solid: data as above.

Methyl 2-methyl-3-nitrobenzoate (52).

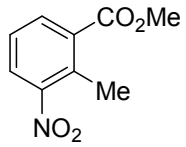

2-Methyl-3-nitrobenzoic acid **57** (10.0 g, 55 mmol) was heated under reflux in MeOH (200 mL) and conc. H_2SO_4 (1 mL) for 48 h, then poured into ice-water (300 mL). The precipitate was filtered, washed (H_2O) and recrystallised (MeOH) to give **52** (10.2 g, 94%) as white crystals; mp 63-64°C (lit.[162] mp 65-66°C); IR ν_{max} 1724 (C=O), 1522 & 1363 (NO_2) cm^{-1}; ^{1}H NMR δ 2.63 (3 H, s, ArMe), 3.94 (3 H, s, OMe), 7.38 (1 H, t, *J* = 8.0 Hz, 5-H), 7.85 (1 H, d, *J* = 7.9 Hz, 4-H), 7.99 (1 H, d, *J* = 7.7 Hz, 6-H).

5-Nitroisocoumarin (56)

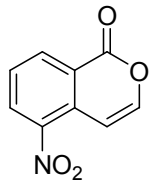

The ester **52** (5.00 g, 25.6 mmol) was heated with dimethylformamide dimethyl acetal (2.5 g, 21 mmol) in DMF (30 mL) at 150°C for 16 h. Evaporation, chromatography (hexane / EtOAc 10:1) and recrystallisation (EtOH) gave **56** (2.6 g, 53%) as pale yellow crystals: R_f = 0.34 (hexane / EtOAc 10:1); mp 171–172°C (lit.[162] mp 171-172°C); IR ν_{max} 1732 (C=O), 1618 (C=C), 1522 & 1342 (NO_2) cm^{-1}; ^1H NMR δ 7.39 (1 H, dd, *J* = 6.0, 0.5 Hz, 4-H), 7.44 (1 H, d, *J* = 6.0 Hz, 3-H), 7.68 (1 H, t, *J* = 8.0 Hz, 7-H), 8.50 (1 H, dd, *J* = 8.0, 1.3 Hz, 6-H), 8.64 (1 H, ddd, *J* = 8.0, 1.3, 0.5 Hz, 8-H).

Ethyl 2-(1-oxo-1,2-dihydroisoquinolin-5-ylamino)acetate (58).

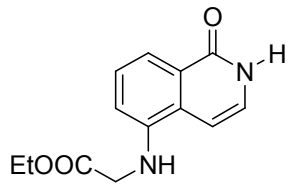

Compound **5** (1.0 g, 4.4 mmol), Pr^i_2NEt (1.4 g, 11 mmol), ethyl bromoacetate (885 mg, 5.3 mmol) and NaI (100 mg, 0.7 mmol) were stirred at 80°C in DMF (60 mL) for 16 h. Evaporation and recrystallisation (MeOH) gave **58** (121 mg, 19%) as buff crystals: R_f = 0.25 (EtOAc / hexane 4:1); mp 199-201°C; IR ν_{max} 3437 (NH), 1728 (C=O), 1654 (C=O) cm^{-1}; ^1H NMR ($(CD_3)_2SO$) δ 1.19 (3 H, t, *J* = 7.2 Hz, Me), 4.01 (2 H, d, *J* = 4.9 Hz, CH_2N), 4.12 (2 H, q, *J* = 7.2 Hz, OCH_2), 6.44 (1 H, t, *J* = 4.9 Hz, CH_2NH), 6.56 (1 H, d, *J* = 7.8 Hz, 4-H), 6.72 (1 H, d, *J* = 7.8 Hz, 3-H), 7.11 (1 H, m, 6-H), 7.22 (1 H, t, *J* = 7.8 Hz, 7-H), 7.46 (1 H, d, *J* = 7.8 Hz, 8-H), 11.2 (1 H, br, NH); ^{13}C NMR δ 14.1, 44.8, 60.4, 99.2, 110.5, 114.4, 125.5, 126.8, 126.9, 127.0, 143.1, 162.0, 171.1. MS (ES +ve) *m/z*

269.0911 (M + Na) ($C_{13}H_{14}N_2O_3Na$ requires 269.0902), 247.1136 (M + H) ($C_{13}H_{15}N_2O_3$ requires 247.1083).

5-(Carboxymethylamino)isoquinolin-1-one hydrochloride (59).

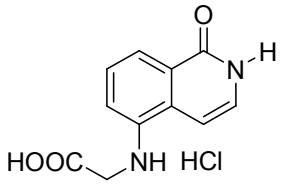

The ester **58** (94.0 mg, 0.39 mmol) was heated under reflux in aq. HCl (17%, 4.0 mL) for 3 h. Evaporation gave **59** (86 mg, 87%) as an amber solid: R_f = 0 (EtOAc); mp 275-280°C (decomp.); IR ν_{max} 3134 (NH), 2523 (OH), 1737 (C=O), 1608 (C=O) cm^{-1}; ^1H NMR ($(CD_3)_2SO$) δ 3.91 (2 H, s, CH_2), 5.23-6.22 (3 H, m, OH, NH_2), 6.58 (1 H, dd, *J* = 7.9, 0.8 Hz, 4-H), 6.72 (1 H, d, *J* = 7.6 Hz, 3-H), 7.10 (1 H, brd, *J* = 7.0 Hz, 6-H), 7.22 (1 H, t, *J* = 8.2 Hz, 7-H), 7.45 (1 H, d, *J* = 7.9 Hz, 8-H), 11.21 (1-H, brs, NH); ^{13}C NMR δ 44.8, 99.2, 110.4, 110.5, 114.2, 135.5, 126.9, 127.0, 143.2, 162.0, 172.5. MS *m/z* 219.0757 (M + H) ($C_{11}H_{11}N_2O_3$ requires 219.0770).

Methyl 3-(5-amino-1-oxoisoquinolin-2(1H)-yl)propanoate (60)

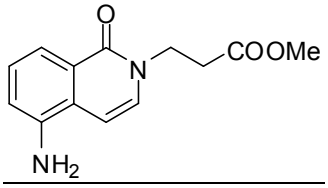

NaH (80 mg, 3.5 mmol) was added to 5 **(0.40 g, 1.8 mmol) in dry THF (40 mL), followed by methyl propenoate (0.17g, 1.9 mmol) and the mixture was stirred for 2 h. Evaporation and recrystallisation (MeOH) gave** 60 **(0.30g, 67%) as pale buff crystals: R_f = 0.35 (EtOAc); mp 188-190°C; IR ν_{max} 3465 (NH), 1715 (C=O), 1674 (C=O) cm^{-1}; ^{1}H NMR ($(CD_3)_2SO$) δ 2.67 (2 H, t, *J* = 7.0 Hz, CH_2CO_2), 4.09 (2 H, t, *J* = 7.0 Hz, NCH_2), 4.36 (3 H, s, CH_3), 5.62-5.91 (2 H, br, NH_2), 6.72 (1 H, d, *J* = 7.5 Hz, 4-H), 6.84 (1 H, d, *J* = 7.5 Hz, 6-H), 7.16 (1 H, t, *J* = 7.8 Hz, 7-H), 7.31 (1 H, d, *J* = 7.4 Hz 3-H), 7.41 (1 H, d, *J* = 7.8 Hz 8-H); ^{13}C NMR (HMBC / HMQC) δ 33.1 (CH_2CO_2), 44.9 (NCH_2), 53.9 (OCH_3), 100.3 (4-C), 114.1 (6-C), 114.8 (8-C), 123.8 (4a-C), 126.4 (8a-C), 127.2 (7-C), 130.6 (3-C), 144.3 (5-C), 161.2 (1-C), 172.6 (COOMe); MS (ES +ve) *m/z* 269.0922 (M + Na) ($C_{13}H_{14}N_2O_3Na$ requires 269.0902), 247.1168 (M + H) ($C_{13}H_{15}N_2O_3$ requires 247.1083).**

3-(5-amino-1-oxoisoquinolin-2(1H)-yl)propanoic acid (62)

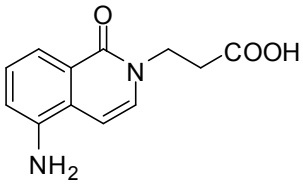

The ester **60** (302 mg, 1.23 mmol) was heated under reflux in aq. HCl (17%, 4.0 mL) for 24 h. Evaporation gave **62** (281 mg, 85%) as an amber solid: R_f = 0 (EtOAc); mp 199-201°C; IR ν_{max} 3240 (NH), 2580 (O-H), 1721 (C=O), 1638 (C=O) cm^{-1}; ^{1}H NMR ($(CD_3)_2SO$) δ 2.68 (2 H, t, *J* = 7.0 Hz, CH_2CO_2), 4.10 (2 H, t, *J* = 7.0 Hz, NCH_2), 5.62-5.91 (2 H, br, 2 × NH), 6.72 (1 H, d, *J* = 7.4 Hz, 4-H), 6.84 (1 H, dd, *J* = 7.8, 1.1 Hz, 6-H), 7.16 (1 H, t, *J* = 7.8 Hz, 7-H), 7.31 (1 H, d, *J* = 7.4 Hz 3-H), 7.41 (1 H, d, *J* = 7.8 Hz 8-H); ^{13}C NMR (HMBC / HMQC) δ 33.1 ($\underline{C}H_2CO_2$), 44.9 ($N\underline{C}H_2$), 53.9, 100.3 (4-C), 114.1 (6-C), 114.8 (8-C), 123.8 (4a-C), 126.4 (8a-C), 127.2 (7-C), 130.6 (3-C), 144.3 (5-C), 161.2 (1-C), 172.6 ($\underline{C}OOH$).MS *m/z* 233.0927 (M + H) ($C_{12}H_{13}N_2O_3$ requires 233.0936).

5-Bromoisoquinolin-1-one (64)

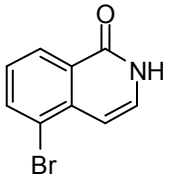

5-Bromo-1-chloroisoquinoline **91** (3.0 g, 12 mmol), AcOH (50 mL) and H_2O (50 mL) were heated to 100°C and allowed to reflux for 48 h. The solution was then allowed to cool and the precipitate was washed (H_2O) and dried to give **64** (1.9g, 70%) as a white solid: R_f = 0.14 (hexane / EtOAc 1:1); mp 240-242°C (lit.[135] 242-244°C); ^{1}H NMR ($(CD_3)_2SO$) δ 6.66 (1 H, d, *J* = 7.2 Hz, 4-H), 7.38 (1 H, d, *J* = 7.1 Hz, 7-H), 7.42 (1 H, d, *J* = 7.2 Hz, 3-H), 8.02 (1 H, d, *J* = 7.1 Hz, 6-H), 8.21 (1 H, d, *J* = 7.1 Hz, 8-H), 11.56 (1 H, br s, NH).

5-Iodoisoquinolin-1-one (65)

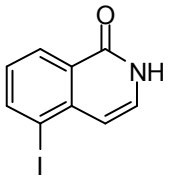

Compound **75** (600 mg, 2.2 mmol) in 2-methoxyethanol (100 mL) was saturated with NH_3 and boiled under reflux for 2 h, then the solvent and excess reagent were evaporated until 5 mL remained. The concentrate was stored at 4°C for 16 h and the precipitated crystals were filtered, washed (H_2O, then EtOH) and recrystallised (acetone) to give **65** (182 mg, 62%) as pale buff crystals: R_f = 0.36 (hexane / EtOAc 2:3); mp 236–244°C (decomp.) (lit.[135] mp 238-244°C); ^{1}H NMR ($(CD_3)_2SO$) δ 6.54 (1 H, d, *J* = 7.3 Hz, 4-H), 7.24 (1 H, t, *J* = 7.8 Hz, 7-H), 7.32 (1 H, d, *J* = 7.3 Hz, 3-H), 8.23 (2 H, m, 6,8-H_2), 11.54 (1 H, br s, NH).

***E*-3-(2-bromophenyl)acrylic acid (70)**

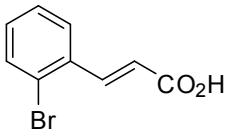

Compound **69** (14.1 g, 50 mmol) was heated under reflux with propenoic acid (4.7 g, 66 mmol), $Pd(OAc)_2$ (111 mg, 0.49 mmol), Et_2N (12.6 g, 124 mmol) in propanenitrile (200 mL) for 1.5 h. HCl (2 M, 800 mL) was then added to the cooled mixture. Filtration of a solution of the resulting precipitate gave the acid **70** (8.5 g, 76%) as a white solid: mp 198-200°C (lit.[135] 202-204°C); ^{1}H NMR δ 6.58 (1 H, d, *J* = 16.2 Hz, 2-H), 7.35 (1 H, dt, *J* = 7.7, 1.5 Hz, Ar 4-H), 7.44 (1 H, t, *J* = 7.7 Hz, Ar 5-H), 7.72 (1 H, dd, *J* = 7.7, 1.5 Hz, Ar 6-H), 7.83 (1 H, d, *J* = 16.2 Hz, 3-H), 7.91 (1 H, dd, *J* = 7.7, 1.5 Hz, Ar 3-H), 12.65 (1 H, br, CO_2H).

_E_-3-(2-bromophenyl)acryloyl chloride (71)

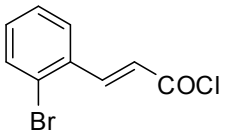

_E_-3-(2-bromophenyl)acryloyl azide (72)

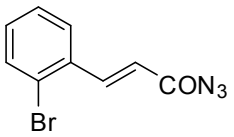

5-Bromoisoquinolin-1-one (64)

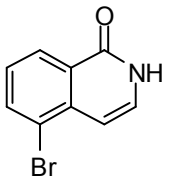

Compound **70** (3.3 g, 15 mmol) was stirred with thionyl chloride (10 mL) and DMF (0.05 mL) for 16 h then the excess reagents were removed by evaporation. The residue (crude **71**) in 1,4-dioxane (5 mL) was added to sodium azide (2.9 g, 44 mmol) in water (6 mL) and 1,4-dioxane (6 mL) over 15 min. The mixture was stirred for 45 min and then diluted

with H_2O (11 mL) extracted with DCM. The dried extract was evaporated to give a residue (crude **64**) which, in DCM (10 mL), was added to boiling bis(2-(2-methoxyethoxy)ethyl) ether (12 mL) in portions. The solution was heated under reflux for 1 h and then cooled. The resulting solid was recrystallised (acetone) to give **64** (0.3 g, 9%) as white crystals: data as above.

5-Aminoisocoumarin (74)

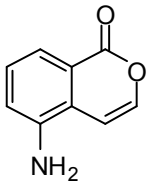

To 5-nitroisocoumarin **56** (1.00g, 5.23 mmol) in THF (100 mL), a slurry of 10% Pd on charcoal (125 mg) in THF (20 mL) was added. The mixture was stirred under H_2 for 2 h. The suspension was then filtered through Celite®. Concentration of the filtrate and drying gave **74** (0.75 g, 89%) as yellow crystals: mp 186-188°C (lit.[176] 185-187°C); ^{1}H NMR ($CDCl_3$) δ 4.02 (2 H, br s, NH), 6.45 (1 H, dd, *J* = 8.0, 0.5 Hz, 4-H), 7.04 (1 H, dd, *J* = 8.0, 1.2 Hz, 6-H), 7.26 (1 H, d, *J* = 8.0 Hz, 3-H), 7.34 (1 H, t, *J* = 8.0 Hz, 7-H), 7.77 (1 H, ddd, *J* = 8.0, 1.2, 0.5 Hz, 8-H).

5-Iodoisocoumarin (75)

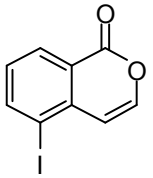

Sodium nitrite (370 mg, 5.33 mmol) in H_2O (30 mL) was added to 5-aminoisocoumarin **74** (1.0 g, 6.2 mmol) in aq. HCl (4.5 M, 36 mL) at 0°C. A solution of KI (1.4g, 8.6 mmol) in H_2O (35 mL) was then added over 10 min. The mixture was stirred for 2 h then extracted with EtOAc. Evaporation and chromatography (hexane/EtOAc 4:1) gave **75** (0.98 g, 58%) as pale yellow crystals: R_f = 0.68 (hexane / EtOAc 4:1); mp 155–156°C (lit.[177] mp 155-156°C); ^{1}H NMR $CDCl_3$ δ 7.31 (1 H, d, *J* = 6.3 Hz, 4-H), 7.36 (1 H, d, *J* =

6.3 Hz, 3-H), 7.60 (1 H, t, *J* = 8.2 Hz, 7-H), 8.41 (1 H, d, *J* = 8.2 Hz, 6-H), 8.56 (1 H, d, *J* = 8.2 Hz, 8-H).

5-Cyanoisoquinolin-1-one (76)

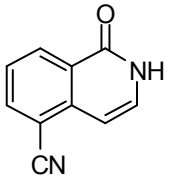

5-Cyanoisocoumarin (77)

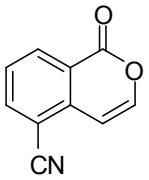

2,6-Dicyanotoluene **41** (1.0 g, 7 mmol) in freshly distilled ethyl formate (25 ml) was stirred at 0-5^{o}C with potassium *tert*-butoxide (4.4 g, 38 mmol) for 25 min. Addition of Et_2O caused a yellow precipitate to form, which was filtered off. The yellow solid was dissolved in water and the solution was acidified with acetic acid, saturated with sodium chloride and extracted with chloroform. The organic extract was dried and the solvent was evaporated. Chromatography (twice) ($CHCl_3$ / EtOAc, 2:1, hexane / EtOAc, 4:1) yielded 5-cyanoisocoumarin **77** (0.33 g, 14%) as colourless crystals: R_f = 0.85 ($CHCl_3$ / EtOAc, 2:1); mp 213-215^{o}C (lit.[131] 212-214 ^{o}C); ^{1}H NMR ($CDCl_3$) δ 6.89 (1 H, d, *J* = 5.7 Hz, 4-H), 7.46 (1 H, d, *J* = 5.7 Hz, 3-H), 7.66 (1 H, t, *J* = 7.7 Hz, 7-H), 8.04 (1 H, d, *J* = 7.7 Hz, 6-H), 8.52 (1 H, d, *J* = 7.7 Hz, 8-H). Further elution gave 5-cyanoisoquinolin-1-one **76** (0.15 g, 6.5%) as a pale yellow solid: R_f = 0.22 (chloroform / ethyl acetate, 2:1); mp 292-294^{o}C (lit.[131] 296-300^{o}C); ^{1}H NMR ($(CD_3)_2SO$) δ 6.60 (1 H, *J* = 7.0 Hz, 4-H), 7.47 (1 H, d, *J* = 7.0 Hz, 3-H), 7.63 (1 H, t, *J* = 7.7 Hz, 7-H), 8.26 (1 H, d, *J* = 7.7 Hz, 6-H), 8.47 (1 H, d, *J* = 7.7 Hz, 8-H), 11.72 (1 H, bs, NH).

5-Bromo-1-chloroisoquinoline (91)

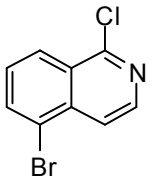

$AlCl_3$ (5.0 g, 37 mmol) and 1-chloroisoquinoline **90** (4.0 g, 24 mmol) were heated to 160°C until molten. Br_2 (5.9 g, 37 mmol) was then added, slowly over 5 h through a sintered condenser. The mixture was allowed to stir for a further 30 min, then allowed to cool and poured onto ice. Extraction (Et_2O), drying and evaporation and washing (MeOH) gave **91** (3.8 g, 65%) as an off-white solid: R_f = 0.68 (hexane/EtOAc 9:1); mp 158-160°C (lit.[145] 159-160°C; ^{1}H NMR ($CDCl_3$) 7.54 (1 H, t, *J* = 8.2 Hz, 7-H), 7.98 (1 H, d, *J* = 5.9 Hz, 4-H), 8.01 (1 H, d, *J* = 8.0 Hz, 6-H), 8.34 (1 H, d *J* = 8.0 Hz, 8-H), 8.37 (1 H, d, *J* = 5.9 Hz, 3-H).

N-(1-Oxo-1,2-dihydroisoquinolin-5-yl)benzamide (101)

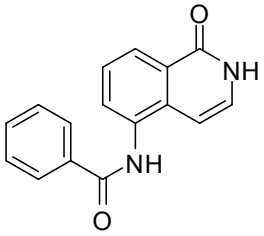

To 5AIQ.HCl **5** (50 mg, 0.25 mmol) in pyridine (2.0 mL) was added benzoyl chloride (0.03 mL, 39 mg, 0.28 mmol). The mixture was stirred at 90°C for 16 h; Evaporation and recrystallisation (EtOAc) gave **101** (57 mg, 86%) as an off-white solid: R_f = 0.16 (EtOAc); mp >310°C (decomp.); ^{1}H NMR ($(CD_3)_2SO$) δ 6.52 (1 H, d, *J* = 7.4 Hz, 4-H), 7.18 (1 H, dd, *J* = 7.4, 5.5 Hz, 3-H), 7.50-7.61 (4 H, m, 7,3',4',5'-H_4), 7.75 (1 H, d, *J* = 7.6 Hz, 6-H), 8.04 (2 H, d, *J* = 7.0 Hz, 2',6'-H_2), 8.13 (1 H, d, *J* = 7.8 Hz, 8-H), 10.33 (1 H, s, PhCONH), 11.32 (1 H, d, *J* = 4.7 Hz, 2-NH); ^{13}C NMR δ 100.6, 124.8, 125.9, 127.0, 127.8 (C_2), 128.5 (C_2), 128.9, 130.5, 131.8, 133.2, 134.1, 134.2, 161.6, 166.0; MS (ESI +ve) *m/z* 287.0801 (M + Na) ($C_{16}H_{12}NaN_2O_2$ requires 287.0796); 265.0952 (M + H)

($C_{16}H_{13}N_2O_2$ requires 265.0977); Anal. Found: C, 72.67; H, 4.48; N, 10.42. Calc. for $C_{16}H_{12}N_2O_2$: C, 72.72; H, 4.58; N, 10.60%.

4-Bromo-N-(1-oxo-1,2-dihydroisoquinolin-5-yl)benzamide (102)

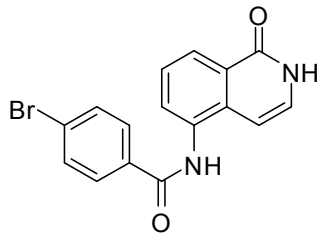

To 5AIQ.HCl **5** (50 mg, 0.25 mmol) in pyridine (2.0 mL) was added 4-bromobenzoyl chloride (61 mg, 0.28 mmol). The mixture was stirred at 90^{o}C for 16 h. Evaporation and recrystallisation (EtOAc) gave **102** (86 mg, 81%) as a yellow solid: R_f = 0.18 (EtOAc); mp 258-260^{o}C; ^{1}H NMR ($(CD_3)_2SO$) δ 6.51 (1 H, d, *J* = 7.4 Hz, 4-H), 7.18 (1 H, dd, *J* = 7.4, 5.7 Hz, 3-H), 7.52 (1 H, t, *J* = 7.8 Hz, 7-H), 7.71 (2 H, d, *J* = 8.2 Hz, Ar 3,5-H_2), 7.74 (1 H, d, *J* = 7.4 Hz, 6-H), , 7.99 (2 H, d, *J* = 8.2 Hz, Ar-2,6-H_2), 8.13 (1 H, d, *J* = 7.8 Hz, 8-H), 10.40 (1 H, s, ArCONH) 11.34 (1 H, d, *J* = 5.1 Hz, 2-NH); ^{13}C NMR 99.9, 125.0, 125.9, 127.0, 128.7, 128.5, 128.9, 129.7, 130.4, 132.9, 132.9, 135.2, 136.6, 161.5, 165.2; MS (ESI +ve) *m/z* 345.0026 (M + H) ($C_{16}H_{12}{}^{81}BrN_2O_2$ requires 345.0062), 343.1414 (M + H) ($C_{16}H_{12}{}^{79}BrN_2O_2$ requires 343.0082); Anal. Found: C, 55.85; H, 3.14; N, 8.02. Calc. for $C_{16}H_{11}BrN_2O_2$: C, 56.00; H, 3.23; N, 8.16%.

4-Methyl-N-(1-oxo-1,2-dihydroisoquinolin-5-yl)benzamide (103)

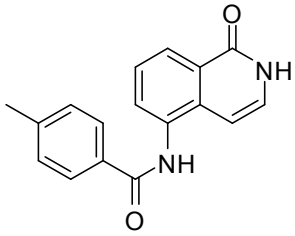

To 5AIQ.HCl **5** (50 mg, 0.25 mmol) in pyridine (2.0 mL) was added 4-methylbenzoyl chloride (0.04 mL, 43 mg, 0.28 mmol). The mixture was stirred at 90°C for 16 h; Evaporation and recrystallisation (EtOAc) gave **103** (57 mg, 82%) as an off-white solid: R_f = 0.19 (EtOAc); mp 297-300°C; ^{1}H NMR δ 2.40 (3 H, s, CH_3), 6.50 (1 H, d, *J* = 7.0 Hz, 4-H), 7.18 (1 H, dd, *J* = 7.2, 6.7 Hz, 3-H), 7.35 (2 H, d, *J* = 7.6 Hz, 3', 5'-H_2), 7.51 (1 H, d, *J* = 8.2 Hz), 7.72 (2 H, d, *J* = 7.6 Hz, 2', 6'-H_2), 8.11 (1 H, d, *J* = 8.2 Hz, 8-H), 10.25 (1 H, s, ArCONH), 11.31 (1 H, br s, 2-NH); ^{13}C NMR δ 21.0, 100.6, 124.7, 127.0, 127.8, 128.8, 129.0, 130.5, 131.3, 133.2, 134.2, 141.8, 161.6, 165.9; MS (ESI +ve) *m/z* 301.0941 (M + Na) ($C_{17}H_{14}NaN_2O_2$ requires 301.0953); 279.1119 (M + H) ($C_{17}H_{15}N_2O_2$ requires 279.1134); Anal. Found: C, 73.23; H, 4.98; N, 10.22. Calc. for $C_{17}H_{14}N_2O_2$: C, 73.37; H, 5.07 10.07.

4-Iodo-N-(1-oxo-1,2-dihydroisoquinolin-5-yl)benzamide (104)

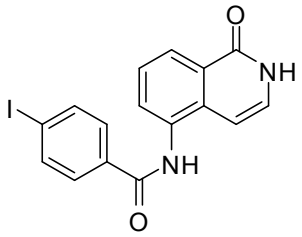

To 5AIQ.HCl **5** (50 mg, 0.25 mmol) in pyridine (2.0 mL) was added 4-iodobenzoyl chloride (74 mg, 0.28 mmol). The mixture was stirred at 90°C for 16 h. Evaporation and recrystallisation (EtOAc) gave **104** (74 mg, 76%) as a pale grey solid: R_f = 0.18 (EtOAc); mp >290 °C; ^{1}H NMR ($(CD_3)_2SO$) δ 6.51 (1 H, d, *J* = 7.4 Hz, 4-H), 7.18 (1 H, dd, *J* = 7.4, 5.7 Hz, 3-H), 7.51 (1 H, t, *J* = 7.8 Hz, 7-H), 7.74 (1 H, d, *J* = 7.4 Hz, 6-H), 7.82 (2 H, d, *J* = 8.2 Hz, Ar 3,5-H_2), 7.95 (2 H, d, *J* = 8.2 Hz, Ar 2,6-H_2), 8.14 (1 H, d, *J* = 7.8 Hz, 8-H), 10.39 (1 H, s, ArCONH) 11.33 (1 H, d, *J* = 5.1 Hz, 2-NH); ^{13}C NMR δ 99.5, 100.6,

124.9, 125.9, 127.0, 128.9,129.7, 130.42, 132.9, 133.6, 134.2, 137.4, 161.6, 165.4; MS (ES +ve) *m/z* 390.9950 (M + H) ($C_{16}H_{12}IN_2O_2$ requires 390.9944); Anal. Found: C, 49.16; H, 2.78; N, 7.32. Calc. for $C_{16}H_{11}IN_2O_2$: C, 49.25; H, 2.84; N, 7.18%.

4-Nitro-N-(1-oxo-1,2-dihydroisoquinolin-5-yl)benzamide (105)

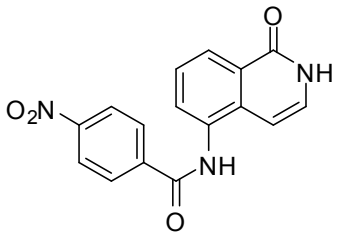

To 5AIQ.HCl **5** (50 mg, 0.25 mmol) in pyridine (2.0 mL) was added 4-nitrobenzoyl chloride (52 mg, 0.28 mmol). The mixture was stirred at 90 ^{o}C for 16 h. Evaporation and recrystallisation (EtOAc) gave **105** (55 mg, 71%) as an orange solid: R_f = 0.15 (EtOAc); mp >190^{o}C (decomp.); ^{1}H NMR ($(CD_3)_2SO$) δ 6.55 (1 H, d, *J* = 7.5 Hz, 6-H), 7.20 (1 H, dd, *J* = 7.5, 5.2 Hz, 3-H), 7.53 (1 H, t, *J* = 7.9 Hz, 7-H), 7.79 (1 H, d, *J* = 7.2 Hz, 4-H), 8.16 (1 H, d, *J* = 7.9 Hz, 8-H), 8.26 (2 H, d, *J* = 8.5 Hz, Ar 3,5-H_2), 8.40 (2 H, d, *J* = 8.54 Hz, Ar 2,6-H_2), 10.66 (1 H, s, ArCONH), 11.36 (1 H, d, *J* = 5.2 Hz, 2-NH); ^{13}C NMR δ 100.46 (5-C), 123.6, 125.2, 126.0, 129.1, 129.3, 130.4, 132.6, 134.1, 139.9, 134.2, 149.3, 161.6, 164.6; MS (ESI +ve) *m/z* 332.0639 (M + Na) ($C_{16}H_{11}NaN_3O_4$ requires 332.0647), 310.0827 (M + H) ($C_{16}H_{12}N_3O_4$ requires 310.0828); Anal. Found: C, 61.96; H, 3.38; N, 13.22. Calc. for $C_{16}H_{11}N_3O_4$: C, 62.14; H, 3.58; N, 13.59%.

N-(1-Oxo-1,2-dihydroisoquinolin-5-yl)-4-(trifluoromethyl)benzamide (106)

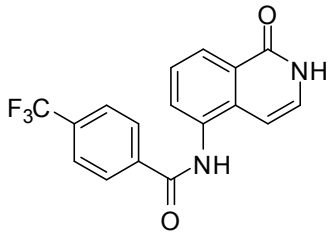

To 5AIQ.HCl **5** (50 mg, 0.25 mmol) in pyridine (2.0 mL) was added 4-trifluoromethylbenzoyl chloride (70 mg, 0.28 mmol). The mixture was stirred at 90 ^{o}C for 16 h. Evaporation and recrystallisation (EtOAc) gave **106** (60 mg, 72%) as a pale orange solid: R_f = 0.15 (EtOAc); mp 319-321°C; ^{1}H NMR ($(CD_3)_2SO$) δ 6.54 (1 H, d, *J* = 7.3 Hz, 4-H), 7.19 (1 H, dd, *J* = 7.3, 4.9 Hz, 3-H), 7.53 (1 H, t, *J* = 7.7 Hz, 7-H), 7.77 (1 H, d, *J* = 7.7 Hz, 6-H), 7.94 (1 H, d, *J* = 7.7 Hz, 8-H), 8.15 (2 H, d, *J* = 8.2 Hz, Ar 3,5-H_2), 8.23 (2 H, d, *J* = 8.2 Hz, Ar 2,6-H_2), 10.56 (1 H, s, ArCONH) 11.35 (1 H, d, *J* = 4.9 Hz, 2-NH); ^{13}C NMR (HMBC / HMQC) δ 100.5 (4-C), 125.1 (8-C), 125.9 (q, *J* = 31.5 Hz, Ph 3,5-C_2), 126.8 (7-C), 126.9 (8a-C), 128.9 (Ph 2,6-C_2), 130.3 (6-H), 130.9 (q, *J* = 31.5 Hz, Ph 4-C), 132.6 (5-C), 134.0 (4a-C), 137.9 (CF_3), 149.5 (Ph 1-C), 161.5 (1-C); MS (ESI +ve) *m/z* 355.0666 (M + Na) ($C_{17}H_{11}F_3NaN_2O_2$ requires 355.0670), 333.0844 (M + H) ($C_{17}H_{12}F_3N_2O_2$ requires 333.0851); Anal. Found: C, 61.23; H, 3.68; N, 8.66. Calc. for $C_{17}H_{11}F_3N_2O_2$: C, 61.45; H, 3.34; N, 8.43%.

4-Fluoro-N-(1-oxo-1,2-dihydroisoquinolin-5-yl)benzamide (107)

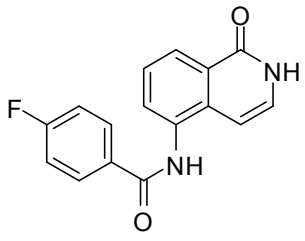

To 5AIQ.HCl **5** (50 mg, 0.25 mmol) in pyridine (2.0 mL) was added 4-fluorobenzoyl chloride (0.04 mL, 46 mg, 0.28 mmol). The mixture was stirred at 90°C for 16 h. Evaporation and recrystallisation (EtOAc) gave **107** (71 mg, 68%) as a pale orange solid: R_f = 0.16 (EtOAc); mp 302-305°C; ^{1}H NMR ($(CD_3)_2SO$) δ 6.54 (1 H, d, *J* = 7.4 Hz, 4-H), 7.18 (1 H, dd, *J* = 7.4, 6.2 Hz, 3-H), 7.33 (2 H, dd, *J* = 9.0, 8.6 Hz, Ar 3,5-H_2), 7.54 (1 H, d, *J* = 8.2 Hz, 7-H), 7.69 (1 H, d, *J* = 8.2 Hz, 6-H), 8.03 (2 H, dd, *J* = 9.0, 5.0 Hz, Ar 2,6-H_2), 8.14 (1 H, d, *J* = 8.2 Hz, 8-H), 10.44 (1 H, br s, ArCONH), 11.33 (1 H, br, 2-NH); ^{13}C NMR δ 102.1, 116.3, 116.5, 126.1, 127.3 (m, CF_3), 129.5, 131.2 (m, Ar 4-C), 131.3, 131.8, 133.6, 135.2, 163.0, 166.7; MS (ESI +ve) *m/z* 305.0710 (M + Na) ($C_{16}H_{11}FNaN_2O_2$ requires 305.0702), 283.0889 (M + H) ($C_{16}H_{12}FN_2O_2$ requires 283.0883) Anal. Found: C, 67.98; H, 3.68; N, 9.62. Calc. for $C_{17}H_{11}F_3N_2O_2$: C, 68.05; H, 3.92; N, 9.92%.

4-Chloro-N-(1-oxo-1,2-dihydroisoquinolin-5-yl)benzamide (108)

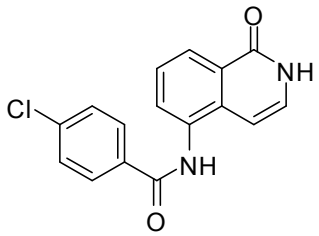

To 5AIQ.HCl **5** (50 mg, 0.25 mmol) in pyridine (2.0 mL) was added 4-chlorobenzoyl chloride (0.04 mL, 49 mg, 0.28 mmol). The mixture was stirred at 90 °C for 16 h. Evaporation and recrystallisation (EtOAc) gave **108** (58 mg, 77%) as a pale orange solid: R_f = 0.17 (EtOAc); mp 347-349°C; ^{1}H NMR ($(CD_3)_2SO$) δ 6.51 (1 H, *J* = 7.5 Hz, 4-H), 7.18 (1 H, dd, *J* = 7.5, 5.2 Hz, 3-H), 7.51 (1 H, *J* = 7.8 Hz, 7-H), 7.63 (2 H, d, *J* = 8.2 Hz, Ar 3,5-H_2), 7.74 (1 H, d, *J* = 7.8 Hz, 6-H), 8.04 (2 H, d, *J* = 8.2 Hz, Ar 2,6-H_2), 8.13 (1 H, d, *J* = 7.8 Hz, 8-H), 10.41 (1 H, s, ArCONH), 11.34 (1 H, d, *J* = 4.6 Hz, 2-NH); ^{13}C NMR δ 100.6, 125.0, 125.9, 127.0, 128.5, 127.0, 128.5 (C_2), 128.9, 129.7 (C_2), 130.4, 132.9, 132.9, 134.2, 136.6, 161.6, 165.0; MS (ESI +ve) *m/z* 323.0334 (M + Na) ($C_{16}H_{11}{}^{37}ClNaN_2$ NaO_2 requires 323.0337) 321.0399 (M + Na) ($C_{16}H_{11}{}^{35}ClNaN_2$ NaO_2

requires 321.0407), 299.0584 (M + H) ($C_{16}H_{12}ClN_2O_2$ requires 299.0587); Anal. Found: C, 64.23; H, 3.68; N, 9.32. Calc. for $C_{16}H_{11}ClN_2O_2$: C, 64.33; H, 3.71; N, 9.38%.

2-Iodo-N-(1-oxo-1,2-dihydroisoquinolin-5-yl)benzamide (109)

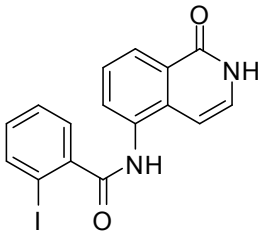

To 5AIQ.HCl **5** (50 mg, 0.25 mmol) in pyridine (2.0 mL) was added 2-iodobenzoyl chloride (74 mg, 0.28 mmol). The mixture was stirred at 90^{o}C for 16 h. Evaporation and recrystallisation (EtOAc) gave **109** (60 mg, 61%) as a pale brown solid: R_f = 0.19 (EtOAc); mp 317-320^{o}C; ^{1}H NMR ($(CD_3)_2SO$) δ 6.77 (1 H, d, *J* = 7.9 Hz, 4-H), 7.20 (1 H, t, *J* = 7.9, 5.6 Hz, 3-H), 7.25 (1 H, dt, *J* = 7.6, 1.8 Hz, Ar 4-H), 7.54-7.63 (3 H, m, 7-H and Ar 3,5-H_2), 7.90 (1 H, d, *J* = 7.9 Hz, 6-H), 7.96 (1 H, d, *J* = 7.9 Hz, 8-H), 8.12 (1H, d, *J* = 7.6 Hz, Ar 6-H), 10.41 (1 H, s, ArCONH), 11.34 (1 H, d, *J* = 5.6 Hz, 2-NH); ^{13}C NMR δ 93.6, 100.5, 124.6, 125.9, 127.1, 128.1, 128.2, 128.7, 129.2, 131.0, 132.5, 133.2, 139.0, 161.5, 166.4; MS (ES +ve) *m/z* 390.9952 (M + H) ($C_{16}H_{12}IN_2O_2$ requires 390.9944) Anal. Found: C, 49.12; H, 2.66; N, 7.26. Calc. for $C_{16}H_{11}IN_2O_2$: C, 49.25; H, 2.84; N, 7.18%.

2-Methyl-N-(1-oxo-1,2-dihydroisoquinolin-5-yl)benzamide (110)

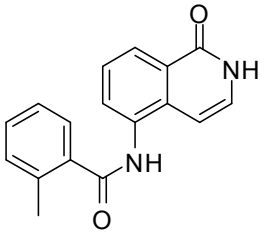

To 5AIQ.HCl **5** (50 mg, 0.25 mmol) in pyridine (2.0 mL) was added 4-methylbenzoyl chloride (0.04 mL, 43 mg, 0.28 mmol). The mixture was stirred at 90 ^{o}C for 16 h. Evaporation and recrystallisation (EtOAc) gave **110** (57 mg, 63%) as an off-white solid: R_f = 0.17 (EtOAc); mp 310-313°C; ^{1}H NMR ($(CD_3)_2SO$) δ 2.54 (3 H, s, Me), 6.62 (1 H, d, *J* = 7.5 Hz, 4-H), 7.21 (1 H, dd, *J* = 7.5, 5.2 Hz, 3-H), 7.29-7.33 (2 H, m, Ar 3,5-H_2), 7.41 (1 H, t, *J* = 7.4 Hz, Ar 4-H), 7.51 (1 H, t, *J* = 7.4 Hz, 7-H), 7.58 (1 H, d, *J* = 7.4 Hz, 6-H) 7.82 (1 H, d, *J* = 7.4 Hz, Ar 6-H), 8.10 (1 H, d, *J* = 7.4 Hz, 8-H), 10.24 (1 H, s, ArCHNH), 11.32 (1 H, d, *J* = 5.1 Hz, 2-NH); ^{13}C NMR δ 19.5, 100.4, 124.5, 125.6, 125.9, 127.0, 127.4, 128.9, 129.7, 130.6, 131.0, 132.9, 133.6, 135.4, 136.8, 161.6, 168.6. MS (ESI +ve) *m/z* 301.0956 (M + Na) ($C_{17}H_{13}N_2NaO_2$ requires 301.0953), 279.1130 (M + H) ($C_{17}H_{14}N_2O_2$ requires 279.1133); Anal. Found: C, 73.33; H, 5.02; N, 10.11. Calc. for $C_{17}H_{14}N_2O_2$: C, 73.37; H, 5.07 10.07%.

N-(1-Oxo-1,2-dihydroisoquinolin-5-yl)thiophene-2-carboxamide (111)

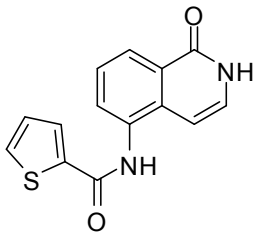

To 5AIQ.HCl **5** (50 mg, 0.25 mmol) in pyridine (2.0 mL) was added thiophene-2-carbonyl chloride (0.03 mL, 41 mg, 0.28 mmol). The mixture was stirred at 90^{o}C for 16 h. Evaporation and recrystallisation (EtOAc) gave **111** (34 mg, 51%) as an off-white solid: R_f = 0.14 (EtOAc); mp 288-291°C; ^{1}H NMR ($(CD_3)_2SO$) δ 6.51 (1 H, d, *J* = 7.4 Hz, 4-H), 7.19 (1 H, dd, *J* = 7.4, 5.4 Hz, 3-H), 7.23 (1 H, dd, *J* = 4.9, 3.6 Hz, Ar 4-H), 7.52 (1 H, t, *J* = 7.8 Hz, 7-H), 7.70 (1 H, d, *J* = 7.8 Hz, 6-H), 7.83 (1 H, d, *J* = 4.9 Hz, Ar 5-H), 8.03 (1 H, d, *J* = 3.6 Hz, Ar 3-H), 8.13 (1 H, d, *J* = 7.8 Hz, 8-H), 10.41 (1 H, s, ArCONH), 11.33 (1 H, d, *J* = 5.4 Hz, 2-NH); ^{13}C NMR δ 100.2, 125.5, 126.6, 127.2, 128.7, 129.3, 129.9, 131.2, 132.3, 132.9, 134.7, 139.4, 161.2, 162.2; MS (ESI +ve) *m/z* 293.0347 (M + Na) ($C_{14}H_{10}N_2NaO_2S$ requires 293.0361), 271.0529 (M + H)

($C_{14}H_{11}N_2O_2S$ requires 271.0541); Anal. Found: C, 61.11; H, 3.55; N, 10.62. Calc. for $C_{14}H_{10}N_2O_2S$: C, 62.21; H, 3.73; N, 10.36%.

N-(1-Oxo-1,2-dihydroisoquinolin-5-yl)cyclohexanecarboxamide (112)

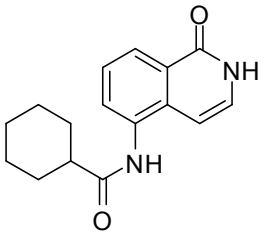

To 5AIQ.HCl **5** (50 mg, 0.25 mmol) in pyridine (2.0 mL) was added cyclohexane-carbonyl chloride (0.04 mL, 41 mg, 0.28 mmol). The mixture was stirred at 90°C for 16 h. Evaporation and recrystallisation (EtOAc) gave **112** (46 mg, 68%) as an off-white solid: R_f = 0.18 (EtOAc); mp 302-305°C; ^{1}H NMR ($(CD_3)_2SO$) δ 1.23 (1 H, *ca.* q, *J* = 12.5 Hz, CH_x, 4_{ax}-H), 1.30 (2 H, *ca.* q, *J* = 12.6 Hz, CH_x, 3_{ax},5_{ax}-H_2), 1.43 (2 H, dq, *J* = 12.1, 2.3 Hz, CH_x, 2_{ax},6_{ax}-H_2), 1.66 (1 H, brd, *J* = 12.1 Hz, CH_x,4_{eq}-H), 1.77 (2 H, *ca.* d, *J* = 12.5 Hz, CH_x, 3_{eq},5_{eq}-H_2), 1.87 (2 H, *ca.* d, *J* = 12.5 Hz, CH_x, 2_{eq},6_{eq}-H_2), 2.50 (1 H, m, CH_x, 1-H). 6.57 (1 H, d, *J* = 7.5 Hz, 4-H), 7.18 (1 H, dd, *J* = 7.3, 6.2 Hz, 3-H). 7.42 (1 H, t, *J* = 7.8 Hz, 7-H), 7.76 (1 H, d, *J* = 7.8 Hz, 6-H), 8.02 (1 H, d, *J* = 7.8 Hz, 8-H), 9.66 (1 H, s, cHexCONH), 11.30 (1 H, d, *J* = 5.1 Hz, 2-NH); ^{13}C NMR δ 25.3 (C_2), 25.4, 29.3 (C_2), 44.2, 100.0, 123.6, 125.8, 126.9, 128.5, 128.6, 132.6, 133.1, 161.6, 174.8; MS (ESI +ve) *m/z* 563.2616 (2 M + Na) ($C_{32}H_{36}N_4NaO_4$ requires 563.2634), 541.2798 (2 M + H) ($C_{32}H_{37}N_4O_4$ requires 541.2815) 293.1248 (M + Na) ($C_{16}H_{18}N_2NaO_2$ requires 293.1266), 271.1140 (M + H) ($C_{16}H_{19}N_2O_2$ requires 271.1147); Anal. Found: C, 71.31; H, 6.52; N, 10.17. Calc. for $C_{16}H_{18}N_2O_2$: C, 71.09; H, 6.71 10.36%.

2,2-Dimethyl-N-(1-oxo-1,2-dihydroisoquinolin-5-yl)propanamide (113)

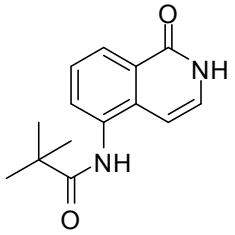

To 5AIQ.HCl **5** (50 mg, 0.25 mmol) in pyridine (2.0 mL) was added 2,2-dimethylpropanoyl chloride (0.03 mL, 34 mg, 0.28 mmol). The mixture was stirred at 90°C for 16 h. Evaporation and recrystallisation (EtOAc) gave **113** (46 mg, 68%) as an off-white solid: R_f = 0.21 (EtOAc); mp 305-307°C; ^{1}H NMR ($(CD_3)_2SO$) δ 1.28 (9 H, s, 3 × Me), 6.38 (1 H, d, *J* = 7.4 Hz, 4-H), 7.18 (1 H, dd, *J* = 7.4, 4.3 Hz, 3-H), 7.45 (1 H, t, *J* = 7.6 Hz, 7-H), 7.53 (1 H, d, *J* = 7.6 Hz, 6-H), 8.08 (1 H, d, *J* = 7.6 Hz, 8-H), 9.36 (1 H, s, Bu^{t}CONH), 11.29 (1 H, br, 2-NH); ^{13}C NMR δ 27.4 (C_3), 40.1, 100.5, 124.6, 125.8, 126.9, 128.7, 130.7, 133.4, 134.5, 161.7, 177.1; MS (ESI +ve) *m/z* 267.1109 (M + Na) ($C_{14}H_{16}N_2NaO_2$ requires 267.1109), 245.1291 (M + H) ($C_{14}H_{17}N_2O_2$ requires 245.1290); Anal. Found: C, 68.68; H, 6.46; N, 11.31. Calc. for $C_{14}H_{16}N_2O_2$: C, 68.83; H, 6.60, 11.47%.

N-(1-Oxo-1,2-dihydroisoquinolin-5-yl)adamantane-1-carboxamide (114)

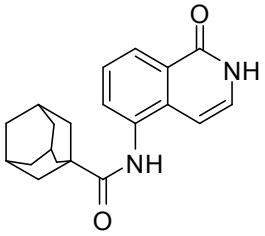

To 5AIQ.HCl **5** (50 mg, 0.25 mmol) in pyridine (2.0 mL) was added adamantane-1-carbonyl chloride (56 mg, 0.28 mmol). The mixture was stirred at 90°C for 16 h. Evaporation and recrystallisation (EtOAc) gave **114** (48 mg, 59%) as an off-white solid: R_f = 0.23 (EtOAc); mp 303-306°C; ^{1}H NMR ($(CD_3)_2SO$) δ 1.73 (6 H, m, 3 × CH_2), 1.97 (6 H, m, 3 × CH_2), 2.04 (3 H, m, 3 × CH), 6.36 (1 H, d, *J* = 7.4 Hz, 4-H), 7.18 (1 H, dd, *J* = 7.4, 6.2 Hz, 3-H), 7.42 (1 H, t, *J* = 7.7 Hz, 7-H), 7.52 (1 H, d, *J* = 7.7 Hz, 6-H), 8.07 (1 H, d, *J* = 7.7 Hz, 8-H), 9.29 (1 H, s, adamantaneCONH), 11.29 (1 H, d, *J* = 4.9 Hz, 2-NH); ^{13}C NMR δ 27.7 (C_3, CH), 36.1 (C_6, CH_2), 38.5, 38.6 (C_6, CH_2), 100.5, 124.5, 125.8, 126.9, 128.7, 130.7, 133.4, 134.4, 161.7, 176.6; MS (ESI +ve) *m/z* 345.1574 (M + Na) ($C_{20}H_{22}N_2$ NaO_2 requires 345.1579), 323.1769 (M + H) ($C_{20}H_{23}N_2O_2$ requires 323.1768); Anal. Found: C, 69.46; H, 6.46; N, 8.06. Calc. for $C_{20}H_{22}N_2O_2$: C, 69.55; H, 6.42; N, 8.11%.

5-Amino-3-(4-chlorophenyl)isoquinolin-1-one hydrochloride (115)

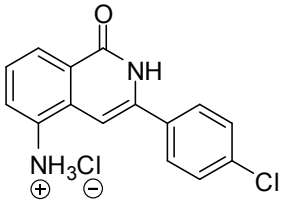

To **139** (170 mg, 0.57 mmol) in EtOH (10 mL) and aq. HCl (34%, 0.4 mL), a slurry of 10% Pd on charcoal (80 mg) in EtOH (5 mL) was added. The mixture was stirred under H_2 for 2 h. The suspension was then filtered through Celite®. The Celite® pad and residue were suspended in water (100 mL) and heated. The hot suspension was filtered through a second Celite® pad. Evaporation of the solvent and drying gave **115** (90 mg, 52%) as a pale buff solid: R_f = 0.74 (MeOH); mp >350°C (lit.[162] mp >350°C); ^{1}H NMR ($(CD_3)_2SO$) δ 7.08 (1 H, s, 4-H), 7.14 (1 H, dd, *J* = 7.8, 1.2 Hz, 6-H), 7.28 (1 H, t, *J* = 7.8 Hz, 7-H), 7.56 (2 H, d, *J* = 9.0 Hz, Ar 3,5-H_2), 7.64 (1 H, dd, *J* = 7.8, 1.2 Hz, 8-H), 7.83 (2 H, d, *J* = 9.0 Hz, Ar 2,6-H_2), 11.50 (1 H, brs, NH).

5-Amino-3-(4-trifluoromethylphenyl)isoquinolin-1-one hydrochloride (116)

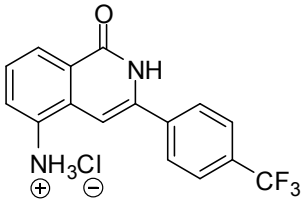

To **140** (140 mg, 0.42 mmol) in EtOH (10 mL) and aq. HCl (34%, 0.4 mL), a slurry of 10% Pd on charcoal (70 mg) in EtOH (5 mL) was added. The mixture was stirred under H_2 for 2 h. The suspension was then filtered through Celite®. The Celite® pad and residue were suspended in water (100 mL) and heated. The hot suspension was filtered through a second Celite® pad. Evaporation of the solvent and drying gave **116** (60 mg, 42%) as a pale buff solid: R_f = 0.76 (MeOH); mp >350°C (lit.[162] mp >350°C); ^{1}H NMR ($(CD_3)_2SO$) δ 7.14 (1 H, dd, *J* = 7.8, 1.2 Hz, 6-H), 7.18 (1 H, s, 4-H), 7.31 (1 H, t, *J* = 7.8 Hz, 7-H), 7.63 (1 H, dd, *J* = 7.8, 1.2 Hz, 8-H), 7.85 (2 H, d, *J* = 8.2 Hz, Ar 3,5-H_2), 8.01 (2 H, d, *J* = 8.2 Hz, Ar 2,6-H_2), 11.60 (1 H, br s, NH); ^{19}F NMR ($(CD_3)_2SO$) δ -59.50 (3 F, s, CF_3).

5-Amino-3-(4-methylphenyl)isoquinolin-1-one hydrochloride (118)

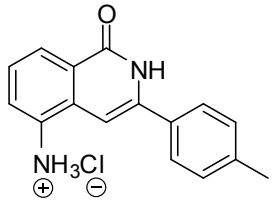

To **141** (160 mg, 0.57 mmol) in EtOH (10 mL) and aq. HCl (34%, 0.4 mL), a slurry of 10% Pd on charcoal (80 mg) in EtOH (5 mL) was added. The mixture was stirred under H_2 for 2 h. The suspension was then filtered through Celite®. The Celite® pad and residue were suspended in water (100 mL) and heated. The hot suspension was filtered through a second Celite® pad. Evaporation of the solvent and drying gave **118** (129 mg, 79%) as a pale buff solid: R_f = 0.72 (MeOH); mp >350°C (lit.[162] mp >350°C); ^{1}H NMR ($(CD_3)_2SO$) δ 2.23 (3 H, s, Me), 6.48 (1 H, s, 4-H), 7.31 (2 H, d, *J* = 7.8 Hz, Ar 3,5-H_2), 7.36 (1 H, t, *J* = 7.8 Hz, 7-H), 7.61 (1 H, d, *J* = 7.8 Hz, 6-H), 7.75 (1 H, d, *J* = 7.8 Hz, 8-H), 7.96 (2 H, d, *J* = 7.8 Hz, Ar 2,6-H_2), 11.47 (1 H, brs, NH).

1-(4-Chlorophenyl)butane-1,3-dione (128)

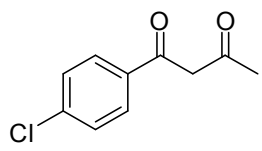

4-Chloroacetophenone **131** (2.3 g, 15 mmol) in Ac_2O (6.2 g, 62 mmol) was added to $BF_3.(AcOH)_2$ (8.6 g, 46 mmol) at 0°C. The mixture was stirred for 30 min and allowed to stand at room temperature for 24 h. The mixture was then poured into aq. NaOAc (13%, 50 mL) and boiled under reflux for 1 h. Extraction (Et_2O), evaporation and chromatography (hexane / EtOAc 4:1) afforded **128** (2.5 g, 84%) as pale orange crystals: R_f = 0.54 (hexane / EtOAc 4:1); mp 56-58°C (lit.[162] mp 58-59°C); ^{1}H NMR ($CDCl_3$) δ 2.20 (2.85 H, s, *enol-form* CH_3), 2.30 (0.15 H, s, *keto-form* CH_3), 4.07 (0.1 H, s, *keto-form* CH_2), 6.13 (0.95 H, s, *enol-form* =CH), 7.40 (1.9 H, d, *J* = 8.6 Hz, *enol-form* Ar 3,5-H_2), 7.43 (0.1 H, d, *J* = 8.6 Hz, *keto-form* Ar 3,5-H_2), 7.79 (1.9 H, d, *J* = 8.6 Hz, *enol-form* Ar 2,6-H_2), 7.87 (0.1 H, d, *J* = 8.2 Hz, *keto-form* Ar 2,6-H_2), 16.09 (0.95 H, br s, *enol-form* OH).

1-(4-Trifluoromethylphenyl)butane-1,3-dione (129)

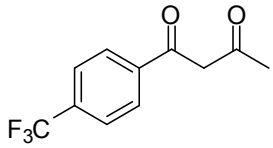

4-(Trifluoromethyl)acetophenone **132** (2.5 g, 13 mmol) in Ac_2O (5.5 g, 54 mmol) was added to $BF_3.(AcOH)_2$ (7.6 g, 40 mmol) at 0°C. The mixture was stirred for 30 min and allowed to stand at room temperature for 24 h. The mixture was then poured into aq. NaOAc (13%, 100 mL) and boiled under reflux for 1 h. Extraction (Et_2O), evaporation and chromatography (hexane / EtOAc 7:3) gave **129** (2.1 g, 68%) as pale orange crystals: R_f = 0.57 (hexane / EtOAc 4:1); mp 48-50°C (lit.[162] mp 48-49°C)**;** ^{1}H NMR ($CDCl_3$) δ 2.23 (2.88 H, s, *enol-form* CH_3), 2.32 (0.12 H, s, *keto-form* CH_3), 4.13 (0.08 H, s, *keto-form* CH_2), 6.19 (0.96 H, s, *enol-form* =CH), 7.68 (2 H, d, *J* = 8.2 Hz, *enol-form* Ar 3,5-H_2), 7.71 (0.08 H, d, *J* = 8.2 Hz, *keto-form* Ar 3,5-H_2), 7.95 (2 H, d, *J* = 8.2 Hz, *enol-form* Ar 2,6-H_2), 8.04 (0.08 H, d, *J* = 8.2 Hz, *keto-form* Ar 2′,6′-H_2), 15.98 (1 H, br s, *enol-form* OH); ^{19}F NMR ($CDCl_3$) δ –63.62 (3 F, s, CF_3).

1-(4-Methylphenyl)butane-1,3-dione (130)

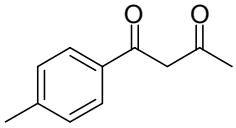

4-Methylacetophenone **133** (2.0 g, 14.9 mmol) in Ac_2O (6.2 g, 61 mmol) was added to $BF_3.(AcOH)_2$ (8.5 g, 45 mmol) at 0°C. The mixture was stirred for 30 min and allowed to stand at room temperature for 24 h. The mixture was then poured into aq. NaOAc (13%, 100 mL) and boiled under reflux for 1 h. Extraction (Et_2O), evaporation and chromatography (hexane / EtOAc 20:1) afforded **130** (2.1 g, 80%) as a colourless oil: R_f = 0.40 (hexane / EtOAc 20:1); ^{1}H NMR ($CDCl_3$) δ 2.20 (2.67 H, s, *enol-form* $COCH_3$), 2.30 (0.33 H, s, *keto-form* $COCH_3$), 2.41 (2.67 H, s, *enol-form* $ArCH_3$), 2.59 (0.33 H, s, *keto-form* $ArCH_3$), 4.08 (0.22 H, s, *keto-form* CH_2), 6.16 (0.89 H, s, *enol-form* =CH), 7.24 (2 H, d, *J* = 8.2 Hz, Ar 3,5-H_2), 7.78 (2 H, d, *J* = 8.2 Hz, Ar 2,6-H_2), 16.22 (0.89 H, br s, *enol-form* OH).

5-Nitro-3-(4-Chlorophenyl)isocoumarin (135)

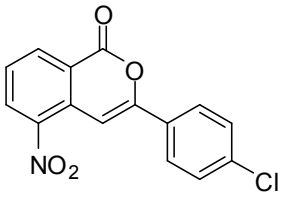

Method A:

To a stirred solution of **34** (7.1 g, 36 mmol) and potassium *t*-butoxide (1.7 g, 15 mmol) in 2-methylpropan-2-ol (50 mL) was added **128** (1.8 g, 7.3 mmol) and Cu powder (47 mg, 0.7 mmol). The mixture was boiled heated reflux for 16 h, then poured into H_2O (350 ml) and acidified with aq. HCl (2 M). Extraction (Et_2O), evaporation and chromatography (hexane / EtOAc 8:1) gave **135** (720 mg, 33%) as pale yellow crystals; R_f = 0.64 (hexane / EtOAc 8:1); mp 203-205°C; (lit.[162] mp 204-205°C); ^{1}H NMR δ 7.47 (2 H, d, *J* = 6.6 Hz, Ar 3,5-H_2), 7.62 (1 H, t, *J* = 8.0 Hz, 7-H), 7.87 (2 H, d, *J* = 6.9 Hz, Ar 2,6-H_2), 7.88 (1 H, brs, 4-H), 8.50 (1 H, dd, *J* = 8.3, 1.9 Hz, 6-H), 8.63 (1 H, brd, *J* = 8.0 Hz, 8-H).

Method B:

$SnCl_4$ (148.5 mg, 0.57 mmol) was added to **56** (100 mg, 0.52 mmol) in $PhNO_2$ (1.0 mL). After 30 min, 4-chlorobenzoyl chloride (217.0 mg, 1.04 mmol) was added and the mixture was stirred at 150°C under Ar for 3 d. The cooled mixture was quenched with ice-water (2.0 mL) and extracted with EtOAc (2 × 20 mL). The combined extracts were washed (NaOH, brine) and dried ($MgSO_4$). Evaporation and chromatography (hexane / EtOAc 15:1) gave **135** (34.5 mg, 29%) as a pale yellow solid; data as above.

5-Nitro-3-(4-trifluorophenyl)isocoumarin (137)

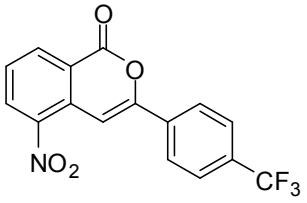

Method A:

To a stirred solution of **34** (3.6 g, 16 mmol) and potassium *t*-butoxide (700 mg, 6.3 mmol) in 2-methylpropan-2-ol (50 mL) was added **129** (760 mg, 3.1 mmol) and Cu powder (20 mg, 0.3 mmol). The mixture was heated under reflux for 16 h, then poured into H_2O (350 mL) and acidified with aq. HCl (2 M). Extraction (Et_2O), evaporation and chromatography (hexane / EtOAc 9:1) gave **137** (125 mg, 12%) as yellow crystals: R_f = 0.52 (hexane / EtOAc 4:1); mp 162-163°C (lit.[162] mp 163-164°C); IR ν_{max} 1724 (C=O), 1626 (C=C), 1537 & 1344 (NO_2) cm^{-1}; ^1H NMR δ 7.67 (1 H, t, *J* = 8.2 Hz, 6-H), 7.75 (2 H, d, *J* = 8.2 Hz, Ar 3,5-H_2), 7.93 (1 H, d, *J* = 0.8 Hz, 4-H), 8.03 (2 H, d, *J* = 8.2 Hz, Ar 2,6-H_2), 8.51 (1 H, dd, *J* = 8.2, 1.6 Hz), 8.57 (1 H, ddd, *J* = 8.2, 1.6, 0.8 Hz, 8-H); ^{19}F NMR δ -63.54 (3 F, s, CF_3).

Method B:

$SnCl_4$ (149 mg, 0.57 mmol) was added to **56** (100 mg, 0.52 mmol) in $PhNO_2$ (1.0 mL). After 30 min, 4-trifluoromethylbenzoyl chloride (217 mg, 1.04 mmol) was added and the mixture was stirred at 150°C under Ar for 3 d. The cooled mixture was quenched with ice-water (2.0 mL) and extracted with EtOAc (2 × 20 mL). The combined extracts were washed (NaOH, brine) and dried ($MgSO_4$). Evaporation and chromatography (hexane / EtOAc 15:1) gave **137** (11.2 mg, 11%) as a pale yellow solid: data as above.

3-(4-Methylphenyl)-5-nitroisocoumarin (138)

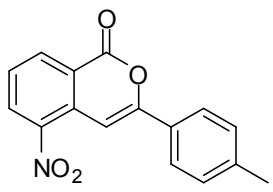

Method A:

To a stirred solution of **34** (22.7 g, 0.1 mol) and potassium *t*-butoxide (5.8 g, 52 mmol) in 2-methylpropan-2-ol (50 mL) was added **130** (6.3 g, 26 mmol) and Cu powder (170 mg, 2.7 mmol). The mixture was heated under reflux for 16 h, then poured into H_2O (350 mL) and acidified with aq. HCl (2 M). Extraction (Et_2O), evaporation and chromatography (hexane / EtOAc 10:1) gave **138** (1.5 g, 20%) as pale yellow crystals: R_f = 0.49 (hexane / EtOAc 4:1); mp 181-182°C (lit.[162] mp 181-182°C); ^{1}H NMR δ 2.42 (3 H, s, Me), 7.29 (2 H, d, *J* = 8.6 Hz, Ar 3,5-H_2), 7.57 (1 H, t, *J* = 8.2 Hz, 7-H), 7.82 (1 H, s, 4-H), 7.83 (2 H, d, *J* = 8.4 Hz, Ar 2,6-H_2), 8.48 (1 H, brd, *J* = 8.2 Hz, 6-H), 8.61 (1 H, brd, *J* = 8.5 Hz, 8-H).

Method B:

$SnCl_4$ (148.5 mg, 0.57 mmol) was added to **56** (100 mg, 0.52 mmol) in $PhNO_2$ (1.0 mL). After 30 min, 4-methylbenzoyl chloride (161 mg, 1.04 mmol) was added and the mixture was stirred at 150°C under Ar for 3 d. The cooled mixture was quenched with ice-water (2.0 mL) and extracted with EtOAc (2 × 20 mL). The combined extracts were washed (NaOH, brine) and dried ($MgSO_4$). Evaporation and chromatography (hexane / EtOAc 15:1) gave **138** (24.2 mg, 23%) as a pale yellow solid; data as above.

3-(4-Chlorophenyl)-5-nitroisoquinolin-1-one (139)

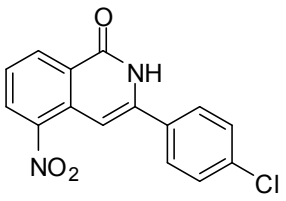

A solution of **135** (180 mg, 0.6 mmol) in 2-methoxyethanol (50 mL) was saturated with NH_3, boiled under reflux for 4 h, then evaporated until 10 mL remained. The concentrate was stored at 4°C for 16 h and the precipitated crystals were filtered, washed (H_2O, then EtOH) and recrystallised (MeOH) to give **139** (460 mg, 64%) as bright yellow crystals: R_f = 0.33 (hexane / EtOAc 1:4); mp 231-233°C (decomp.) (lit.[162] mp 231-232°C (decomp.)); ^{1}H NMR ($(CD_3)_2SO$) δ 7.22 (1 H, d, *J* = 0.8 Hz, 4-H), 7.59 (2 H, d, *J* = 8.6 Hz, Ar 3,5-H_2), 7.65 (1 H, t, *J* = 8.2 Hz, 7-H), 7.79 (2 H, d, *J* = 8.6 Hz, Ar 2,6-H_2), 8.47 (1 H, dd, *J* = 8.2, 1.2 Hz, 6-H), 8.58 (1 H, ddd, *J* = 8.2, 1.2, 0.8 Hz, 8-H), 12.13 (1 H, br s, NH).

5-Nitro-3-(4-trifluoromethylphenyl)isoquinolin-1-one (140)

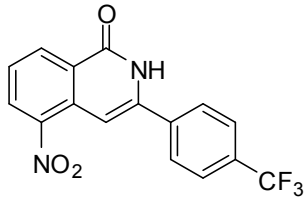

A solution of **137** (280 mg, 0.84 mmol) in 2-methoxyethanol (25 mL) was saturated with NH_3, boiled under reflux for 4 h and then evaporated until 10 mL remained. The concentrate was stored at 4°C for 16 h and the precipitated crystals were filtered, washed (H_2O, then EtOH) and recrystallised (MeOH) to give **140** (67 mg, 24%) as yellow crystals: R_f = 0.43 (hexane / EtOAc 1:4); mp 228-230°C (lit.[162] mp 230-231°C); ^{1}H NMR ($(CD_3)_2SO$) δ 7.28 (1 H, s, 4-H), 7.68 (1 H, t, *J* = 7.8 Hz, 7-H), 7.88 (2 H, d, *J* = 8.2 Hz, Ar 3,5-H_2), 7.97 (2 H, d, *J* = 8.2 Hz, Ar 2,6-H_2), 8.47 (1 H, dd, *J* = 7.8, 1.2 Hz, 6-H), 8.58 (1 H, d, *J* = 7.8, 1.2 Hz, 8-H), 12.21 (1 H, br s, NH); ^{19}F NMR ($(CD_3)_2SO$) δ -61.84 (3 F, s, CF_3).

3-(4-Methylphenyl)-5-nitroisoquinolin-1-one (141)

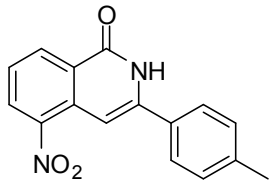

A solution of **138** (250 mg, 0.89 mmol) in 2-methoxyethanol (30 mL) was saturated with NH_3, boiled under reflux for 4 h, then evaporated until 10 mL remained. The concentrate was stored at 4°C for 16 h and the precipitated crystals were filtered, washed (H_2O, then EtOH) and recrystallised (MeOH) to give **141** (199 mg, 80%) as bright yellow crystals: R_f = 0.23 (hexane / EtOAc 3:2); mp 175-176°C; (lit.[162] mp 174-175°C); ^{1}H NMR ($(CD_3)_2SO$) δ 2.37 (3 H, s, Me), 7.20 (1 H, d, *J* = 0.8 Hz, 4-H), 7.32 (2 H, d, *J* = 8.2 Hz, Ar 3,5-H_2), 7.62 (1 H, t, *J* = 8.2 Hz, 7-H), 7.66 (2 H, d, *J* = 8.2 Hz, Ar 2,6-H_2), 8.45 (1 H, dd, *J* = 8.2, 1.2 Hz, 6-H), 8.56 (1 H, ddd, *J* = 8.2, 1.2, 0.8 Hz, 8-H), 12.03 (1 H, br s, NH).

2-Benzoyl-5-nitroisoquinolin-1-one (145)

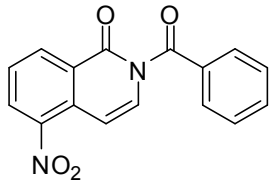

$AlCl_3$ (70.6 mg, 0.53 mmol) was added to **38** (100 mg, 0.53 mmol) in benzoyl chloride (3.1 g, 22.3 mmol) and the mixture was stirred at 100°C under Ar for 3 d. The cooled mixture was quenched with ice-water (5.0 mL) and extracted with EtOAc (2 × 20 mL). The combined extracts were washed (aq. NaOH, brine) and dried. Evaporation, chromatography (hexane / EtOAc 4:1) and recrystallisation gave **145** (40 mg, 26%) as pale yellow crystals: R_f = 0.61 (hexane / EtOAc 2:3); mp 151-153°C; IR ν_{max} 1668 (C=O), 1662 (C=O) 1626 (C=C), 1519 & 1340 (NO_2) cm^{-1}; ^{1}H NMR δ 7.41 (1 H, dd, *J* = 8.2, 0.9 Hz, 4-H), 7.50 (2 H, t, *J* = 8.7 Hz, Ph 3,5-H_2), 7.59-7.65 (3 H, m, 3,7-H_2, Ph 4-H), 7.81 (2 H, d, *J* = 8.7 Hz, Ph 2,6-H_2), 8.44 (1 H, dd, *J* = 8.2, 1.1 Hz, 8-H), 8.66 (1 H, d, *J* = 8.2 Hz, 6-H); ^{13}C NMR δ 101.8,. 126.6, 127.6, 128.6, 128.8, 129.2, 130.4, 138.9, 131.0, 131.2, 132.4, 134.2, 134.4, 145.2, 160.2, 170.1. MS (ES +ve) *m/z* 317.0524 (M + Na) ($C_{16}H_{10}N_2O_4Na$ requires 317.0538).

4-Acetyl-5-nitroisoquinolin-1-one (146)

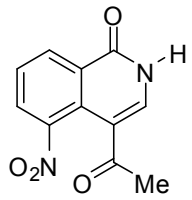

Compound **38** (80 mg, 0.42 mmol) in Ac_2O (3 mL) and conc. H_2SO_4 (50 μL) were heated at 100°C for 22 h. Evaporation, chromatography (acetone) and recrystallisation (EtOH) gave **146** (36 mg, 36%) as yellow crystals: R_f = 0.63 (EtOAc); mp 303-305 °C; IR ν_{max} 3436 (NH), 1761 (C=O), 1661 (C=O), 1518 & 1315 (NO_2) cm^{-1}; ^1H NMR ($(CD_3)_2SO$) δ 2.47 (3 H, s, Me), 7.73 (1 H, t, *J* = 7.8 Hz, 7-H), 8.19 (1 H, d, *J* = 7.8 Hz, 3-H), 8.26 (1 H, d, *J* = 7.8 Hz, 6-H), 8.52 (1 H, d, *J* = 8.2 Hz, 8-H) 12.86 (1 H, brs, NH); ^{13}C NMR (HMBC / HMQC) δ 27.4 (2'-C), 125.9 (4a-C), 127.5 (7-C), 129.4 (8a-C), 129.6 (6-C), 132.0 (8-C), 133.3 (4-C), 137.9 (3-C), 146.9 (5-C), 160.5 (1-C), 196.1 (1'-C); Anal. Found: C, 56.38; H, 3.26; N, 12.26. Calc. for $C_{11}H_8N_2O_4$: C, 56.90; H, 3.47; N, 11.86%.

5-Nitro-3-phenyl-3-[^{13}C]-isocoumarin (148)

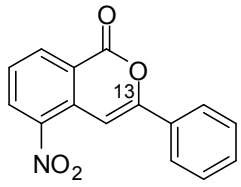

$SnCl_4$ (148.5 mg, 0.57 mmol) was added to **56** (100 mg, 0.52 mmol) in $PhNO_2$ (1.0 mL). After 30 min, [*Carbonyl*-^{13}C]-benzoyl chloride (140.5 mg, 1.04 mmol) was added and the mixture was stirred at 150°C under Ar for 3 d. The cooled mixture was quenched with ice-water (2.0 mL) and extracted with EtOAc (2 × 20 mL). The combined extracts were washed (NaOH, brine) and dried ($MgSO_4$). Evaporation and chromatography (hexane / EtOAc 15:1) gave **148** (37 mg, 39%) as a pale yellow solid: R_f =0.57 (hexane/EtOAc 4:1); mp 145-146°C (lit.[158] 142-143°C for unlabelled compound); ^1H NMR δ 7.49-7.51 (3 H, m, Ph 3,4,5-H_3), 7.60 (1 H, t, *J* = 8.2 Hz, 7-H), 7.87 (1 H, brd, *J* = 5.5 Hz, 4-H),

7.94 (2 H, m, Ph 2,6-H_2), 8.49 (1 H, dd, *J* = 8.2, 1.2 Hz, 6-H), 8.61 (1 H, ddd, *J* = 7.8, 1.2, 0.8 Hz, 8-H); ^{13}C NMR (HMBC / HMQC) δ 96.3 (d, *J* = 75.1 Hz, 4-C), 122.3 (d, *J* = 3.8 Hz, 4a-C or 8a-C), 125.9 (d, *J* = 1.5 Hz, Ph 2,6-C_2 or Ph 3,5-C_2), 127.1 (CH, s), 129.0 (CH, d, *J* = 4.6 Hz), 131.1 (d, *J* = 68.2 Hz, Ph 1-C), 131.2 (s, CH), 131.6 (s, CH), 131.9 (s, 8a-C or 4a-C), 135.8 (s, 8-C), 144.3 (d, *J* = 5 Hz, 5-C), 156.8 (s, 3-C), 156.8 (d, *J* = 75.9 Hz, 3-C for 3,4-$^{13}C_2$ isotopomer), 156.8 (d, *J* = 67.5 Hz, 3-C for 1',3-$^{13}C_2$ isotopomer), 160.3 (d, *J* = 3.1 Hz, 1-C); MS (ES +ve) *m/z* 559.1052 (2 M + Na) ($^{13}C_2{}^{12}C_{28}H_{18}N_2Na_1O_8$ requires 559.1028), 537 (2 M + H), 291.0476 (M + Na) ($^{13}C_1{}^{12}C_{14}H_9N_1Na_1O_4$ requires 291.0463), 269 (M + H).

5-Nitro-3-(4-nitrophenyl)isocoumarin (154)

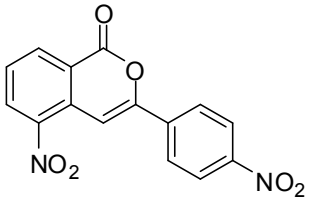

$SnCl_4$ (148.5 mg, 0.57 mmol) was added to **56** (100 mg, 0.52 mmol) in $PhNO_2$ (1.0 mL). After 30 min, 4-nitrobenzoyl chloride (193 mg, 1.04 mmol) was added and the mixture was stirred at 150°C under Ar for 3 d. The cooled mixture was quenched with ice-water (2.0 mL) and extracted with EtOAc (2 × 20 mL). The combined extracts were washed (NaOH, brine) and dried ($MgSO_4$). Evaporation and chromatography (hexane / EtOAc 15:1) gave **154** (9.8 mg, 12%) as a pale yellow solid: R_f =0.54 (hexane/EtOAc 4:1); mp 211-214 °C; IR ν_{max} 1724 (C=O), 1626 (C=C), 1537 & 1344 (NO_2) cm^{-1}; ^{1}H NMR δ 7.70 (1 H, d, *J* = 8.0 Hz, 7-H), 8.03 (1 H, brs, 4-H), 8.11 (2 H, d, *J* = 7.2 Hz, Ar 2,6-H_2), 8.36 (2 H, d, *J* = 7.2 Hz, Ar 3,5-H_2), 8.54 (1 H, dd, *J* = 8.3, 1.1 Hz, 6-H), 8.67 (1 H, brd, *J* = 8.2 Hz, 8-H); ^{13}C NMR (HMBC / HMQC) δ 99.2 (4-C), 122.8 (C_q), 124.3 (2',6'-C_2), 126.7 (3',5'-C_2), 128.5 (CH), 131.0 (C_q), 131.2 (C_q), 131.8 (CH), 135.9 (CH), 137.0 (C_q), 149 (C_q), 154 (C_q), 159 (1-C); MS m/z 335.0288 (M + Na) ($C_{15}H_8N_2NaO_6$ requires 335.0280); Anal. Found: C, 57.64; H, 2.51; N, 8.79. Calc. for $C_{15}H_8N_2O_6$: C, 57.70; H, 2.58; N, 8.97%.

3-(3-Methylphenyl)-5-nitroisocoumarin (155)

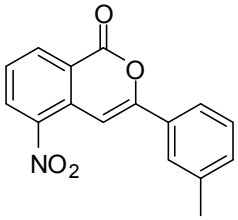

$SnCl_4$ (148.5 mg, 0.57 mmol) was added to **56** (100 mg, 0.52 mmol) in $PhNO_2$ (1.0 mL). After 30 min, 3-methylbenzoyl chloride (161 mg, 1.04 mmol) was added and the mixture was stirred at 150°C under Ar for 3 d. The cooled mixture was quenched with ice-water (2.0 mL) and extracted with EtOAc (2 × 20 mL). The combined extracts were washed (aq. NaOH, brine) and dried ($MgSO_4$). Evaporation and chromatography (hexane / EtOAc 15:1) gave **155** (21.3 mg, 21%) as a pale yellow solid: R_f =0.53 (hexane:EtOAc; mp 152-154°C; IR ν_{max} 1731 (C=O), 1621 (C=C), 1518 & 1337 (NO_2) cm^{-1}; ^1H NMR δ 2.43 (3 H, s, Me) 7.30 (1 H, d, *J* = 7.4 Hz, Ar 4-H), 7.40 (1 H, t, *J* = 7.7 Hz, Ar 5-H), 7.58 (1 H, t, *J* = 8.0 Hz, 7-H), 7.71 (1 H, d, *J* = 7.7 Hz, Ar 6-H), 7.73 (1 H, s, Ar 2-H), 7.83 (1 H, s, 4-H), 8.47 (1 H, d, *J* = 8.2 Hz, 6-H), 8.61 (1 H, d, *J* = 7.7 Hz, 8-H); MS *m/z* 282.0761 (M + H) ($C_{16}H_{12}NO_4$ requires 282.0766); Anal. Found: C, 68.58; H, 4.07; N, 4.79. Calc. for $C_{16}H_{12}NO_4$: C, 68.32; H, 3.94; N, 4.98%.

5-Amino-3-(2-methylphenyl)isoquinolin-1-one hydrochloride (157)

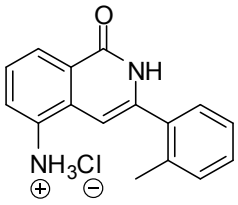

To **158** (200 mg, 0.71 mmol) in EtOH (10 mL) and aq. HCl (34%, 0.4 mL), a slurry of 10% Pd on charcoal (80 mg) in EtOH (5 mL) was added. The mixture was stirred under H_2 for 2 h. The suspension was then filtered through Celite®. The Celite® pad and residue were suspended in water (100 mL) and heated. The hot suspension was filtered through a second Celite® pad. Evaporation of the solvent and drying gave **157** (161 mg, 52%) as a

buff solid: R_f = 0.36 (MeOH); mp >350°C (decomp); ^{1}H NMR ($(CD_3)_2SO$) δ 2.32 (3 H, s, Me), 6.61 (1 H, s, 4-H), 7.16 (1 H, t, *J* = 7.2 Hz, 7-H), 7.32-7.38 (5 H, m, 6-H and Ar-, 3,4,5,6-H_4), 7.66 (1 H, d, *J* = 7.2 Hz, 8-H), 11.40 (1 H, s, NH); ^{13}C NMR δ 19.7, 99.9, 123.1, 124.1, 125.8, 126.6, 127.4, 129.5, 129.5, 130.3, 132.4, 133.6, 135.3, 135.4, 136.1, 155.2; MS (ESI +ve) *m/z* 273.1001 (M + Na) ($C_{16}H_{14}NaN_2O$ requires 273.1004); 251.1191 (M + H) ($C_{16}H_{15}N_2O$ requires 251.1184).

5-Amino-3-(3-methylphenyl)isoquinolin-1-one (159)

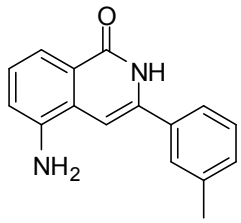

To **155** (320 mg, 1.14 mmol) in EtOH (30 mL), a slurry of 10% Pd on charcoal (160 mg) in EtOH (10 mL) was added. The mixture was stirred under H_2 for 2 h. The suspension was then filtered through Celite®. Evaporation of the solvent from the filtrate and drying gave **159** (177 mg, 62%) as a pale buff solid: R_f = 0.12 (hexane / EtOAc 1:4); mp 340-342°C; ^{1}H NMR ($(CD_3)_2SO$) δ 2.39 (3 H, s, Me), 5.76 (2 H, br s, NH_2), 6.88 (1 H, d, *J* = 7.6 Hz, 6-H), 7.09 (1 H, s, 4-H), 7.18 (1 H, d, *J* = 7.6 Hz, 8-H), 7.24 (1 H, t, *J* = 7.6 Hz, 7-H), 7.34-7.38 (1 H, d, Ar 4-H), 7.42 (1 H, t, *J* = 7.4 Hz, Ar 5-H), 7.63 (1 H, d, *J* = 7.4 Hz, Ar 6-H), 7.68 (1 H, s, Ar 2-H) 11.25 (1 H, br s, NH); ^{13}C NMR δ 21.0, 98.5, 113.9, 115.2, 124.5, 125.6, 126.8, 127.0, 127.1, 129.3, 130.7, 134.3, 137.6, 138.2, 144.7, 163.0; MS (ESI +ve) *m/z* 273.0987 (M + Na) ($C_{16}H_{14}NaN_2O$ requires 273.1104); 251.1182 (M + H) ($C_{16}H_{15}N_2O$ requires 251.1184).

5-Nitro-3-(4-iodophenyl)isocoumarin (159)

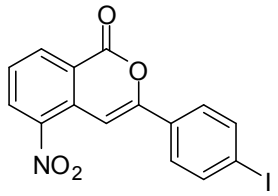

$SnCl_4$ (148.5 mg, 0.57 mmol) was added to **56** (100 mg, 0.52 mmol) in $PhNO_2$ (1.0 mL). After 30 min, 4-iodobenzoyl chloride (277.1mg, 1.04 mmol) was added and the mixture was stirred at 150°C under Ar for 3 d. The cooled mixture was quenched with ice-water (2.0 mL) and upon standing a precipitate developed which was collected by filtration. Washing (EtOAc) and drying gave **156** (76.0 mg, 34%) as a pale yellow solid: R_f = 0.66 (hexane / EtOAc 10:1); mp 211-213°C; ^{1}H NMR ($(CD_3)_2SO$) δ 7.24 (1 H, s, 4-H), 7.62 (1 H, t, *J* = 7.8 Hz, 7-H), 7.66 (2 H, d, *J* = 8.4 Hz, Ar 3,5-H_2), 7.88 (2 H, d, *J* = 8.4 Hz, Ar 3,5-H_2), 8.50 (1 H, dd, *J* = 7.8, 1.2 Hz, 6-H), 8.65 (1 H, dd, *J* = 7.8, 1.2 Hz, 8-H); ^{13}C NMR δ 90.7, 96.6, 127.3, 127.5, 128.3, 128.5, 131.5, 135.8, 137.9, 138.3, 143.4, 144.9, 152.4. MS (ESI +ve) *m/z* 415.9390 (M + Na) ($C_{15}H_8NaINO_4$ requires 415.9396); 393.9581 (M + H) ($C_{15}H_9INO_4$ requires 393.9576).

3-(4-Iodophenyl)-5-nitroisoquinolin-1-one (160)

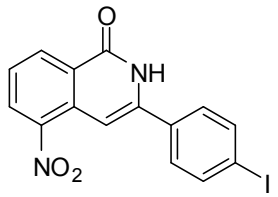

A solution of **159** (360 mg, 1.2 mmol) in 2-methoxyethanol (80 mL) was saturated with NH_3 and boiled under reflux for 4 h. The solvent and excess reagent were evaporated until 10 mL remained. The concentrate was stored at 4°C for 16 h and the precipitated crystals were filtered, washed (H_2O, then EtOH) and recrystallised (MeOH) to give **160** (198 mg, 59%) as bright yellow crystals: R_f = 0.31 (hexane / EtOAc 1:4); mp 254-256°C; ^{1}H NMR ($(CD_3)_2SO$) δ 7.26 (1 H, s, 4-H), 7.60 (2 H, d, *J* = 8.4 Hz, Ar 3,5-H_2), 7.69 (1 H, t, *J* = 7.8 Hz, 7-H), 7.92 (1 H, d, *J* = 8.4 Hz, Ar 2,6-H_2), 8.47 (1 H, dd, *J* = 7.8, 1.2 Hz, 6-H), 8.60 (1 H, dd, *J* = 7.8, 1.2 Hz, 8-H), 12.12 (1 H br s, NH); ^{13}C NMR δ 97.2, 97.4,

125.9, 126.7, 129.2, 129.9, 130.8, 133.0, 133.1, 137.4, 137.7, 143.3, 144.4, 161.3; MS (ESI +ve) *m/z* 414.9560 (M + Na) ($C_{15}H_9NaIN_2O_3$ requires 414.9556); 392.9731 (M + H) ($C_{15}H_{10}IN_2O_3$ requires 392.9736).

5-Amino-3-(4-iodophenyl)isoquinolin-1-one (161)

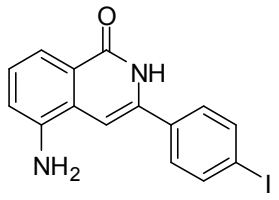

A mixture of **160** (588 mg, 1.5 mmol) and $SnCl_2$ (870 mg, 4.6 mmol) in EtOH (40 ml) was heated at 70°C for 4 h, then poured into ice-H_2O (200 ml). The resulting suspension was made alkaline (aq. NaOH) and the precipitate was filtered. Extraction of the filtrate (EtOAc), evaporation and recrystallisation (hexane, EtOAc) gave **161** (277 mg, 51%) as a pale buff powder: R_f = 0.26 (hexane / EtOAc 1:4); mp 238-241°C; ^{1}H NMR ($(CD_3)_2SO$) δ 5.81 (2 H, br s, NH_2) 7.26 (1 H, d, *J* = 7.8 Hz, 6-H), 7.39 (1 H, s, 4-H), 7.14 (1 H, d, *J* = 7.8 Hz, 8-H), 7.39 (1 H, t, *J* = 7.8 Hz, 7-H), 7.64 (2 H, d, *J* = 8.4 Hz, Ar 3,5-H_2), 7.83 (2 H, d, *J* = 8.4 Hz, Ar 2,6-H_2) 11.89 (1 H, br s, NH); ^{13}C NMR δ 99.0, 99.9, 113.7, 115.2, 128.4, 129.8, 130.1, 133.0, 135.9, 137.3, 137.9, 144.6, 145.0, 164.8; MS (ESI +ve) *m/z* 384.9808 (M + Na) ($C_{15}H_{11}INaN_2O$ requires 384.9814); 369.9987 (M + H) ($C_{15}H_{12}IN_2O$ requires 362.9994).

3-(2-Methylphenyl)-5-nitroisoquinolin-1-one (162)

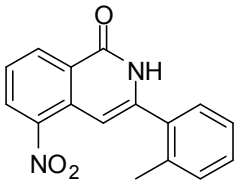

A solution of **163** (360 mg, 1.2 mmol) in 2-methoxyethanol (80 mL) was saturated with NH_3 and boiled under reflux for 4 h. The solvent and excess reagent were evaporated until 10 mL remained. The concentrate was stored at 4°C for 16 h and the precipitated crystals were filtered, washed (H_2O, then EtOH) and recrystallised (MeOH) to give **162** (198 mg, 59%) as bright yellow crystals: R_f = 0.31 (hexane / EtOAc 1:4); mp 254-256°C; ^{1}H NMR ($(CD_3)_2SO$) δ 2.33 (3 H, s, Me), 7.34 (2 H, t, *J* = 8.0 Hz, Ar 4,5-H_2), 7.40 (2 H, d, *J* = 8.2 Hz, Ar 3,6-H_2), 7.67 (1 H, t, *J* = 8.0 Hz, 7-H), 8.48 (1 H, dd, *J* = 8.0, 1.2 Hz, 6-H), 8.61 (1 H, dd, *J* = 8.0, 1.2 Hz, 8-H); ^{13}C NMR δ 19.5, 99.0, 125.6, 125.9, 126.6, 129.3, 129.6, 129.7, 130.5, 133.2, 134.5, 134.5, 136.0, 144.6, 145.0, 160.9; MS (ESI +ve) *m/z* 303.0752 (M + Na) ($C_{16}H_{12}NaN_2O_3$ requires 303.0746), 281.0922 (M + H) ($C_{16}H_{13}N_2O_3$ requires 281.0926).

3-(2-Methylphenyl)-5-nitroisocoumarin (163)

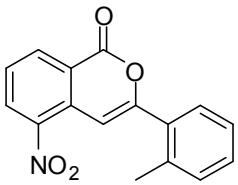

$SnCl_4$ (148.5 mg, 0.57 mmol) was added to **56** (100 mg, 0.52 mmol) in $PhNO_2$ (1.0 mL). After 30 min, 2-methylbenzoyl chloride (161 mg, 1.04 mmol) was added and the mixture was stirred at 150°C under Ar for 3 d. The cooled mixture was quenched with ice-water (2.0 mL) and extracted with EtOAc (2 × 20 mL). The combined extracts were washed (NaOH, brine) and dried ($MgSO_4$). Evaporation and chromatography (hexane / EtOAc 15:1) gave **163** (37 mg, 25%) as a bright yellow solid: R_f = 0.51 (hexane / EtOAc 4:1); mp 132-134°C; ^{1}H NMR ($CDCl_3$) δ 2.54 (3 H, s, Me), 7.29-7.34 (2 H, m, Ar 4,5-H_2), 7.40 (1 H, dt, *J* = 7.2, 1.6 Hz, Ar 3-H), 7.52 (1 H, d, *J* = 0.8 Hz, 4-H), 7.57 (1 H, dd, *J* =

7.2, 1.6 Hz, Ar 6-H), 7.64 (1 H, t, *J* = 8.0 Hz, 7-H), 8.51 (1 H, dd, *J* = 8.0, 1.2 Hz, 6-H), 8.67 (1 H, ddd, *J* = 8.0, 1.2, 0.8 Hz, 8-H); ^{13}C NMR δ 20.9, 100.6, 100.6, 122.2, 126.3, 127.4. 129.4, 130.6, 131.4, 131.5, 131.8, 132.1, 135.8, 137.0, 144.3, 158.9, 160.6; MS (ESI +ve) *m/z* 304.0581 (M + Na) ($C_{16}H_{11}NaNO_4$ requires 304.0586); 251.0769 (M + H) ($C_{16}H_{12}NO_4$ requires 282.0766).

5-Nitro-3-(3-methylphenyl)isoquinolin-1-one (164)

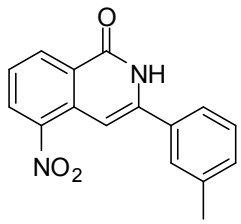

Method A:

A solution of **155** (360 mg, 1.2 mmol) in 2-methoxyethanol (80 mL) was saturated with NH_3 and heated under reflux for 4 h. The solvent and excess reagent were evaporated until 10 mL remained. The concentrate was stored at 4°C for 16 h and the precipitated crystals were filtered, washed (H_2O, then EtOH) and recrystallised (MeOH) to give **164** (198 mg, 59%) as bright yellow crystals: R_f = 0.31 (hexane / EtOAc 1:4); mp 325-328°C; ^{1}H NMR ($(CD_3)_2SO$) δ 2.46 (3 H, s, Me), 7.22 (1 H, s, 4-H), 7.34 (1 H, d, *J* = 7.4 Hz, Ar 4-H), 7.42 (1 H, t, *J* = 7.4 Hz, Ar 5-H), 7.57 (1 H, d, *J* = 7.5, Ar 6-H), 7.62 (1 H, s, Ar 2-H), 7.65 (1 H, t, *J* = 7.9 Hz, 7-H), 8.47 (1 H, dd, *J* = 7.8, 1.1 Hz, 6-H), 8.59 (1 H, dd, *J* = 7.8, 1.1 Hz, 8-H); ^{13}C NMR δ 20.9, 97.0, 124.3, 125.2, 126.5, 127.6, 128.8, 129.7, 130.7, 130.9, 133.1, 133.4, 138.2, 144.3, 144.7, 161.3; MS (ESI +ve) *m/z* 281.0922 (M + H) ($C_{16}H_{13}N_2O_3$ requires 281.0926).

Method B:

Compound **173** (250 mg, 0.8 mmol) was stirred in ag. HBr (78 %, 40 mL) at 80°C for 4 h. Evaporation and recyrstallisation gave **155** (195 mg, 85%) as bright yellow crystals: data as above.

1,3-Dichloro-5-nitroisoquinoline (168)

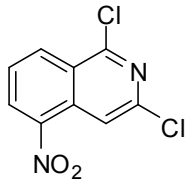

To a cooled solution of 1,3-dichloroisoquinoline **172** (1.00 g, 5.05 mmol) in conc. H_2SO_4 (5 mL) was added aq. HNO_3 (70%, 0.43 g, 6.7 mmol) in conc. H_2SO_4 (3 mL) dropwise at 0-5°C. The mixture was stirred at 0°C for 2 h, then poured onto ice. The precipitate was collected, washed (H_2O), dried under vacuum and recrystallised (EtOAc / hexanes) to give **168** (1.12 g, 91%) as pale yellow needles: mp 175-177°C (lit.[178] mp 168-170°C); ^{1}H NMR δ 7.79 (1 H, t, *J* = 7.8 Hz, 7-H), 8.53 (1 H, s, 4-H), 8.61 (1 H, dd, *J* = 7.8, 0.8 Hz, 6-H), 8.70 (1 H, dd, *J* = 7.8, 0.8 Hz, 8-H).

3-Chloro-1-methoxy-5-nitroisoquinoline (171)

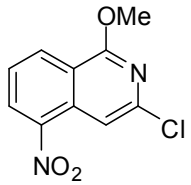

To **168** (6.0 g, 25 mmol) in anhydrous MeOH (90 mL) was added finely divided sodium (0.7 g, 31.5 mmol) and the mixture was heated under reflux for 16 h. The excess solvent was then evaporated until 20 mL remained and the residue was diluted with H_2O and extracted ($CHCl_3$). Evaporation of the solvent and drying gave **171** (4.8 g, 82%) as a yellow solid: R_f = 0.54 (hexane / EtOAc 10:1); mp 172-174°C; ^{1}H NMR δ 4.04 (3 H, s, OMe), 7.60 (1 H, t, *J* = 8.0 Hz, 7-H), 8.22 (1 H, s, 3-H), 8.51 (1 H, dd, *J* = 8.0, 1.2 Hz, 6-H), 8.58 (1 H, dd, *J* = 8.0, 1.2 Hz, 8-H); ^{13}C NMR δ 55.1, 109.8, 119.4, 119.4, 125.0,

129.3, 131.5, 131.9, 147.4. 160.9; MS *m/z* 239.0216 (M + H) ($C_{10}H_8{}^{35}ClN_2O_3$ requires 239.0223).

1-Methoxy-3-(3-methylphenyl)-5-nitroisoquinoline (173)

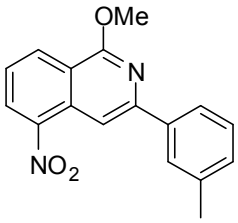

Compound **171** (0.84 g, 3.53 mmol), $Pd_2(dba)_3$ (0.18 g, 0.35 mmol), SPhos (0.14 g, 0.70 mmol), K_3PO_4 (1.5g, 7.06 mmol) and 3-methylphenylboronic acid (0.72g 5.30 mmol) were placed in a dry flask. Degassed toluene (20 mL) was added and the mixture was stirred at 100°C for 16 h. Evaporation and chromatography (hexane/EtOAc 15:1) gave **173** (0.70 g, 67%) as yellow crystals: R_f = 0.69 (hexane / EtOAc 10:1); mp 166-169°C; ^{1}H NMR ($CDCl_3$) δ 2.36 (3 H, s, ArMe), 4.11 (3 H, s, OMe), 7.13 (1 H, d, *J* = 7.8 Hz, Ar 4-H), 7.27 (1 H, t, *J* = 7.8 Hz, Ar 5-H), 7.36 (1 H, t, *J* = 7.4 Hz, 7-H), 7.83 (1 H, s, Ar 2-H), 7.85 (1 H, d, *J* = 7.6 Hz Ar 6-H), 8.23-8.26 (2 H, m, 6-H and 4-H), 8.39 (1 H, d, *J* = 7.4 Hz 8-H); ^{13}C NMR (HMBC / HMQC) δ 21.6 (ArMe), 54.0 (OMe), 104.9 (4-C), 124.2 (Ar 6-C), 124.2 (7-C), 127.6 (Ar 2-C) 128.5 (6-C), 128.6 (Ar 5-C), 130.1 (Ar 4-C), 131.1 (8-C), 131.3 (C_q), 138.2 (Ar 1-C), 138.5 (C_q),151.8 (3-C), 151.9 (5-C), 160.3 (1-C); MS *m/z* 295.1076 (M + H) ($C_{17}H_{15}N_2O_3$ requires 295.1083).

2,6-Dicyanoethylbenzene (174)

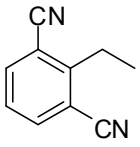

$LiN(SiMe_3)_2$ in dry THF (1.0 M, 15.4 mL, 15.4 mmol) was added to 2,6-dicyanotoluene **41** (2.0 g, 14 mmol) in dry THF (30 mL) at -78°C under N_2. After 30 min, MeI (2.1 mL, 2.39 g, 16.8 mmol) was added; the mixture allowed to warm to room temperature and was stirred for a further 2 h. The reaction mixture was quenched with ice-water and extracted with $CHCl_3$. Evaporation and recrystallisation gave **174** (1.7 g, 78%) as pale

yellow crystals: R_f = 0.91 (hexane / EtOAc 4:1); mp 115-117°C (lit.[170] mp 116-118°C); ^{1}H NMR δ 1.36 (3 H, t, *J* = 7.6 Hz, Me), 3.06 (2 H, q, *J* = 7.6 Hz, CH_2), 7.42 (1 H, t, *J* = 7.7 Hz, 4-H), 7.82 (2 H, *J* = 7.7 Hz, 3,5-H_2).

(±)-3-Cyano-2-(1-methyl-2-oxoethyl)benzonitrile (176)

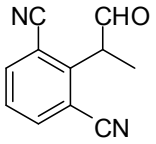

Compound **174** (1.0 g, 6 mmol) was boiled under reflux in dimethylformamide dimethyl acetal (10.0 g, 84 mmol) under N_2 for 5 d. 4-Methylbenzenesulfonic acid monohydrate (100 mg, 0.53 mmol) was added and the mixture was stirred for a further 2 d. Evaporation and chromatography (hexane / EtOAc 3:2) gave **176** (136 mg, 12%) as a yellow solid: R_f = 0.77 (hexane / EtOAc 4:1); mp 229-232°C; ^{1}H NMR δ 1.80 (3 H, d, *J* = 7.7 Hz, Me), 4.24 (1 H, q, *J* = 7.4 Hz, CH), 7.56 (1 H, t, *J* = 7.8 Hz, 5-H), 7.92 (2 H, d, *J* = 7.8 Hz, 4,6-H_2), 9.84 (1 H, s, CHO); ^{13}C NMR δ 14.3, 51.1, 114.8, 116.2, 128.8, 137.5, 146.4, 197.5. MS (ES +ve) *m/z* 185.0720 (M + H) ($C_{11}H_9N_2O$ requires 186.0555).

5-Cyano-4-methylisocoumarinn (177)

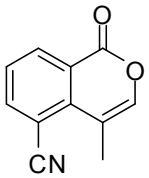

Compound **176** (100 mg, 0.54 mmol) was stirred with Pr^i_2NH (60 mg, 0.59 mmol) in THF (10 mL) for 24 h. Evaporation and chromatography (hexane/EtOAc 6:1) gave **177** (13 mg, 13%) as a white solid: R_f = 0.61 (hexane / EtOAc 4:1); mp 237-239°C; ^{1}H NMR δ 2.52 (3 H, d, *J* = 1.2 Hz, Me), 7.17 (1 H, q, *J* = 1.2 Hz, 3-H), 7.62 (1 H, t, *J* = 7.8 Hz, 7-H), 8.08 (1 H, dd, *J* = 7.8, 1.2 Hz, 6-H), 8.57 (1 H, dd, *J* = 7.8, 1.2 Hz); ^{13}C NMR δ 15.4, 107.8, 111.7, 122.8, 128.2, 135.1, 135.2, 137.4, 141.7, , 143.8, 160.8. MS (ES +ve) *m/z*

186.0552 (M + H) ($C_{11}H_8NO_2$ requires 186.0555) 208.0372 (M + Na) ($C_{11}H_7NNaO_2$)requires 208.0374.

5-Amino-4-bromoisoquinolin-1(2*H*)-one (184)

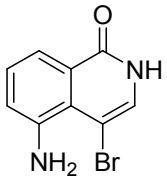

A mixture of **49** (0.27 g, 1.0 mmol) and $SnCl_2$ (0.65 g, 3.2 mmol) in EtOH (10 mL) was heated at 80°C for 4 h, then poured into ice-H_2O (40 mL). The resulting suspension was made alkaline with aq. NaOH and the precipitate was filtered. Extraction of the filtrate (EtOAc), evaporation and chromatography (EtOAc:hexane 4:1) gave **189** (0.14 g, 54%) as a buff solid: R_f = 0.33 (EtOAc:hexane 1:4); mp 213-216°C (lit[175] 210-212°C); ^{1}H NMR ($(CD_3)_2SO$) δ 5.91 (2 H, br s, NH_2), 7.74 (1 H, s, 3-H), 7.02 (1 H, dd, *J* = 8.4, 1.5 Hz, 6-H), 7.20 (1 H, s, 3-H), 7.26 (1 H, t, *J* = 8.4 Hz, 7-H), 7.54 (1 H, dd, *J* = 8.0, 1.4 Hz, 8-H), 11.34 (1 H, br s, NH)

4-Bromo-1-chloro-5-nitro-isoquinoline (189)

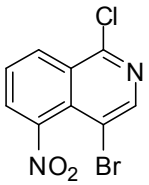

Vilsmeier's reagent was prepared by adding oxalyl chloride (5.3 mL, 7.67 g, 60.4 mmol) dropwise over 30 min to DMF (4.7 mL, 4.4 g, 60.4 mmol) in 1,2-dichloroethane (35 mL) at 0°C. The suspension was stirred at room temperature for 10 min, then **49** (7.3 g, 27.3 mmol) was added. The mixture was then heated at 80°C for 6 h, allowed to cool and diluted with CH_2Cl_2. Washing (H_2O), drying and evaporation of solvent gave **189** (7.0 g, 89%) as a yellow solid: mp 164-166°C; ^{1}H NMR ($CDCl_3$) δ 7.82 (1 H, t, *J* = 7.6 Hz, 7-H), 8.01 (1 H, dd, *J* = 7.6, 1.2 Hz, 6-H), 8.62 (1 H, s, 3-H), 8.65 (1 H, dd, *J* = 7.6, 1.2 Hz,

8-H); ^{13}C NMR δ 112.4, 127.1, 127.8, 128.2, 128.6, 131.0, 147.4, 147.6, 152.0; MS (ESI +ve) *m/z* 240.0682 (M + Na) ($C_{12}H_{11}NaNO_3$ requires 240.0637); 218.0819 (M + H) ($C_{16}H_{15}N_2O$ requires 218.0817).

1-Methoxy-4-methyl-5-nitroisoquinoline (190)

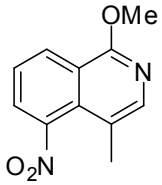

Method A:

To **46** (100 mg, 0.35 mmol) in dry THF (9 mL) was added *n*-BuLi in THF (1.6 M, 0.24 mL, 0.38 mmol) at -78°C. The suspension was stirred for 20 min. Iodomethane (55.4 mg, 0.39 mmol) in THF (1 mL) was added and the mixture allowed to warm to room temperature over 1 h. The reaction was quenched with H_2O and extracted (CH_2Cl_2). Evaporation and chromatography (hexane/EtOAc 15:1) gave **190** (7 mg, 9%)as a yellow-orange solid: R_f = 0.54 (hexane / EtOAc 5:1); mp 90-93°C; ^{1}H NMR ($CDCl_3$) δ 2.91 (3 H, s, 4-Me), 4.09 (3 H, s, OMe), 7.50 (1 H, t, *J* = 8.6 Hz, 7-H), 7.75 (1 H, d, *J* = 7.4 Hz, 8-H), 7.87 (1 H, s, 3-H) 8.42 (1 H, d, *J* = 7.4 Hz, 6-H); ^{13}C NMR (HMBC / HMQC) δ 16.00 (4-Me), 53.94 (OMe), 120.00 (4-C), 125.02 (7-C), 125.34 (4a-C), 125.66 (8-C), 128.34 (6-C), 128.91 (8a-C), 143.24 (5-C), 143.58 (3-C), 159.99 (1-C); MS (ES +ve) *m/z* 241.0582 (M + Na) ($C_{10}H_{10}N_2NaO_3$ requires 241.0589), 219.0772 (M + H) ($C_{10}H_{11}N_2O_3$ requires 219.0770).

Method B:

Compound **46** (1.00 g, 3.52 mmol), $Pd_2(dba)_3$ (0.18 g, 0.35 mmol), SPHOS (0.14 g, 0.70 mmol) and $SnMe_4$ (0.95 g, 5.28 mol) were placed in a dry flask. Degassed toluene (20 mL) was added and the mixture was stirred at 100°C for 7 d. Evaporation and chromatography (hexane/EtOAc 15:1) gave **190** (0.77 g, 72%) as a yellow-orange solid: data as above.

4-Phenyl-1-methoxy-5-nitroisoquinoline (194)

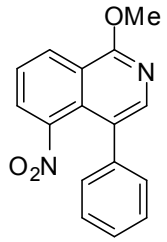

Compound **46** (1.00 g, 3.53 mmol), $Pd_2(dba)_3$ (0.18 g, 0.35 mmol), SPhos (0.14 g, 0.70 mmol), K_3PO_4 (1.5g, 7.06 mmol) and benzeneboronic acid (0.64g 5.30 mmol) were placed in a dry flask. Degassed toluene (40 mL) was added and the mixture was stirred at 100°C for 16 h. Evaporation and chromatography (hexane / EtOAc 10:1) gave **194** (0.85 g, 86%) as yellow crystals: R_f = 0.79 (hexane / EtOAc 1:1); mp 118-120°C; ^{1}H NMR ($CDCl_3$) δ 4.20 (3 H, s, OMe), 7.27-7.31 (2 H, m, Ph 2,6-H_2), 7.38-7.43 (3 H, m, Ph 3,4,5-H_3), 7.62 (1 H, t, *J* = 8.0 Hz, 7-H), 7.97 (1 H, dd, *J* = 8.0, 1.2 Hz, 6-H or 8-H), 8.06 (1 H, s, 3-H), 8.60 (1 H, dd, *J* = 8.0, 1.2 Hz, 8-H or 6-H); ^{13}C NMR δ 54.4, 120.7, 124.5, 125.5, 127.4, 127.7, 127.8, 128.1, 128.4, 129.1, 137.5, 144.7, 147.6, 160.3; MS (ES +ve) *m/z* 303.0740 (M + Na) ($C_{16}H_{11}NaN_2O_3$ requires 303.0746); 281.0915 (M + H) ($C_{16}H_{12}N_2O_3$ requires 281.0926); Anal. Found: C, 68.50; H, 4.26; N, 10.19. Calc. for $C_{16}H_{12}N_2O_3$: C, 68.57; H, 4.32; N, 10.00%.

5-Amino-4-phenylisoquinolin-1-one (195)

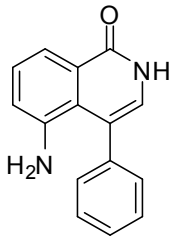

To **196** (46 mg, 0.17 mmol) in EtOH (10 mL), a slurry of 10% Pd on charcoal (50 mg) in EtOH (5 mL) was added. The mixture was stirred under H_2 for 6 h. The suspension was then filtered through Celite®. Evaporation of the solvent and drying gave **195** (21 mg, 51%) as a pale yellow solid: R_f = 0.47 (hexane / EtOAc, 1:1); mp 236-240°C; ^{1}H NMR ($(CD_3)_2SO$) δ 4.45 (2 H, s, NH_2), 6.70 (1 H, brs, 3-H), 6.86 (1 H, dd, *J* = 7.8, 1.2 Hz, 6-H), 7.23 (1 H, t, *J* = 7.8 Hz, 7-H), 7.36 (2 H, dd, *J* = 7.3, 1.2, Ph 2,6-H_2), 7.41-7.47 (3 H, m, Ph 3,4,5-H_3), 7.60 (1 H, d, *J* = 7.8, 1.2 Hz, 8-H), 11.20 (1 H, br, NH); ^{13}C NMR (HMBC / HMQC) δ 116.2 (8-C), 118.40 (6-C), 122.6 (4a-C) 125.4 (4-C), 127.4 (3-C), 128.0 (7-C), 128.3 (Ph 4-C), 129.1 (Ph 3,5-C_2), 130.2 (8a-C), 130.3 (Ph 2,6-C_2), 141.1 (Ph 1-C), 142.3 (5a-C), 160.1 (1-C); MS (ES +ve), *m/z* 259.0841 (M + Na) ($C_{15}H_{11}NaN_2O$ requires 259.0847), *m/z* 237.1017 (M + H) ($C_{15}H_{12}N_2O$ requires 237.1022); Anal. Calcd. for $C_{15}H_{12}N_2O$: C, 76.26; H, 5.12; N, 11.37. Found: C, 76.68; H, 5.46; N, 11.43.

5-Nitro-4-phenylisoquinolin-1-one (196)

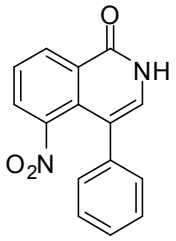

Compound **194** (182 mg, 0.65 mmol) was stirred in aq. HBr (48 %, 30ml) at 50°C for 4 h. Evaporation and recyrstallisation (hexane / EtOAc) gave **196** (112 mg, 65%) as yellow crystals solid: R_f = 0.34 (hexane / EtOAc 1:1); mp 211-214°C; ^{1}H NMR ($(CD_3)_2SO$) δ 7.20 (3 H, m, 3-H and Ph 2,6-H_2), 7.32 (3 H, m, Ph 3,4,5-H_3), 7.70 (1 H, t, *J* = 7.6 Hz, 7-

H), 8.14 (1 H, dd, J = 7.8, 1.2 Hz, 6-H), 8.58 (1 H, dd, J = 7.8, 1.2 Hz, 8-H); ^{13}C NMR δ 113.5, 126.4, 127.2, 127.6, 128.0, 128.2, 128.5, 129.0, 131.6, 133.1, 136.7, 147.0, 159.7; MS (ES +ve) *m/z* 289.0598 (M + Na) ($C_{15}H_{10}NaN_2O_3$ requires 289.0589); 267.0761 (M + H) ($C_{15}H_{11}N_2O_3$ requires 267.0770); Anal. Found: C, 68.60; H, 3.48; N, 10.49. Calc. for $C_{15}H_{10}N_2O_3$: C, 67.67; H, 3.59; N, 10.52%.

5-Amino-4-(4-trifluoromethylphenyl)isoquinolin-1-one (197)

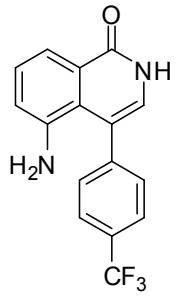

To **199** (56 mg, 0.18 mmol) in EtOH (10 mL), a slurry of 10% Pd on charcoal (50 mg) in EtOH (5 mL) was added. The mixture was stirred under H_2 for 6 h. The suspension was then filtered through Celite®. Evaporation of the solvent and drying gave **197** (29mg, 53%) as a pale yellow solid: R_f = 0.52 (hexane / EtOAc, 1:1); mp 265-267°C; ^{1}H NMR ($(CD_3)_2SO$) δ 4.37 (2 H, s, NH_2), 6.81 (1 H, brs, 3-H), 6.93 (1 H, dd, J = 7.8, 1.2 Hz, 6-H), 7.27 (1 H, t, J = 7.8 Hz, 7-H), 7.57 (2 H, d, J = 7.6 Hz, Ar 2,6-H_2), 7.63 (1 H, dd, J = 7.8, 1.2 Hz, 6-H), 7.77 (1 H, d, J = 7.6 Hz, 8-H), 11.31 (1 H, brs, NH); ^{13}C NMR δ 112.9, 114.7, 115.8, 118.2, 120.9, 124.9 (m, Ph 3,5-C_2), 127.5, 127.8, 127.9 (m, CF_3), 128.8 (m, Ph C-4), 130.2, 130.5, 143.0, 144.2, 161.5; MS (ES +ve) *m/z* 327.0729 (M + Na) ($C_{17}H_{11}F_3NaN_2O$ requires 327.0712), 305.0905 (M + H) ($C_{17}H_{12}F_3N_2O$ requires 305.0902); Anal. Calcd. for $C_{17}H_{11}F_3N_2O$: C, 63.16; H, 3.64; N, 9.21. Found: C, 63.21; H, 3.69; N, 9.30%

.

1-Methoxy-5-nitro-4-(4-trifluoromethylphenyl)isoquinoline (198)

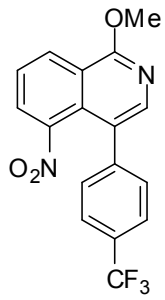

Compound **46** (1.00 g, 3.53 mmol), $Pd_2(dba)_3$ (0.18 g, 0.35 mmol), SPhos (0.14 g, 0.70 mmol), K_3PO_4 (1.5g, 7.06 mmol) and (4-trifluoromethylphenyl)boronic acid (1.00 g, 5.30 mmol) were placed in a dry flask. Degassed toluene (40 mL) was added and the mixture was stirred at 100°C for 16 h. Evaporation and chromatography (hexane/EtOAc 10:1) gave **198** (1.00 g, 81%) as yellow crystals; R_f = 0.76 (hexane / EtOAc 1:1); mp 95-97°C; ^{1}H NMR ($CDCl_3$) δ 4.25 (3 H, s, OMe), 7.43 (2 H, d, *J* = 8.8 Hz, Ar 2,6-H_2), 7.68-7.72 (3 H, m, 7-H and Ar 3,5-H_3), 8.05 (1 H, dd, *J* = 8.4, 1.2 Hz, 6-H), 8.07 (1 H, s, 3-H), 8.66 (1 H, dd, *J* = 8.4, 1.2 Hz, 8-H); ^{13}C NMR δ 54.5, 120.7, 123.1, 125.4 (q, *J* = 3.7 Hz, Ar 3.5-C_2), 125.8, 127.3 (m, CF_3), 127.6, 128.3, 129.4, 130.0 (m, Ar 4-C), 141.2, 145.0, 160.8; MS (ES +ve) *m/z* 371.0631 (M + Na) ($C_{17}H_{11}F_3NaN_2O_3$ requires 371.0619), 349.0805 (M + H) ($C_{17}H_{12}F_3N_2O_3$ requires 349.0800); Anal. Calcd. for $C_{17}H_{11}F_3N_2O_3$: C, 58.63; H, 3.18; N, 8.05. Found: C, 58.47; H, 3.23; N, 7.96.

5-Nitro-4-(4-trifluoromethylphenyl)isoquinolin-1-one (199)

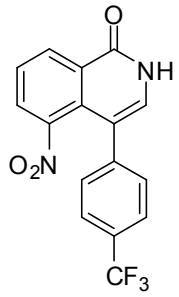

Compound **198** (182 mg, 0.65 mmol) was stirred in aq. HBr (48 %, 30 mL) at 50°C for 4 h. Evaporation and recrystallisation gave **199** (112 mg, 65%) as yellow crystals: R_f = 0.37 (hexane / EtOAc 1:1); mp 283-285°C; ^{1}H NMR ($(CD_3)_2SO$) δ 7.34 (1 H, d, *J* = 6.5 Hz, 3-H), 7.46 (2 H, d, *J* = 7.8 Hz, Ar 3,5-H_2), 7.70 (2 H, d, *J* = 7.8 Hz, Ar 2,6-H_2), 7.73 (1 H, t, *J* = 8.2 Hz, 7-H), 8.22 (1 H, dd, *J* = 8.2, 1.2 Hz, 6-H), 8.61 (1 H, dd, *J* = 8.2, 1.2 Hz, 8-H), 12.09 (1 H, d, *J* = *ca*. 5.5 Hz, NH); ^{13}C NMR δ 112.0, 125.1 (q, *J* = 3.8 Hz, Ar 3,5-C_2), 126.7, 127.7, 128.0, 128.1, 128.2, 129.3, 131.9 (m, Ar 4-C), 134.0 (m, CF_3), 141.1, 146.7, 159.8; Anal. Calc. for $C_{16}H_9F_3N_2O_3$: C, 57.50; H, 2.71; N, 8.38. Found: C, 57.14; H, 2.67; N, 8.04 %.

5-Amino-4-(4-methoxyphenyl)isoquinolin-1-one (200)

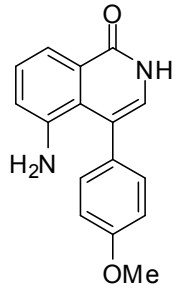

To **203** (100 mg, 0.26 mmol) in EtOH (15 mL), a slurry of 10% Pd on charcoal (80 mg) in EtOH (8 mL) was added. The mixture was stirred under H_2 for 16 h. The suspension was then filtered through Celite®. Evaporation of the solvent and drying gave **200** (32 mg, 47%) as a pale buff solid: R_f = 0.55 (hexane / EtOAc, 1:1); mp 240-243°C; ^{1}H NMR ($(CD_3)_2SO$) δ 4.03 (3 H, s, Me), 4.62 (2 H, br s, NH_2), 6.85 (1 H, dd, *J* = 7.8, 1.2 Hz, 6-H), 6.93 (2 H, d, *J* = 8.6 Hz, Ar 3,5-H_2), 7.34 (2 H, d, *J* = 8.6 Hz, Ar 2,6-H_2), 7.39 (1 H,

d, J = 8.6 Hz, Ar 3.5-H_2), 7.46 (1 H, t, J = 7.8 Hz, 7-H), 7.60 (1 H, d, J = 7.8, 1.2 Hz, 8-H), 10.86 (1 H, br, NH); ^{13}C NMR; 55.4, 112.1, 112.7, 113.9, 114.3, 115.0, 122.4, 126.8, 127.4, 127.5, 130.5, 143.4, 159.0, 161.4; MS (ES +ve) *m/z* 267.1105 (M + H) ($C_{16}H_{15}N_2O_2$ requires 267.1134; Anal. Calcd. for $C_{16}H_{14}N_2O_2$: C, 76.26; H, 5.12; N, 11.37. Found: C, 76.68; H, 5.46; N, 11.43%.

1-Benzyloxy-4-bromo-5-nitroisoquinoline (201)

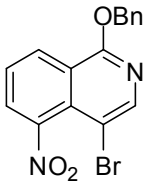

4-Bromo-1-dimethylamino-5-nitroisoquinoline (202)

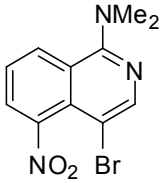

To NaH (300 mg, 12.5 mmol) in anhydrous DMF (10 mL) was added BnOH (680 mg, 6.3 mmol) and the mixture was stirrred for 30 min. **189** (1.5 g, 5.2 mmol) in anhydrous DMF (30 mL) was added and the suspension was heated at 100°C for 48 h. The excess solvent was then evaporated until 5 mL remained and the residue was diluted with H_2O and extracted ($CHCl_3$). Evaporation and chromatography (hexane / EtOAc 15:1) gave **201** (1.3 g, 71%) as a yellow solid: mp 106-108°C; R_f = 0.67 (hexane / EtOAc 10:1); ^{1}H NMR ($CDCl_3$) δ 5.58 (2 H, s, CH_2), 7.40 (3 H, m, Ph 3,4,5-H_3), 7.52 (2 H, d, J = 7.1 Hz, Ph 2,6-H_2), 7.62 (1 H, t, J = 7.8 Hz, 7-H), 7.90 (1 H, dd, J = 7.1, 1.2 Hz, 8-H), 8.33 (1 H, s, 3-H), 8.55 (1 H, dd, J = 7.1, 1.2 Hz, 6-H); ^{13}C NMR ($CDCl_3$) δ 68.96 (CH_2), 104.5, 122.0, 126.3, 126.9, 127.0, 128.2, 128.3, 128.5, 128.6, 136.1, 146.2, 147.1, 159.7; MS (ESI +ve) *m/z* 382.9826 ($C_{16}H_{11}{}^{81}BrNaN_2O_3$ requires 382.9830); 380.9860 (M + Na) ($C_{16}H_{11}{}^{79}BrNaN_2O_3$ requires 380.9851), 359.0039 (M + H) ($C_{16}H_{12}{}^{79}BrN_2O_3$ requires 359.0031).

Further elution gave **202** (184 mg, 12%) as a red-orange solid mp 127-130°C; R_f = 0.37 (hexane / EtOAc 10:1); ^{1}H NMR ($CDCl_3$) δ 3.14 (6 H, s, $NMe)_2$, 7.52 (1 H, t, *J* = 7.6 Hz, 7-H), 7.88 (1 H, dd, *J* = 7.6, 1.2 Hz, 6-H), 8.26 (1 H, dd, *J* = 7.6, 1.2 Hz, 8-H), 8.30 (1 H, s, 3-H); ^{13}C NMR ($CDCl_3$) (HMQC / HMBC) δ 43.06 NMe_2, 103.28 (4-C), 122.78 (8a-C), 124.21 (4-C), 126.38 (6-C), 127.95 (4a-C), 130.65 (8-C), 147.04 (3-C), 147.42 (5-C), 160.87 (1-C); MS (ESI +ve) *m/z* 319.9840 (M + Na) ($C_{11}H_{10}{}^{81}BrNaN_3O_2$ requires 319.9834); 317.9848 (M + Na) ($C_{11}H_{10}{}^{79}BrNaN_3O_2$ requires 317.9854).

1-Benzyloxy-4-(4-methoxyphenyl)-5-nitroisoquinoline (203)

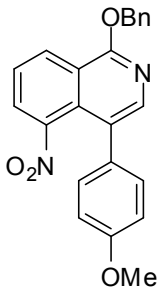

Compound **201** (500 mg, 1.4 mmol), $Pd_2(dba)_3$ (72 mg, 0.14 mmol), SPhos (168 mg, 0.70 mmol), K_3PO_4 (594 mg, 2.8 mmol) and 4-methoxyphenylboronic acid (317 mg, 2.1 mmol) were placed in a dry flask.Degassed toluene (20 mL) was added and the mixture was stirred at 100°C for 16 h. Chromatography (hexane / EtOAc, 20:1) gave **203** (330 mg, 61%) as a yellow solid: R_f = 0.74 (hexane / EtOAc, 10:1); mp 162-164°C; ^{1}H NMR ($CDCl_3$) δ 3.85 (3 H, s, OMe), 5.64 (2 H, s, CH_2), 6.93 (2 H, d, *J* = 8.6 Hz, Ar 3,5-H_2), 7.21 (2 H, d, *J* = 8.6 Hz, Ar 2,6-H_2), 7.36-7.45 (3 H, m, Ph 3,4,5-H_3), 7.55 (2 H, d, *J* = 7.5 Hz, Ph 2,6-H_2), 7.60 (1 H, t, *J* = 8.2 Hz, 7-H), 7.95 (1 H, d, *J* = 7.4 Hz, 6-H or 8-H), 8.04 (1 H, s, 3-H), 8.63 (1 H, d, *J* = 7.4 Hz, 8-H or 6-H); ^{13}C NMR (HMBC / HMQC) δ 55.2 (Me), 68.6 (CH_2), 108.7, 113.8 (Ar 3,5-C_2), 120.7 (8a-C), 124.4 (Ar 1-C), 125.4 (7-C), 127.2 (6-C), 128.0 (Ph 4-C), 128.1 (4a-C), 128.2 (Ph 3.5-C_2), 128.6 (Ph 2,6-C_2), 129.0 (8-C), 129.3 (Ar 2,6-C_2), 129.8 (4-C), 131.5 (Ar 4-C), 136.7 (Ph 1-C), 147.7 (3-C), 159.2 (5-C), 159.5 (1-C); MS (ES +ve) *m/z m/z* 409.1164 (M + Na) ($C_{23}H_{17}N_2NaO_4$

requires 409.1164), 387.1366 (M + H) ($C_{23}H_{19}N_2O_4$ requires 387.1345); Anal. Calc. for $C_{23}H_{18}N_2O_4$: C, 71.49; H, 4.70; N, 7.25. Found: C, 71.56; H, 4.82; N, 7.31%.

1-(Benzyloxy)-5-nitro-4-(phenanthren-9-yl)isoquinoline (204)

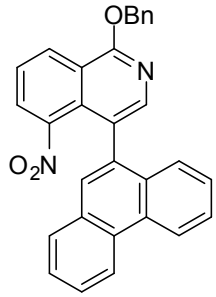

Compound **201** (1.26 g, 3.53 mmol), $Pd_2(dba)_3$ (0.18 g, 0.35 mmol), SPhos (0.14 g, 0.70 mmol), K_3PO_4 (1.5 g, 7.06 mmol) and benzeneboronic acid (1.00 g 5.30 mmol) were placed in a dry flask. Degassed toluene (50 mL) was added and the mixture was stirred at 100°C for 16 h. Evaporation and chromatography (hexane/EtOAc 20:1) gave **204** (0.67 g, 42%) as yellow-orange crystals: R_f = 0.72 (hexane / EtOAc 10:1); mp 102-105°C; ^{1}H NMR ($CDCl_3$) δ 7.41 (1 H, t, *J* = 7.8 Hz, Ph 4-H), 7.47 (2 H, t, *J* = 7.8 Hz, Ph 3,5-H_2), 7.52 (1 H, td, *J* = 7.8, 1.2 Hz, Ar 3 or 6-H), 7.56 (1 H, s, Ar 9-H), 7.60-7.65 (3 H, m, Ph 2,6-H_2 and 7-H), 7.66-7.71 (2 H, m,), 7.82 (2 H, t, *J* = 7.4 Hz, Ar 2,7-H_2), 7.85 (1 H, dd, *J* = 7.6, 1.2 Hz, 6-H), 8.71 (1 H, dd, *J* = 7.6, 1.2 Hz, 8-H), 8.74 (1 H, d, *J* = 7.8 Hz, Ar 4 or 5-H), 8.79 (1 H, d, *J* = 7.8 Hz, Ar 4 or 5-H); ^{13}C NMR δ 68.8 (CH_2), 120.8, 122.1 (Ar 1-C), 122.7 (Ar), 123.1, 125.6, 126.4 (Ar 2 or 7-C), 126.6, 126.8, 127.0 (8-C), 127.0, 128.2 (Ph 2,6-C_2), 128.3 (Ph 4-C), 128.4, 128.7, 128.8 (Ph 3,5-C_2), 129.0 (Ar 2 or 7-C), 129.2, 130.3, 130.6, 131.0, 131.4, 132.7, 136.7 (Ph 1-C), 145.8 (3-C), 147.7 (5-C), 160.0 (1-C);); MS (ES +ve) *m/z* 479.1360 (M + Na) ($C_{30}H_{20}N_2NaO_3$ requires 479.1372), 457.1571 (M + H) ($C_{30}H_{21}N_2O_3$ requires 457.1552).

5-Amino-4-(phenanthren-9-yl)isoquinolin-1-one (205)

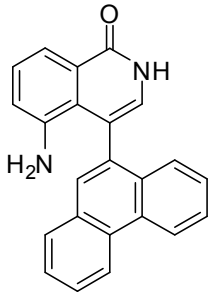

To **204** (200 mg, 0.44 mmol) in EtOH (10 mL), a slurry of 10% Pd on charcoal (100 mg) in EtOH (10 mL) was added. The mixture was stirred under H_2 for 40 h. The suspension was then filtered through Celite® and the precipitate was collected to give **205** (39mg, 26%) as a buff solid.

This compound could not be fully characterised due to solubility issues.

MS (ES +ve) *m/z* 359.1196 (M + Na) ($C_{23}H_{16}NaN_2O$ requires 359.1160), *m/z* 337.1331 (M + H) ($C_{23}H_{17}N_2O$ requires 337.1341).

4-Methyl-5-nitroisoquinolin-1-one (206)

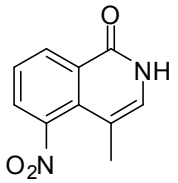

Compound **190** (200 mg, 0.92 mmol) was stirred in aq. HBr (48 %, 30 mL) at 80°C for 4 h. Evaporation and recrystallisation (hexane / EtOAc) gave **206** (131 mg, 70%) as a pale buff solid mp: R_f = 0.34 (hexane / EtOAc 1:1); mp 211-214°C (lit.[175] mp 209-211°C); ^{1}H NMR ($(CD_3)_2CO$) δ 2.02 (3 H, s, Me), 7.22 (1 H, d, *J* = 5.1 Hz, 3-H), 7.66 (1 H, t, *J* = 7.8 Hz, 7-H), 8.13 (1 H, dd, *J* = 7.8, 1.3 Hz, 6-H), 8.50 (1 H, dd, 7.8, 1.3 Hz, 8-H), 11.64 (1 H, br, NH).

5-Amino-4-methylisoquinolin-1-one hydrochloride (207)

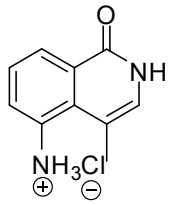

To **206** (116 mg, 0.56 mmol) in EtOH (10 mL) and aq. HCl (34%, 0.4 mL), a slurry of 10% Pd on charcoal (0.1 g) in EtOH (4 mL) was added. The mixture was stirred under H_2 for 2 h. The suspension was then filtered through Celite®. The Celite® pad and residue were suspended in water (100 mL) and heated. The hot suspension was filtered through a second Celite® pad. Evaporation of the solvent and drying gave **207** (78 mg, 65%) as a pale buff solid: mp 225-228°C (lit.[175] mp 227-229°C); ^{1}H NMR (D_2O) δ 2.37 (3 H, s, Me), 6.94 (1 H, s, 3-H), 7.42 (1 H, t, *J* = 8.2 Hz, 7-H), 7.63 (1 H, d, *J* = 7.8 Hz, 6-H), 8.14 (1 H, d, *J* = 8.2 Hz, 8-H).

1-Methoxy-5-nitro-4-phenylaminoisoquinolinine (208)

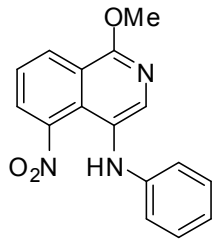

Compound **46** (1.00 g, 3.53 mmol), $Pd_2(dba)_3$ (0.18 g, 0.35 mmol), SPhos (0.14 g, 0.70 mmol), potassium *tert*-butoxide (0.79 g, 7.06 mmol) and aniline (0.49 g, 5.30 mmol) were placed in a dry flask. Degassed dioxane (40 mL) was added and the mixture was stirred at 100°C for 16 h. Evaporation and chromatography (hexane / EtOAc 10:1) gave **208** (0.47 g, 45%) as a deep red solid; mp 124-126°C; ^{1}H NMR ($CDCl_3$) δ 4.17 (3 H, s, OMe), 5.56 (1 H, s, NH), 6.61 (2 H, dd, *J* = 7.4, 1.1 Hz, Ph 2,6-H_2), 6.79 (1 H, t, *J* = 7.4 Hz, Ph 4-H), 7.14 (2 H, t, *J* = 7.4 Hz, Ph 3,5-H_2), 7.59 (1 H, d, *J* = 8.2 Hz, 7-H), 7.80 (1 H, dt, *J* = 8.2, 1.2 Hz, 8-H), 8.14 (1 H, d, *J* = 1.1 Hz, 3-H), 8.51 (1 H, dd, *J* = 8.2, 1.2 Hz, 6-H); ^{13}C NMR δ 54.3, 114.2, 119.5, 121.2, 124.7, 125.8, 126.3, 127.8, 128.7, 129.3,

142.3, 146.8, 158.7; MS (ES +ve) *m/z* 318.0850 (M + Na) ($C_{16}H_{13}N_3NaO_3$ requires 318.0855), 296.1027 (M + H) ($C_{16}H_{14}N_3O_3$ requires 296.1035).

N-(3-Methyl-1-oxo-1,2-dihydroisoquinolin-5-yl)benzamide (215)

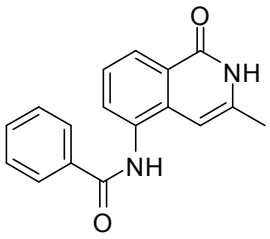

To 5AIQ:HCl **5** (53 mg, 0.25 mmol) in pyridine (2.0 mL) was added benzoyl chloride (0.03 mL, 39 mg, 0.28 mmol). The mixture was stirred at 90°C for 16 h; Evaporation and recrystallisation (EtOAc) gave **215** (38 mg, 72%) as an off-white solid: R_f = 0.19 (EtOAc); mp >310°C (decomp.); ^{1}H NMR ($(CD_3)_2SO$) δ 2.12 (3 H, s, Me), 6.33 (1 H, s, 4-H), 7.42 (1 H, t, *J* = 7.8 Hz, 7-H), 7.55 (2 H, t, *J* = 7.9 Hz, Ar 3,5-H_2), 7.62 (1 H, t, *J* = 7.9 Hz, Ar 4-H), 7.69 (1 H, dd, *J* = 7.8, 1.2 Hz, 6-H), 8.04-8.09 (3 H, m, Ar 2,6-H_2 and 8-H), 10.28 (1 H, s, PhCONH), 11.35 (1 H, s, 2-NH); ^{13}C NMR δ 19.0, 98.7, 124.7, 124.9, 125.1, 127.8, 128.4, 130.6, 131.7, 132.5, 134.2, 134.6, 138.5, 162.3, 166.0; MS (ES +ve) *m/z* 301.0948 (M + Na) ($C_{17}H_{14}NaN_2O_2$ requires 301.0953), *m/z* 279.1142 (M + H) ($C_{17}H_{15}N_2O_2$ requires 279.1134); Anal. Calcd. for $C_{17}H_{14}N_2O_2$: C, 73.37; H, 5.07; N, 10.07. Found: C, 73.42; H, 5.06; N, 10.13%.

N-(1-Oxo-3-phenyl-1,2-dihydroisoquinolin-5-yl)benzamide (216)

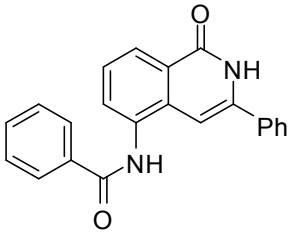

To 5AIQ:HCl **5** (68 mg, 0.25 mmol) in pyridine (2.0 mL) was added benzoyl chloride (0.03 mL, 39 mg, 0.28 mmol). The mixture was stirred at 90°C for 16 h; Evaporation and recrystallisation (EtOAc) gave **216** (54 mg, 64%) as an off-white solid: R_f = 0.22 (EtOAc); mp >325°C (decomp.); ^{1}H NMR ($(CD_3)_2SO$) δ 6.82 (1 H, s, 4-H), 7.45-7.58 (7-

H, m, Ph 3,4,5-H_3, COPh 3,4,5-H_3 and 7-H), 7.61 (1 H, t, *J* = 7.6 Hz, 7-H), 7.75 (2 H, *J* = 6.8 Hz, Ph 2,6-H_2), 7.83 (1 H, d, *J* = 7.6 Hz, 6-H), 8.05 (2 H, d, *J* = 6.8 Hz, COPh 2,6-C-$_2$), 8.15 (1 H, d, *J* = 7.6 Hz, 8-H), 10.38 (1 H, s, PhCONH), 11.66 (1 H, s, 2-NH); ^{13}C NMRδ 99.3, 124.5, 125.8, 126.0, 126.8, 127.9, 128.5, 128.8, 129.3, 129.3, 130.3, 131.8, 33.5, 133.5, 134.1, 134.3, 140.0, 162.6, 166.2; MS (ES +ve) *m/z* 363.1119 (M + Na) ($C_{22}H_{16}NaN_2O_2$ requires 363.1109), *m/z* 341.1303 (M + H) ($C_{22}H_{17}N_2O_2$ requires 341.1290).

N-(1-Oxo-4-phenyl-1,2-dihydroisoquinolin-5-yl)benzamide (217)

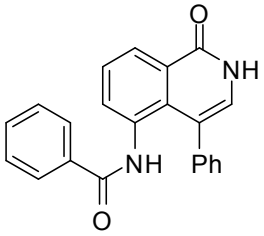

To 5AIQ:HCl **5** (68 mg, 0.25 mmol) in pyridine (2.0 mL) was added benzoyl chloride (0.03 mL, 39 mg, 0.28 mmol). The mixture was stirred at 90^{o}C for 16 h; Evaporation and chromatography (EtOAc then EtOAc / MeOH 4:1) gave **217** (31 mg, 36%) as a pale pink solid: R_f = 0.22 (EtOAc); mp >230-232^{o}C (decomp.); ^{1}H NMR (CD_3OD) δ 7.10-7.16 (3 H, m, Ph 3,4,5-H_3), 7.24 (1 H, s, 3-H), 7.26-7.36 (4 H, m, 7-H and COPh 3,4,5-H_3), 7.62 (2 H, d, *J* = 7.2 Hz, Ph 2,6-H_2), 7.71 (1 H, d, *J* = 7.8 Hz, 6-H), 7.78 (1 H, d, *J* = 7.4 Hz,COPh 2,6-H_2), 8.42 (1 H, d, *J* = 7.8 Hz, 8-H); ^{13}C NMR δ 119.5, 127.7, 127.6, 128.4, 128.6, 128.9, 129.2, 129.4, 129.9, 130.3, 130.9, 131.8, 133.0, 134.6, 140.2, 164.1, 168.3; MS (ES +ve) *m/z* 363.1133 (M + Na) ($C_{22}H_{16}NaN_2O_2$ requires 363.1109), *m/z* 341.1312 (M + H) ($C_{17}H_{15}N_2O_2$ requires 341.1290).

4-Iodo-N-(1-oxo-3-phenyl-1,2-dihydroisoquinolin-5-yl)benzamide (218)

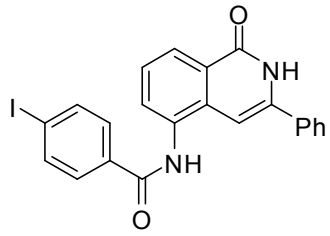

To 5AIQ:HCl **5** (68 mg, 0.25 mmol) in pyridine (2.0 mL) was added 4-iodobenzoyl chloride (75 mg, 0.28 mmol). The mixture was stirred at 90^{o}C for 16 h; Evaporation and recrystallisation (EtOAc) gave **218** (72 mg, 64%) as an off-white solid: R_f = 0.23 (EtOAc); mp >325^{o}C (decomp.); ^{1}H NMR ($(CD_3)_2SO$) δ 6.82 (1 H, s, 4-H), 7.48-7.50 (3 H, m, Ph 3,4,5-H_3) 7.54 (1 H, t, *J* = 7.6 Hz, 7-H), 7.51 (2 H, dd, *J* = 8.0, 1.2 Hz, Ph 2,6-H_2), 7.72 7.82 (2 H, d, *J* = 8.2 Hz, Ar 3,5-H_2), 7.83-7.86 (3 H, m, Ar 2,6-H_2 and 6-H), 8.17 (1 H, d, *J* = 7.6 Hz, 8-H), 10.42 (1 H, s, PhCONH), 11.63 (1 H, d, *J* = 4.7 Hz, 2-NH); ^{13}C NMR δ 99.0, 99.4, 124.6, 125.8, 125.9, 126.8, 128.8, 129.3, 129.8, 130.3, 133.3, 133.5, 133.8, 134.1, 137.3, 139.9, 162.5, 165.6; MS (ES +ve) *m/z* 467.0267 (M + H) ($C_{22}H_{16}IN_2O_2$ requires 467.0256); Anal. Calcd. for $C_{22}H_{15}IN_2O_2$: C, 56.67; H, 3.24; N, 6.01. Found: C, 56.51; H, 3.38; N, 6.13%.

1-Chloro-5-nitroisoquinoline (219)

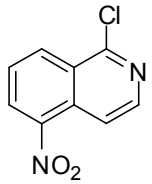

To a cooled solution of 1-chloroisoquinoline **90** (2.00g, 12.2 mmol) in conc. H_2SO_4 (10 mL) was added aq. HNO_3 (70%, 0.85g, 13.4 mmol) in conc. H_2SO_4 (5 mL) dropwise at 0-5°C. The mixture was stirred at 0°C for 2 h, then poured onto ice. The precipitate was collected, washed (H_2O), dried under vacuum and recrystallised (EtOAc / hexanes) to give **219** (2.34g, 92%) as pale yellow crystals: mp 181-183°C (lit.[179] mp 183-184°C); ^{1}H NMR ($CDCl_3$) □ 7.81 (1 H, t, *J* = 8.2 Hz, 7-H), 8.41 (1 H, dd, *J* = 6.3, 1.2 Hz, 4-H), 8.49 (1 H, d, *J* = 6.3 Hz, 3-H), 8.56 (1 H, dt, *J* = 8.2, 1.2 Hz, 8-H) 8.75 (1 H, dd, *J* = 8.2, 1.2 Hz, 6-H),

References

1. Chambon, P.; Weill, J. D.; Mandel, P. Nicotinamide mononucleotide activation of new DNA-dependent polyadenylic acid synthesizing nuclear enzyme. *Biochem. Biophys. Res. Commun.* **1963,** *11*, 39-43.
2. Nguewa, P. A.; Fuertes, M. A.; Valladares, B.; Alonso, C.; Perez, J. M. Poly(ADP-ribose) polymerases: homology, structural domains and functions. Novel therapeutical applications. *Prog. Biophys. Mol. Biol.* **2005,** *88*, 143-172.
3. Auer, B. N. U.; Herzog, H.; Schneider, R.; Schweiger, M. Human nuclear NAD^+ ADP-ribosyltranferase(polymerising): organization of the gene. *DNA.* **1989,** *8*, 575-580.
4. Shizuta, Y.; Kameshita, I.; Ushiro, H.; Matsuda, M.; Suzuki, S.; Mitsuuchi, Y.; Yokoyama, Y.; Kurosaki, T. The domain structure and the function of poly(ADP-ribose) synthetase. *Adv. Enzyme Regul.* **1986,** *25*, 377-84.
5. Zahradka, P.; Ebisuzaki, K. Poly(ADP-ribose) polymerase is a zinc metalloenzyme. *Eur. J. Biochem.* **1984,** *142*, 503-509.
6. Langelier, M. F.; Servent, K. M.; Rogers, E. E.; Pascal, J. M. A third zinc-binding domain of human poly(ADP-ribose) polymerase-1 coordinates DNA-dependent enzyme activation. *J. Biol. Chem.* **2008,** *283*, 4105-4114.
7. Schreiber, V.; Molinete, M.; Boeuf, H.; de Murcia, G.; Menissier-de Murcia, J. The human poly(ADP-ribose) polymerase nuclear localization signal is a bipartite element functionally separate from DNA binding and catalytic activity. *EMBO. J.* **1992,** *11*, 3263-3269.
8. Kaufmann, S. H.; Desnoyers, S.; Ottaviano, Y.; Davidson, N. E.; Poirier, G. G. Specific proteolytic cleavage of poly(ADP-ribose) polymerase: an early marker of chemotherapy-induced apoptosis. *Cancer Res.* **1993,** *53*, 3976-3985.
9. Boulares, A. H.; Yakovlev, A. G.; Ivanova, V.; Stoica, B. A.; Wang, G.; Iyer, S.; Smulson, M. Role of poly(ADP-ribose) polymerase (PARP) cleavage in apoptosis. Caspase 3-resistant PARP mutant increases rates of apoptosis in transfected cells. *J. Biol. Chem.* **1999,** *274*, 22932-22940.
10. Koonin, E. V.; Altschul, S. F.; Bork, P. BRCA1 protein products ...Functional motifs... *Nature Genet.* **1996,** *13*, 266-268.
11. Zhang, X.; Morera, S.; Bates, P. A.; Whitehead, P. C.; Coffer, A. I.; Hainbucher, K.; Nash, R. A.; Sternberg, M. J.; Lindahl, T.; Freemont, P. S. Structure of an XRCC1 BRCT domain: a new protein-protein interaction module. *EMBO J.* **1998,** *17*, 6404-6411.
12. Uchida, K.; Hanai, S.; Ishikawa, K.; Ozawa, Y.; Uchida, M.; Sugimura, T.; Miwa, M. Cloning of cDNA encoding Drosophila poly(ADP-ribose) polymerase: leucine zipper in the auto-modification domain. *Proc. Natl. Acad. Sci. USA.* **1993,** *90*, 3481-3485.
13. Ruf, A.; Mennissier de Murcia, J.; de Murcia, G.; Schulz, G. E. Structure of the catalytic fragment of poly(AD-ribose) polymerase from chicken. *Proc. Natl. Acad. Sci. USA.* **1996,** 93, 7481-7485.
14. Rolli, V.; O'Farrell, M.; Menissier-de Murcia, J.; de Murcia, G. Random mutagenesis of the poly(ADP-ribose) polymerase catalytic domain reveals amino acids involved in polymer branching. *Biochemistry* **1997,** *36*, 12147-12154.
15. Schreiber, V.; Ame, J. C.; Dolle, P.; Schultz, I.; Rinaldi, B.; Fraulob, V.; Menissier-de Murcia, J.; de Murcia, G. Poly(ADP-ribose) polymerase-2 (PARP-2) is

required for efficient base excision DNA repair in association with PARP-1 and XRCC1. *J. Biol. Chem.* **2002,** *277*, 23028-23036.
16. Davidovic, L.; Vodenicharov, M.; Affar, E. B.; Poirier, G. G. Importance of poly(ADP-ribose) glycohydrolase in the control of poly(ADP-ribose) metabolism. *Exp. Cell. Res.* **2001,** *268*, 7-13.
17. Okayama, H.; Honda, M.; Hayaishi, O. Novel enzyme from rat liver that cleaves an ADP-ribosyl histone linkage. *Proc. Natl. Acad. Sci. USA.* **1978,** *75*, 2254-2257.
18. Poirier, G. G.; de Murcia, G.; Jongstra-Bilen, J.; Niedergang, C.; Mandel, P. Poly(ADP-ribosyl)ation of polynucleosomes causes relaxation of chromatin structure. *Proc. Natl. Acad. Sci. USA.* **1982,** *79*, 3423-3427.
19. D'Amours, D.; Desnoyers, S.; D'Silva, I.; Poirier, G. G. Poly(ADP-ribosyl)ation reactions in the regulation of nuclear functions. *Biochem. J.* **1999,** *342*, 249-268.
20. Huet, J.; Laval, F. Potentiation of cell killing by inhibitors of poly(adenosine diphosphate-ribose) synthesis in bleomycin-treated Chinese hamster ovary cells. *Cancer. Res.* **1985,** *45*, 987-991.
21. Ben-Hur, E.; Chen, C. C.; Elkind, M. M. Inhibitors of poly(adenosine diphosphoribose) synthetase, examination of metabolic perturbations, and enhancement of radiation response in Chinese hamster cells. *Cancer. Res.* **1985,** *45*, 2123-2127.
22. Simbulan-Rosenthal, C. M.; Rosenthal, D. S.; Ding, R.; Jackman, J.; Smulson, M. E. Depletion of nuclear poly(ADP-ribose) polymerase by antisense RNA expression: influence on genomic stability, chromatin organization, DNA repair, and DNA replication. *Prog. Nucleic. Acid. Res. Mol. Biol.* **1996,** *55*, 135-156.
23. Stevnsner, T.; Ding, R.; Smulson, M.; Bohr, V. A. Inhibition of gene-specific repair of alkylation damage in cells depleted of poly(ADP-ribose) polymerase. *Nucleic. Acids. Res.* **1994,** *22*, 4620-4624.
24. Ding, R.; Pommier, Y.; Kang, V. H.; Smulson, M. Depletion of poly(ADP-ribose) polymerase by antisense RNA expression results in a delay in DNA strand break rejoining. *J. Biol. Chem* **1992,** *267*, 12804-12812.
25. Ding, R.; Smulson, M. Depletion of nuclear poly(ADP-ribose) polymerase by antisense RNA expression: influences on genomic stability, chromatin organization, and carcinogen cytotoxicity. *Cancer. Res.* **1994,** *54*, 4627-4634.
26. de Murcia, J. M.; Niedergang, C.; Trucco, C.; Ricoul, M.; Dutrillaux, B.; Mark, M.; Oliver, F. J.; Masson, M.; Dierich, A.; LeMeur, M.; Walztinger, C.; Chambon, P.; de Murcia, G. Requirement of poly(ADP-ribose) polymerase in recovery from DNA damage in mice and in cells. *Proc. Natl. Acad. Sci. USA.* **1997,** *94*, 7303-7307.
27. Ame, J. C.; Spenlehauer, C.; de Murcia, G. The PARP superfamily. *Bioessays* **2004,** *26*, 882-893.
28. Caldecott, K. W. XRCC1 and DNA strand break repair. *DNA Repair* **2003,** *2*, 955-969.
29. Fortini, P.; Pascucci, B.; Belisario, F.; Dogliotti, E. DNA polymerase beta is required for efficient DNA strand break repair induced by methyl methanesulfonate but not by hydrogen peroxide. *Nucleic Acids Res.* **2000,** *28*, 3040-3046.
30. Yang, Y.-G.; Cortes, U.; Patnaik, S.; Jasin, M.; Wang, Z.-Q. Ablation of PARP-1 does not interfere with the repair of DNA double-strand breaks, but compromises the reactivation of stalled replication forks. *Oncogene* **2004,** *23*, 3872-3882.

31. Audebert, M.; Salles, B.; Calsou, P. Effect of double-strand break DNA sequence on the PARP-1 NHEJ pathway. *Biochem. Biophys. Res. Commun.* **2008,** *369*, 982-988.
32. Featherstone, C.; Jackson, S. P. Ku, a DNA repair protein with multiple cellular functions? *Mutat. Res.* **1999,** *434*, 3-15.
33. Tuteja, R.; Tuteja, N. Ku autoantigen: a multifunctional DNA-binding protein. *Crit. Rev. Biochem. Mol. Biol.* **2000,** *35*, 1-33.
34. Chang, P.; Jacobson, M. K.; Mitchison, T. J. Poly(ADP-ribose) is required for spindle assembly and structure. *Nature* **2004,** *432*, 645-649.
35. Glover, D. M.; Leibowitz, M. H.; McLean, D. A.; Parry, H. Mutations in aurora prevent centrosome separation leading to the formation of monopolar spindles. *Cell* **1995,** *81*, 95-105.
36. Crosio, C.; Fimia, G. M.; Loury, R.; Kimura, M.; Okano, Y.; Zhou, H.; Sen, S.; Allis, C. D.; Sassone-Corsi, P. Mitotic phosphorylation of histone H3: spatio-temporal regulation by mammalian Aurora kinases. *Mol. Cell. Biol.* **2002,** *22*, 874-885.
37. Monaco, L.; Kolthur-Seetharam, U.; Loury, R.; Murcia, J. M.; de Murcia, G.; Sassone-Corsi, P. Inhibition of Aurora-B kinase activity by poly(ADP-ribosyl)ation in response to DNA damage. *Proc. Natl. Acad. Sci. USA* **2005,** *102*, 14244-14248.
38. Kanai, M.; Uchida, M.; Hanai, S.; Uematsu, N.; Uchida, K.; Miwa, M. Poly(ADP-ribose) polymerase localizes to the centrosomes and chromosomes. *Biochem. Biophys. Res. Commun.* **2000,** *278*, 385-389.
39. Hassa, P. O.; Hottiger, M. O. The functional role of poly(ADP-ribose)polymerase 1 as novel coactivator of NF-kappaB in inflammatory disorders. *Cell. Mol. Life Sci.* **2002,** *59*, 1534-1553.
40. Kraus, W. L.; Lis, J. T. PARP goes transcription. *Cell* **2003,** *113*, 677-683.
41. Hassa, P. O.; Hottiger, M. O. A role of poly (ADP-ribose) polymerase in NF-kappaB transcriptional activation. *Biol. Chem.* **1999,** *380*, 953-959.
42. Tulin, A.; Spradling, A. Chromatin loosening by poly(ADP)-ribose polymerase (PARP) at Drosophila puff loci. *Science* **2003,** *299*, 560-562.
43. Kim, M. Y.; Mauro, S.; Gevry, N.; Lis, J. T.; Kraus, W. L. NAD^+-dependent modulation of chromatin structure and transcription by nucleosome binding properties of PARP-1. *Cell* **2004,** *119*, 803-814.
44. Hernandez, A. I.; Wolk, J.; Hu, J. Y.; Liu, J.; Kurosu, T.; Schwartz, J. H.; Schacher, S. Poly-(ADP-ribose) polymerase-1 is necessary for long-term facilitation in Aplysia. *J. Neurosci.* **2009,** *29*, 9553-9562.
45. Oliver, F. J.; Menissier-de Murcia, J.; Nacci, C.; Decker, P.; Andriantsitohaina, R.; Muller, S.; de la Rubia, G.; Stoclet, J. C.; de Murcia, G. Resistance to endotoxic shock as a consequence of defective *NF-κB* activation in poly (ADP-ribose) polymerase-1 deficient mice. *EMBO. J.* **1999,** *18*, 4446-4454.
46. Andreone, T. L.; O'Connor, M.; Denenberg, A.; Hake, P. W.; Zingarelli, B. Poly(ADP-ribose) polymerase-1 regulates activation of activator protein-1 in murine fibroblasts. *J. Immunol.* **2003,** *170*, 2113-2120.
47. Yu, S. W.; Wang, H.; Poitras, M. F.; Coombs, C.; Bowers, W. J.; Federoff, H. J.; Poirier, G. G.; Dawson, T. M.; Dawson, V. L. Mediation of poly(ADP-ribose) polymerase-1-dependent cell death by apoptosis-inducing factor. *Science* **2002,** *297*, 259-263.

48. Boulares, A. H.; Zoltoski, A. J.; Sherif, Z. A.; Jolly, P.; Massaro, D.; Smulson, M. E. Gene knockout or pharmacological inhibition of poly(ADP-ribose) polymerase-1 prevents lung inflammation in a murine model of asthma. *Am. J. Respir. Cell. Mol. Biol.* **2003,** *28*, 322-329.
49. Suzuki, Y.; Masini, E.; Mazzocca, C.; Cuzzocrea, S.; Ciampa, A.; Suzuki, H.; Bani, D. Inhibition of poly(ADP-ribose) polymerase prevents allergen-induced asthma-like reaction in sensitized Guinea pigs. *J. Pharmacol. Exp. Ther.* **2004,** *311*, 1241-1248.
50. Wayman, N.; McDonald, M. C.; Thompson, A. S.; Threadgill, M. D.; Thiemermann, C. 5-aminoisoquinolinone, a potent inhibitor of poly (adenosine 5'-diphosphate ribose) polymerase, reduces myocardial infarct size. *Eur. J. Pharmacol.* **2001,** *430*, 93-100.
51. Thiemermann, C.; Bowes, J.; Myint, F. P.; Vane, J. R. Inhibition of the activity of poly(ADP ribose) synthetase reduces ischemia-reperfusion injury in the heart and skeletal muscle. *Proc. Natl. Acad. Sci. USA* **1997,** *94*, 679-683.
52. Zingarelli, B.; Cuzzocrea, S.; Zsengeller, Z.; Salzman, A. L.; Szabo, C. Protection against myocardial ischemia and reperfusion injury by 3-aminobenzamide, an inhibitor of poly (ADP-ribose) synthetase. *Cardiovasc. Res.* **1997,** *36*, 205-215.
53. Roesner, J. P.; Vagts, D. A.; Iber, T.; Eipel, C.; Vollmar, B.; Noldge-Schomburg, G. F. Protective effects of PARP inhibition on liver microcirculation and function after haemorrhagic shock and resuscitation in male rats. *Intensive Care Med.* **2006,** *32*, 1649-1657.
54. Chatterjee, P. K.; Chatterjee, B. E.; Pedersen, H.; Sivarajah, A.; McDonald, M. C.; Mota-Filipe, H.; Brown, P. A.; Stewart, K. N.; Cuzzocrea, S.; Threadgill, M. D.; Thiemermann, C. 5-Aminoisoquinolinone reduces renal injury and dysfunction caused by experimental ischemia/reperfusion. *Kidney Int.* **2004,** *65*, 499-509.
55. McDonald, M. C.; Mota-Filipe, H.; Wright, J. A.; Abdelrahman, M.; Threadgill, M. D.; Thompson, A. S.; Thiemermann, C. Effects of 5-aminoisoquinolinone, a water-soluble, potent inhibitor of the activity of poly (ADP-ribose) polymerase on the organ injury and dysfunction caused by haemorrhagic shock. *Br. J. Pharmacol.* **2000,** *130*, 843-850.
56. Shiratora, Y.; Aoki, S.; Takada, H.; Kiriyama, H.; Ohto, K.; Hai, K.; Teraoka, H.; Matano, S.; Matsumoto, K.; Kamii, K. Oxygen-derived free radical generating capacity of polymorphonuclear cells in patients with ulcerative colitis. *Digestion* **1989,** *44*, 163-171.
57. Zingarelli, B.; Szabo, C.; Salzman, A. L. Blockade of Poly(ADP-ribose) synthetase inhibits neutrophil recruitment, oxidant generation, and mucosal injury in murine colitis. *Gastroenterology* **1999,** *116*, 335-345.
58. Cuzzocrea, S.; Mazzon, E.; Di Paola, R.; Genovese, T.; Patel, N. S.; Muia, C.; Threadgill, M. D.; De Sarro, A.; Thiemermann, C. 5-Aminoisoquinolinone reduces colon injury by experimental colitis. *Naunyn. Schmiedebergs. Arch. Pharmacol.* **2004,** *370*, 464-473.
59. Jijon, H. B.; Churchill, T.; Malfair, D.; Wessler, A.; Jewell, L. D.; Parsons, H. G.; Madsen, K. L. Inhibition of poly(ADP-ribose) polymerase attenuates inflammation in a model of chronic colitis. *Am. J. Physiol. Gastrointest. Liver Physiol.* **2000,** *279*, 641-651.

60. Mazzon, E.; Dugo, L.; Li, J. H.; Di Paola, R.; Genovese, T.; Caputi, A. P.; Zhang, J.; Cuzzocrea, S. GPI 6150, a PARP inhibitor, reduces the colon injury caused by dinitrobenzene sulfonic acid in the rat. *Biochem. Pharmacol.* **2002,** *64*, 327-337.
61. Mabley, J. G.; Jagtap, P.; Perretti, M.; Getting, S. J.; Salzman, A. L.; Virag, L.; Szabo, E.; Soriano, F. G.; Liaudet, L.; Abdelkarim, G. E.; Hasko, G.; Marton, A.; Southan, G. J.; Szabo, C. Anti-inflammatory effects of a novel, potent inhibitor of poly (ADP-ribose) polymerase. *Inflamm. Res.* **2001,** *50*, 561-569.
62. Negri, C.; Scovassi, A. I.; Cerino, A.; Negroni, M.; Borzi, R. M.; Meliconi, R.; Facchini, A.; Montecucco, C. M.; Astaldi Ricotti, G. C. Autoantibodies to poly(ADP-ribose)polymerase in autoimmune diseases. *Autoimmunity* **1990,** *6*, 203-209.
63. Scovassi, A. I.; Negri, C.; Negroni, M.; Dal, V.; Borzi, R. M.; Meliconi, R.; Facchini, A.; Montecucco, C. M.; Astaldi Ricotti, G. C. Detection of circulating autoantibodies to poly(ADP-ribose)polymerase in autoimmune diseases. *Ann. N.Y. Acad. Sci.* **1992,** *663*, 508-509.
64. Pacher, P.; Beckman, J. S.; Liaudet, L. Nitric oxide and peroxynitrite in health and disease. *Physiol. Rev.* **2007,** *87*, 315-424.
65. Pacher, P.; Szabo, C. Role of the peroxynitrite-poly(ADP-ribose) polymerase pathway in human disease. *Am. J. Pathol.* **2008,** *173*, 2-13.
66. Ame, J. C.; Rolli, V.; Schreiber, V.; Niedergang, C.; Apiou, F.; Decker, P.; Muller, S.; Hoger, T.; Menissier-de Murcia, J.; de Murcia, G. PARP-2, A novel mammalian DNA damage-dependent poly(ADP-ribose) polymerase. *J. Biol. Chem.* **1999,** *274*, 17860-17868.
67. Menissier de Murcia, J.; Ricoul, M.; Tartier, L.; Niedergang, C.; Huber, A.; Dantzer, F.; Schreiber, V.; Ame, J. C.; Dierich, A.; LeMeur, M.; Sabatier, L.; Chambon, P.; de Murcia, G. Functional interaction between PARP-1 and PARP-2 in chromosome stability and embryonic development in mouse. *EMBO J.* **2003,** *22*, 2255-2263.
68. Masson, M.; Niedergang, C.; Schreiber, V.; Muller, S.; Menissier-de Murcia, J.; de Murcia, G. XRCC1 Is Specifically Associated with Poly(ADP-Ribose) Polymerase and Negatively Regulates Its Activity following DNA Damage. *Mol. Cell. Biol.* **1998**, *18*, 3563-3571.
69. Fisher, A. E.; Hochegger, H.; Takeda, S.; Caldecott, K. W. Poly(ADP-ribose) polymerase 1 accelerates single-strand break repair in concert with poly(ADP-ribose) glycohydrolase. *Mol. Cell. Biol.* **2007,** *27*, 5597-5605.
70. Griffith, J. D.; Comeau, L.; Rosenfield, S.; Stansel, R. M.; Bianchi, A.; Moss, H.; de Lange, T. Mammalian telomeres end in a large duplex loop. *Cell* **1999,** *97*, 503-514.
71. Muftuoglu, M.; Wong, H. K.; Imam, S. Z.; Wilson, D. M., 3rd; Bohr, V. A.; Opresko, P. L. Telomere repeat binding factor 2 interacts with base excision repair proteins and stimulates DNA synthesis by DNA polymerase beta. *Cancer Res.* **2006,** *66*, 113-124.
72. Wright, W. E.; Shay, J. W. Telomere-binding factors and general DNA repair. *Nature Genet.* **2005,** *37*, 116-118.
73. Dantzer, F.; Giraud-Panis, M. J.; Jaco, I.; Ame, J. C.; Schultz, I.; Blasco, M.; Koering, C. E.; Gilson, E.; Menissier-de Murcia, J.; de Murcia, G.; Schreiber, V. Functional interaction between poly(ADP-Ribose) polymerase-2 (PARP-2) and TRF-2: PARP activity negatively regulates TRF-2. *Mol. Cell. Biol.* **2004,** *24*, 1595-1607.
74. de Lange, T. Protection of mammalian telomeres. *Oncogene* **2002,** *21*, 532-540.

75. Popoff, I.; Jijon, H.; Monia, B.; Tavernini, M.; Ma, M.; McKay, R.; Madsen, K. Antisense oligonucleotides to poly(ADP-ribose) polymerase-2 ameliorate colitis in interleukin-10-deficient mice. *J. Pharmacol. Exp. Ther.* **2002,** *303*, 1145-1154.
76. Kofler, J.; Otsuka, T.; Zhang, Z.; Noppens, R.; Grafe, M. R.; Koh, D. W.; Dawson, V. L.; de Murcia, J. M.; Hurn, P. D.; Traystman, R. J. Differential effect of PARP-2 deletion on brain injury after focal and global cerebral ischemia. *J. Cereb. Blood Flow Metab.* **2006,** *26*, 135-141.
77. Yelamos, J.; Monreal, Y.; Saenz, L.; Aguado, E.; Schreiber, V.; Mota, R.; Fuente, T.; Minguela, A.; Parrilla, P.; de Murcia, G.; Almarza, E.; Aparicio, P.; Menissier-de Murcia, J. PARP-2 deficiency affects the survival of $CD4^{+}CD8^{+}$ double-positive thymocytes. *EMBO J.* **2006,** *25*, 4350-4360.
78. Bai, P.; Houten, S. M.; Huber, A.; Schreiber, V.; Watanabe, M.; Kiss, B.; de Murcia, G.; Auwerx, J.; Menissier-de Murcia, J. Poly(ADP-ribose) polymerase-2 controls adipocyte differentiation and adipose tissue function through the regulation of the activity of the retinoid X receptor/peroxisome proliferator-activated receptor-gamma heterodimer. *J. Biol. Chem.* **2007,** *282*, 37738-33746.
79. Dantzer, F.; Mark, M.; Quenet, D.; Scherthan, H.; Huber, A.; Liebe, B.; Monaco, L.; Chicheportiche, A.; Sassone-Corsi, P.; de Murcia, G.; Menissier-de Murcia, J. Poly(ADP-ribose) polymerase-2 contributes to the fidelity of male meiosis I and spermiogenesis. *Proc. Natl. Acad. Sci. USA* **2006,** *103*, 14854-14859.
80. Johansson, M. A human poly(ADP-ribose) polymerase gene family (ADPRTL): cDNA cloning of two novel poly(ADP-ribose) polymerase homologues. *Genomics* **1999,** *57*, 442-445.
81. Augustin, A.; Spenlehauer, C.; Dumond, H.; Menissier-De Murcia, J.; Piel, M.; Schmit, A. C.; Apiou, F.; Vonesch, J. L.; Kock, M.; Bornens, M.; De Murcia, G. PARP-3 localizes preferentially to the daughter centriole and interferes with the G1/S cell cycle progression. *J. Cell. Sci.* **2003,** *116*, 1551-1562.
82. Lehtio, L.; Jemth, A. S.; Collins, R.; Loseva, O.; Johansson, A.; Markova, N.; Hammarstrom, M.; Flores, A.; Holmberg-Schiavone, L.; Weigelt, J.; Helleday, T.; Schuler, H.; Karlberg, T. Structural basis for inhibitor specificity in human poly(ADP-ribose) polymerase-3. *J. Med. Chem.* **2009,** *52*, 3108-3111.
83. Kickhoefer, V. A.; Siva, A. C.; Kedersha, N. L.; Inman, E. M.; Ruland, C.; Streuli, M.; Rome, L. H. The 193-kD vault protein, VPARP, is a novel poly(ADP-ribose) polymerase. *J. Cell. Biol.* **1999,** *146*, 917-928.
84. Kickhoefer, V. A.; Vasu, S. K.; Rome, L. H. Vaults are the answer, what is the question? *Trends Cell Biol.* **1996,** *6*, 174-178.
85. Kickhoefer, V. A.; Rajavel, K. S.; Scheffer, G. L.; Dalton, W. S.; Scheper, R. J.; Rome, L. H. Vaults are up-regulated in multidrug-resistant cancer cell lines. *J. Biol. Chem.* **1998,** *273*, 8971-8974.
86. Raval-Fernandes, S.; Kickhoefer, V. A.; Kitchen, C.; Rome, L. H. Increased susceptibility of vault poly(ADP-ribose) polymerase-deficient mice to carcinogen-induced tumorigenesis. *Cancer Res.* **2005,** *65*, 8846-8852.
87. Smith, S.; Giriat, I.; Schmitt, A.; de Lange, T. Tankyrase, a poly(ADP-ribose) polymerase at human telomeres. *Science* **1998,** *282*, 1484-1487.
88. Bennett, V. Ankyrins. Adaptors between diverse plasma membrane proteins and the cytoplasm. *J. Biol. Chem.* **1992,** *267*, 8703-8706.

89. De Rycker, M.; Price, C. M. Tankyrase polymerization is controlled by its sterile alpha motif and poly(ADP-ribose) polymerase domains. *Mol. Cel.l Biol.* **2004,** *24*, 9802-9812.
90. Chiang, Y. J.; Hsiao, S. J.; Yver, D.; Cushman, S. W.; Tessarollo, L.; Smith, S.; Hodes, R. J. Tankyrase 1 and tankyrase 2 are essential but redundant for mouse embryonic development. *PLoS One* **2008,** *3*, e2639, 1-10.
91. Seimiya, H.; Smith, S. The telomeric poly(ADP-ribose) polymerase, tankyrase 1, contains multiple binding sites for telomeric repeat binding factor 1 (TRF1) and a novel acceptor, 182-kDa tankyrase-binding protein (TAB182). *J. Biol. Chem.* **2002,** *277*, 14116-14126.
92. Cook, B. D.; Dynek, J. N.; Chang, W.; Shostak, G.; Smith, S. Role for the related poly(ADP-Ribose) polymerases tankyrase 1 and 2 at human telomeres. *Mol. Cell. Biol.* **2002,** *22*, 332-342.
93. Incles, C. M.; Schultes, C. M.; Kempski, H.; Koehler, H.; Kelland, L. R.; Neidle, S. A G-quadruplex telomere targeting agent produces p16-associated senescence and chromosomal fusions in human prostate cancer cells. *Mol. Cancer Ther.* **2004,** *3*, 1201-1206.
94. Strahl, C.; Blackburn, E. H. Effects of reverse transcriptase inhibitors on telomere length and telomerase activity in two immortalized human cell lines. *Mol. Cell. Biol.* **1996,** *16*, 53-65.
95. Dikmen, Z. G.; Gellert, G. C.; Jackson, S.; Gryaznov, S.; Tressler, R.; Dogan, P.; Wright, W. E.; Shay, J. W. In vivo inhibition of lung cancer by GRN163L: a novel human telomerase inhibitor. *Cancer Res.* **2005,** *65*, 7866-7873.
96. Schreiber, V.; Dantzer, F.; Ame, J. C.; de Murcia, G. Poly(ADP-ribose): novel functions for an old molecule. *Nat. Rev. Mol. Cell Biol.* **2006,** *7*, 517-528.
97. Ma, Q.; Baldwin, K. T.; Renzelli, A. J.; McDaniel, A.; Dong, L. TCDD-inducible poly(ADP-ribose) polymerase: a novel response to 2,3,7,8-tetrachlorodibenzo-p-dioxin. *Biochem. Biophys. Res. Commun.* **2001,** *289*, 499-506.
98. Gao, G.; Guo, X.; Goff, S. P. Inhibition of retroviral RNA production by ZAP, a CCCH-type zinc finger protein. *Science* **2002,** *297*, 1703-6.
99. Ladurner, A. G. Inactivating chromosomes: a macro domain that minimizes transcription. *Mol. Cell* **2003,** *12*, 1-3.
100. Karras, G. I.; Kustatscher, G.; Buhecha, H. R.; Allen, M. D.; Pugieux, C.; Sait, F.; Bycroft, M.; Ladurner, A. G. The macro domain is an ADP-ribose binding module. *EMBO J.* **2005,** *24*, 1911-1920.
101. Yu, M.; Schreek, S.; Cerni, C.; Schamberger, C.; Lesniewicz, K.; Poreba, E.; Vervoorts, J.; Walsemann, G.; Grotzinger, J.; Kremmer, E.; Mehraein, Y.; Mertsching, J.; Kraft, R.; Austen, M.; Luscher-Firzlaff, J.; Luscher, B. PARP-10, a novel Myc-interacting protein with poly(ADP-ribose) polymerase activity, inhibits transformation. *Oncogene* **2005,** *24*, 1982-1993.
102. Cortes, U.; Tong, W. M.; Coyle, D. L.; Meyer-Ficca, M. L.; Meyer, R. G.; Petrilli, V.; Herceg, Z.; Jacobson, E. L.; Jacobson, M. K.; Wang, Z. Q. Depletion of the 110-kilodalton isoform of poly(ADP-ribose) glycohydrolase increases sensitivity to genotoxic and endotoxic stress in mice. *Mol. Cell. Biol.* **2004,** *24*, 7163-7178.

103. Clark, J. B.; Ferris, G. M.; Pinder, S. Inhibition of nuclear NAD nucleosidase and poly ADP-ribose polymerase activity from rat liver by nicotinamide and 5'-methyl nicotinamide. *Biochim. Biophys. Acta.* **1971,** *238*, 82-85.
104. Banasik, M.; Ueda, K. Inhibitors and activators of ADP-ribosylation reactions. *Mol. Cell. Biochem.* **1994,** *138*, 185-197.
105. Shall, S. Proceedings: Experimental manipulation of the specific activity of poly(ADP-ribose) polymerase. *J. Biochem.* **1975,** *77*, 2-4.
106. Purnell, M. R.; Whish, W. J. Novel inhibitors of poly(ADP-ribose) synthetase. *Biochem. J.* **1980,** *185*, 775-777.
107. Banasik, M.; Komura, H.; Shimoyama, M.; Ueda, K. Specific inhibitors of poly(ADP-ribose) synthetase and mono(ADP-ribosyl)transferase. *J. Biol. Chem.* **1992,** *267*, 1569-1575.
108. Sims, J. L.; Sikorski, G. W.; Catino, D. M.; Berger, S. J.; Berger, N. A. Poly(adenosinediphosphoribose) polymerase inhibitors stimulate unscheduled deoxyribonucleic acid synthesis in normal human lymphocytes. *Biochemistry* **1982,** 21, 1813-1821.
109. Griffin, R. J.; Pemberton, L. C.; Rhodes, D.; Bleasdale, C.; Bowman, K.; Calvert, A. H.; Curtin, N. J.; Durkacz, B. W.; Newell, D. R.; Porteous, J. K. Novel potent inhibitors of the DNA repair enzyme poly(ADP-ribose)polymerase (PARP). *Anticancer Drug Des.* **1995,** *10*, 507-514.
110. Suto, M. J.; Turner, W. R.; Arundel-Suto, C. M.; Werbel, L. M.; Sebolt-Leopold, J. S. Dihydroisoquinolinones: the design and synthesis of a new series of potent inhibitors of poly(ADP-ribose) polymerase. *Anticancer Drug Des.* **1991,** *6*, 107-117.
111. White, A. W.; Almassy, R.; Calvert, A. H.; Curtin, N. J.; Griffin, R. J.; Hostomsky, Z.; Maegley, K.; Newell, D. R.; Srinivasan, S.; Golding, B. T. Resistance-modifying agents. 9. Synthesis and biological properties of benzimidazole inhibitors of the DNA repair enzyme poly(ADP-ribose) polymerase. *J. Med. Chem.* **2000,** *43*, 4084-4097.
112. Skalitzky, D. J.; Marakovits, J. T.; Maegley, K. A.; Ekker, A.; Yu, X. H.; Hostomsky, Z.; Webber, S. E.; Eastman, B. W.; Almassy, R.; Li, J.; Curtin, N. J.; Newell, D. R.; Calvert, A. H.; Griffin, R. J.; Golding, B. T. Tricyclic benzimidazoles as potent poly(ADP-ribose) polymerase-1 inhibitors. *J. Med. Chem.* **2003,** *46*, 210-213.
113. Southan, G. J.; Szabo, C. Poly(ADP-ribose) polymerase inhibitors. *Curr. Med. Chem.* **2003,** *10*, 321-340.
114. Loh, V. M., Jr.; Cockcroft, X. L.; Dillon, K. J.; Dixon, L.; Drzewiecki, J.; Eversley, P. J.; Gomez, S.; Hoare, J.; Kerrigan, F.; Matthews, I. T.; Menear, K. A.; Martin, N. M.; Newton, R. F.; Paul, J.; Smith, G. C.; Vile, J.; Whittle, A. J. Phthalazinones. Part 1: The design and synthesis of a novel series of potent inhibitors of poly(ADP-ribose)polymerase. *Bioorg. Med. Chem. Lett.* **2005,** *15*, 2235-2238.
115. Cockcroft, X.-l.; Dillon, K. J.; Dixon, L. Phthalazinones 2: Optimisation and synthesis of novel potent inhibitors of poly(ADP-ribose)polymerase. *Bioorg. Med. Chem. Letters* **2006,** *16*, 1040-1045.
116. Menear, K. A.; Adcock, C.; Boulter, R.; Cockcroft, X.-l.; Copsey, L.; Cranston, A.; Dillon, K. J.; Drzewiecki, J.; Garman, S.; Gomez, S.; Javaid, H.; Kerrigan, F.; Knights, C.; Lau, A.; Loh Jr, V. M.; Matthews, I. T. W.; Moore, S.; O'Connor, M. J.; Smith, G. C. M.; Martin, N. M. B. 4-[3-(4-Cyclopropanecarbonylpiperazine-1-carbonyl)-

4-fluorobenzyl]-2H- phthalazin-1-one: A Novel Bioavailable Inhibitor of Poly(ADP-ribose) Polymerase-1. *J. Med. Chem.* **2008,** *51*, 6581-6591.
117. Penning, T. D.; Zhu, G. D.; Gandhi, V. B.; Gong, J.; Thomas, S.; Lubisch, W.; Grandel, R.; Wernet, W.; Park, C. H.; Fry, E. H.; Liu, X.; Shi, Y.; Klinghofer, V.; Johnson, E. F.; Donawho, C. K.; Frost, D. J.; Bontcheva-Diaz, V.; Bouska, J. J.; Olson, A. M.; Marsh, K. C.; Luo, Y.; Rosenberg, S. H.; Giranda, V. L. Discovery and SAR of 2-(1-propylpiperidin-4-yl)-1H-benzimidazole-4-carboxamide: A potent inhibitor of poly(ADP-ribose) polymerase (PARP) for the treatment of cancer. *Bioorg. Med. Chem.* **2008,** *16*, 6965-6975.
118. Plummer, R.; Jones, C.; Middleton, M.; Wilson, R.; Evans, J.; Olsen, A.; Curtin, N.; Boddy, A.; McHugh, P.; Newell, D.; Harris, A.; Johnson, P.; Steinfeldt, H.; Dewji, R.; Wang, D.; Robson, L.; Calvert, H. Phase I study of the poly(ADP-ribose) polymerase inhibitor, AG014699, in combination with temozolomide in patients with advanced solid tumors. *Clin. Cancer Res.* **2008,** *14*, 7917-7923.
119. Rottenberg, S.; Jaspers, J. E.; Kersbergen, A.; van der Burg, E.; Nygren, A. O.; Zander, S. A.; Derksen, P. W.; de Bruin, M.; Zevenhoven, J.; Lau, A.; Boulter, R.; Cranston, A.; O'Connor, M. J.; Martin, N. M.; Borst, P.; Jonkers, J. High sensitivity of BRCA1-deficient mammary tumors to the PARP inhibitor AZD2281 alone and in combination with platinum drugs. *Proc. Natl. Acad. Sci. USA* **2008,** *105*, 17079-17084.
120. Evers, B.; Drost, R.; Schut, E.; de Bruin, M.; van der Burg, E.; Derksen, P. W.; Holstege, H.; Liu, X.; van Drunen, E.; Beverloo, H. B.; Smith, G. C.; Martin, N. M.; Lau, A.; O'Connor, M. J.; Jonkers, J. Selective inhibition of BRCA2-deficient mammary tumor cell growth by AZD2281 and cisplatin. *Clin. Cancer. Res.* **2008,** *14*, 3916-3925.
121. Perkins, E.; Sun, D.; Nguyen, A.; Tulac, S.; Francesco, M.; Tavana, H.; Nguyen, H.; Tugendreich, S.; Barthmaier, P.; Couto, J.; Yeh, E.; Thode, S.; Jarnagin, K.; Jain, A.; Morgans, D.; Melese, T. Novel inhibitors of poly(ADP-ribose) polymerase/PARP1 and PARP2 identified using a cell-based screen in yeast. *Cancer Res.* **2001,** *61*, 4175-4183.
122. Iwashita, A.; Mihara, K.; Yamazaki, S.; Matsuura, S.; Ishida, J.; Yamamoto, H.; Hattori, K.; Matsuoka, N.; Mutoh, S. A new poly(ADP-ribose) polymerase inhibitor, FR261529 [2-(4-chlorophenyl)-5-quinoxalinecarboxamide], ameliorates methamphetamine-induced dopaminergic neurotoxicity in mice. *J. Pharmacol. Exp. Ther.* **2004,** *310*, 1114-1124.
123. Oliver, A. W.; Ame, J. C.; Roe, S. M.; Good, V.; de Murcia, G.; Pearl, L. H. Crystal structure of the catalytic fragment of murine poly(ADP-ribose) polymerase-2. *Nucleic Acids Res.* **2004,** *32*, 456-464.
124. Ruf, A.; de Murcia, G.; Schulz, G. E. Inhibitor and NAD+ binding to poly(ADP-ribose) polymerase as derived from crystal structures and homology modeling. *Biochemistry* **1998,** *37*, 3893-3900.
125. Ishida, J.; Yamamoto, H.; Kido, Y.; Kamijo, K.; Murano, K.; Miyake, H.; Ohkubo, M.; Kinoshita, T.; Warizaya, M.; Iwashita, A.; Mihara, K.; Matsuoka, N.; Hattori, K. Discovery of potent and selective PARP-1 and PARP-2 inhibitors: SBDD analysis via a combination of X-ray structural study and homology modeling. *Bioorg. Med. Chem.* **2006,** *14*, 1378-1390.
126. Schraufstatter, I. U.; Hyslop, P. A.; Hinshaw, D. B.; Spragg, R. G.; Sklar, L. A.; Cochrane, C. G. Hydrogen peroxide-induced injury of cells and its prevention by

inhibitors of poly(ADP-ribose) polymerase. *Proc. Natl. Acad. Sci. USA* **1986,** *83*, 4908-4912.
127. Cheung, A.; Zhang, J. A scintillation proximity assay for poly(ADP-ribose) polymerase. *Anal. Biochem.* **2000,** *282*, 24-28.
128. Lee, S.; Koo, H. N.; Lee, B. H. Development of a miniaturized assay for the high-throughput screening program for poly(ADP-ribose) polymerase-1. *Methods Find. Exp. Clin. Pharmacol.* **2005,** *27*, 617-622.
129. Dillon, K. J.; Smith, G. C.; Martin, N. M. A FlashPlate assay for the identification of PARP-1 inhibitors. *J. Biomol. Screen.* **2003,** *8*, 347-352.
130. Wenkert, E.; Wenkert. Derivatives of Hemimellitic Acid. A Synthesis of Erythrocentaurin1. *J. Org. Chem.* **1964,** *29*, 2534-2542.
131. Watson, C. Y.; Whish, W. J.; Threadgill, M. D. Synthesis of 3-substituted benzamides and 5-substituted isoquinolin-1(2H)-ones and preliminary evaluation as inhibitors of poly(ADP-ribose)polymerase (PARP). *Bioorg. Med. Chem.* **1998,** *6*, 721-734.
132. Woon, C. Y., Dhami, A., Sunderland, P. T., Threadgill, M. D. Reductive Cyclisation of 2-Cyanomethyl-3-Nitrobenzoates. *Lett. Org. Chem.* **2006,** *3*, 571-578.
133. Heck. Palladium-catalyzed vinylic hydrogen substitution reactions with aryl, benzyl, and styryl halides. *J. Org. Chem.* **1972,** *37*, 2320-2322.
134. Mizoroki, T., Mori, K., Ozaki, A. Arylation of olefin with aryl iodide catalyzed by palladium. *Bull. Chem. Soc. Jpn.* **1971,** *44*, 581.
135. Berry, J. M. W., C. Y.; Whish, W. J. D.; Threadgill, M. D. 5-Nitrofuran-2-ylmethyl group as a potential bioreductively activated pro-drug system. *J. Chem. Soc. Perkin Trans. 1* **1997**, 1147-1156.
136. Plevyak. Selective palladium-catalyzed vinylic substitutions with bromoiodo aromatics. *J. Org. Chem.* **1979,** *44*, 4078-4080.
137. Carda, M.; Gonzalez, F.; Sanchez, R.; Marco, J. A. Stereoselective synthesis of (-)-cytoxazone. *Tetrahedron: Asymmetry* **2002,** *13*, 1005-1010.
138. Kim, S.; Ko, H.; Kim, E.; Kim, D. Stereocontrolled Total Synthesis of Pancratistatin. *Org. Lett.* **2002,** *4*, 1343-1345.
139. Ponticello. Useful synthesis of 4-substituted indoles. *J. Org. Chem.* **1979,** *44*, 4003-4005.
140. March, J. In *Advanced Organic Chemistry*, 2nd ed.; McGraw-Hill.: London, 1977, 816-817.
141. Banwell, M., G. Cowden, C, J. Convergent Routes to the <1,3>Dioxolo<4,5-j>phenanthridin-6(5H)-one and 2,3,4,4a-Tetrahydro<1,3>dioxolo<4,5-j>phenanthridin-6(5H)-one Nuclei. Application to Syntheses of the Amaryllidaceae Alkaloids Crinasiadine, N-Methylcrinasiadine and Trisphaeridine. *Aust. J. Chem.* **1994,** *47*, 2235-2254.
142. Bisagni, E.; Landras, C.; Thirot, S.; Huel, C. A convenient way to dibenzo[c,h]-1,5-naphthyridines (11-aza-benzo[c] phenanthridines). *Tetrahedron* **1996,** *52*, 10427-10440.
143. Iley, J., Carvalho, E., Norberto, F., Rosa, E. . Reaction of N-Aryl- and N-Alkyl-benzimidoyl Chlorides with Silver Nitrate. *J. Chem. Soc., Perkin Trans. 2.* **1992,** *2*, 281-290.

144. Gordon. The Swamping Catalyst Effect. VI. The Halogenation of Isoquinoline and Quinoline1. *J. Org. Chem.* **1964,** *29*, 329-332.
145. Braye. *Eur. J. Med. Chem.* **1977,** *9*, 197-200.
146. Palucki, M.; Buchwald, S. L. Palladium-Catalyzed Î±-Arylation of Ketones. *J. Am. Chem. Soc.* **1997,** 119, 11108-11109.
147. Moradi, W. A.; Buchwald, S. L. Palladium-Catalyzed Î±-Arylation of Esters. *J. Am. Chem. Soc.* **2001,** *123*, 7996-8002.
148. Zeevaart, J. G.; Parkinson, C. J.; de Koning, C. B. Palladium-catalysed arylation of acetoacetate esters to yield 2-arylacetic acid esters. *Tetrahedron Lett.* **2004,** *45*, 4261-4264.
149. Zeevaart, J. G.; Parkinson, C. J.; de Koning, C. B. Copper(I) iodide-catalysed arylation of acetoacetate to yield 2-arylacetic acid esters. *Tetrahedron Lett.* **2007,** *48*, 3289-3293.
150. Ozdemir, I.; Yigit, M.; Cetinkaya, E.; Cetinkaya, B. Synthesis of arylacetic acid derivatives from diethyl malonate using in situ formed palladium(1,3-dialkylimidazolidin-2-ylidene) catalysts. *Tetrahedron Lett.* **2004,** *45*, 5823-5825.
151. Culkin, D. A.; Hartwig, J. F. Palladium-Catalyzed Î±-Arylation of Carbonyl Compounds and Nitriles. *Acc.Chem. Res.* **2003,** *36*, 234-245.
152. Milstein. A general, selective, and facile method for ketone synthesis from acid chlorides and organotin compounds catalyzed by palladium. *J. Am. Chem. Soc.* **1978,** *100*, 3636-3638.
153. Milstein. Palladium-catalyzed coupling of tetraorganotin compounds with aryl and benzyl halides. Synthetic utility and mechanism. *J. Am. Chem. Soc.* **1979,** *101*, 4992-4998.
154. Milstein. Mechanism of reductive elimination. Reaction of alkylpalladium(II) complexes with tetraorganotin, organolithium, and Grignard reagents. Evidence for palladium(IV) intermediacy. *J Am. Chem. Soc.* **1979,** *101*, 4981-4991.
155. Woon, E. C.; Threadgill, M. D. Poly(ADP-ribose)polymerase inhibition - where now? *Curr. Med. Chem.* **2005,** *12*, 2373-2392.
156. Eltze, T.; Boer, R.; Wagner, T.; Weinbrenner, S.; McDonald, M. C.; Thiemermann, C.; Burkle, A.; Klein, T. Imidazoquinolinone, imidazopyridine, and isoquinolindione derivatives as novel and potent inhibitors of the poly(ADP-ribose) polymerase (PARP): a comparison with standard PARP inhibitors. *Mol. Pharmacol.* **2008,** *74*, 1587-1598.
157. Pellicciari, R.; Camaioni, E.; Costantino, G.; Formentini, L.; Sabbatini, P.; Venturoni, F.; Eren, G.; Bellocchi, D.; Chiarugi, A.; Moroni, F. On the way to selective PARP-2 inhibitors. Design, synthesis, and preliminary evaluation of a series of isoquinolinone derivatives. *Chem.Med. Chem.* **2008,** *3*, 914-23.
158. Woon, C. Y., Dhami, A., Mahon, F., Threadgill, M. D. 5-Nitroisocoumarins from tandem Castro-Stephens coupling-6-*endo*-dig cyclisation of 2-iodo-3-nitrobenzoic acid and arylethynes and ring-closure of methyl 2-alkynyl-3-nitrobenzoates with electrophiles. *Tetrahedron* **2006,** *62*, 4829-4837.
159. Hurtley, W., R., H. Replacement of halogen in orthobromo-benzoic acid. *J. Chem. Soc.* **1929**, 1870-1873.
160. Cirigottis, K., A., Ritchie, E., Taylor, W., C. Studies on the Hurtley reaction. *Aust. J. Chem.* **1974,** *27*, 2209-2228.

161. Ames, D., R., Ribeiro., O. Heterocyclic synthesis from o-halogeno-acids. Part III. Synthesis of 2-methylindole-4-carboxylic acid and related compounds and of some derivatives of 3-phenylisoquinolin-1(2H)-one. *J. Chem. Soc. Perkin Trans. 1* **1976,** *1*, 1073-1078.
162. Woon, E. C. Y. PhD Thesis, University of Bath, 2004.
163. Kim. Synthesis of 4-Acetylisocoumarin: First Total Syntheses of AGI-7 and Sescandelin. *J. Org. Chem.* **2002,** *67*, 3127-3130.
164. Kama, A., Robertson, A., Tittensor, R. Hydroxy-carbonyl compounds. Part XIV. The syntheses of some isocoumarins. *J. Chem. Soc.* **1950,** 3375-3380.
165. Chatterjee, J., N., Mukherjee, S., K., Bhakta, C., Jha, H., C., Zilliken, F. Eine neue Synthese von Tetrahydrocapillarin, O-Methylglomellin und Oospolacton *Chem. Ber.* **1980,** *113*, 3927-3931.
166. Ford, A.; Sinn, E.; Woodward, S. Exploitation of differential reactivity of the carbon-chlorine bonds in 1,3-dichloroisoquinoline. Routes to new N,N-chelate ligands and 1,3-disubstituted isoquinolines. *J. Chem. Soc., Perkin Trans. 1.* **1997**, 927 - 934.
167. Gamage, S. A.; Spicer, J. A.; Rewcastle, G. W.; Milton, J.; Sohal, S.; Dangerfield, W.; Mistry, P.; Vicker, N.; Charlton, P. A.; Denny, W. A. Structure-Activity Relationships for Pyrido-, Imidazo-, Pyrazolo-, Pyrazino-, and Pyrrolophenazinecarboxamides as Topoisomerase-Targeted Anticancer. *J. Med. Chem.* **2002,** *45*, 740 - 743.
168. Elpern; Hamilton. *J. Am. Chem. Soc.* **1946,** *68*, 1436.
169. Secel, A., D. Sanchez., J., P. Hollis Showalter, H., D.,. Simple Synthesis of 4-Substituted 1(2H)-Isoquinolinones via Electrophilic Trapping of Lithiated Mono- and Dianion Precursors *Synth. Commun* **2007,** *37*, 4199-4208.
170. Mao. Syntheses of dihydropyrenes with functionality in the cavity of the pi.-electron cloud. *J. Org. Chem.* **1980,** *45*, 2746-2749.
171. Horning, D., E., Lacasse, G., Muckowski, J., M. Isocarbostrils. I. Electrophilic Substitution Reactions. *Can. J. Chem.* **1971,** *49*, 2785-2796.
172. Barder. Catalysts for SuzukiMiyaura Coupling Processes: Scope and Studies of the Effect of Ligand Structure. *J. Am. Chem. Soc.* **2005,** *127*, 4685-4696.
173. Wong, M. S.; Zhang, X. L. Ligand promoted palladium-catalyzed homo-coupling of arylboronic acids. *Tetrahedron Lett.* **2001,** *42*, 4087-4089.
174. Smith, J. A.; Jones, R. K.; Booker, G. W.; Pyke, S. M. Sequential and selective Buchwald-Hartwig amination reactions for the controlled functionalization of 6-bromo-2-chloroquinoline: synthesis of ligands for the Tec Src homology 3 domain. *J. Org. Chem.* **2008,** *73*, 8880-8892.
175. Dhami, A. PhD Thesis, University of Bath, 2008.
176. Parveen, I.; Naughton, D. P.; Whish, W. J. D.; Threadgill, M. D. 2-nitroimidazol-5-ylmethyl as a potential bioreductively activated prodrug system: reductively triggered release of the PARP inhibitor 5-bromoisoquinolinone. *Bioorg. Med. Chem. Lett.* **1999,** *9*, 2031-2036.
177. Ferrer, S. N., D., Parveen, I., Threadgill, M.D. N- and O-Alkylation of isoquinolin-1-ones in the Mitsunobu reaction: development of potential drug delivery systems. *J. Chem. Soc., Perkin Trans. 1.* **2002**, 335-340.
178. Nair, M. D.; Mehta, S. R. *Ind. J. Chem.* **1967,** *5*, 403-408.

179. Gamage, S. A.; Spicer, J. A.; Rewcastle, G. W.; Milton, J.; Sohal, S.; Dangerfield, W.; Mistry, P.; Vicker, N.; Charlton, P. A.; Denny, W. A. Structure Activity Relationships for Pyrido-, Imidazo-, Pyrazolo-, Pyrazino-, and Pyrrolophenazinecarboxamides as Topoisomerase-Targeted Anticancer Agents. *J. Med. Chem.* **2002,** *45*, 740-743.